A Kinetic and Thermodynamic Study of the Reduction of Peroxyacids by Iodide and Aryl Alkyl Sulfides in the Presence of Non-ionic Surfactants and α-Cyclodextrin.

SALEM MANSOUR MOUSA

PhD

2009

A Kinetic and Thermodynamic Study of the Reduction of Peroxyacids by Iodide and Aryl Alkyl Sulfides in the Presence of Non-ionic Surfactants and α-Cyclodextrin.

A thesis submitted in partial fulfilment

of the requirements of the

University of Northumbria at Newcastle

For the degree of

Doctor of Philosophy

Research undertaken in the School of applied Science

at Northumbria University

2009

ACKNOWLEDGMENT

All powers belong to almighty God, the creator of whole universe, who provide me the knowledge and strength to complete this work.

I wish to express my sincere gratitude to my supervisors Dr. Michael Deary and Dr. Martin Davies for their guidance and cooperation throughout this work, and also speciall thanks to Dr Michael Deary for reading the manuscript of this thesis and making many suggestions which helped materially to clear and improve this thesis.

Also I wish to express my thanks to Mr Gary Askwith, for his assistance during this research work.

Also I am indebted to my sponsor, Libyan Government, for paying the fees and living expense during my study.

Finally I would like to acknowledge my parents and wife for their help and encouragement at each and every step.

Declaration

I declare that the work contained in this thesis has not been submitted for any other award and that it is all my own work.

Name: SALEM MANSOUR MOUSA

Signature:

Date: 07/05/2009

Abstract

The objectives of this study were two-fold: firstly to add to existing knowledge about the reaction of peracid with both iodide and sulfides in the presence of micelles (anionic and non-ionic) and α-cyclodextrin. The reaction between iodide and peracid had previously been studied only at 25°C in non-ionic, anionic micellar and alpha cyclodextrin; while the reaction of sulfides and peracid had only been investigated in the presence of α-cyclodextrin at one temperature. This study has investigated the previously undetermined effect of temperature on these reactions and how changes in temperature can affect the process of reactants binding to the micelle or cyclodextrin catalyst. The second objective was to obtain quantitative information about reactivity in ordered aqueous media such as micellar systems and cyclodextrins, and find out how these media can affect and control these reactions. This might have implications for fields such as cell biology, specifically for process occurring in living cells since both cyclodextrins and micelles might be considered simple models for protein and membranes in terms of their hydrophobicity. In addition, little information is known about bimolecular reactions involving two neutral reactants in non-ionic micelles where only the hydrophobic interaction is likely to influence the reaction due to the absence of charge-charge interaction.

A kinetic and thermodynamic investigation of the reactions between peracids and different reductants i.e. iodide and series of aryl alkyl sulfides in presence non-ionic micelle and α- cyclodextrin is reported in this work. The kinetics were conducted by monitoring spectrophotometrically the increase or decrease in the absorbance due to formation of triioidide or disappearance of sulfides respectively, and absorbance versus time plots were fitted to nonlinear equation in order to obtain the observed pseudo first order rate constants.

For reactions carried out in micellar systems the kinetic data were treated using the multiple micellar pseudophase model developed by Davies which considers the partition of reactants between water in the bulk aqueous phase and that in the micellar pseudophases. Important parameters in this model include the binding constant of reactants to Brij (non-ionic micelle) and k_{mic} (reaction rate in micelle). For reactions in α-cyclodextrin, data was fitted to rate equations containing first and second order dependencies on cyclodextrin using non linear regression techniques.

The work was carried out in the presence of 0.003 M nitric acid as reaction medium. The effect of inorganic electrolytes (sodium nitrate, sulfate, actetate, perchlorate and chloride)

on the rate of oxidation of iodide in the absence and presence of non-ionic surfactant brij-35 was also studied. The critical micelle concentration (CMC) of the surfactants was determined using kinetic techniques and was found to be inversely proportional to the salt concentration and also to the temperature. The CMC was also found to decrease as the length of the hydrophobic part of the Brij surfactants was increased, possibly due to the decrease of interfacial energy on micellization, which generally increases in with increasing hydrophobic chain length.

It was shown from analysis of the kinetic data that all non-ionic micelles in the (absence of salts) and α-CD studied in this work enhanced the rate of the iodide oxidation by MCPBA and that the rate showed saturation type kinetics. Sulfate ions were shown to accelerate the reaction further, whereas perchlorate caused an inhibition of the iodide oxidation (compared to the reaction only in nitric acid) in presence of Brij-35, but an increase in the presence of α-cyclodextrin. For the oxidation of sulfides by MCPBA in micelles and α-CD the observed rate increases to a maximum with increasing micelle or α-CD concentration and then subsequently declines. In the case of sulfide oxidation by the anionic peracid, peroxymonosulfate (PMS), there was only inhibition in the rate, due to separation of reactants.

The effect of temperature on both rate and equilibrium processes for these systems was determined over the range 15 to 35°C. The results showed a linear decrease in the binding of metachloroperbenzoic (MCPBA) acid and aryl alkyl sulfides to both micelle and α-CD with increasing the temperature.

The thermodynamic and activation parameters for the reactions were determined by using Van't Hoff and Eyring plots. Comparison of the micellar association constants of MCPBA and the apparent micellar association constant of the transition state for the reaction with iodide, suggested that orientational restriction imposed on the peracid by Brij-35 are similar to that in the transition state. For the same reactions carried out in α-cyclodextrin at different temperatures it was determined that the binding constant enthalpy and entropy of substrates, (peracid and iodide) are more negative than that obtained in the presence of brij-35 which indicates that stronger interactions are involved and more restriction imposed on the reactant in presence of α-CD compared to brij-35.

A similar approach was employed for the reaction of series of aryl alkyl sulfides with peracids (PMS and MCPBA) in presence of Brij-35 and α-CD. The aryl alkyl sulfides can form both 1:1 and 2:1 host: guest complexes in cyclodextrin; the 2:1 inclusion

complexes for some sulfides were larger than the 1:1 complexes, indicating cooperative binding, with the driving force for this possibly being a substrate induced dipole-dipole interaction between the two cyclodextrin molecules. Linear free energy studies indicate that the catalytic species is the bound peracid reacting with the unbound sulfides; sulfide binding results in steric inhibition of the reaction. The reaction of the non-binding PMS with sulfides results only in inhibition as cyclodextrin concentration is increased.

The enthalpy and entropy for sulfide oxidation by peracids was calculated by means of a Van't Hoff plot. The reaction in α-CD associated with more negative entropy and enthalpy for the inclusion 2:1 while for 1:1 some substrates associated with positive entropy and small negative enthalpy while other show the usual behaviour observed for complex formation (negative values for both enthalpy and entropy).

In all studied reactions (related reactions) there were good relationships between enthalpy and entropy (isokinetic relationships or enthalpy-entropy compensation). Whilst in some cases it is difficult to explain why enthalpy-entropy compensation might be observed, we have suggested that in the case of binding of sulfides to cyclodextrin these plots can act as probes into the orientation of the substrate within the cyclodextrin cavity.

The nature of the catalytic mechanism for the reactions of peracids with sulfides and iodide in the presence of micelles and α-cyclodextrin was examined by comparing the transition state stabilisation parameters, K_{TS1}, for the same reaction in the two catalytic systems. It was found that for three out of five sulfides the degree of transition state stabilisation was almost identical in both Brij-35 and α-cyclodextrin, perhaps suggesting the same catalytic mechanism in each system; this could be via either decreased stabilisation of the peracid ground state in the absence of a protic solvent and / or the prevention of significant charge development in the transition state as a result of an intramolecular proton transfer step involving the peracid that is facilitated by the absence of water. Other possibilities exist, such as general acid catalysis, though these would be more dependent on the nature of the catalytic system. There was a less clear relationship for iodide.

Table of content

Chapter 1: Review of literature

1.1. General introduction

As this work deals with the reactions of peracids with iodide and alkyl aryl sulfides in the presence of non-ionic micelles and cyclodextrin, thus the next sections will detail the general features of first the peroxides and their physical and chemical properties, structure and preparation. In the second part detail about surfactants and micelles formation and their effect on the chemical reactions in the absence and presence of salts, also the Hofmeister series will be considered as it related to the current study. The third section deals with cyclodextrin, its properties and its effect on rate of chemical reactions. All these are pertinent to the discussion in this thesis, with final section of this chapter discussing the rationale and aim for such investigation.

1.2. Peroxides and related compounds

1.2.1. Backgrounds

Organic peroxides can have a range of characteristics depending on their chemical structure and reactivity. The reactivity of peroxides depends on the peroxide group configuration and on the type of substituents. Organic peroxides can be classified into different groups depending on their chemical structures.

Peroxy compounds play an important role in oxidation reaction and they are generally produced by a reaction with molecular dioxygen or its activated form, e.g. superoxide anion radical. These species also play an important role in combustion, polymerisation, biological metabolism and as environmental friendly agents[1].

Peroxides constitute a group of chemicals that all contain peroxygen i.e the O-O bond. Hydrogen peroxide is the simplest peroxide and is the parent compound from which other classes can be derived [2]. The main classes are alkyl hydroperoxide of the form ROOH, where R is an alkyl group; dialkylperoxides of the form ROOR; and acyl peroxides of the form RCOOOR, which include peroxyacid, peroxyester and diacylperoxides. And in Figure1.1 shows some classes of the peroxides compounds.

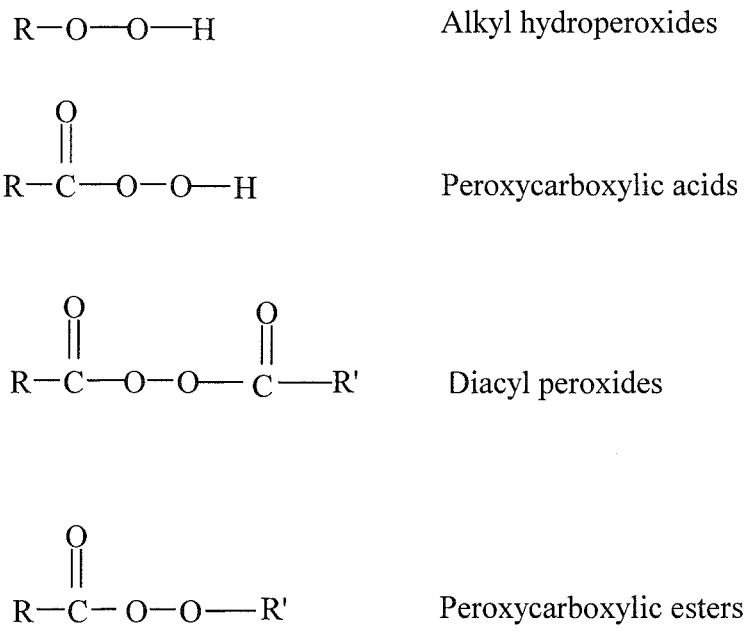

Figure 1.1: general structures of some peroxids compounds

Peroxyacid has been used as an environmentally friendly agent. For example, polycyclic aromatic hydrocarbons are found ubiquitously in the environment and have been determined to exhibit mutagenic and carcinogenic properties, both in humans and animals. Therefore, they should be treated as a pollutant and have to be removed. One method used for the removal of this compound from the environment is called the peroxy-acid process, which involves the degradation of polycyclic aromatic hydrocarbon in soil. The compounds tested were α-methylnaphthalene and benzo(a)pyrene [3]. Recently, other types of polycyclic aromatic hydrocarbon have been tested for the peroxy acid process, including fluorene, phenanthrene, anthracene and pyrene; all these compounds were degraded [4].

1.2.2. Peroxyacids

Peracids are compounds that have become known and utilised as oxidation reagents. They can behave as an electrophiles causing olefin epoxidation and amine oxidation and are also used for the oxidation of substrates such as sulfides and iodide, they can act as nucleophiles for example in the oxidation of ketones into ester.

The synthesis, properties and reactions of peroxyacids and their related compounds have been reviewed extensively [5]. As they are related to this study the next section will give some detail about their properties, preparation, structure and chemical properties.

1.2.2.1. Properties of Peracids and hydrogen peroxids

In aqueous solution peracid dissociate into peroxy anion and hydrogen ion according to following Equation:

$$RCOOOH \underset{}{\overset{K_a}{\rightleftharpoons}} RCO_3^- + H^+$$

And the dissociation constant is defined by the following Equation:

$$Ka = [RCO_3^-]\,[H^+] / [RCO_3H]$$

The pKa value of the peracid is usually higher than the corresponding carboxylic acid: 7.1 to 8.2 for peracid, and 3.6 to 4.9 for parent acid. For example, peroxyacetic acid has a pK_a value of 8.2, whereas acetic acid has a pka of 4.7. Two explanations have been proposed for this difference. The first is the intramolecular hydrogen bonding present in the peroxy acid, which stabilises the peracid relative to its anion. The second is that the peroxyanion lacks the stabilisation of the carboxylate anion[2]. In addition, the pK_a of the hydroperoxides (11.6 to 12.8) is higher than that of peracid for the same reason [6].

Oxygen containing reactive species can be classified into two groups based on their electronic and chemical properties. The first class is the cationic species, including $O^{\cdot+}$, HO^+ and H_2O^+, which act as electrophiles toward organic substitutes; alkene and aromatic compounds, for example. The second class is the anionic species, including HO^- and $O_2^{\cdot-}$, which act as nucleophiles toward electron deficient substrates [6]. Some of the reactions of peroxide as nucleophiles and electrophiles will be considered in the coming section, but firstly the main property of the parent compound hydrogen peroxide is described.

Hydrogen peroxide has a high redox potential (1.76 v), and it seems as though the compound could be a relatively powerful oxidant. This is not the case, however, as it requires activation in some way or another in the majority of its applications, e.g. for bleaching purposes. Hydrogen peroxide can be both an electrophile and nucleophile agent. Its nucleophilic behaviour arises from the fact that peroxyanions HOO^- is a

powerful nucleophile and the undissociated H_2O_2 behaves as a electrophile, being about 10^4 times more reactive than water [7]. The neutral oxygen radical is considered an electrophile and reacts with electron-rich species such as alkene [6].

Depending on the structure of the peroxide, the peroxide bond can be cleaved homolytically or heterolytically. In the case of alkylhydroperoxides, they undergo homolytic cleavage to give two $RO^{\bullet}$, and are often used for initiating a radical chain reaction. Heterolysis cleavage can be achieved under certain circumstances.

Hydrogen peroxide often decomposes exothermically into water and oxygen gas spontaneously [2]. This process is favourable and it has a ΔH° of -98 kJ/ mol and a ΔG° of -119.2 kJ/mol and a ΔS° of 70.5 J/mol K [7].

These compounds have a lower melting point than their corresponding carboxylic acids. Table 1.1 shows some of the properties of 3-chloroperbenzoic acid and other peroxyacids. Their boiling point is low, which is attributed to the high stability of the monomeric form with intramolecular hydrogen bonding [7] (see the Figure 1.2). From Table 1.1 it can be seen that the peracids are weaker than their parent acids, as shown by the pK_a value. Electron attracting substituents increases the acidity of the peroxyacids. For example, the pk_a value of trifluoro acetic acid is estimated to be 3.7, owing to the strong electron attracting CF_3 group [8].

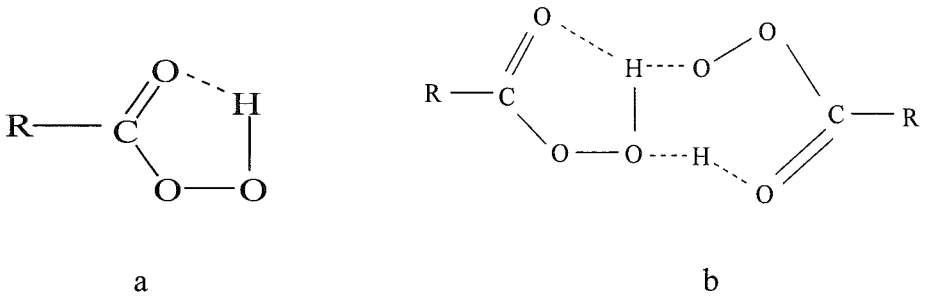

a b

Figure 1.2: Intramolecular hydrogen bonding.

Table 1.1: Physical properties of peroxy acid (taken from reference 5).

Peroxy acids	**Melting point C^0**	**pK_a**
$3\text{-}ClC_6H_4CO_3H$	92	7.2
CF_3CO_3H		3.7
$PhCO_3H$	41	7.78
HCO_3H	-18	7.1
$MeCO_3H$	0	8.2

1.2.2.2. Preparation and structure

Preparation from carboxylic acid:

The reaction between H_2O_2 and carboxylic acid or anhydride in acidic medium is shown in Scheme1.1 below:

$$RCOOH + H_2O_2 \longrightarrow RCOOOH + H_2O$$

$$(RCO)_2O + H_2O_2 \longrightarrow RCOOOH + RCOOH$$

Scheme1.1

Also, perhydrolysis of acid chloride in alkaline hydrogen peroxide:

$$RCOCl + H_2O_2 + NaOH \longrightarrow RCO_3H + H_2O + NaCl$$

The addition of an excess amount of hydrogen peroxide is pertinent since the molar ratio RCOCl: H_2O_2 is 2:1 lead to formation of diacylperoxide [5].

Peracetic acid can be prepared by the oxidation of acetaldehyde [5] and also by the reaction of tetraacetylethylenediamine (TAED) in the presence of an alkaline hydrogen peroxide solution [9]. Other methods are used to prepare peroxyacids (for more detail reference to 7).

Davison [10] found strong evidence, using infrared spectroscopy, that perbenzoic acid exists in monomeric form due to an intramolecular hydrogen bond between the carbonyl oxygen and the hydroxyl oxygen atoms of the percarboxyl group, as shown in Structure 1.1a. More evidence supporting this was obtained by infrared study and x-ray diffraction on the aliphatic peracid. The results show that in solution the peracid exists as an intramolecularly chelated monomer containing a five-membered ring; while in the solid

state, x-ray diffraction shows that the peracid exists as dimers, in which two monomer link through intermolecular hydrogen bonds, as shown in Figure 1.1b [11].

Giguere and Olmos [12] have suggested that the stability of lower chain aliphatic peracids (performic and peracetic acids) may be due to intramolecular hydrogen bonds of peracid which result in a five-membered ring with no angle strain. The energy of these hydrogen bonds is estimated to be about 7 kcal. per mole [12].

The electric dipole moments of five long-chain aliphatic peracids indicate considerable puckering in the five-membered chelate ring, formed by hydrogen bonding between the hydroxyl oxygen and the carbonyl oxygen atoms [13].

1.2.2.3 Nucleophilicity of peracids

The peroxy anion is considered to be a strong nucleophile compared to the hydroxide anion. The peroxy anion can react via nucleophilic attack on several substrates; for example, the acyl transfer reaction of peroxybenzoate ions which acts as a nucleophile with p-nitrophenyl acetate, and also the reaction of MCPBA anion with p-nitrophenyl phosphate [5]. The reactivity difference between peroxy anion and hydroxide anion is about 10^4 for an attack upon benzonitrile [14, 15]. Peracids and other types of hydroperoxide show nucleophilic behaviour toward an electrophilic centre, whereby they can displace the existing group or pair of electrons or addition, as shown in Scheme 1.2a and 1.2b respectively [5]. The product of the reaction is stable but will decompose by rapid redox reaction, resulting in the cleavage of the O-O bond homolyticaly or heterolytically depending on the peroxide, or the peroxide bond [15].

The high nucleophility of peroxide and its anion has been described in terms of the alpha effect (two adjacent atoms bearing lone pairs of electron) [15].

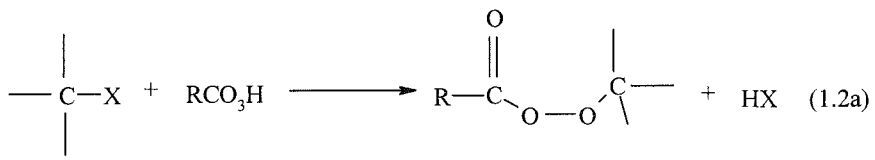

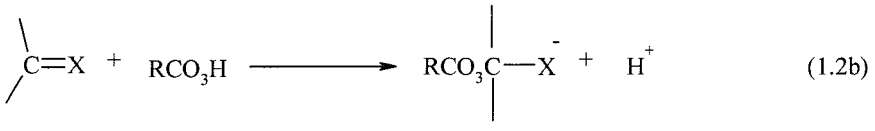

Scheme 1.2: Nucleophilic reaction of peracid.

Peroxyacid or hydrogen peroxide (especially m-chloroperbenzoic acid) is used in the Baeyer-Villiger oxidation of ketone to ester because it is cheap to do so. Scheme 1.3 shows a reaction in which the deprotonated peracid, which is a good nucleophilic species, attacks the carbonyl carbon and forms tetrahedral intermediate, and then by rearrangement arrangement forms the ester [21].

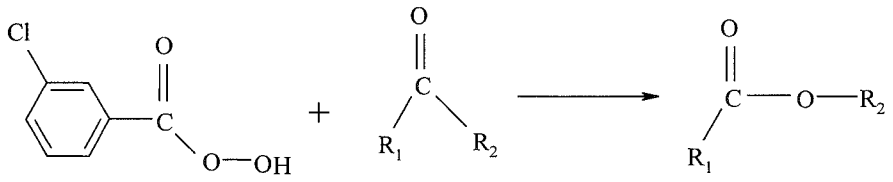

Scheme1.3: Oxidation of ketone by peracid.

1.2.2.4. Electrophilicity of peroxyacid

The most characteristic reaction of peroxyacid is electrophilic oxygen transfer, where an oxygen atom of the peracid transfers to a substrate nucleophile containing a lone pair; the transfer is accelerated by an electron attracting group on the peracid and electron donating substitutes on the substrate. The latter case will be observed in chapter 4 for the reaction of peracid with substituted alkyl aryl sulfides. When a nucleophile denoted S:, approaches the peroxide bond, along a line formed by the two peroxidic oxygens, the oxygen close to the nucleophile becomes partially positive and so behaves as an electrophile [5] (see Scheme 1.4).

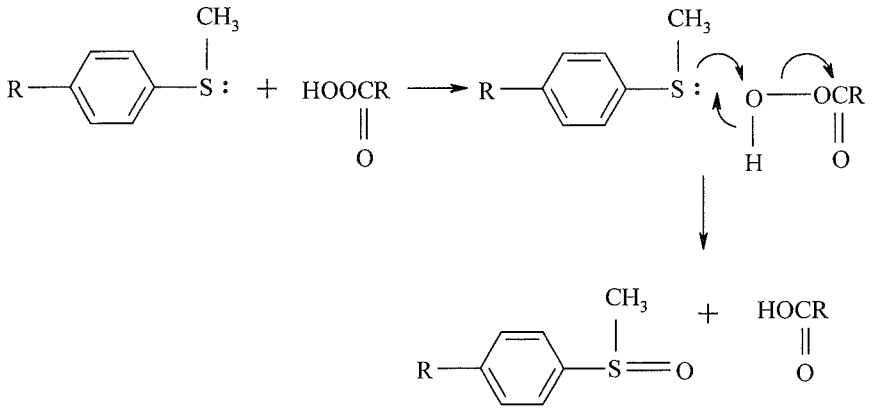

Scheme 1.4

The most important reaction of this type for the present work is the reaction of the peracid with iodide. The reaction of peracid with this and other halide ions is well known, with the formation of hypohalides being the rate determining step [16]. Also, the oxidation of sulfides by peracid shows it behaves as an electrophilic reagent. The mechanism of the reaction involves attack of the nucleophile on the outer oxygen of the peracid, and this reaction is considered to be fast [17].

Another example of the use of peroxyacids such as 3-chloroperbenzoic acid, which is a strong oxidizing agent, is the epoxidation of alkenes; the epoxidation reaction of olefins can also be achieved by applying a variety of oxidants. However, peroxycarboxylic acids are widely used stoichiometric reagents for epoxidation in industrial and academic research [18], along with alkylhydroperoxides, hydrogen peroxide [19], and oxygen [20]. Most oxidants have the disadvantage that in addition to the oxidised products, stoichiometric amounts of waste products are formed which have to be separated from the epoxides.

The main advantages of the use of peroxides are the low cost and the absence of oxidant waste products. Therefore, oxygen containing comppunds is among the most important oxidants for large-scale industrial application [19]. In general, this reaction is accelerated by increasing the electron density on the double bond in the alkene, which is the nucleophile, as well as the electron attracting group on the peroxyacid in which the oxygen is considered an electrophile [2]. Scheme 1.5 shows the epoxidation of alkene by peracid.

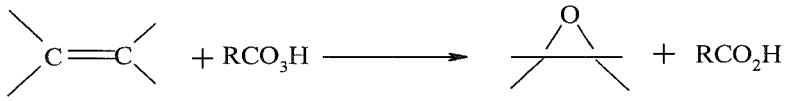

Scheme 1.5

1.2.3. Decomposition of peroxyacid

The thermal decomposition of peroxyacids in aqueous solutions to form the parent acid and oxygen has been extensively investigated. An increase in temperature by about 10°C results in a 2-3-fold increase in decomposition rate. The reactivity of organic peroxides is affected to a high degree by the type of substituents on the carbon atom adjacent to the peroxy bond. An extensive review of peroxy compounds has been carried out by Ando [1].

Peracids are sensitive to decomposition and it has been shown to occur by means of several processes [1].

The addition in Scheme 1.6 relates to the decomposition of peracid in solution. In the absence of any metal ion catalysed decomposition reactions, a second order decomposition with respect to the peracid is observed, whereby the rate is at its highest when the pH of the solution equals the pK_a of the peracid. This is because at the pKa there is equal and relatively maximal amount of both protonated and unprotonated forms of the peracid. The decomposition is accepted as the nucleophilic attack of the anion of the peracid on the protonated form [22, 5]. The protonated form of the peracid exhibits electrophilic behaviour, as shown in Scheme 1.6 below:

$$RCO_3H + RCO_3^- \longrightarrow 2RCO_2^- + H^+ + O_2$$

Scheme 1.6

The autodecomposition of peroxyacid has been shown to proceed in the presence of sequestRants such as sodium and calcium salts of EDTA [2]. The rate law equation is as follows: $v = k [RCO_3H] [RCO_3^-]$.

Two mechanisms for this reaction are postulated, in which the peracid anion can attack either the outer peroxidic oxygen or the carbonyl of the molecular peracid [23].

Peroxyacids can absorb radiation in the ultraviolet region, which results in homolytic cleavage of the O-O bond. Heat also has the same effect [24]. The photolysis of peroxyacid is highly effective and yields radicals at any temperature. For example, irradiation of peroxyacetic acid in cyclohexane produces cyclohexanol in 90% yield [25], and heating this peroxyacid above 80°C leads to O-O homolysis producing radicals [25].

The oxyl radicals derived from the photolysis or thermolysis of a peroxide compound can abstract atomic hydrogen from a wide range of organic substrates to yield an organic radical species [24]. Leffort and colleagues [26] systematically studied the radical decomposition of peracids. Several radicals were formed by the thermolysis of different peroxyacids. These reactions are outlined in the equations below (Scheme 1.7):

$RCO_3H \longrightarrow RCO_2^{\cdot} + HO^{\cdot}$

$RCO_2^{\cdot} \longrightarrow R^{\cdot} + CO_2^{\cdot}$

$R^{\cdot} + HO_2COR \longrightarrow ROH + RCO_2^{\cdot}$

Scheme 1.7

The decarboxylation in the second step is very fast and the reactivity of the radical with the peracid is correlated with the ionisation potential and explained by the polar effect, as shown in Structure 1.1 below:

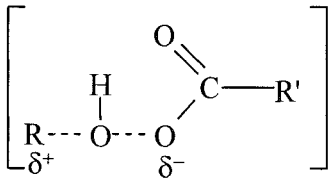

Structure 1.1 (taken from reference 5).

Another route for peracid decomposition is via metal ion interactions. In this case, the decomposition of peracid and organic peroxide in general is catalysed by the presence of a small amount of transition metal ions. The reaction is suppressed by EDTA at high pH[27]. The hydrolysis of peracid gives rise to parent acid and hydrogen peroxide [28].

1.2.4. Acyl transfer

Acyl transfer reactions and their mechanism have been studied for their structure-reactivity relationships. In general, the mechanism by which acyl reactions occur is proposed [29] as either a stepwise mechanism which involves the formation of an intermediate, or a concerted mechanism where bond forming and bond breaking are linked and occur almost instantaneously (see Scheme 1.8).

The acyl transfer happens either through the formation of ionic intermediate acylium ion step (1) - in which the nucleophile is weak and the leaving group is strong and so the attack by the nucleophile occurs after the formation of acylium ion[29] - or an intermediate adduct is formed where the nucleophile is strong and the leaving group is poor (see

Scheme 1.8). The concerted mechanism lies between these two mechanisms, where the bond formation and breaking are coupled [29].

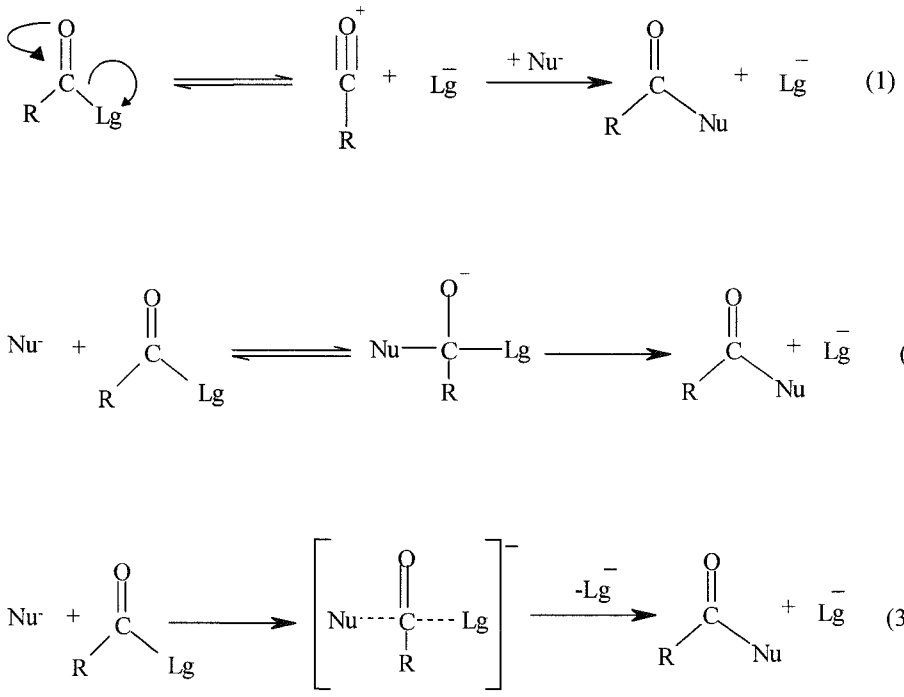

Scheme 1.8: The mechanism routes for acyl transfer reaction (nucleophilic carbonyl addition reactions): (1) elimination-addition mechanism with formation of ion; (2) addition-elimination pathway with the formation of tetrahedral intermediate; (3) concerted mechanism with a single transition state formation.

1.3. Surfactants

1.3.1. Overview

Generally, surfactants (surface active agents) consist of diphilic moieties: one is called hydrophobic (lipophilic or lipid loving) and the other hydrophilic (lipophobic or lipid hating). The structures of ionic surfactants can be represented by RX, where R stands for the hydrocarbon chain containing 8–18 carbon atoms present in an alkyl/aromatic moiety or other kind of hydrophobic residue, and X is an ionic moiety [30, 31]. Depending on the nature of charge on X, the surfactants are classified as anionic and cationic surfactants. For the anionic surfactants, the hydrophilic moiety contains groups that may be sulfate, sulfonate, phosphate or carboxylate. The examples are as follows: $CH_3(CH_2)_nOSO_3^-M^+$, $CH_3(CH_2)_nSO_3^-M^+$, $CH_3(CH_2)_nCO_2^-M^+$ (where M^+ can be Li^+, Na^+, K^+, and $n = 7–17$). In this group, sodium dodecyl sulfate (SDS) $C_{12}H_{25}OSO_3^-Na^+$ is a representative example. For the cation-active surfactants, the hydrophilic moiety is generally a quaternary ammonium, pyridinium or phosphonium group. The examples are as follows: $CH_3(CH_2)nN^+(CH_3)_3X^-$, $CH_3(CH_2)nN^+(C_6H_5)_3X^-$ (where X^- can be Cl^-, Br^-, OH^-, and $n = 7–17$). The representative example is cetyltrimethylammonium bromide (CTAB), $C_{16}H_{33}N^+Me_3Br^-$. The structures of non-ionic surfactants may also be denoted by RX, where X (which is electrically neutral) generally represents a polyoxyethylene residue. Polyoxyethylene (23) dodecanol (Brij-35) is a representative example [32]. The following section describes the surfactant in more detail, emphasising the non-ionic surfactant because this was the type of surfactant used in the present work

1.3.2. General classification of surface active agent

1.3.2.1. Non-ionic surfactant

This is the second largest class of surfactants and they do not have an apparent ionic charge. They generally have polyether or polyhydroxyl as their head group, in addition to a hydrophobic portion which can be a long hydrocarbon chain (an epoxy group). An example of a non-ionic surfactant is Triton X-100, whose structure is shown in Structure 1.2, where n is 9-10. Usually, non-ionic surfactants are polydisperse and an average molecular weight is quoted. The micellar structure consists of a hydrophobic core surrounded by a mantle region comprised of mainly the hydrophilic head groups. Polyoxyethylene chains have been shown to be hydrated [33].

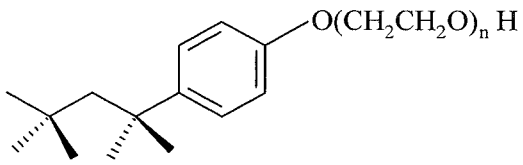

Structure 1.2: Non-ionic surfactant polyethylene glycol tert-octylphenyl (Triton-100).

The preparation of polyoxyethylene surfactants involves adding ethylene oxide to a compound containing a hydrophobic hydrocarbon chain and a reactive hydrogen atom (see Scheme 1.9).

The absence of ions in these micelle systems renders them useful as a detergent, an emulsifier, and allows their structure to be elucidated. The predominant use of non-ionic surfactants is as a food and drink additive, and an ingredient for pharmaceutical and skin care products. There is one major problem with many non-ionic surfactants, namely they are temperature dependent [32]. At higher temperatures, this class of surfactants is less soluble in water and tends to precipitate out of the solvents. As a result, the use of these surfactants is limited by temperature.

Scheme 1.9: Preparation of non-ionic surfactants X can be O, N or any functionality capable of linking the POE (polyoxyethylene) chain to the R group.

1.3.2.1.1. Brij-35

Brij-35 (polyoxyethylene (23) lauryl ether) is a typical non-ionic surfactant which has an n- alkyl poly(oxyethylene) monoether structure with the general formula C_nE_m, where n and m denote the length of the hydrophobic and hydrophilic chains respectively. Using the light scattering photometry Becher [34] has reported, the CMC and the aggregation number of Brij-35 is ca. 0.11g/L and 40 respectively. From geometric constraints, he proposed that Brij-35 can form rod-like micelles assuming that surfactants with a long polyoxyethylene chain would not form spherical micelles. The aggregation number of

Brij-35 micelles has been measured using quasi-elastic light scattering. An increase in temperature results in an increase in aggregation number according to Phillies [35].

The mean aggregation number of a non-ionic micelle depends on concentration and temperature (as stated above, a value of 40 was obtained in reference [34]). Also, value ranges from 37-47 for temperatures of 10-40°C were reported in reference 27; Maire [36] also found a value of 40. However, there is some debate over the type of micelles formed: Becher stated a rod-like micelle, Tanford[37] proposed oblate ellipsoids, and Phillies [35] proposed a spherical two shell model with a hydrophobic core and a hydrated shell. The critical micelle concentration of Brij-35 to form a micelle is in the rang 0.04-0.1 g/L.[38]. Table 1.2 shows a list of CMC and aggregation numbers for series of non-ionic surfactants with a general structural formula C_nE_m where n and m denote the hydrophobic and hydrophilic portions of the non-ionic surfactants.

Table 1.2: Critical micelle concentrations and aggregation numbers for C_nE_m type non-ionic surfactants (data taken from reference 32).

Surfactants	Temperature/°C	N/aggregation number	CMC/ Mol dm^{-3}
C_8E_3	25	-	7.5×10^{-3}
C_8E_5	25	-	9.2×10^{-3}
$C_{10}E_5$	25	-	7.6×10^{-4}
C_8E_6	25	-	9.9×10^{-3}
C_8E_6	18	30	-
C_8E_6	30	41	-
$C_{10}E_6$	35	260	-
$C_{12}E_{18}$	25	51	-
$C_{12}E_{23}$	25	40	-
$C_{16}E_9$	25	219	2.1×10^{-6}
$C_{16}E_{12}$	25	152	2.3×10^{-6}
$C_{16}E_{21}$	25	70	3.9×10^{-6}

1.3.2.2. Anionic surfactants

The most widely used surfactants of this class are alkali or alkaline earth metal salt of the fatty acid and sulphuric, sulfonic and phosphoric acids containing saturated or unsaturated hydrocarbon substitute [39]. Anionic surfactants are also long chain hydrocarbons with a charged polar head group. However, in these surfactants the head group is negatively charged.

The general structure of anionic surfactants is shown in Structure 1.3, where X represents the head group and most often is carboxylates (COO^-), sulfates (SO_4^{-2}), sulfonates (SO_3^-) or phosphates (PO_4^{-3}), and M represents the counter ions. The most commonly used counterions are sodium and potassium because they impart water solubility [32].

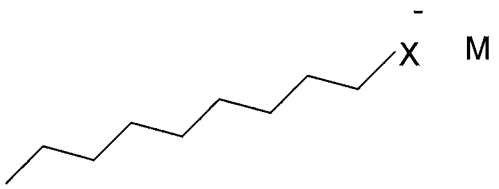

Structure 1.3: The general structure of an anionic surfactant.

One of the most commonly used is sodium dodecyl sulfate (SDS), which consists of a long alkyl chain and a small head group. It is used in low temperature detergents for delicate fabric. The structure of SDS is shown in Structure 1.4 below:

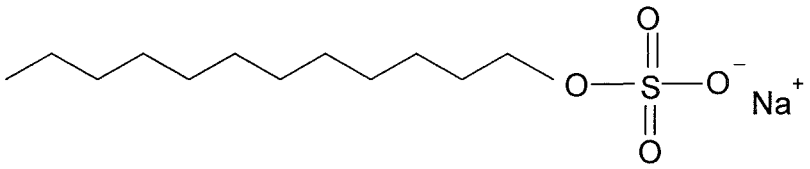

Structure 1.4: Structure of the anionic surfactant sodium dodecyl sulfate (SDS).

The hydrophobic interior of the micelle is surrounded by a region containing mainly head groups. About half of the counter ions are found in a Stern layer along with water. The rest of the counter ions are contained in the Gouy-Chapman portion of the electrical double layer which extends into the aqueous medium [32].

The critical micelle concentration of SDS in water is ca. 8.3×10^{-3} M; above this concentration spherical micelles are formed. At higher concentrations of about 6.5×10^{-2} mol dm^{-3} the micelles become ellipsoidal and the aggregation number increases. Several techniques have been used to confirm this observation [40].

The addition of salt to an anionic surfactant results in a decrease in the critical micelle concentration, as shown in Table 1.3. In addition, the micelles become more elongated and like rods in structure with an increase in aggregation number [41].

Table 1.3: Effect of added electrolyte on the critical micelle concentration of SDS solutions (taken from reference 32).

[NaCl]/mol dm^{-3}	0	0.1	0.2	0.4
CMC/ 10^{-3} mol dm^{-3}	8.2×10^{-3}	1.62×10^{-3}	8.3×10^{-4}	5.2×10^{-4}

1.2.2.3. Cationic surfactants

Cationic surfactants are comprised of a long alkyl hydrocarbon chain with a positively charged polar head group. This type of surfactant has the general form $R_x N^+ Y^-$, where R denotes the hydrophobic group, N^+ is the hydrophilic part of the surfactant (any element capable of forming positive ion), and Y^- is its counter ion.

Most cationic surfactants are long chain amines and their salts, quaternary ammonium salt, pyridinium compounds, or polyoxyethylenated long chain amines. In most cases, the head group is either a quaternary ammonium or phosphonium ion paired with a counter ion such as chloride, bromide, iodide, hydroxide or a carboxylate [30, 42]. Salts of long chain amines were the first cationic surfactants to be synthesised. In strongly acidic medium the amine protonates, resulting in a positively charged head group. However, it is known that at higher pH the amines deprotonate to form an uncharged molecule.

Surfactants of quaternary ammonium salt are the most common and versatile since they are very stable and are not affected by pH, thus maintaining their positive charge in acidic, neutral and alkaline media. A typical cationic surfactant is shown in Structure 1.5 below:

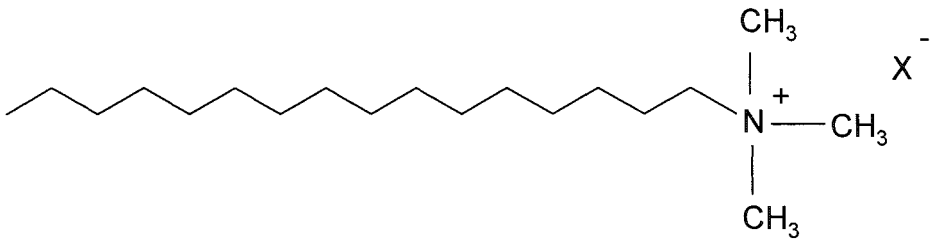

Structure 1.5: Cationic surfactant cetyltrimethylammonium halide $X^- = Br^-, Cl^-$.

In addition to their use as a detergent, a wetting agent and an emulsifier, cationic surfactants have been used as germicides, fungicides, disinfectants, antistatic agents and dispersants in the treatment of fabric to make it water repellent. They have also been used in drug delivery systems and in pharmaceutical formulations.

1.2.2.4. Zwitterionic (amphoteric) surfactants

Zwitterionic surfactants possessing both the cationic and anionic sites in polar head groups are biologically and industrially quite important [42, 32]. The most common amphoterics surfactants are trimethyl glycine $Me_3N^+CH_2COO^-$ (known as betaine); an example of this type of zwitterionic surfactant is lauryl amido propyl dimethyl betaine, shown in Structure 1.6. Other classes of zwitterionic surfactants include the N-alkyl amino propionates with a chemical formula $R\text{-}N^- CH_2CH_2COO^-$ [76].

The charges of zwitterionic surfactants change with pH, and this affects their properties, such as wetting, foaming and detergency. At an isolectric point these surfactants resemble non-ionic surfactants, below this point they shift towards cationic surfactants, while above this point they behave like anionic surfactants. They are widely used in industry and due to their low eye irritation they are used for cosmetics; they can often be found in shampoos, hand soaps, hair conditioners, cleaning lotions and cream [76].

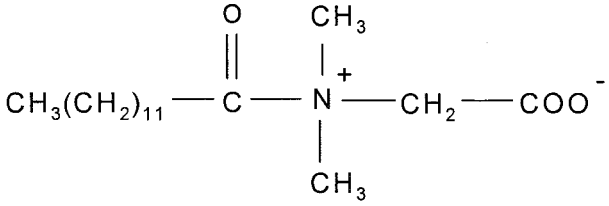

Structure 1.6: Structures of Lauryl amido propyl dimethyl betaine..

1.3.3. Micelles

When surfactants as solutes are introduced into aqueous solution, and due to hydrophobic interaction, the solute particles have a tendency to aggregate spontaneously to form thermodynamically stable bigger particles of colloidal dimension. The hydrophobic effect arises when a non-polar solute is inserted into water and the hydrocarbons have an inability to form a hydrogen bond with the water. The hydrophobic effect can be distinguished from hydrophobic interactions, which result from the association of two non-polar moieties in water [43].

It is believed that when small hydrophilic solute molecules are inserted into water, the solvent will dissolve it due to the fact that solvation energy is equal or larger than the energy needed to create a cavity in the solvent for that solute. In the case of a surfactant whose hydrophobic group becomes large, it starts to aggregate because it is energetically easier to form a large cavity than a smaller one for each molecule [43, 44].

Tanford [43] has stated that the attraction of non-polar groups (such as hydrocarbon chains) to each other plays only a minor role in the hydrophobic effect, but this force arises primarily from the strong attraction force between water molecules. The hydrophobic effect is typically attributed to the ordering of water molecules around an unassociated hydrophobic molecule. At the interface between hydrocarbon and water, water has a higher energy state because hydrogen bonds are lost. This effect leads to a decrease in the entropy; the entropy loss can be offset when the association of hydrophobic molecules into micelles occurs because this leads to an increase in entropy as the 'structured water' structure is broken up. Dill [45] has argued that the hydrophobic effect is more subtle and depends on solute size as well as shape.

Different factors control the supramolecular structure of the self-assembly of the surfactant molecules [31, 32]. At low concentrations, the surfactant molecules behave just like ordinary solutes, and ionic ones behave like an electrolyte, but after reaching a certain concentration they aggregate (the aggregation number denoted by N may vary from 20 to 100 depending on the conditions) to form micelles. This smallest concentration at which micellization starts is called the critical micelle concentration (CMC). The driving force which leads to aggregation of surfactant molecules is the hydrophobic interaction among the hydrocarbon chains [43]. Growth of micelles leading to separation of the surfactant as a macrophase is prohibited by hydration of the hydrophilic moiety, electrostatic repulsion among the micellar head groups of the approaching

micelles (in the case of ionic reactants), steric factors, and entropy losses. Therefore, the micelles do not come together to create a continuous phase, but are rather homogeneously distributed in the aqueous medium to generate a micellar pseudo-phase [30].

The strength of the head group repulsion depends on the nature of the surfactant. With non-ionic surfactants the head group repulsion is mainly the result of steric hindrance, and with ionic surfactants the repulsion is due to an electrostatic character. The electrostatic repulsion between head groups can be reduced with the addition of an electrolyte, which can screen the electrostatic repulsion [32].

Micelles are in dynamic equilibrium with their monomer surfactants, and the micelles themselves are constantly disintegrating and reforming. Two relaxation processes are related to this equilibrium: a fast one in a microsecond time scale (the residence time of an individual surfactant molecule in a micelle), or in other words associated with the quick exchange of individual monomers between the micelles and the bulk aqueous phase; and a slower one in a millisecond time scale (10^{-3} - 10^{-1} seconds), associated with the complete dissolution of the micelles into monomers, which is called the lifetime of a micelle [46].

As the inter-conversion between the micelles and surfactant solute molecules is a reversible process that occurs in a few milliseconds, it is possible to destroy the micelles to produce the original simple solution of surfactants by simple dilution (provided the concentration of the surfactant falls below the critical micelle concentration). Hoffmann [47] has stated that factors that lower the cmc usually increase the lifetime of the micelle, as well as the residence time of surfactant molecules in the micelle.

Aqueous micelles have different forms (e.g. spherical, rod-like, etc.) [39, 32], but all have a common property: the hydrophilic groups projected outward in contact with the bulk solvent water and the hydrocarbon ends directed towards the interior side produce a hydrophobic core. This is why aqueous micelles can be simply described as oil in water (o/w: oil represents the non-polar hydrophobic core). The ionic head groups of ionic surfactants and some of the counter ions form the Stern layer, in which 60–70% of the micellar charge is neutralised; the remaining counterions form a diffuse Gouy-Chapman layer [34]. Thus, to neutralise the charge of the micellar head groups, the counter ions are attracted to form electrical double layers. The hydrophobic core of the aqueous micelle

is very similar to a liquid hydrocarbon. Thus, the hydrophobic core of a micelle is suitable to extract the non-polar and hydrophobic substrates from an aqueous phase.

From a detailed structure of a micelle showing the three main regions [37] it is clear that the inner region of the hydrophobic core consists primarily of the hydrocarbon tail of the surfactant, and so it is non-polar. This region is surrounded by the Stern layer which consists of the polar head group as well as a few of the counter ions, and therefore it is a polar region. The outermost region of the micelle is referred to as the Gouy-Chapman double layer and consists of the majority of counter ions and some water [32]. The water molecules may be entrapped by the micelle and the amount of water in the micelle core varies from one surfactant to another [44].

A simplified model of ionic micelles is shown in Figure 1.3 below:

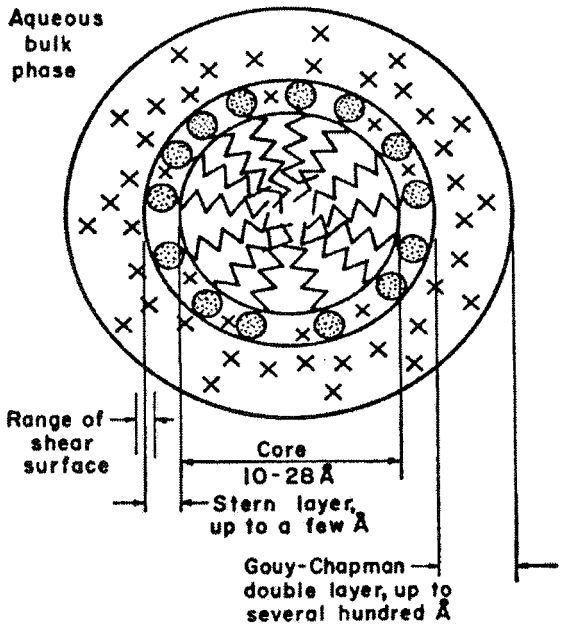

Figure 1.3: Schematic presentation of ionic micelle (taken reference [39]).

In addition to a normal micelle, an inverted or reverse micelle can be formed. When surfactants are present in non polar solvents the reverse micelle is formed (water in oil, w/o) [48]. If reverse micelles are produced in non-polar hydrocarbon solvents, the hydrophobic hydrocarbon portion of the surfactant forms the outer layer in contact with the non-polar solvent, while the hydrophilic groups of the surfactant remains projected towards the interior containing the water. The properties of reverse micelles largely

depend on the ratio $w_0 = [H_2O] / [surfactant]$ [49]. Reverse micelles formed by sodium bis(2-ethylhexyl)sulfosuccinate), which is abbreviated as AOT, are well recognized [49] (see Structure 1.7). The structure of water confined within the core is drastically affected because of the charged interior surface. In the water pool (which is spherical in shape) of the reverse micelles, the hydrophilic reactants are stabilized. In the small aqueous compartment, the solubilised polar substrates are more firmly bound than the substrates in aqueous media. Thus, the reverse micelles can strongly influence different types of chemical reactions, including enzymatic reactions [50].

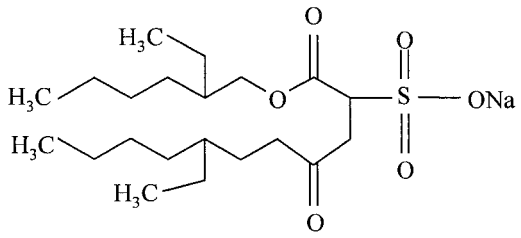

Structure 1.7: sodium bis (2-ethylhexyl) sulfosuccinate) AOT.

1.3.4. Micelle association number and critical micelle concentration

Micelle formation, or micellization, is an important parameter due to a number of important interfacial phenomena, such as detergency and solubilisation which depend on the existence of micelles in solution. Furthermore, micelles have become a subject of great interest in organic chemistry and biochemistry because of their unusual catalysis of organic reactions and their similarity to biological membranes and globular proteins [32, 39].

As mentioned previously, the driving force behind micellization is hydrophobic force. The strong interaction between water molecules repels the hydrocarbon chain out of the water bulk phase. This drives the surfactants to form aggregates whereby the hydrocarbon chains are concealed by hydrophilic head groups [43]. Micelle formation is therefore more likely to take place at lower concentrations for surfactants with long chains than surfactants with short chains. A rule of thumb is that for each added methylene group the CMC decreases by a factor of 2 for an ionic surfactant and by a factor of 3 for a non-ionic surfactant[32]. Every surfactant has a definite CMC at a given temperature. The shorter the hydrocarbon chain, the smaller the decrease in free energy of the micellization process, and consequently the higher the CMC. However, the cmc of a particular surfactant is dependent on the chemical composition of the solution in which

the micellization is carried out [30]. For ionic surfactants, the factors that reduce electrostatic repulsion among hydrophilic moieties (micellar head groups) favour micelle formation. The counter ions, being oppositely charged, are attracted by micellar head groups and the charge is neutralised. Thus, an increase in the concentration of counter ions reduces cmc values [31].

For non-ionic surfactants, micellization is favoured by a rise in temperature, which disfavours the hydration of their hydrophilic groups. In general, micellization occurs in a narrow range of surfactant concentrations, around the CMC at which there is a sharp change in several properties of a solution (e.g. viscosity, electrical conductivity, surface tension, light scattering), which indicates the formation of micelles [30]. Figure 1.4 shows physical properties plotted against surfactant concentrations. A break in the line for a particular property represents the critical micellar concentration.

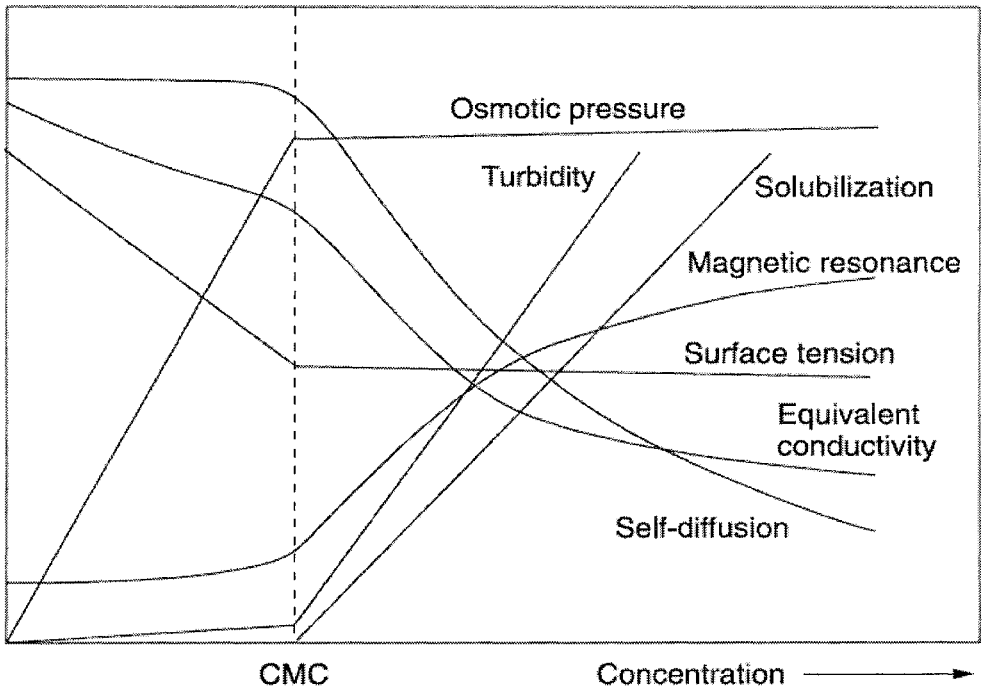

Figure 1.4: changes in the concentration dependence of a wide range of physic-chemical change around the critical micelle concentration, CMC, (taken from reference 51).

The cmc also depends on the head group of the surfactant. In general, ionic surfactants have a much higher cmc compared to non-ionic surfactants. In the micellization process of ionic surfactants, the counter ion of the surfactant will seek out the bulk phase due to the entropy gain of this process. However, in the absence of added electrolyte, about 80% of surfactant counter ions are bound to the micelle and around 20% are free in

solution. Therefore, micelle forms at high CMC due to electrostatic repulsion. When salt is added to the solution, the ionic surfactant head group will be screened out by the salt counter ions; thus, the micelle formation is favoured at low CMC. The cmc of an ionic surfactant is higher than the cmc of a non-ionic surfactant with corresponding chain length [32].

Aggregation numbers of micelles are an important quantity and determine the size of micelles, which are dependent on the length of the hydrocarbon chain as well as the concentration of the surfactant[32]. Many techniques have been used to calculate aggregation numbers, including NMR and light scattering [52]. Based on the geometric aspect of the micelle, the aggregation number tends to increase rapidly with an increase in the length of the hydrophobic group of the surfactant molecule, and decreases with an increase in the cross sectional area of the hydrophilic head group [32]. Adding salt to an ionic surfactant solution has the effect of drawing ions away from the surface of the micelle, resulting in a decrease of the repulsive interactions of the head group. This is known as the electrostatic screening effect. Lowering the head group repulsions also lowers the CMC. Since less energy is needed to overcome this repulsion force, it becomes more favourable to form micelles at a lower CMC. Also, because the head group can fit closer together, association numbers will increase [32, 39]. Aggregation numbers do depend on ionic strength, and the aggregation number for sodium dodecyl sulfate increases from 95 to 117 to 132 as the NaCl concentration is elevated from 0.00 to 0.10 to 0.40 M [53].

Mohamed Benrraou [54] has studied the effect of counter ions on the properties of anionic surfactants (CMC and aggregation number of micelles) tetramethyl-, tetraethyl-, tetrapropyl- and tetrabutylammonium dodecyl sulfate, which can be abbreviated as TMADS, TEADS, TPADS, and TBADS respectively. He has observed unusual behaviour in that both the aggregation number and the CMC tend to decrease as the radius of the counter ion increases; whereas it is usually observed that the aggregation number decreases as the cmc increases. He proposes that the counter ion TAA^+ 'tetraalkylammonium ions' is so large that steric hindrance impedes the binding to the micelle and causes the aggregation number to decrease.

1.3.5. Factors affecting the micelle formation

1.3.5.1. The hydrophobic group

In aqueous medium, the CMC decreases linearly with an increase in the carbon number in the alkyl chain length of the hydrophobic portion of the surfactants. When the hydrophobic group is branched, the carbon atoms on the branches appear to have about one-half the effect of carbon atoms on a straight chain [32].

1.3.5.2. The hydrophilic group

In aqueous medium, ionic surfactants have much higher CMC than non-ionic surfactants containing equal hydrophobic groups. For the usual type of polyoxyethylene (in which the hydrophobic group is a hydrocarbon residue), the CMC in aqueous medium increases with an increment in the number of oxyethylene units in the polyoxyethylene chain. Due to the fact that commercial polyoxyethylene (POE) non-ionics are mixtures containing POE chains with different numbers of oxyethylene units, which are clustered about a certain mean value, CMC is slightly less than for those of the single species containing the same hydrophobic group and with oxyethylene content corresponding to that particular mean value. This is probably because the component with low oxyethylene content in the commercial material reduces the CMC more than it is raised by those with high oxyethylene content [55].

1.3.5.3. The effect of temperature

The effect of temperature on the CMC is usually moderate. However, the solubility of the surfactant decreases with decreasing temperature, and if the solubility is below the cmc then the compound will precipitate as solid crystals. The temperature at which this occurs is known as the Krafft temperature [32].

The effect of temperature on the CMC of surfactants in aqueous medium is complex [32]. Rosen [32] points out that the value appears first to decrease with the temperature to a minimum and then increases with a further increase in temperature. An increase in temperature causes a reduction of the hydration of the hydrophilic group, which favours micellization. However, a temperature increase also causes disruption of the structured water surrounding the hydrophobic group, an effect which does not favour micellization. Consequently, the relative magnitude of these two rival effects determines whether the

cmc increases or decreases over a particular temperature range. From the data available in literature, the minimum CMC temperature curve appears to be around 25 °C for ionic surfactants [56] and around 50 °C for non-ionic surfactants [55]. However, for some surfactants an increase in CMC value with an increase in temperature can be observed, in striking contrast to the usual behaviour of non-ionic surfactants which show a gradual trend of decreasing CMC with an increase in temperature. The CMC values of both ethylene glycol mono n-dodecyl ether (EGDE) and ethylene glycol mono n-tetradecyl ether (EGTE) increase with an increase in temperature [57], and no explanation has been given for this.

1.3.5.4. Salts effect

Adding electrolyte to an aqueous solution of surfactant usually decreases the CMC of ionic surfactants, but such an effect is less pronounced when the surfactant is non-ionic. Salts tend to screen electrostatic repulsions between head groups and make the surfactant effectively more hydrophobic. This increases hydrophobic interactions among the surfactants which cause them to aggregate at lower concentration; thus the CMC is decreased [32]. Pandite [58] has shown that the effect of electrolyte decreasing the CMC of a high molecular weight non-ionic of the POE polyoxypropylene type follows the order $Na_3PO_4 > Na_2SO_4 > NaCl$, while NaSCN leads to an increase in the CMC due to its affect on water structure.

1.3.6. Cloud point

The higher solubility of the polyoxyethylene chains is due to the hydrogen bonding between the solvent and the ether oxygen atoms in the head group. As this bonding is sensitive to temperature, there will be a temperature at which the amount of hydrogen bond will be minimised, resulting in phase separation. This temperature is called the cloud point [60].

Polyoxyethylene non-ionic surfactants exhibit an interesting feature above a certain temperature called the cloud point, whereby separation takes place. One phase is micellar rich and the other is a micellar free phase. This phenomenon occurs above the CMC. Salts have a significant effect on the cloud point temperature of such a surfactant. Doscher and colleagues [59] have measured the turbidity of Triton-100 as a function of added salts, finding that some salts, like sodium chloridel, salt out the surfactant and

decrease the temperature of the cloud point, while the salting in effect of such salts as calcium chloride increases the temperature at which the phase separation occurs. Other investigations of the salt effect on temperature (reference 60, for example) have measured the salting out effect of univalent and multivalent salt on TX-100. The results have shown there is a good correlation between the cloud point temperature and the ionic strength of the added salts.

Many researchers ([61, 62, 63, 64]) have studied the effect of the number of inorganic salts on a solution of polyoxyethylene non-ionic surfactant. Their findings show that salts like potassium thiocyanate, urea and sodium iodide, salt in the surfactant as a result of their effect on the structure of water, in which they break the water structure and thus increase the number of available water molecules for hydrogen bonding with the ether oxygen of the polyoxyethylene head group. This leads to their hydration and consequently results in an increase in the cloud point temperature. Other salts, such as sodium sulfate, have been observed to salt out the surfactants as a result of the dehydradation of the polyoxyethylene head groups [61].

Schott[61,62] discussed the salt effect very extensively and attributed the salting out effect to the dehydration of the polyoxyethylene head group, which is due to the competition for water between the hydrated salt ions. Salting in, on the other hand, occurs because of increased hydration of the head group due to destruction of the water structure by the large polarizable anion, or by complexing of the salt cations with the ether oxygen of the polyoxyethylene head group[65].

Paresh [66] has shown that the salting out effect, lowering the cloud point temperature, is more effective for sodium sulfate than the salting out of sodium fluoride, sodium chloride, and sodium bromide, and attributes it to the higher charge on the sulphate ion, which plays a more major role in the salting out process than ion-solvent interaction does.

The addition of salts to a non-ionic surfactant solution does change the temperature at which the cloud point occurs. Sharma [67] has investigated the effect of various electrolytes and non-electrolytes on the cloud point of non-ionic surfactants of the type $C_{12}E_{10}$. $C_{12}E_9$ and $C_{12}E_6$. The results show that thiocyanate causes the cloud point temperature to increase as it enhances the hydrogen bonding by its effect on water structure, as described above. On the other hand, salts like sodium chloride and potassium chloride decrease the cloud point. For non-electrolytes (studied by Sharma [67])

tetra butyl ammonium iodide (TBAI) and tetra methyl ammonium bromide (TMAB), the cloud point is increased in the presence of the former compound and decreased in the presence of the latter. TMAB is a water structure former which decreases the availability of non-associated water molecules to hydrate the ether oxygen of the POE chain[32], thus lowering the cloud point.

1.3.7. Structure packing parameters of surfactant

Early studies [68] have shown that lamellar micelles are formed where ionic single alkyl chain compounds dissolve in the aqueous phase. Also, Menger [69] has described the micelle as a spherical aggregate in which an alkyl group forms a hydrocarbon liquid-like core and its polar head groups from a charged surface. After that, micelles of very different shapes were encountered. The different geometries were found to depend mainly on the structure of the surfactant, as well as environmental conditions (for example, concentration, temperature, pH and electrolyte content, as mentioned above).

In the process of micelle formation, molecular geometry plays an important role and it is essential to understand how surfactants are packed. The main structures encountered are spherical micelles, bilayers, vesicles or inverted micelles. As described previously, two opposing forces control the self-association process: firstly hydrocarbon-water interaction that favours aggregation (i.e. pulling surfactant molecules out of the bulk phase), and secondly head group interaction that works in the opposite way. The first term can be considered an attractive interfacial tension and the second, repulsion due to the nature of the head group [32].

To understand which parameters determine the aggregate structure in aqueous bulk solution and the change of surfactant micellar structure from spherical, through rod-like structure to bilayers or vesicle, Ninham and Mitchell [70] and Israelachvili [71] have established packing parameters based on molecular geometry. The key parameters are the minimum interfacial area occupied by the head group a_O, the volume of the hydrophobic tail (v), and the maximum extended chain length of the tail in the micelle core (L_c) (see Equation 1.1).

$$cpp = \frac{v}{L_c\ a_O} \qquad 1.1$$

Where CPP are critical packing parameters.

For spherical micelles, L_c are assumed to be equal or less than the micelle core radius R_{mic}. For such shapes with N surfactants, the aggregation number N is to the ratio between the micellar core volume $V_{mic}$and the volume of one chain see Equation 1.2

$$N = \frac{V_{mic}}{v} = \frac{(4/3)\pi R_{mic}^3}{v} \qquad 1.2$$

Also, the aggregation number N is equal to the ratio of the area of a micelle A_{mic}, to the cross sectional area.

$$N = \frac{A_{mic}}{a_0} = \frac{4\pi R_{mic}^2}{a_0} \qquad 1.3$$

Equating Equation 1.2 and 1.3 leads to Equation 1.4

$$1/3 = \frac{V}{a_o R_{mic}} \qquad 1.4$$

And since Lc can not exceed R_{mic} for a spherical micelle Equation 1.4 become.

$$\frac{1}{3} \geq \frac{v}{a_o l_c} \qquad 1.5$$

Ionic surfactants have a large head group area due to the repulsion between equally charged groups, and typically have CPP values of 1/3 or lower, meaning that they form spherical micelles. If an ionic surfactant has two chains, the CPP increases with the increasing volume of the hydrocarbon tail. Such surfactants will form rod-shaped micelles or lamellar sheets (e.g. phospholipids in organic cell membranes [72]). Surfactants that form spherical micelles at low concentrations may form rod-like micelles at higher concentrations. Surfactants with a small head group area, such as fatty alcohols and fatty acids, will typically have high CPP values [76].

1.3.8. Thermodynamics of micelle formation

When surfactant molecules adsorb at an interface they provide an expanding force and cause the interfacial tension to decrease (at least up to the CMC). This is illustrated by the general Gibbs adsorption equation, from which the surface excess concentration of a surfactant in a monolayer and the area per adsorbed molecule can be calculated. Numerous examples are given by Rosen [32]. The micelle formation thermodynamics are based on the Gibbs equation $\Delta G = \Delta H - T\Delta S$. The process of micelle formation at room temperature is assumed to be characterised by small positive values of enthalpy, and high positive values of entropy, which is considered to be the main driving force for the process. This high positive value of ΔS is in contrast to the aggregation process in which the system become more ordered as one single entity (micelle) is formed from many monomers, and should result in negative contribution to entropy as the formation of micelle leads to order of surfactant monomer. Also, ΔH should be larger since hydrocarbon groups have very little solubility in water and hence a high enthalpy of solution.

The larger entropy increase of micellization in aqueous medium has been explained in two ways. The first is based on the structure of water during the formation of micelle, and as the hydrophobic residues aggregate the highly structured water around each chain collapses back to bulk water, which accounts for the large gain in entropy of micellization. The second factor is the increased movement of hydrocarbon chains in the non-polar interior of the micelle compared to the aqueous phase [73, 43].

The surface tension of a aqueous solution shows little change when the concentration of surfactant exceeds the CMC. This well-known behaviour suggests that micelles can be approximated as a phase since the chemical potential is kept nearly constant, irrespective of the amount of the material [74].

There are two models which are used to describe the micelle formation: one is called the mass action model in which the micelle and monomers are in equilibrium, and the other is the phase separation model in which the micelle is considered to constitute a new phase in the system at and above the cmc. These two models are well documented in literature and have been explained by Engberts [75].

The process of micelle formation can be described as equilibrium between surfactant monomer and micelles, which in the case of non-ionic surfactants can be expressed by Equation 1.6 below:

$$nS \underset{}{\overset{K_m}{\rightleftharpoons}} S_n \qquad 1.6$$

Where n is the number of molecules of surfactants S, associating with micelle S_n, and equilibrium between micelle and monomers is assumed with corresponding equilibrium constant K_m:

$$K_m = \frac{[S_n]}{[S]^n} \qquad 1.7$$

The brackets indicate the concentration and n, the number of monomers in the micelle, aggregation number.

From Equation 1.7, the standard free energy of micellization per mole of micelle is given by:

$$\Delta G_m^o = -RT \ln K_m = -RT \ln S_n + nRT \ln S \qquad 1.8$$

The standard free energy change per mole of monomer can be obtained by dividing the Equation 1.8 by n (aggregation number) which is assumed to be about 100 times larger for many micellar systems. It is also assumed that S is approximately equal to S_n at the CMC. Thus, the first term in the right hand of the equation can be ignored and the free energy of micellization per mole of surfactant becomes as shown in Equation 1.9, assuming S is approximately equal to S_n at the cmc [30, 76].

$$\Delta G_m^o = RT \ln CMC \qquad 1.9$$

1.3.9. Solubilisation by surfactants

Solubilisation is usually defined as the process of incorporating an insoluble substance (which is usually referred to as the substrate or solubilisate) into surfactant micelles (which are termed the solubiliser) [76]. The solubilisation process involves the transfer of co-solute from a pure state, either crystalline solid or liquid, to micelle [77]. The co-solute can either be non-polar or polar.

The most important characteristics of micelles are their ability to solubilise a wide variety of organic solutes and take up all kinds of substance. Hydrophobic and electrostatic interaction is generally the main factor affecting the binding of substances to micelles. Dynamically, solubilisation is similar to that which is observed for the entrance

and exit of surfactant monomer molecules and their uptake is like diffusion control [78]. Solubilisation is dealt with by the pseudophase model, in which the bulk aqueous phase is regarded as one phase and the micellar pseudophase another. This can permit the affinity of the solubilised compound for the micelle to be quantified by the partition coefficient, which is defined as the ratio of the concentration of the solubilisate in the micellar pseudophase and the aqueous phase [31].

Micelles possess a complete range of solublisation environments, ranging from the non-polar hydrophobic core of the micelle to the relatively polar micelle-water interface. This different polarity of the micelle plays an important role in determining the nature and relative magnitude of the factors that contribute to solubilisation; thus, solute of a different structural type might solubilise in distinct regions within the micelle. On the other hand, solutes with a similar structure and differing hydrophobicities might also solubilise in different locations of the micelle. Saturated hydrocarbons (cyclohexane) show a preference for the interior of the micelle, while benzene and toluene are adsorbed in small quantities into the micelle surface. However, with additive concentrations they have been found in the micellar core (micellar sodium octylsulfate) [79]. Solubilisates that possess hydrophilic substituents, such as alcohol or amines, prefer the surface of the micelle in which the hydrophilic groups can remain largely hydrated [80]. In the case of a solublisate that is amphiphilic itself, the apolar parts will be directed towards the interior of the micelle and the polar ones to the hydrophilic part of the micelle itself. Many studies have focused on the position of aromatic hydrocarbon. Investigations have focused on the distribution of benzene in aqueous solutions of cetyltrimethylammonium bromide and sodium dodecylsulphate. Some authors have claimed that this compound stays mainly in the interior of micelles [81, 82], while others have stated that these solubilisates residue at the interface [83] or in both regions simultaneously [84].

These different findings can be attributed to the concentration of the solubilised benzene. At a low concentration these compounds reside at the outer region of the micelle, but at a high concentration and when the interfacial region is saturated, solubilisates penetrate deeper into the micelle with concomitant swelling of the micelle [80, 85]. Mukerjee [86] has stated that from a molecular point of view, the preference of benzene for the micelle-water interface can be attributed to the ability of the pi-electron system to accept hydrogen bonds.

The high Laplace pressure of small aggregates has been frequently cited [87] as the cause of the high pressure in the interior of the small aggregate to repel out the solublisate, which

can then bind to the interface. However, Marqusee and Dill have pointed out that the Laplace pressure can not be the dominant factor, because worm-like and spherical micelles show comparable solubilisation behaviour. However, worm-like micelles have small Laplace pressure [88].

Micelles are known to have an anisotropic water distribution inside their structure. In other words, the water concentration decreases from the surface in the direction of the core of the micelle. As a result, the spatial position of a solubilised substance in a micelle will depend on its polarity: non-polar molecules will be solubilised in the micellar core, and substances with intermediate polarity will be distributed along the surfactant molecules in certain intermediate positions [89].

With regard to the solubility of a weakly soluble molecule as a function of the concentration of surfactant, the solubility is very small at surfactant concentration below cmc, and as surfactant concentration reaches the CMC and above the CMC the solubility increases linearly with the concentration of the surfactant, indicating that solubilisation is related to micellization [89].

The site of incorporation of a solubilisate is closely related to its chemical nature. The factor controlling the solubilisation process and the possible locations in the micelle have been reviewed [90, 91]. The possible location of incorporation of this solublisate in the micelle is as follows (from Rosen [32]):

1 On the surface of the micelle at the micelle-solvent interface.
2 Between the hydrophilic head groups, for example in the polyoxyethylene shell of the micelle of non-ionic surfactants.
3 In the palisade layer of the micelle between the hydrophilic groups and the first few carbon atoms of the hydrophobic groups which comprise the micelle outer core.
4 More deeply in the palisade layer.
5 In the inner core of the micelle.

These possible sites are illustrated in Figure1.4.

According to the model of Menger [69], for the micellar structure the solublisation can take place in three regions of the micelle: the hydrophobic core, the hydrate micellar grooves, and the bulk aqueous phase. A more important consideration is the localization of the reacting species in the relatively small volume of the micelles compared to the bulk

solution which leads to a great rise in the effective concentration; the observed rate increases for this reason [69].

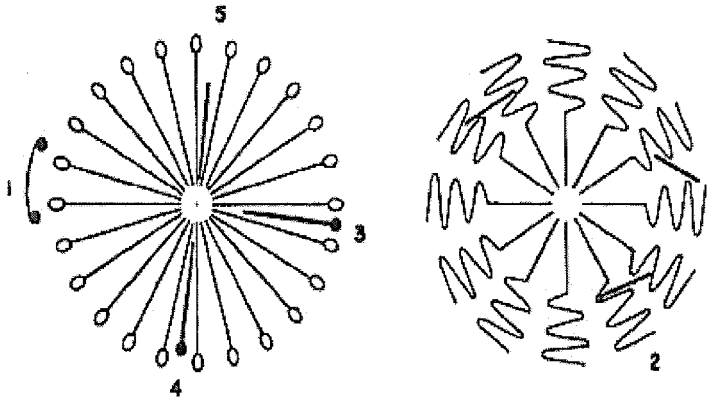

Figure1.5: Locus of solublisation of material in surfactant micelles (taken from Rosen [32]).

As stated above, the micelle offers several binding sites for relatively apolar molecules. These include the hydrophobic core and hydrophobic binding sites located in the Stern region. The latter region is particularly flexible in binding molecules as it contains the highly hydrophilic surfactant head groups and hydrophobic domains, in part due to backfolding of the surfactant tails, as well as water molecules [92].

A number of techniques are suitable for the study of binding locations inside micelles. These methods include aromatic ring current effects, which induce changes of NMR chemical shifts [93] fluorescence probing experiments[78]. From the results of various studies applying the techniques mentioned above (among others), it is commonly assumed that polar molecules preferably bind to micelles in the Stern region [69]. Moreover, it is also usually assumed that, up to a critical concentration, aromatic molecules also bind in the Stern region [94]. However, for benzene the binding depends on the surfactant structure, with the preference for binding in the Stern region being higher for trimethylammonium head groups (DTAB and CTAB) than for sulfate head groups (SDS) [95].

In general, non-polar molecules are usually attracted to the relatively hydrophobic inner core of micelles, whereas ionic reactants and products are either associated with the Stern and Gouy-Chapman layers or repelled from the micelles, depending on the sign of electrostatic interaction [92].

Non-ionic surfactants are often used because of their lower critical micelle concentration compared to ionic surfactants, their higher degree of surface-tension reduction, and their relatively constant properties in the presence of salt, which result in better performance and lower concentration requirements. In particular, the non-ionic ethoxylate surfactants have been suggested for the removal of organic contaminants from soil because of their high solubilisation capacity and biodegradability.

Recently, the effect of non-ionic surfactant type nonylphenyl ethoxylate with a different ethylene oxide group was used to remove the naphthalene from sand [96].

1.3.10. Micellar kinetic models

1.3.10.1. Assumptions made about models and their origin

Menger and Portony developed the basic kinetics equation for the inhibition in micelle of ester saponification [97]. There are numbers of assumptions stated for the treatment of the kinetic data, which include.

i. The concentration of monomers in aqueous solution is equal to the CMC and considered constant.
ii. Below the CMC the substrate reacts at a rate similar to its concentration in water; the rate is k_w.
iii. Above the cmc the binding of the substrate is increased by increasing the concentration of the surfactant; the rate in the micelle is k_m.
iv. The concentration of the surfactant is always higher than that for the substrate and the catalytic properties of the micelle are not altered by binding of the substrate. In addition, change in the aggregation number of the micelle structure does not affect the reactivity of the reactants in the micelle.

The homogeneity of the micellar environment was considered and by experimental evidence the micellar reaction/solubilisation environment was found not to be completely homogeneous in terms of polarity/dielectric constant, water concentration, water structure, viscosity, and ionic strength (for ionic micelles only). However, these properties change gradually in going from the exterior to the deep core of the micelle [98].

It has been recognised that there is resemblance between an enzyme catalysed reaction and a micellar catalysed reaction. The effect of micellar has also received a considerable amount of attention by researchers [99, 39]. Similar to an enzyme catalysed reaction, where

the catalyst binds the substrate and effects the reaction, the micelle can cooperatively take the substrate and also affect the reaction. In addition, reaction in micelles can be regarded a model for enzyme-catalysed reactions in a biological system [39] since like an enzyme, it has a non-polar region which is the core, shielded by the hydrophilic head group from the water. However, while micellar and enzymic catalysis have similar characteristics, but no micellar system has the specificity and catalytic advantage of an enzyme [39].

Catalysis by micelles involves at least three main steps: (i) binding of the substrate(s) to the micelle; (ii) the actual chemical transformation in the micelle (usually at the micellar surface); and (iii) release of products. In the case of nonfunctionalized surfactant micelles, the actual micellar rate effect is caused by a composite of noncovalent interactions between the micelle on the one hand and the reactants and activated complex on the other.

Micellar systems have been considered a simple model of biological membrances [39]. It can therefore be said that the study of chemical reaction in the presence of micelles may be better than studying it in the presence of water in order to draw a conclusion about the stability and rate of reaction in a biological system, such as the rate of sugar consumption by the body. Based on this view, the present study is designed to assess the influence of various surfactants on the rate of chemical reaction and their effect on substrate activity.

Surfactant aggregates often accelerate chemical reactions; however, they also inhibit reactions. The term 'micellar catalysis' was first applied to describe increases in rates of chemical reactions produced by aqueous association colloids, especially micelles [31]. Surfactant micelles can enhance sensitivity and can bring about changes in solubility, pK_a, chemical equilibria, reaction rates and mechanisms [31].

Surfactants have been used for changing the kinetics of reactions, and various kinetic models have been developed to describe the micellar effect on chemical reactions. Kinetic treatments have been developed and most of them are for reactions in the presence of aqueous micelles. These models have been proposed to treat the kinetic data obtained experimentally. The next section discusses some of them.

1.3.10.2. Berezin's model

Kinetic treatments have been developed most extensively for reactions in the presence of aqueous micelles. In the pseudo-phase kinetic model proposed by Berezin [31] reactions are assumed to take place in the bulk aqueous and micellar pseudo-phases. The micellised surfactant is in equilibrium with solutes throughout the reaction, and observed rates can be treated as the sum of rates of concurrent reactions in each pseudophase. A large amount of kinetic data has been explained successfully by the pseudo-phase model [100]. However, the model fails to describe some of the kinetic data obtained in the presence of charged micelles and it is unsuitable for accounting for electrolyte effects on the rates of micelle catalysed reactions [100].

According to the Berezin approach [31], a solution above the critical micelle concentration (cmc) can be regarded as a two-phase system, made up of an aqueous phase and a micellar pseudo-phase. The reactants A and B may be distributed as shown in Scheme 1.10. In the pseudo-phase kinetic model proposed by Berezin [31], reactions occur in both the phases mentioned above. The micellised surfactant is in equilibrium with reactants throughout the reaction, and observed rates can be treated as the sum of rates of concurrent reactions in each pseudophase.

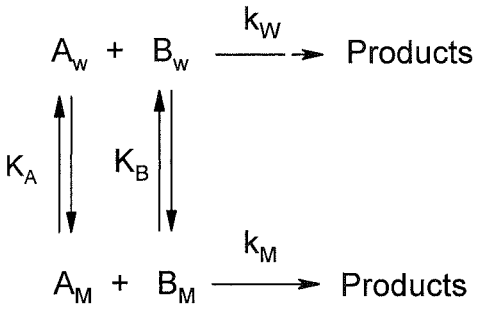

Scheme 1.10

A quantitative rate expression for a bimolecular reaction Scheme1.10 which occurs only in the aqueous k_W and micellar k_M phase for the reactants A and B, is given in Equation 1.10 below:

$$k = \frac{\{k_M P_A P_B CV + k_W(1-CV)\}}{\{1+(P_A-1)CV\}\{1+(P_B-1)CV\}} \qquad 1.10$$

Here, k is the observed second-order rate constant in the aqueous micellar system, C is the total surfactant concentration in molarity minus cmc, $C = [D]_T - CMC$, V is the partial molar volume of the surfactant in the micelle, CV and (1−CV) stand for the fractions by

volume of the micellar phase and aqueous phase respectively, and k_M and k_W are the rate constants for the reaction occurring in the micellar phase and aqueous phase respectively. The relation between binding constants (K) of species is related to their partition coefficients P as $K_A = (P_A - 1)$ CV and $K_B = (P_B - 1)$ CV. For dilute surfactant solutions, where the volume fraction of the micellar phase is small (i.e. 1 - $CV \approx 1$), Equation 1.10 reduces to Equation 1.11.

$$k = \frac{k_M P_A P_B CV + k_W}{(1+K_A C)(1+K_B C)} \qquad 1.11$$

However, this model fails to explain some of the kinetic data obtained in the presence of charged micelles and it is inappropriate for accounting for electrolyte effects on the rates of micelle-catalysed reactions [100].

1.3.10.3. Menger–Portnoy model

The Menger–Portnoy model [97] considers the partitioning of just one reactant; for example, it considers A between the micellar and aqueous phase (Scheme 1.11).

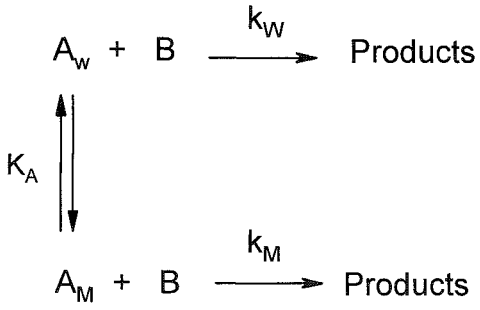

Scheme 1. 11

Scheme 1.11 leads to the following rate law equation [97]:

$$k_\psi = \frac{k_M K_A C + k_W}{1+K_A C} \qquad 1.12$$

Where K_A is the binding constant in terms of the micellised surfactant, k_M and k_W are the first-order rate constants in the micellar and aqueous phase, C is the concentration of the micelle, and as has been already defined above, is the observed second-order rate constant. Bunton[115] have used the above equation for the oxidation of ferrocene by ferricyanide ion in presence of sodium dodecyl sulfate (SDS) which inhibits the reaction

by excluding the ions and binding of organic substrate. The applicability of this model restricted to reactions where partition of one reactant between micelle and bulk phases occurs and where rate retardation by micelle observed as result of reactants separations[115].

1.3.10.4. Multiple micelle pseudophase model

It should first be mentioned that the equation derivative from this model has been used throughout the present work. Davies [101] has suggested that the micelle pseudophase should not be thought of as only one or two phases, as in the single pseudophase models[31] but, rather as multiple phases. As described earlier, due to the change in the micellar polarity in going from the exterior to the interior of the micelle, also the molecules could assume several different orientations within the micelle pseudophase, thus the multiple micelle pseudophase model (MMPP) was introduced. This model divided the micellar system into arbitrary pseudophases and every phase has a different partition coefficient for the reactants, as well as a different mean rate constant.

The model has been used to treat the kinetic data obtained for reactions between iodide and peracids in non-ionic (Brij-35, Triton-100), anionic (SDS) and mixed non-ionic anionic surfactants [101, 102].

In this work the data in chapter 3 and 4 is fitted according to Equation 1.13, which is derived using the multiple micellar pseudophase (MMPP) model [101].

$$k_{obs} = \frac{k_w + (k_{mic} - k_w \bar{V}_{mic})([S] - CMC)}{\{1 + (K^{PH}_{mic} - \bar{V}_{mic})([S] - CMC)\}\{1 + (K^{I}_{mic} - \bar{V}_{mic})([S] - CMC)\}} \qquad 1.13$$

The terms in this equation will be defined in Chapter 3.

1.3.11. Hofmeister series

The Hofmeister series [103] shown below in Scheme1.12 originates from a test looking at the ability of a variety of ions to precipitate a mixture of hen egg white proteins:

$SO_4^{-2} > HPO_4^{-2} > OH^- > F^- > HCOO^- > CH_3COO^- > Cl^- > Br^- > NO_3^- >$

$I^- > SCN^- > ClO_4^-$

Cations: $Mg^{2+} > Li^+ > Na^+ > K^+ > NH_4^+$.

Scheme 1.12

The effect of anions was proved to be much stronger than the cations in terms of their ability to affect the catalytic efficiency of proteins [103]. The anions on the left hand are called kosmotropic salts and they 'salt out' electrolytes. Generally, these anions are small, have high charge density and are highly hydrated. Chloride is in the border while the salts on the right hand side exhibit salting in affect, have a weak electric field and are less hydrated [104]. Jencks [105] has stated that salts that affect protein can be divided into two classes: those that cause protein to precipitate (which includes the salts on the left in Scheme 1.12), and those that induce the disaggregating of protein (which includes those on the right hand of Scheme 1.12). Two mechanisms have been proposed to explain the effect of salts. First is that salts affect the solvent quality of water; salts on the left hand side of the Hofmeister series are considered to be a water structure makers, while salt on the right hand side are considered to be a water structure breakers. The other mechanism is the phenomena whereby ions adsorb or are depleted at the water solute interface, thus modifying the phase equilibrium. However, the exact mechanism governing the effect of salts has not been determined yet, and these two mechanisms have been used in parallel to interpret the effect of salts on the poly (ethylene oxide)-block-poly (propylene oxide)-block-poly (ethylene (tri-copolymer). The presence of LiCl, KCl, NaCl, and NaBr decreases cloud point, CP, (in the order $Cl^- > Br^-$ and $Na^+ > K^+ > Li^+$), whereas the addition of NaSCN and urea results in an increase of CP in the order NaSCN > urea [106].

According to McDevit [107], the energy required to create the volume in water which is needed to accommodate a non-polar solute is increased in electrolyte solutions due to ion-water interactions. This results in an increase in the activity of the nonelectrolyte and hence its salting out.

Baptista [108] studied the change of water structure induced by nonelectrolyte and a supramolecular system which included Brij-35 CTAB, SB-2, and SDS. The study was based on the measurement of temperature of maximum refractive index TMR, which was found to be lower in the presence of solutes like urea, which is a water structure breaker, whereas TMR increased in the presence of a water structure maker such as tert-butyl alcohol. Also, in the presence of micellised surfactants the water structure tends to decrease more efficiently than when the surfactant is in a monomeric form. In addition, the molecular structure of the surfactant affects the water structure: below the cmc the disruption of the water structure was observed to decrease in the order Brij-35 >> CTAB > SB-12 > SDS. Brij-35 has the most profound effect on the structure of water compared to the others, which are almost similar [108]. Due to their strong tendency for hydration, kosmotropic ions compete for water around the POE chains in the surfactant molecular assemblies, such as micelles [109].

Recently, Cremer and colleagues [110] have argued that the effect of salt can not be explained on the basis of affecting the water structure, as mentioned and stated previously [104]. This was proved by them using time resolved and thermodynamic studies of water molecules in salt solutions. They found that the change in bulk water structure is the main reason behind the salt effect in the Hofmeister series, but also that the ion-macromolecule interaction and interaction with water molecules in the adjacent hydration shell of the colloid can be used to explain the salt effect [110].

1.3.12. Effect of micelles on reaction rate in the presence and/or absence of salt

Bimolecular reactions in micellar systems have been modelled by Berezin and colleagues [31]. They have suggested that partitioning of the reactants between the bulk aqueous phase and the micellar pseudophase leads to the catalysis and inhibition of reactions when the reactants are first concentrated and then diluted in the micellar pseudophase, as the concentration of the surfactant is increased. Davies and colleagues [101,102] have studied the effect of surfactants, including Brij-35, on the kinetics of the reaction of iodide with different peracids. The reaction of iodide and MCPBA has been investigated in the mixed surfactant system of Brij-35/SDS. Brij-35 by itself enhances the rate; however by adding sodium dodecyl sulphate the rate is inhibited [102].

The effects of inorganic electrolyte on the micellar catalysis of several substrates have been extensively investigated. The addition of a wide variety of salts leads to change in micellar structure and results in wide variation in the catalytic efficiency of the micelle. Also, it has been stated that surface potential of the ionic micelles decreases with an increase in the concentration of the counterions [31]. This reduces the cmc and can also change the shape and size of the micelles, as stated above [31, 32]. These effects are more marked for the counterions of higher charge and hydrophobicity. Very often, the micellar catalysis in bimolecular reactions is retarded by the addition of electrolytes [31, 111]. This rate retarding effect mainly depends on the nature of the counterions. Counterions from added electrolytes compete with reactive counterions for a micellar binding site. This rate retarding effect generally increases with an increase in hydrophobicity of added counterions, and hydrophobicity favours the micellar binding of counterions.

The inhibition of micellar catalysis by added electrolytes may also be interpreted by considering the change of the size of the micelles in the presence of salts. The presence of salts increases the aggregation number, and consequently the shape and size of the micelles [112]. An increase in aggregation number will reduce the number of micelles, and as a result the catalytic efficiency of the aggregate decreases.

There is considerable amount of information available about the effect of salt on the catalytic behaviour of micelles in hydrolytic reactions. In his study about the effect of electrolyte on the attack of hydroxide ions upon carboxylic ester catalysed by cationic micelle, Cordes [113] has shown that bromide and nitrate ions reduce the reaction rate to such an extent that the catalytic effect of the micelle is totally reversed. The effect of salt was explained in terms of increasing the extent of charge neutralisation of the micelle surface, and hence reducing the catalytic effect; the affinity of the anions for the micelle surface is larger for larger anions, with low charge density ions which interact strongly with the micelle. The other explanation assigned by Cordes is displacement of one reactant from the micellar surface by electrolyte [114].

The effect of electrolytes on micelle-catalysed reactions can be discussed in terms of their competition with the reagent for an available binding site, as well as their ability to alter the micellar structure [113].

Bunton and colleagues [115a] have studied the effect of electrolytes on the reaction of 2,4-dinitrochlorobenzene with hydroxide ion in the presence of cationic micelle CTAB.

They used a number of inorganic salts at different concentrations and observed inhibition of micellar catalysis. Their conclusion was that the extent of inhibition depends upon the nature of the anions, and is least for anions of high charge density. Also, they investigated the effect of non-ionic and anionic micelles on the same reaction, observing that the former has no effect on the reaction and the later type of micelle inhibits the reaction due to electrostatic repulsion between the micelle head group and the anionic reagent [115b].

Bunton and colleagues [115b] have also investigated the effect of electrolytes on the reactions between 2,4-dinitrofluorobenzene and hydroxide in presence of cationic, anionic and noionic micelles, which were observed to be catalysed strongly in the presence of CTAB, were inhibited by adding salts. The inhibition was largest with anions of low charge density. Also it inhibited by anonic micelle while non-ionic micelle has no effect [115b].

Lucia and colleagues [116] have investigated the effect of electrolyte potassium chloride, potassium bromide and sodium salicylate, on the alkaline hydrolysis of p-nitrophenyl ethyl chloromethylphosphonate occurring in cetlypyridinium bromide. It was suggested that the inhibition of the reaction occurs as a result of the structure change of the micelle and the decrease of the concentration of the nucleophile in the micelle, which is due to a decrease in the surface potential.

The effect of the non-ionic micelles (Tweens, which is an ethoxylated derivative of fatty acids of ester)[76] polyoxyethylene (20) sorbitan monolaurate (Tween 20), polyoxyethylene (20) sorbitan (monooleate) (Tween 80) on the elimination reaction between 2-(*p*-nitrophenyl) ethyl bromide and OH^- ions has been studied[117] and a pseudophase model was used for treatment of kinetic data. The results of the work show that the presence of a non-ionic micelle inhibits the reaction. The inhibition observed was explained to be as a result of the large equilibrium binding constants found in Tween 20 and Tween-80 micellar solutions. The strong binding can result in the 2- (*p*-nitrophenyl) ethyl bromide molecules being incorporated deeper in the micellar interior of the non-ionic micelle and, as a consequence, the organic substrate molecules will be hindered from the hydrophilic hydroxide ions, hence inhibiting the reaction. Also, the inhibition is more in Tween-80 than in Tween 20 due to the large binding of organic substrate in the former.

Elsoud and colleagues have studied the pH independent hydrolysis of 4-nitrophenyl chloroformate[118] and 4-nitrophenyl 2, 2 dichloropropionate[119] (NPDCP) in various surfactants, including sodium dodecyl sulfate, alkyltrimethylammonium chlorides, alkyldimethylbenzylammonium chlorides and polyoxyethylene (9) nonylphenyl ether. They observed that the rate in the former case is enhanced by a cationic micelle and inhibited by other micelles due to stabilization/destabilization of transition state induced by a charged micelle. The rate reaction of the latter compounds was found to be faster in water than in a cationic micelle. This difference was attributed to low water activity at the reaction site in the presence of NPDCP. This was supported by thermodynamic parameters obtained by varying the temperature at fixed surfactant concentrations, which shows that there is high entropy and enthalpy of activation of the micelle reaction compared to that in water for the NPDCP.

The effect of surfactants on chemical reactions has been well studied; for example, the oxalic acid catalyzed oxidation of different aromatic azo compounds by Cr(VI) has been investigated by Reddy and co-workers [120]. Both SDS and CTAB (cetyltrimethylammonium bromide) were found to inhibit the reaction, while the non-ionic surfactant polyoxyethylene (23) dodecanol (Brij 35) catalyzes the reaction. The neutral Cr(VI)–oxalic acid complex has been suggested as the active oxidant. It is preferably accumulated in the aqueous phase in the presence of both the cationic and anionic micelle, but it gets partitioned between the aqueous and micellar pseudophase in the presence of a non-ionic micelle. The aromatic azo-compound is preferably accumulated in the micellar phase due to the hydrophobic interaction in all cases (SDS, CTAB and Brij-35). The observed micellar effects were explain by the different patterns of partitioning of the reactants in the presence of different types of surfactants.

The oxidation of ethylenediaminetetraacetic (EDTA) by chromic acid in the presence of the non-ionic surfactant Triton X-100 have been studied [121]. The pseudo-first-order rate constant of the process has been found to increase monotonically with the increase of surfactant concentration. The observed micellar catalysis has been rationalized by considering the fact that the reactants bind with the non-ionic micellar head groups (ether oxygen of the polyoxyethylene) through hydrogen bonding and the reactants are concentrated in the Stern layer [121].

1.3.13. The micellar effect on sulfide oxidation

1.3.13.1. Background

The general characteristics of these reactions are similar to other cases of nucleophilic displacement on peroxidic oxygen, and the mechanism of the reaction of sulfur compounds and peroxide involves nucleophilic attack of outer peroxidic oxygen by a sulphur atom, producing sulfoxide and leaving groups, as in Scheme 1.13. The mechanism also involves build up of positive charge on the sulphur in the transition state as the electrons transfer to the peracid, and this is seen in the positive value of ρ (reaction constant) for substituted peroxy benzoic acid [122]. Sulfones are synthesised with 1:2 molar ratio at high temperature [2].

$$R_2S: + YOOH \longrightarrow YOH + R_2S{=}O$$

$$R_2S{=}O + YOOH \longrightarrow R_2SO_2$$

Scheme 1.13

R can be an alkyl or aryl group, and Y is a leaving group in peracid.

The reaction is speeded up by an electron releasing group at the para position in the sulfide and reduced by an electron withdrawing group [123]. For the peroxide, on the other hand, reactivity increases as the basicity of the leaving group is weak and the pK_a of the leaving group is lower [122].

The oxidation of sulfide compounds by peroxy compounds has been studied extensively and it has been concluded that hydrogen peroxide is less reactive than peroxyacids. Also, the peracid monperoxosulfate is more reactive and peroxoborate is less reactive [125]. Figure1.6 shows the plot of the pK_a of parent acid versus log k, indicating the lower reactivity of hydrogen peroxide compared to other peroxides [124].

The oxidation of organic sulfide by hydrogen peroxide itself is less effective and has to be activated to get a good oxidation yield. For example, it can be activated by conversion into peroxyacid. Also, the molybdate ion has been used to activate peroxide and the reaction produces peroxymolybdate, which is a better oxidant [125]. Also the Hydrogencarbonate ion and H_2O_2 generate a peroxocarbonate which is an effective oxidant [126].

Richardson [127] has also used bicarbonate for the conversion of H_2O_2 to peroxycarbonate, which easily oxidises sulfide in mildly alkaline conditions. The oxidation of thioanisole (PhSMe) by H_2O_2 is activated by acetonitrile (MeCN), and the reaction of HO_2^- with nitriles generates short-lived peroxyimidates which convert alkenes into epoxides, and oxidize sulfides to sulfoxides and sulfones [128].

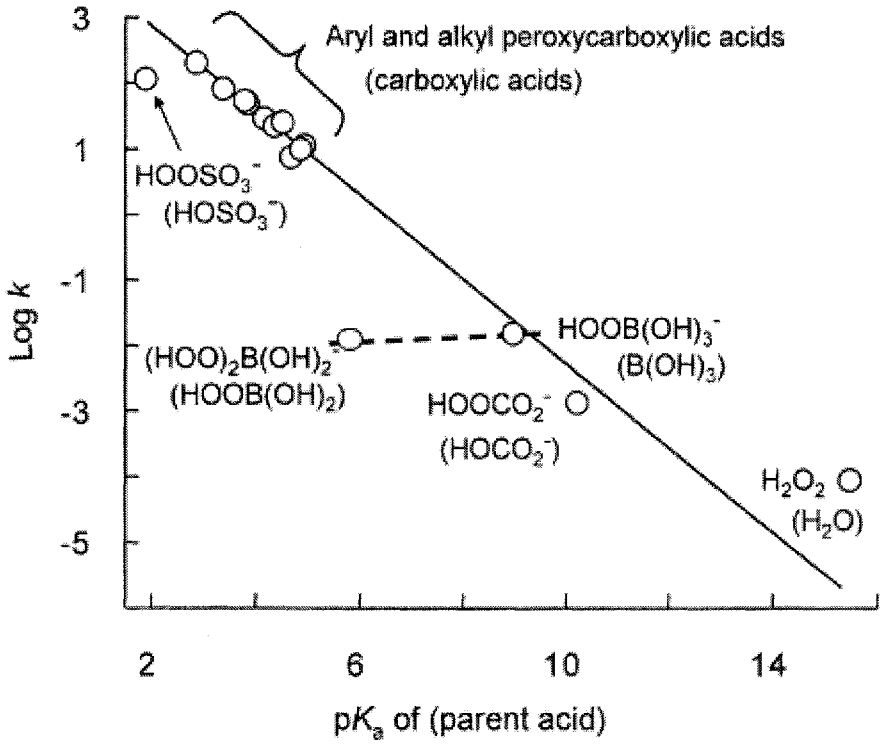

Figure 1.6: Brønsted-type plot, including parent Lewis acids, for the reactions of peroxides with methyl 4-nitrophenyl sulfide (taken from reference 124).

1.2.13.2. Effect of micelles on oxidation of organic sulfides

The reaction of anions with hydrophobic organic substrate is strongly inhibited by micelles of a similar charge and accelerated by micelles of counter charge [129]. However the oxidation of sulfides by periodate [130] and peroxymonosulfate [123] is inhibited by cationic micelles, even though this reactant carries an opposite charge to the micelle head group.

Anionic micelle SDS inhibits the oxidation of dipropyl and dibutyl sulfide and 1-methoxy-4-(methythio) benzene by periodate. Also, at high SDS there is residual reaction, as the periodate is not completely excluded from the micelle. The second order rate constant is lower than in water by a factor of 2-6[130], and by addition of Me_4NBr the

rate has been observed to increase with an increase in the SDS concentration, as the negative charge of the micelle is decreased due to incorporation of the Me_4N^+ and hence the periodate is less excluded from the interfacial area of the micelle. Also, a decrease in polarity is assumed to be the factor inhibiting the reaction in the micelle [130]. In general, the results observed were explained as follows: the inhibition was explained as a result of the build up of positive charge on the sulfur atom in the transition state, which leads to the expulsion of the organic substrate from the cationic micelle due to electrostatic repulsion. However, no explanation has been given as to why the rate is inhibited by an anionic micelle if the transition state involves positive charge.

The effect of solvent polarity on the rate was seen to be a major factor causing a decrease in the rate of alkene bromination by Br_3^- in the presence of a cationic micelle, despite the fact that both reactants are incorporated in the micelle [131]. In addition, Bunton [132] and colleagues have investigated the oxidation of 3-chloroethyl phenyl sulfide and 1-methoxy-4(methylthio) benzene by HSO_5^-, as well as the periodate oxidation of aryl methyl sulfide ArSMe in the presence of zwitterionic micelle N-tetradecyl-N,N-dimethyl-3-ammonio-1-propanesulfonate (SB-14). Their results show that this micelle inhibits oxidation, and the main reason for this is the lower polarity of the micellar medium, as in the case of a cationic micelle mentioned above [130].

Tetraperoxymolybdate was also used for the oxidation of phenyl methyl sulfide in the presence of cationic micelle cetylpyridinium chloride; the reaction was inhibited compared to that in bulk aqueous solution. The inhibition of the reaction between PhSMe and $Mo(O_2)_4^{-2}$ was attributed to a decrease in polarity and the water content of the medium, as with other oxygen transfer processes. In addition, Bunton assumed that the high phase volume and low polarity of the reaction region in the micelle relative to the water inhibits the reaction [133].

Rajkumar [134] found the opposite effect of cationic micelle CTAB and SDS on the electron transfer from sulfide to [CrV(ehba)2] (ehba means (2-ethyl-2-hydroxy butyric acid), in which the rate is increased in the presence of the former micelle, which is in contrast to the previous study of Bunton with IO_4^-, HSO_5^- and HCO_4^- oxidation of organic sulfides as stated above. SDS micelles show the same behaviour as those observed by Bunton [130], and the explanation was as follows: the decrease in the rate in presence of SDS is a result of the electrostatic repulsion between the anionic oxidant and the negative charge on the head group of the micelle, low polarity of the micelle, and partition of the hydrophobic substrate between phases.

It is important to recall that $[CrV(ehba)_2]K$ oxidation of organic sulfides proceeds by an electron transfer mechanism, and of anionic peroxidants by the electrophilic attack of the oxidant at the sulfur centre of the substrate and proton transfer (an SN_2 type mechanism). Thus, the positive charge developed on the sulfur centre in the transition state is less with $[CrV(ehba)_2]^-$ oxidation compared to anionic peroxidants oxidation. These results also support the importance of charge–charge interaction in the transition state on the overall rate of the reaction in the micellar phase. Also, in general the catalysis were due to a concentration effect which offset the charge-charge interaction between the cationic micellar and the positive charge on the sulphur centre [138]. A similar explanation has been given by Drummond and Grieser [135] for micellar catalysis in H_2O_2-mediated oxidation reactions.

Rajkumar [136] has also recently investigated the oxidation of organic sulfides by iron (III)-polypyridyl complexes in the presence of cationic and anionic micelles, which resulted in catalysis of the reaction in both cases. The micelle catalysis in the presence of SDS was attributed to the strong binding of the cationic oxidant to the anionic micelle and the build up of positive charge on the sulfur centre in the transition state; while the catalysis observed in the presence of CTAB, even with a build up of positive charge on the sulfur atom, indicates the importance of the hydrophobic interaction between the micelle and the hydrophobic ligand of the cationic reactant. This is in contrast to the previous results of Bunton [130], which attribute the inhibition of sulfide oxidation in the presence of cationic micelle to the build up of positive charge on the sulfur centre of the substrate in the transition state, which leads to electrostatic repulsion so that the micelle catalysis can not be explained precisely unless a complete investigation is undertaken.

SDS has been found to catalyze the Cr(VI) oxidation of dialkyl sulfides [137], while the cationic surfactant cetyltrimethylammonium chloride (CTACl) retards the reaction. It has been explained by the fact that the reaction takes place both in the aqueous and micellar phases. The reaction is catalyzed by SDS because of the enhanced local concentrations of the reactants in the micellar phase. The reaction is acid catalyzed and the H^+ ion gets preferentially concentrated in the anionic micellar phase. The cationic surfactant inhibits the reaction because the approach of H^+ ion to the cationic micellar surface (in which both the reactants are preferentially concentrated) is unfavourable due to an electrostatic repulsion. Moreover, oxidation of an organic sulfide involves electron transfer from sulfide to Cr(VI), and a build up of positive charge on the sulfur is unfavourable due to a repulsive interaction with the cationic micellar head groups. In

fact, this is also in agreement with the observed micellar catalysis in the presence of anionic surfactant, SDS. Here, the change of polarity of the medium (specifically in the intermicellar zone in which the reactants are positioned), with the addition of surfactant to influence the observed micellar effect, has been analyzed.

Das [138] has studied the picolinic acid (PA) catalyzed oxidation of dimethyl sulfoxide (DMSO) to dimethyl sulfone by chromium (VI) in the absence and presence of the surfactants sodium dodecyl sulfate and cetylpyridinium chloride (CPC). The main observation was that the rates are catalyzed in the presence of SDS and inhibited in the presence of CPC. The catalysis by SDS was explained as follows: Cr(VI)–PA complex is the active oxidant formed at the pre-equilibrium step and is positively charged. Due to the electrostatic attraction, it is preferably partitioned in the SDS micellar phase which is also enriched with the neutral substrate concentration due to hydrophobic interaction. The process is strongly catalyzed by H^+, and H^+ ions are also preferentially concentrated in the anionic micellar pseudophase. Thus, in the presence of SDS the reaction in the micellar phase is facilitated. On the other hand, in the cationic micellar phase, the neutral substrate is preferably accumulated due to hydrophobic interaction, but the other reactants (positively charged Cr (VI)–PAcomplex and H ions) are repelled by the cationic micellar phase due to electrostatic repulsion, and the reaction is mainly restricted in the aqueous phase by a reduced concentration of DMSO. Consequently, the overall rate decreases with the increase of $[CPC]_T$.

Lobachev and coworkers [139] have studied the effect of different surfactants on the rate of diethyl sulfide (Et_2S) oxidation by hydrogen peroxide and peroxymonocarbonate (HCO_4^-) in aqueous solutions. The surfactants used were Triton X-100 (neutral), sodium dodecyl sulfate (SDS) (anionic), and cetyltrimethylammonium bromide (CTAB) (cationic surfactant). Their results showed that in all cases the rates decreased, except for the oxidation of sulphide by HCO_4^- in a cationic micelle, where both the reactants were concentrated into the micellar system due to the electrostatic attraction between the HCO_4^- and the micellar head group, and also due to hydrophobic interaction in the case of diethyl sulfide.

A very important endeavour is to look out for new systems of rapid oxidation of organic sulfides, which are active components of toxic agents. Therefore, in current work we have studied the kinetics of the oxidation of methyl phenyl sulfide and other substituent sulfides with MCPBA and peroxymonosulfate in aqueous solutions of Brij-35.

Methyl phenyl sulfide has been considered a model analogue for mustard gas, both in its hydrophobic properties and reactivity [126]. However, the details of the non-ionic micellar effect on the oxidation of sulfide aided by peracid are not well documented in literature. This has prompted us to study the micellar effect on the kinetics of this reaction.

1.4. Isokinetic relationships and enthalpy–entropy compensation

In general, if a linear relationship between enthalpy and entropy is observed in a chemical reaction, then a phenomenon known as enthalpy-entropy compensation will be observed, in which the magnitude of the change in the Gibbs free energy is small. Mathematically, this is because of the Gibbs free energy equation $\Delta G = \Delta H - T\Delta S$, where the term in enthalpy (ΔH) and the term in entropy ($T\Delta S$) have opposite signs and ΔG will change very little if both enthalpy and entropy increase. For example, in a reaction where the chemical bonds become stronger or they are formed throughout the reaction, a negative ΔH value will occur. At the same time, this aforementioned act of forming or even strengthening a bond will limit the movement of the molecule in terms of the molecule's ability to rotate, vibrate and hence decrease the entropy of the molecule, which leads to a fairly small ΔG value.

When a series of structurally related substrates undergo the same general reaction, or when the reaction conditions for a single substrate are changed in a systematic way, the enthalpies and entropies of activation sometimes satisfy Equation 1.14 [140, 141].

$$\delta\Delta H^{\#} = \text{constant} + \beta\, \delta\Delta S\# \qquad 1.14$$

This equation is said to represent an isokinetic relationship, where the parameter β is called the isokinetic temperature and the temperature T or β at which all members of a series obeying the isokinetic relationship react at the same rate. Supposed isokinetic relationships established by direct correlation of ΔH with ΔS are often spurious and the calculated value of β is meaningless because errors in ΔH lead to compensating errors in ΔS [140, 141].

Exner has recommended a simple method to assess the isokinetic relationship[142]. It consists of plotting the logarithms of rate constants for the same member of a reaction series at two temperatures ($T_2 > T_1$) against each other according to Equation 1.15.

$$\text{Log } k_2 = a + b \log k_1 \qquad 1.15$$

If a linear correlation is obtained that suggests valid existence of an isokinetic relationship, then the isokinetic temperature readily is readily obtained from slope *b* using Equation 1.16.

$$B = T_1 T_2 (b-1)/ bT_2 - T_1 \qquad 1.16$$

The advantage of this method is that the relationship is evaluated from two independent data sets, unlike that for the enthalpy–entropy compensation which is evaluated from the same data set so that the error is correlated for ΔH and ΔS [140]. This method will be used in the present study in parallel with an enthalpy–entropy plot, and the isokinetic temperature obtained from both methods will be compared.

Exner [141] has also shown that the existence of isokinetic relationships can be discovered by plotting natural logarithm of rate or equilibrium constant versus 1/T and if a common point of intersection exists it suggests the existence of such a relationship. Also, Exner has shown that the presence of a good linear correlation between ΔH and ΔS does not mean that there is a common point of intersection for the same reactions when log k is plotted versus 1/T.

There are two related but not synonymous terms that have been used to explain thermodynamic relationships: the first is the compensation effect and the second is the isokinetic or isoequilbrium effect. Karpinski [143] has defined the two terms as follows: the compensation effect means that there is an excellent linear correlation between ln A versus energy of activation and between enthalpy change and entropy change, as well as between enthalpy of activation and entropy of activation of a similar reaction. Figure 1.7 and Figure 1.8 show such relationships. The isokinetic or isoequilibrium effect is defined as the existence of a common point of intersection in a Arrhenius or Van't Hoff plot.

Xing [144] has stated that the existence of the compensation effect can be inferred from statistical analysis in which the correlation coefficient of the linear plot is used to indicate the existence of this phenomenon; the higher the r^2 the better the relationship. On the other hand, the existence of isokinetic relationships is based on the closeness of the reaction rates or equilibrium to each other at the isokinetic temperature. The existence of one does not mean the other process is present. Furthermore, Xing [144] has shown that as an experimental error can lead to such apparent correlations; thus, statistical analysis can be used to confirm the compensation effect is correct as error bars can be drawn. For

isokinetic relationships, all lines describing the kinetics or thermodynamics of the reaction series can be overlaid on one plot to see if there is a point of intersection or not.

Enthalpy-entropy compensation means that, at a specific temperature, the enthalpy variations are compensated by a change in entropies, such that the net change in free energies remains constant in physicochemical processes [144]. For example, when EEC (enthalpy-entropy compensation) is observed for different solutes, a plot of enthalpy against entropy changes is linear, with a slope called compensation temperature; the slope is constant for processes having a similar interaction mechanism [145].

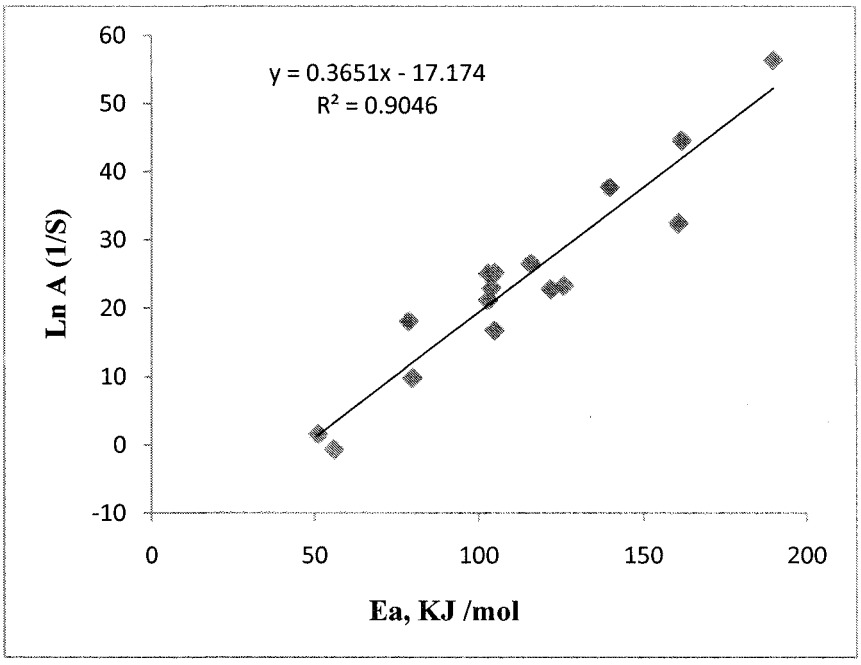

Figure 1.7: Relationships between frequency factor and activation energy of polysaccharide depolymerisation (taken from reference 149).

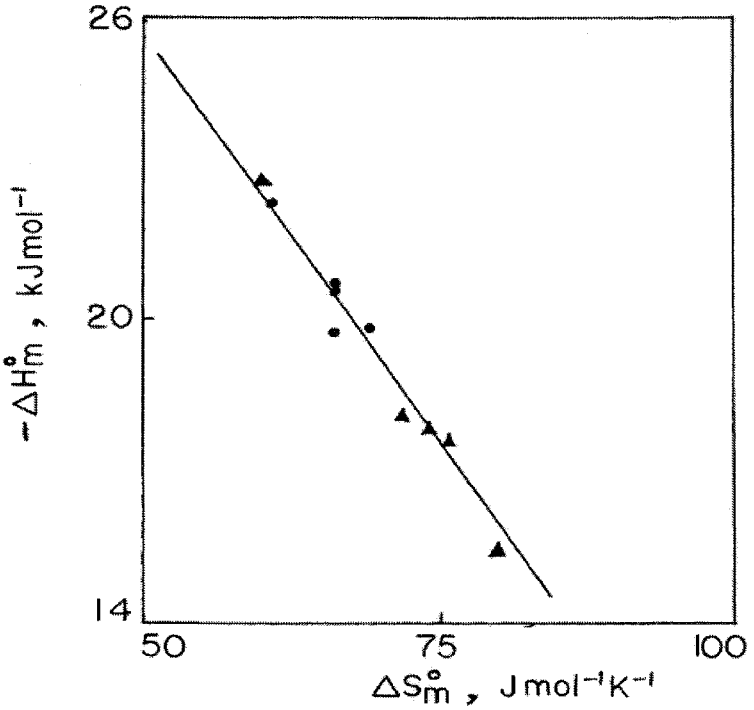

Figure 1.8: Enthalpy-entropy plot for the micellisation of non-ionic surfactant poly(oxyethylene(10)) lauryl ether [$C_{12}H_{25}(OCH_2CH_2)_{10}$ OH] in aqueous solution in the presence of both polyethylene glycol 400 (circle) and sucrose (triangular shape) (taken from reference 150).

Krug [146] developed methods to test whether enthalpy-entropy compensation exists. According to Krug's [146] test, the following conditions have to be met for enthalpy-entropy compensation to exist: firstly the lines of lnK or ΔG versus 1/T for all compounds must interconnect at a single temperature. Secondly, when enthalpy-entropy compensation is real, then ΔH versus ΔG must form a linear plot. Engberts and co-workers [147] have investigated different micelles including cationic, anionic and a series of non-ionic micelles on the 1,3-dipolar cycloaddition of benzonitrile oxide with a series of N-substituted maleimides. The effect of the cationic and anionic micelles on the acceleration rate is higher than that for non-ionic micelles. Also, they have studied the effect of temperature ranging from 15°C-35° C on the same reaction in the presence of $C_{16}E_{20}$. Their results show that the binding of reactants does not depend on temperature and that temperature has no effect on the morphology of the micelle. However, they also found that a linear relationship exists between the enthalpy and entropy of activation for the reaction between 1,3-dipolar benzonitrile oxide and *n*-butyl- maleimides in different media at 25°C, as shown in Figure 1.9.

Bunton and co-workers [148] have carried out a temperature dependent experiment on the cyclization of 3-halopropyloxyphenoxide ion in the presence of cationic micelles (cetyltrimethylammonium bromide). Their results show that the process is speeded up in the presence of the micelle due to a decrease in the enthalpy of activation. Also, the effect of micellar structure induced by temperature change on the value of determined activation parameters is very small. The same researchers [148] argue that for bimolecular reaction, estimation of the thermodynamic parameters from kinetic data should take into account the distribution of the reactants as it is difficult to measure temperature effect on distribution. Also, this phenomenon has been found in ionisation of substituted aniline; studies show a good linear correlation between ΔS and ΔH when plotted against each other using the relationship above. In addition, when ΔG is plotted versus ΔH no dependence is observed and the values of ΔG are approximately constant in comparison with ΔH variation. So, the linear correlation between ΔH and ΔS can express the fact that ΔG is approximately constant [141].

Some researchers [140, 141, 144] have argued that enthalpy-entropy is probably a statistical artefact which can result in observance of a relationship between two variables. This may at first seem reasonable, but is in fact false because the relationship being observed does not actually exist. Xing [144] demonstrates that for a series of related reactions a good correlation can be obtained by plotting Ln k versus temperature, but for the same series a poor correlation is obtained by plotting ΔH versus ΔS. Sometimes a graph that is plotted against temperature will be used to obtain a value of enthalpy and entropy, when in fact this is not the proper way to measure these values. Calorimetry experiments can yield the proper measurements of enthalpy and entropy compensation since there is no worry about false compensation between Van't Hoff enthalpy and entropy [141]. However, calorimetric data are generally scarce and most literature does not deal with values from this technique.

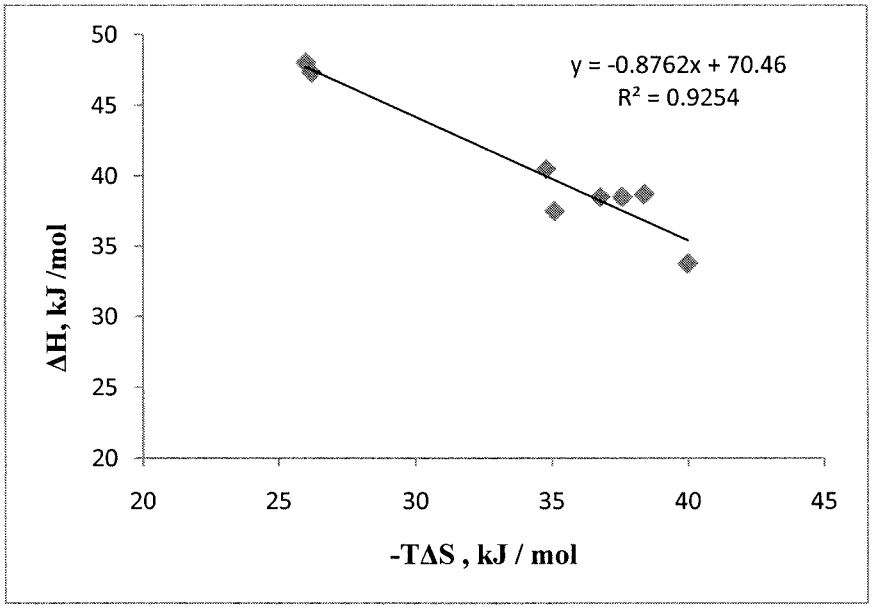

Figure 1.9: Enthalpy-entropy plot for the reaction between 1,3-dipolar benzonitrile oxide and *n*-butyl- maleimides at 25°C (taken from reference 147).

1.5. Cyclodextrins

1.5.1. Introduction

In addition to the micellar catalysis of the sulfides / peroxyacid reaction, the effect of cyclodextrins on these reactions will be investigated.

In this section certain aspects of cyclodextrin properties will be mentioned, including their physical properties, their structure and their complex inclusion, as well as their effect on chemical reactions. Cyclodextrins are macrocycles formed by (1-4) linked units of -D-glucopyranose. Cyclodextrins are created by the action of enzyme on starch; the enzyme is called cyclodextrin glucosyl transferase enzyme (CGTase). Cyclodextrins consist of six (α-cyclodextrin), seven (β-cyclodextrin), and eight (γ-cyclodextrin) α-(1,4) linked glucopyranose units forming a conical cylinder. As a consequence of the $^4C_1$ conformation of the glucopyranose units, all secondary hydroxyl groups are situated on one of the two edges of the ring, whereas all the primary ones are placed on the other edge. The ring is frequently characterized as a doughnut or wreath-shaped truncated cones [151]. The chemical structure of β-cyclodextrin is illustrated in Figure 1.10, with molecular shape portrayed in the form of a truncated cone.

For β-cyclodextrin the seven primary hydroxy groups are situated at the narrower end of the cylinder and the 14 secondary hydroxy groups form the wider open. The hydrogen bonding between the secondary hydroxy groups on adjacent glucopyranose units lends

the molecule a more rigid structure than α-cyclodextrin, where one of its six glucopyranose units is in a distorted position and the hydrogen bond belt is incomplete [151]. The hydrogen bonding is all 3-OH (donor) and 2-OH (acceptor) in α-cyclodextrin, but in the case of β- and γ-cyclodextrins the opposite occurs, where all 3-OH become acceptor and 2-OH acts as the hydrogen bond (donor) [152].

The CD cavity is hydrophobic in character as a result of the two lone pairs of ether oxygen which is located in the middle of cavity and this gives the cyclodextrin some Lewis-based character [151]. In addition, there is hydrophobicity due to C3-H, C5- H and C6-H2 hydrogens. Consequently, this cavity can host many molecules which are insoluble in the bulk water. The exterior of the cyclodextrin rings are hydrophilic due to the presence of 2- and 3-OH groups on the wider rim and the narrower rim displaying 6-OH groups, thus rendering the cyclodextrin soluble in water [152].

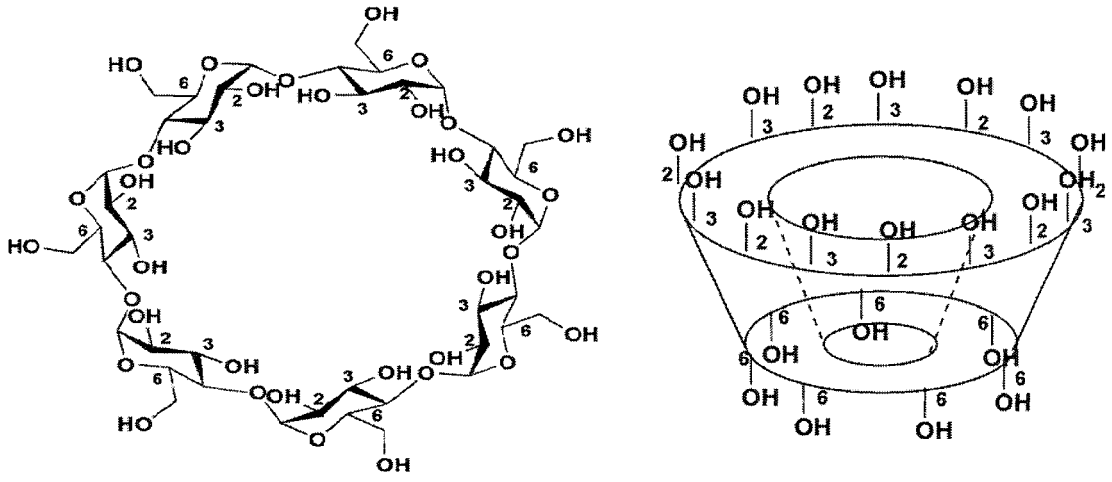

a b

Figure 1.10: Chemical structure of β-cyclodextrin (taken from reference 155).

In an aqueous solution, the slightly apolar cyclodextrin cavity is engaged by water molecules, which are energetically unfavoured (polar-apolar interaction) and therefore can be readily replaced by the appropriate guest molecules, which are less polar than water [152]. In an aqueous solution, this hydrophobic cavity contains about 3 (α-DC), 7 (β-DC) or 9 (γ-DC) water molecules. Table 1.4 shows the main properties of cyclodextrins [153].

Cyclodextrins (CDs) are compounds widely used in the pharmaceutical industry. They enhance solubility, bioavailability and stability of many drugs and also aid the absorption

of drugs by the body. Cyclodextrins are also used in the petroleum industry to separate aromatic hydrocarbons and in agriculture to reduce the volatility of insecticides [153].

Properties of the main cyclodextrins					
Cyclodextrin	Mass	Outer diameter, (A^o)	Cavity diameter (A^o)	Solubility, $g/100mL^{-1}$ H_2O 2b	Number of H_2O, [154]
α-CD	972	14.6±0.4	4.7 - 5.3	14.5	6.4
β-CD	1134	15.4±0.4	6.0 - 6.5	1.85	9.6
γ-CD	1296	17.5±0.4	7.5 – 8.3	23.2	14.2

Table 1.4: Physical properties of cyclodextrins (taken from reference 155 unless stated).

1.5.2. Cyclodextrin inclusions complex

Many driving forces for the complexation of CD with substrate have been proposed [152, 156], including van der Waals forces of hydrophobic interaction, hydrogen bonding, and release of energy upon complexation. The two main components of the driving force of the inclusion process are the repulsive forces between the included water molecules and the apolar CD cavity on one hand, and between the bulk water and the apolar guest on the other [152]. Tabushe [156a] has stated that the two main driving forces for the inclusion of benzene, p-iodoaniline, and methyl orange by α-CD are van der Waals interaction and the release of water molecules around the apolar guest compound [156a].

Upon encapsulation of a molecule, many properties of the guest molecular are altered. For example, the stability, solubility, and volatility are modified. The reactivity of the guest molecule is modified and in most cases the reactivity decreases, i.e. the guest is stabilized. However, in many cases due to the hydrophobic properties of the CD and its similarity to an enzyme which also has a hydrophobic pocket it can provide a strong recognition site for substrates. Thus, cyclodextrins have attracted the interest of enzyme mimic chemistry and as mimics of antibodies binding. Such comparisons can give information about the enzyme-substrate interaction [156b]. Also, CD can accelerate various reactions and modify the reaction pathway [152]. The use of cyclodextrins as an enzyme model has been comprehensively reviewed by Hoffmann[152] and Connors [157].

Notwithstanding the above, Breslow [158] has stated that binding constants are too weak to allow simple cyclodextrins to be good antibody mimics, and that the complexes are often too flexible to enable simple cyclodextrin derivatives to be ideal enzyme mimics. To overcome this problem he suggests the use of cyclodextrin dimers. When two cyclodextrin units are linked, the binding of substrates that can occupy both cavities is generally much stronger, and the geometry of the resulting complex is better defined since the substrate is grasped at both ends and held across the linker that ties the two cyclodextrins together [159]. The most studied type of complex type is the 1:1 host-guest complex. Also, the possibility of simultaneous formation of complexes with different stoichiometries has also been found. Four types of CD-guest complexes with 1:1, 1:2, 2:1 and 2:2 stoichiometry, have been observed depending on the size and structural features of the guest with respect to the host cavity [160].

The encapsulation of the guest into the cyclodextrin can include dipole-dipole and ion-dipole interaction; in the latter case complexation of CD with ClO_4^- and NO_3^- was observed, though for ions of high charge density such as SO_4^{-2} no such interaction was observed. This is attributed to the fact that SO_4^{-2} is more strongly solvated by water and such complexation with CD is unfavourable [161]..

1.5.3. The effect of cyclodextrins on chemical reactions

The first use of cyclodextrins as a catalyst was reported by Bender and colleagues, who studied the hydrolysis of phenyl acetate in the presence of CD and discovered significant substrate specificity in the reaction rates in which the hydrolysis of meta- substituted phenyl acetate by CD was accelerated considerably, while for para- and ortho-susbtituted phenyl acetate it was marginally accelerated. Since then, reactions catalyzed by CDs have been continuously reported [160, 161].

The effects of CDs on organic reactions can be divided largely into two types. The first is called covalent catalysis, whereby the CD and the reactant at first form a CD-reactant reaction intermediate involving a covalent bond, which is followed by the formation of the products. This type involves the nucleophilic attack of the secondary hydroxyl group of the CD on the substrate forming cyclodextrin-covalent intermediate, which is then hydrolysed to the final product. An example of this type is the hydrolysis of phenyl acetate: in the first step of this reaction there is nucleophilic attack of the secondary hydroxide group of cylodextrin toward carbonyl carbon of the substrate, which is located

in the cavity of the CD. Then the phenol group is removed from carbonyl carbon and acetyl-CD is formed, followed by hydrolyses of this intermediate into products.

The second effect shows no covalent bond and is called non-covalent catalysis. This mechanism is attributed to the hydrophobic cavity of the CD and conformational effect due to the guest geometric inclusion. In these cases, the CD mediates the reactions and is not used as a catalyst [160, 161]. An example of this type of catalysis is provided by the reaction of sulfides with peracid, as reported by Davies [162] who carried out a detailed and systematic study of the reaction between para-substituted aryl alkyl sulfides and substituted perbenzoic acid, and alkyl percarboxylic acids in the presence of α-CD. Davies suggests a mechanism for this reaction as outlined in Equation 1.17 to Equation 1.26 [162], in which the main pathway is the reaction of the 2:1 CD-peracid complex with the unbound sulfide, even though the extent of transition state stabilization by the second CD molecule is only about the same as its stabilization of the peracid in the ground state [162]. Also, a reaction between iodide and substituted perbenzoic acids has been carried out in the presence of α-CD [163]. It was concluded that the mechanism of the catalysis of these reactions by cyclodextrin is common to both sulfides and iodide. The substituted perbenzoic acids were found to bind to α-cyclodextrin with the OOH at the narrow end of the cavity, which constitutes the positively charged end of the cyclodextrin dipole and enhances electrophilicity [162], and decreases the apparent pKa of the peracid due to repulsion of the proton [163]; the iodide or sulfide nucleophile is then attracted to the outer peroxidic oxygen [162].

$$PH + CD \overset{K_{p11a}}{\rightleftharpoons} PH,CD \qquad 1.17$$

$$PH,CD + CD \overset{K_{p12a}}{\rightleftharpoons} PH,(CD)_2 \qquad 1.18$$

$$S + CD \overset{K_{S11}}{\rightleftharpoons} S,CD \qquad 1.19$$

$$S,CD + CD \overset{K_{S12}}{\rightleftharpoons} S,(CD)_2 \qquad 1.20$$

In these equations PH and S denote the peracid and sulfides respectively. Equations 1.17 and 1.18 represent peracid–cyclodextrin complexes and Equation 1.19 and Equation 1.20 represent sulfide–cyclodextrin complexes.

The following equations (1.21 to 1.26) describe the pathway for the oxidation of sulphides by peracids catalysed by cyclodextrins:

$$PH + S \xrightarrow{k_o} Products \qquad 1.21$$

$$PH, CD + S \xrightarrow{k_{1a}} Products \qquad 1.22$$

$$PH + S, CD \xrightarrow{k_{1b}} Products \qquad 1.23$$

$$PH, CD + S, CD \xrightarrow{k_{2a}} Products \qquad 1.24$$

$$PH, (CD)_2 + S \xrightarrow{k_{2b}} Products \qquad 1.25$$

$$PH + S, (CD)_2 \xrightarrow{k_{2C}} Products \qquad 1.26$$

And the kinetic data is described by Equation 1.27,

$$k_{obs} = \frac{k_o + k_{1obs}[CD] + k_{2obs}[CD]^2}{(1 + K_{S11}[CD] + K_{S11}K_{S12}[CD]^2)} \times \frac{1}{(1 + K_{P11a}[CD] + K_{P11a}K_{p12a}[CD]^2)} \qquad 1.27$$

k_{1obs} and k_{2obs} in Equation 1.27 are defined in Equations 1.28 and 1.29

$$k_{1obs} = k_{1a}K_{P11a} + k_{1b}K_{S11} \qquad 1.28$$

$$k_{2obs} = k_{2a}K_{P11a}K_{S11} + k_{2b}K_{P11a}K_{p12a} + k_{2c}K_{S11}K_{S12} \qquad 1.29$$

The term will be described elsewhere.

Using the spectrophotomeric titration method, the binding of a series of para substituted aryl alkyl sulfides to α-cyclodextrin has been investigated. It is believed that the shape of the sulfur containing group is the most important factor for determining the orientation and strength of the binding of sulfide, and that steric hindrance is responsible for the complexation. Also, binding of type 2:1 has been observed and it is assumed that

substrates induce and promote the interaction between opposite dipoles of cyclodextrin, as illustrated in Figure 1.11 in which head to head or head to tail complex can be formed. Davies preferred the latter structure in which the driving force is the interaction between opposite dipoles of the cyclodextrin, possibly stabilised by hydrogen bonding [164].

The effect of the electronic character of the substituent on aromatic ring has much effect on the binding of the substrate to the α- CD. For example, good correlation between the Hammett sigma values, σ, and log K_{11} for α-CD complexes with 4-substituted benzoic acid and their anions was obtained and it is suggested that the carboxylate group COOH is directed toward the primary end of the cyclodextrin. For the 4-substituted benzoic acid series the binding is enhanced by an electron releasing group from the para subtituent, while for the anions electron withdrawing group there is an increase in binding to α- CD as the para substituent becomes the actual binding site. Figure 1.12 shows log K_{11} versus Hammett sigma values for this process [157].

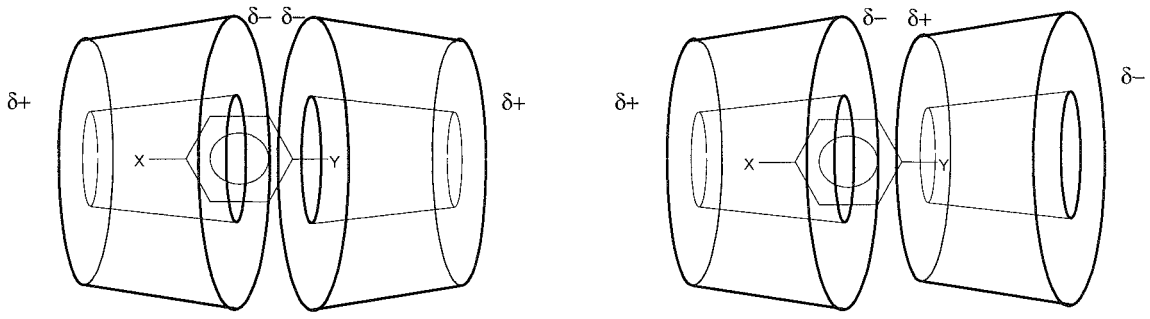

2:1 head to head 2:1 head to tail

Figure 1.11: Ligand dimerization (taken from reference 164).

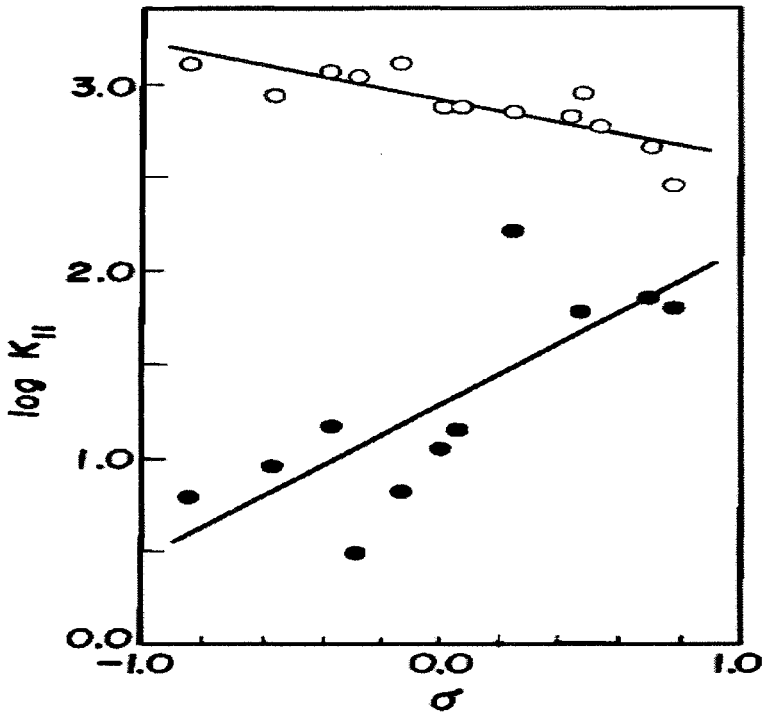

Figure1.12: Plot of the Hammett sigma values versus log K_{11} for encapsulation of 4-substituted benzoic acid (open circle) and their anions (filled circle) (taken from reference 157).

The same factor was observed to control the complexation of benzene derivatives with α-CD, with emphasis placed on the electronic effect of the substituents in the substrate. The binding constant shows good correlation with the Hammett constant and molar refractivies R_m of the substituents. The latter parameters represent the volume and the polarizability of the substrate. It is easier for the host to polarise and thus enhance the binding, and it has been observed that R_m correlates well with log K_{11}[165].

Guo [166] and colleagues have utilised the plot of log K_{11} (binding constant of guest) for the complexation of α- CD and β-CD with monosubstituted versus substituent molar refraction R_m, hydrophobic constant and Hammett constant of benzene derivatives. It was observed that for α- CD the main driving force was predominantly van der Waals, as good correlation between R_m and log K_{11} was observed; while for β-CD both van der Waals force and hydrophobic interactions were found to govern the inclusion due to the better correlation between log K_{11} and both R_m and hydrophobic constant [166]. The contribution of the Hammett sigma constant for the complexation of the guest with α-CD is so small that it can be considered absent [166]. It seems obvious that the driving force for the inclusion of the guest is affected by several factors and it is different from

one system to another; correlation of particular parameters with association constant that can be observed in one case seem to have no effect in another. However, despite the great number of studies undertaken looking at the inclusion complexation of cyclodextrins with substrate, the driving force controlling the complexation process is still unclear [157].

1.5.4. Effect of temperature on the stability constant of CD-guest complex

The host–guest complexation is an equilibrium process where the strength of the binding is affected by the temperature of the system. In most cases, as the temperature increases the binding constant decreases. For example, the association constant for a Naproxen molecule with beta-cyclodextrin decreases from 1379 to 975 to 788 as the temperature increases from 25°C to 35°C to 45°C respectively [167].

The effect of temperature on the inclusion complex of five amino amide-type local anaesthetics, bupivacaine, etidocaine, lidocaine, mepivacaine and prilocaine with beta cyclodextrin, have been investigated at 25°C and 37 °C. It was found that the stability constant K (M^{-1}) of the LA-CD complex decreased with an increase in temperature for all the drugs studied. For example, the stability constant of bupivacaien at 25°C and 37°C was 112 ± 6 and 87 ± 1 respectively. The only exception was mepivacaine, which was found not to be affected by temperature, although no suggestion was made to explain this [168].

Zarzycki and colleagues have studied the effect of temperature ranging from 10 to 70°C on the association constant of β-Cyclodextrin-phenolphthalein inclusion complex. The binding K_{11} at 10°C and 70°C was found to be 7.44 and 0.26 $\times 10^4$ M^{-1} respectively, which shows that the increase in temperature results in a decrease in the binding constant [169]. Moreover, the influence of temperature on the binding constant of propyl gallate to cyclodextrins has been investigated by measuring the fluorescence intensity at different temperatures ranging from 15°C to 60°C. The results show that the binding constant decreases with an increase in temperature; for example, values of 833 M^{-1} and 151 M^{-1} were obtained at 15°C and 60°C respectively [170].

With most of the effects of temperature on the cyclodextrin complexation mentioned above, good correlation between the enthalpy and entropy has been found. An extensive study on this phenomenon was carried out by Guo[171], who studied cyclodextrin complexation with different types of substrate, including hydrophobic, hydrophilic and

charged substrates. The results showed the presence of good relationships between the enthalpy and entropy of this process, especially with the hydrophobic substrates rather than the hydrophilic and charged substrates, which show higher values of correlation coefficients. A model composed of two portions was used: a non-compensated portion and a compensated portion, the former portion being related to the interaction of the host and the guest and their environment, and the latter being due to the reorganization of water. Hence, for charged and hydrophilic guests the compensation will be poor, as the interaction between the guest and water will be strong, contributing to the non-compensated part which will disfavour the occurrence of the compensation. The explanation given was based on the solvent reorganisation being a physical origin of this compensation [171].

In general, it has been proposed that the complexation process is driven by enthalpy, with large and negative enthalpy and negative entropic changes being exhibited. The negative value of enthalpy is attributed to the van der Waals interaction and hydrogen bonding between the guest and the cavity of the cyclodextrin; whereas the negative entropy change is a result of the restriction of the motion of the guest molecules upon inclusion due to the size limit and shape of the cyclodextrin cavity, which imposes more order on the guest. Most of the thermodynamic studies of inclusion complexation and temperature dependence deal with stoichiometry of 1:1 and 1:2 inclusion complexations [156a].

1.6. Transition state theory and its application to catalysis

The acceleration of the reaction rate originates from the stabilisation of the transition state by the catalyst, and the catalyst enhances the reaction by decreasing the free energy of the transition state relative to the ground state or reactants [172] (see Figure 1.12). As can be seen in Figure 1.12, the catalyst binds to the substrate and the complex formed is lower in energy than the substrate. However, it can also be seen that the binding of the transition state is even stronger, which leads to a lowering of the activation energy for the catalysed reaction and an increase in the rate. In general, to achieve the catalyst the transition state must be stabilised more by the catalyst than the ground state.

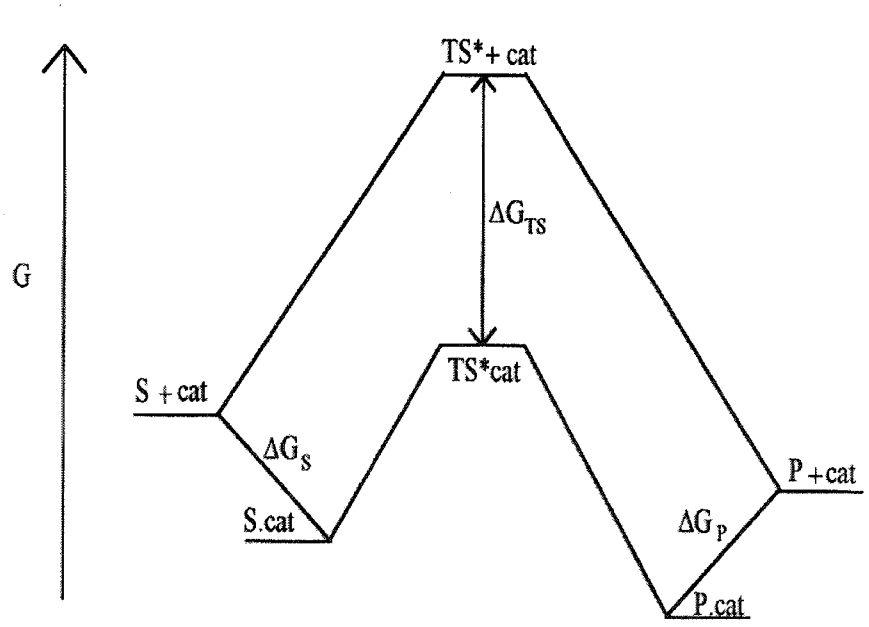

Figure 1.12: Schematic illustration of free energy profile, showing the stabilization of the transition state TS* by the catalyst relative to that of the substrate S. ΔG represents the Gibbs free energy between species not associated with the catalyst and those that are (taken from reference 172).

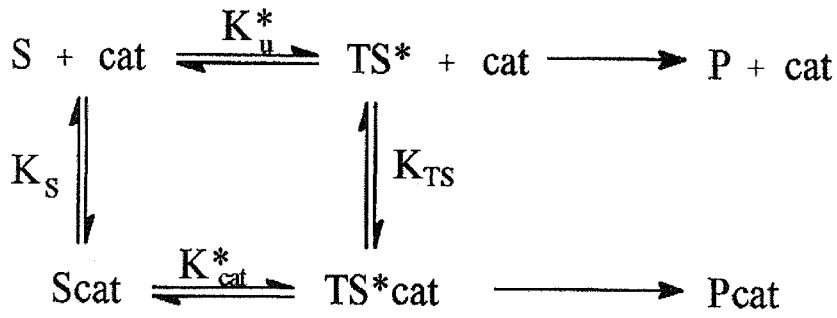

Scheme 1.16: Thermodynamic cycle showing the substrate and the transition state binding to the catalyst. Here, K_S and K_{TS} represent the binding constant of the substrate and the transition state to the catalyst: S = substrate, Cat = catalyst and TS = transition state.

From transition state theory the following Eyring equations are produced (1.28 and 1.29), representing the rate for uncatalysed and catalysed reactions, in which the equilibria between the substrate and the transition state when bound to catalyst K^*_{cat} and free in solution K^*_u are proportional to catalysed and uncatalysed rate constants:

$$k_{cat} = \kappa\,(kT/h)\,K^*_{cat} \qquad 1.28$$

$$k_u = \kappa\,(kT/h)\,K^*_u \qquad 1.29$$

k_{cat}, k_u are the observed rate constants for catalysed and catalysed reactions respectively, κ is the transmission coefficient, k is the Boltzmann constant, h is the planck constant and T is absolute temperature.

By comparing the rate constant for the catalysed reaction with the one for the uncatalysed reaction, Equation 1.30 is obtained.

$$\frac{k_{cat}}{k_u} = \frac{\kappa\left(\frac{kT}{h}\right)K^*_{cat}}{\kappa\left(\frac{kT}{h}\right)K^*_u} \qquad 1.30$$

As transmission is equal to 1 for a reaction in solution [173] and the term (kT/h) is constant, Equation 1.31 becomes:

$$\frac{k_{cat}}{k_u} = \frac{K^*_{cat}}{K^*_u} \qquad 1.31$$

From the thermodynamic cycle Scheme 1.16, the quotient of the constant formation of the transition state $\frac{K^*_{cat}}{K^*_u}$ can be equated with that of dissociation of the substrate K_S and the transition state K_{TS}. Thus, Equation 1.32 is obtained.

$$\frac{k_{cat}}{k_u} \approx \frac{K_{TS}}{K_S} \qquad 1.32$$

The tighter binding between the transition state and the catalyst, as compared to the binding between the catalyst and the ground state, is the source of the catalysis in the rate acceleration [173].

Tee [174] has shown that the transition state stabilisation model can be applied to micelle and cyclodextrin catalysed reactions to get information about the binding energy of the transition state to the catalyst, which is independent of any mechanism and the path of reaction, so K_{TS} can be compared with association constant of the reactants . Tee has stated that catalysis occurs due to stabilization of the transition state more than the ground state reactants by the catalyst [174].

1.7. Objective

In this work, detailed kinetic information will be presented concerning the reduction of peracid by iodide and sulfides in aqueous solvent, organized aqueous media (including non-ionic micelles), and α-cyclodextrin. The present study has several objectives. One is to add to existing knowledge about the reaction of peracid with both iodide and sulfides. The reaction between iodide and peracid has been studied previously at 25°C in non-ionic, anionic micellar and alpha cyclodextrin; while the reaction of sulfides and peracid has only been investigated in the presence of alpha cyclodextrin at one temperature. Therefore, this study will go further to investigate the effect of temperature on these reactions and show how a change in temperature can affect the process of reactants binding to the catalyst.

Another objective of the present study is to obtain quantitative information about reactivity in ordered aqueous media such as micellar systems and cyclodextrins, and find out how these media can effect and control these reactions. This could provide information about the process occurring in living cells by assuming that these organised media are similar to protein and membranes in their hydrophobicity. In addition, little information is known about bimolecular reactions involving two neutral reactants in non-ionic micelles where only the hydrophobic interaction is likely to influence the reaction due to the absence of charge-charge interaction.

Chapter 3 details the effect of buffer component concentrations and sodium perchlorate and sodium sulfate on the rate of reaction of iodide and 3-chloroperbenzoic acid in the absence and presence of a fixed amount of Brij-35. Following this there is a study of the nature and concentration of salt effects (including both those kosmotropic and chaotropic) on the rate constants and the substrate binding to Brij-35 of the reaction between iodide and 3-chloroperbenzoic (MCPBA). In addition, the influence of temperature on the reaction will be studied in the absence and presence of 0.35 M, 1 M SO_4^{-2}, and ClO_4^- respectively.

The multi micelle pseudo-phase model is used to analyze the kinetic data. The kinetic data will then be fitted to an appropriate equation to obtain certain parameters which will be used to construct a Van't Hoff and Eyring plot to calculate the enthalpy and entropy for the association constant from the binding constant, and the activation enthalpy and entropy from the rate constant respectively.

In Chapter 4, the reactions of a selected number of alkyl aryl sulfides with peroxymonosulfate (PMS) and 3-chloroperbenzoic have been studied in Brij-35 micelle. The effect of substituent position on the rate was also studied using ortho, meta and para-chlorothioanisole; the kinetic data was fitted universally. Universal fit allows us to get reliable values of thermodynamic and common K_P for all reactions, regardless of the sulfide substituent. Enthalpy and entropy changes obtained for the binding of sulfides from universal fit will be calculated.

These thermodynamic values will be calculated from both the Van't Hoff and Eyring plots. Such an analysis also indicates that the enthalpy-entropy compensation that previously existed for the reaction series is not an artefact, which is proved further by the method adopted in [142], where linear correlation between ln k_2 and ln k_1 is present.

Chapter 5 reports on a systematic study of the effects of α-CD on the rates of a range of alkyl aryl sulfides with peracid, namely MCPBA and PMS, at different temperatures. Cyclodextrins can form an inclusion complex with a wide range of guests, thus making them of special interest for use as a drug carrier, a preservative, or an odour mask. So, formation of an inclusion complex between cyclodextrins and sulfides can result in enhancement of solubility and also reduce the odour of some sulfides (such as phenyl methyl sulfides). However, it also makes them open to electrophilic attack by peracid. From this study the binding constant of the reactant and the transition state pseudo equilibrium constant will be calculated and compared with values found in literature. Also, from Van't Hoff plots the thermodynamic parameters for the binding of the substrate and the transition state will be obtained, which will give some insight into the force driving the binding.

Chapter 6 discusses the effect of α-cyclodextrin on the oxidation of iodide by MCPBA at different temperatures. From this study the thermodynamic parameters will be calculated, allowing some insight into the force and the mechanism driving the complexation.

Chapter 2 Materials and Methods

2.1. Materials

2.1.1. Peroxyacids

2.1.1.1. Source and preparation

The main oxidizing agent used in this work is 3-chloroperbenzoic acid (MCPBA), which was purchased from Sigma Chemical Company. It has purity of 80%, with the main impurity being the parent acid, 3-chlorobenzoic acid. As the solid 3-chloroperbenzoic acid is sparingly soluble in water, solutions of 3-chloroperbenzoic acid were normally prepared every four days by adding the required amount to distilled water and stirring for about an hour using a magnetic stirrer. This was filtered with a Duran Buchner funnel (75 ml) with a sintered disc (45 mm) of 16-40 micrometer pore diameter. The concentration of MCPBA was determined iodometrically, as described below. The required concentration for the working solution was obtained by further dilution in distilled water. The stock solutions of the MCPBA required regular standardisation due to their decomposition; they were normally used for up to four days. The other oxidant used was monoperoxysulfate, which was purchased from Sigma Aldrich as the triple salt, $KHSO_5.KHSO_4.K_2SO_4$. Due to its solubility the solid was weighted out, dissolved and made up to the required volume with distilled water to give the required stock solution concentration.

2.1.1.2. Iodometric titration acid determination

The concentration of peracid was determined by iodometric titration. Many methods to determine organic peracids exist [175]. Analytical reactions using iodine as the oxidizing agent are called iodimetry, while procedures using iodide ion as the reducing agent are called iodometry. The usual procedure involves the addition of an excess of iodide ion to the oxidizing agent analyte, in this case peracid, which produces iodine. This can be titrated with standard sodium thiosulfate solution.

The general method followed will now be explained. About 5 ml of 0.03 M potassium iodide and 10 ml of 2 M sulphuric acid were mixed in a 250 ml conical flask and 5.0 ml of the peracid was added by pipette and the mixture mixed thoroughly. The liberated iodine was titrated with the standard solution of sodium thiosulfate (0.01 M) until a pale yellow colour was obtained. Then a small amount of iodine indicator was added toward

the end of the titration. The end point was determined by a change in colour from pale blue to colourless. The reactions that take place are illustrated in Equation 2.1 to 2.3.

$$RCO_3H + 2\ I^- + 2\ H^+ \longrightarrow RCO_2H + H_2O + I_2 \qquad 2.1$$

$$2\ S_2O_3^{2-} + I_2 \longrightarrow S_4O_6^{2-} + 2\ I^- \qquad 2.2$$

From Equations 2.1 and 2.2

$$2I^- \equiv 2S_2O_3^{-2} \equiv RCO_3H \qquad 2.3$$

Therefore, the strength of metachloroperbenzoic acid can be calculated by the following equation:

[MCPBA] = V of $Na_2S_2O_3$ × 0.01 M / 2 × volume of MCPBA

[MCPBA] = 0.01 × titre / 10

So the measured volume of $Na_2S_2O_3$ in cm^3 is directly equal to the concentration of MCPBA in 10^{-3} mol dm^{-3}.

2.1.2. Surfactants and other materials

Potassium iodide (Analar reagent, 99.5%), sulphuric acid with minimum assay of 95%, glacial acetic acid (analytical reagent grade), sodium chloride (Analar reagent 99.9%), and sodium sulphate anhydrous (99%) were purchased from BDH. Sodium acetate (99%) and sodium nitrate (99%) were obtained from Aldrich. Sodium thiosulfate (99%) was purchased from Fisher Chemical Company. The four non-ionic surfactants used in this study are Brij 35 ($C_{12}E_{23}$), polyoxyethylene 10 lauryl ether ($C_{12}E_{10}$), Brij 700 ($C_{18}E_{100}$) and Brij 58 ($C_{16}E_{20}$). These linear polyoxyethylene (POE) alcohol surfactants are often represented as C_nE_m, where n is the number of carbons in the alkyl chain and m is the number of ethylene oxide units in the POE chain. These surfactants were purchased from the Aldrich Chemical Co. Ltd and were of the highest grade available. Also, non-ionic triblock copolymer, which is also known as pluronic-104, was purchased from BSFA.

The reactants and reagents were prepared in distilled water. In the case of other solid salts, the exact amount was weighed out and dissolved in distilled water and made up to the required volume with distilled water to obtain the stock solution. Brij-35 (25 g) was dissolved in about 200 ml of distilled water with a little heat (40 C^o), using a magnetic

stirrer to speed up the process. This took about two hours and was then made up to 250 ml with distilled water to obtain the required stock solution. Potassium iodide (4.15g) was dissolved and made up to 250 ml in a volumetric flask to obtain a stock solution of 0.1 M.

2.1.3. Sulfides source and its preparation

The organic sulfides used as nucleophiles in this study were all obtained from Aldrich. Their chemical structures and purity levels are listed in Table 2.1 below. They were used without further purification. The solution of sulfide was prepared as previously stated [164], and a small amount was weighted and dissolved in distilled water and stirred for several hours. It was then filtered with a scintered glass to remove undissolved materials. The concentrations of each sulfide were calculated based on their extinction coefficient [164]. Absorbance of the stock solution of the alkyl aryl sulfide was measured using a UV spectrophotometer, and from the absorbance the concentrations were calculated using the Beer-Lambert low equation shown below:

$$A = c\,l\,e$$

A denotes the absorbance and c, l and e represent the concentration, cell length and absorpitvity respectively.

The other chemical compounds used included peroxymonosulfate (98%) obtained from Aldrich and MCPBA, which have already been mentioned in the first section along with all the other chemicals.

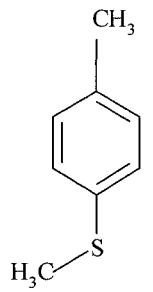

methyl p-tolyl sulfide

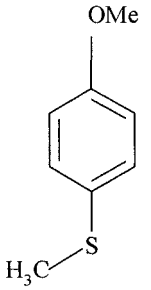

4-methoxythioanisole

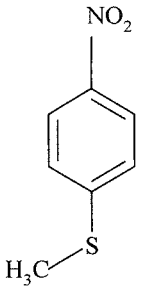

4-nitrothioanisole

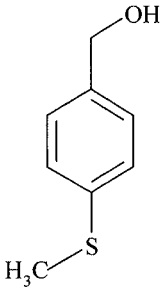

4-(methylthio)benzyl alcohol

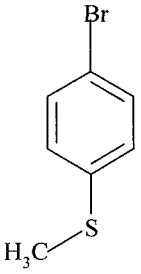

4-bromothioanisole

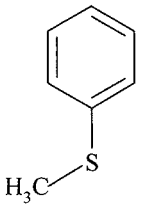

methyl phenyl sulfide

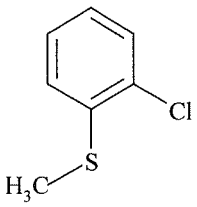

2-chlorothioanisole

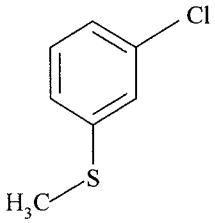

3-chlorothioanisole

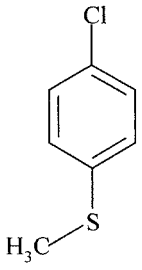

4-chlorothioanisole

Table 2.1: Chemical structures of aryl alkyl sulfides used in this study.

2.2. Methods

2.2.1. UV/visible spectrophotometry

The spectrum of the product of the reaction between peracid and iodide was measured using an Ultraviolet 300 evolution spectrophotometer. The machine was zeroed using distilled water in the two cell compartments and the reference spectrum was taken. Then the required volume of the reactant was mixed in the cuvette, which was introduced into the front cell compartment, and its spectrum was measured. Maximum absorption of iodine (as triiodide) occurs at 351 nm. This wavelength was used in the subsequent experiments to follow the reaction kinetically.

2.2.2. Stopped flow method

Usual spectrophotometric techniques cannot be used when investigating reactions that take place at millisecond rates. If reactants are added by hand and then stirred for a few seconds to allow adequate mixing, the reaction is over and no changes in spectra are recorded. For some reactions the time required to mix the reactants together may be comparable to the reaction time. That is, the half-life of the reaction occurs in approximately the same timescale as the mixing. This is overcome by using a stopped-flow apparatus.

An SX-17MV Stopped Flow Reaction Analyser from Applied Photophysics was used to measure the rate of the reaction between iodide and MCPBA, and also the oxidation of sulfides with peracids: In this method, the reactants are injected simultaneously into a mixing chamber, where they begin to react, and are then moved quickly through a spectrophotometer cell and finally to a stopping syringe. This stopping syringe fills and drives its plunger back against a stopping block. This stops the flow and triggers the activation of data acquisition on a computer. The progress of the reaction is followed by monitoring a change in absorbance of either a reactant or product in the spectrophotometer cell. The time that is required for the reactant and products to travel to the spectrophotometer cell is known as the dead time.

Calibration of the stopped flow is carried out before every experiment using distilled water in both syringes. Following that, the syringes are filled with the relevant solutions. Air bubbles are removed before the runs by flushing backward and forward between the drive syringes and the reservoir syringes many times. The kinetic run and the depression of the two reactants from syringes into the reactor chamber are done automatically. This forces the unreacted solution into the flow cell and also forces the reacted solution out of the cell.

Where different concentrations were used, care was taken to flush the system with water. Emptying the stopping syringe was done by turning the control valve to the drive position and pushing the water manually from the drive syringe through the flow circuit and into the stopping syringe. The stopping syringe was empted three or more times to ensure the system was flushed out effectively.

For the kinetic run, first the wavelength 351 nm for the reaction between MCPBA and iodide was set up, and for each reaction an average of about 5 runs (unless otherwise stated) was automatically obtained. The temperature was controlled using a circulating

water heating bath with temperature controller. The temperature in the reaction chamber was measured by a thermocouple attached to it and the reading was shown on the computer. The reduction of MCPBA by the iodide in acetate buffer and 0.003 M nitric acid was followed by measuring the absorbance of the product, triiodide anion, at 351nm using the stopped flow method.

2.2.3. Analysis of the kinetic data

The pseudo-first order rate constant obtained from the stopped flow was calculated using single exponential, floating end point, non-linear regression for the change of absorbance with time by the stopped flow programme.

The equation used is of the form

$$A_\infty - A = (A_\infty - A_0)\, e^{-kobs\, t}$$

Here, k_{obs} denotes the pseudo-first order rate constant, A_0 is the initial absorbance, A_∞ is the final absorbance, and t is the time. The path length of the spectrophotometer cell is 1 cm.

Chapter 3 The reduction of 3-chloroperbenzoic acid by iodide in presence of non-ionic surfactants.

3.1. Introduction

This chapter details the reaction of iodide with 3-chloroperbenzoic acid (MCPBA) in different conditions and at different reactant concentrations and temperatures. It will also discuss the effect of salt, from which the mechanism and the factors affecting the rate can be inferred. The main objective of this chapter is to investigate the effect of Brij on the peracid – iodide reaction at varying temperatures and salt concentrations. From the temperature dependence, which has not been reported before for this reaction, the binding of the substrate to the micelle, as well as the thermodynamic parameters, can be calculated and compared for different conditions.

The reaction between 3-chloroperbenzoic acid (MCPBA) and iodide is a very well known reaction, having previously been studied by Secco and Venturini [17]. They found that the reaction is independent of salt and hydrogen ion concentrations. However, a hydrogen bond accepting solvent like 1,4- dioxane decreases the rate of the reaction because it stabilises the initial state with respect to the transition state; while the reaction rate is enhanced by hydrogen bond donor solvents, which minimise charge separation and stabilise the transition state structure 3.1 (with R = H for water) [17].

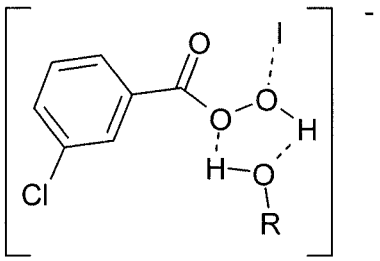

Structure 3.1

The reaction is outlined in Scheme 3.2. The nucleophilic iodide attacks the outer oxygen of the peracid to form IOH and the corresponding parent acid, IOH, reacts with I^- to form iodine, which equilibrates with iodide to form triiodide.

$$RCO_3H + I^- \longrightarrow IOH + RCO_2^-$$

$$IOH + I^- \longrightarrow I_2 + HO^-$$

$$I_2 + I^- \rightleftharpoons I_3^-$$

Scheme 3.2

Bimolecular reactions in micellar systems have been modelled by Berezin and co-workers [31]. They suggest that partitioning of the reactants between the bulk aqueous phase and the micellar pseudophase leads to the catalysis and inhibition of reactions when the reactants are first concentrated and then diluted in the micellar pseudophase as the concentration of the surfactant is increased. Davies and co-workers [101] have studied the effect of surfactants, including Brij-35 and Triton.100, on the kinetics of the reaction of iodide with different peracids. The reaction of iodide and MCPBA has also been investigated in the mixed surfactant system of Brij-35/SDS. A non-ionic micelle enhances the rate to a maximum at higher surfactant concentrations and then becomes stable, which indicates that the micelle is saturated by reactants. Also, by adding the anionic surfactant, sodium dodecyl sulfate, the rate is inhibited, which is attributed to the exclusion of the iodide from the anionic micelle as a result of electrostatic repulsion [102].

3.2. Experimental work

3.2.1. Kinetic measurements

The reactions were studied on an Applied Photophysics SX17 MV stopped-flow spectrophotometer, as stated in Chapter 2. The temperature was maintained at 25°C by circulating water from a thermostated bath around the injection syringes and the chamber of reaction.

A typical run was carried out by filling one of the injection syringes with a solution containing the peracid and the surfactant, and another with the iodide and buffer or the salts. Pseudo first order conditions of the reaction were assured by using a large excess of

iodide over MCPBA. Rapid mixing of the reaction mixtures from the reservoirs in this apparatus was performed using high pressure nitrogen gas (5 bar).

3.2.2. Determination of the rate constant

The initial concentrations of peracid and iodide were 4 x 10^{-6} M and 1.5 x 10^{-3} M respectively, unless stated otherwise. Reactions were carried out in 0.003 M nitric acid. At this level of acidity the parent 3-chlorobenzoic acid that is present as an impurity in the peracid, and a product of its reaction with iodide, is unionised, and so will not contribute any charge to the micelles. Also, the acidity is sufficiently low so that the acid catalysed aerobic oxidation of iodide, which interferes with the measurement of its reaction with peracid, is negligible, except in the most unfavourable conditions of high surfactant and sulfate concentrations.

The reaction was followed by monitoring the absorbance of the triiodide I_3^- at 351 nm for experiments where acetate buffer was used, and at 290 nm when the reaction was carried out in nitric acid of 0.003 M. Pseudo first order rate constants were evaluated from the nonlinear plots of absorbance versus time using Equation 3.4 (shown below); the change in the absorbance is proportional to the amount of triiodide formed, which from Scheme 3.2 is equivalent to the amount of MCPBA consumed.

$$\frac{-d[MCPBA]}{dt} = k_{obs}\,[MCPBA] \qquad 3.1$$

$$\frac{-d[MCPBA]}{[MCPBA]} = k_{obs} \times dt$$

$$\ln[MCPBA] = -k_{obs} \times t + C \qquad 3.2$$

when t = o, [MCPBA] = $[MCPBA]_o$

$$C = \ln\,[MCPBA]_O$$

Substituting C in Equation 3.2 gives

$$\ln[MCPBA] = -k_{obs} \times t + \ln[MCPBA]_O$$

Which can be written as

$$\ln(A_\infty - A_t) = -k_{obs} \times t + \ln(A_\infty - A_O) \qquad 3.3$$

This can be written in another form

$$(A_\infty - A_t) = (A_\infty - A_o) \exp -k_{obs} \times t \qquad 3.4$$

Here, k_{obs} denotes the pseudo first order rate constant Equation 3.5, A_o is the initial absorbance, A_∞ is the final absorbance, and t is the time.

$$k_{obs} = k\ [I^-] \qquad 3.5$$

Where k is the second order rate constant and can be obtained from the plot of the observed first order rate versus the concentration of iodide.

3.2.3. Fitting of the kinetic data

All the kinetic data for the oxidation of iodide by MCPBA obtained from the stopped flow machine was fitted locally using the Grafit programme [176] to Equation 3.6.

$$k_{obs} = \frac{k_w + (k_{mic} - k_w \bar{V}_{mic})([S] - CMC)}{\{1 + (K^{PH}_{mic} - \bar{V}_{mic})([S] - CMC)\}\{1 + (K^{I}_{mic} - \bar{V}_{mic})([S] - CMC)\}} \qquad 3.6$$

For the multiple micellar pseudophase (MMPP) model [101], k_w is the pseudo first order rate constant in the aqueous pseudophase at the cmc, k_{mic} is the observed second-order rate constant in the micellar pseudophase, K^{PH}_{mic} and K^{I}_{mic} are the micellar equilibrium constants of the respective reactants, and $\bar{V}_{mic}$ is the molar volume of the micellized surfactant, which is estimated to be 1.2 $dm^3\ mol^{-1}$ [1, 102].

3.3. Results

3.3.1. Rate-dependence on the reactants concentration.

In a typical run for the uncatalysed reaction, a plot of k_{obs} versus iodide concentration gave a straight line with a slope equal to $(4.5 \pm 0.101) \times 10^3$ M^{-1} s^{-1}. Figure 3.1 indicates that the reaction under the chosen conditions follows the pseudo first order rate kinetic in which the rate is increased by increasing the iodide concentration; hence the order with respect to iodide is unity. The influence of the concentration of MCPBA acid on the reaction rate was studied in different experimental conditions with 0.0015 M of iodide and 0.1 M buffer acetate in presence of 0.01 M of Brij-35, as shown in Figure 3.2. There was no effect of varying the peracid concentration on the rate constant; for example, 4.2×10^{-5} M gives a rate constant of 19.12 s^{-1}, which is close to the value obtained at 2.1×10^{-4} M of MCPBA (19.23 s^{-1}), thus confirming that k_{obs} is independent of MCPBA.

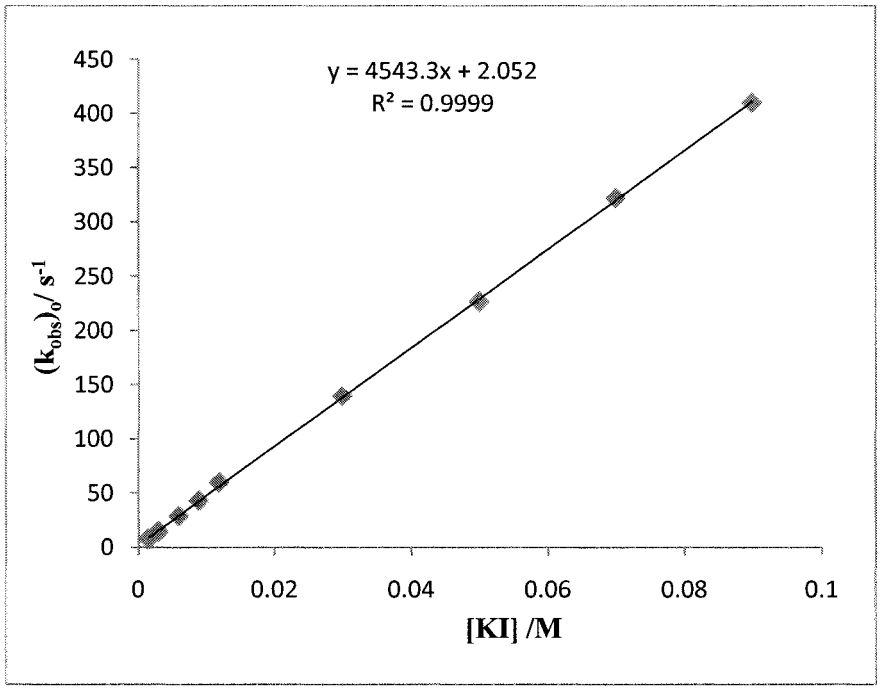

Figure 3.1: Plot of observed rate constant versus iodide concentration with 4.5×10^{-6} M MCPBA and 0.1 M buffer at 25°C.

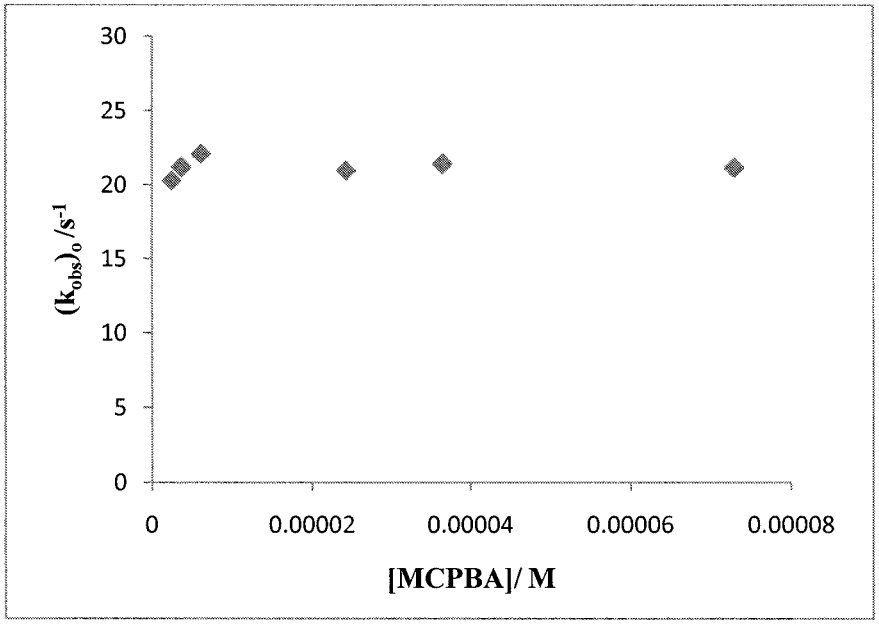

Figure 3.2: Plot of observed rate constant against concentration of MCPBA at 0.0015 M potassium iodide and 0.1 M acetate buffer in presence of 0.01 M at 25°C.

3.3.2. The effect of varying the buffer concentration and ionic strength in the absence and presence of Brij-35

In this section the effect of various reagents, including the buffer component, on the reduction of peracid by iodide will be investigated in the absence and presence of Brij-35. The effect of varying the acetate buffer concentration from 0.01 to 0.1 while keeping the ionic strength constant at 0.1 M using sodium nitrate is illustrated in Figure 3.3a Figure 3.3b shows the effect of sodium nitrate concentrations on the k_{obs} in two different conditions (absence and presence of 0.0033 M Brij-35). It can be seen that there is quite a decline in the rate as the sodium nitrate concentrations increase in the presence of 0.0033 M of Brij-35, and that the decrease in the rate is greater in the presence of high Brij-35, which can be seen from the slope in Figure 3.3b, compared to that in the absence of Brij-35. The influence of an added buffer was analysed as the added salt effect. The concentration of sodium acetate was varied at constant concentration of acetic acid and sodium nitrate. In this case not much of an effect was observed. For comparison, the effect of varying the buffer components on the rate constant in the absence and presence of 0.0033 M of Brij-35 is plotted in Figure 3.3c and Figure 3.3d.

In addition, the effect of the ionic strength on the rate of the reaction was investigated by varying the concentration of $NaNO_3$ from 0.01 to 0.09 M, keeping other conditions

constant, and in the absence of Brij-35. The results obtained are graphically plotted in Figure 3.4. Log of k_{obs} versus square root of ionic strength is linear with a slope of 0.03, which shows that one of the reactants bears no charge and thus the rate is independent of the ionic strength.

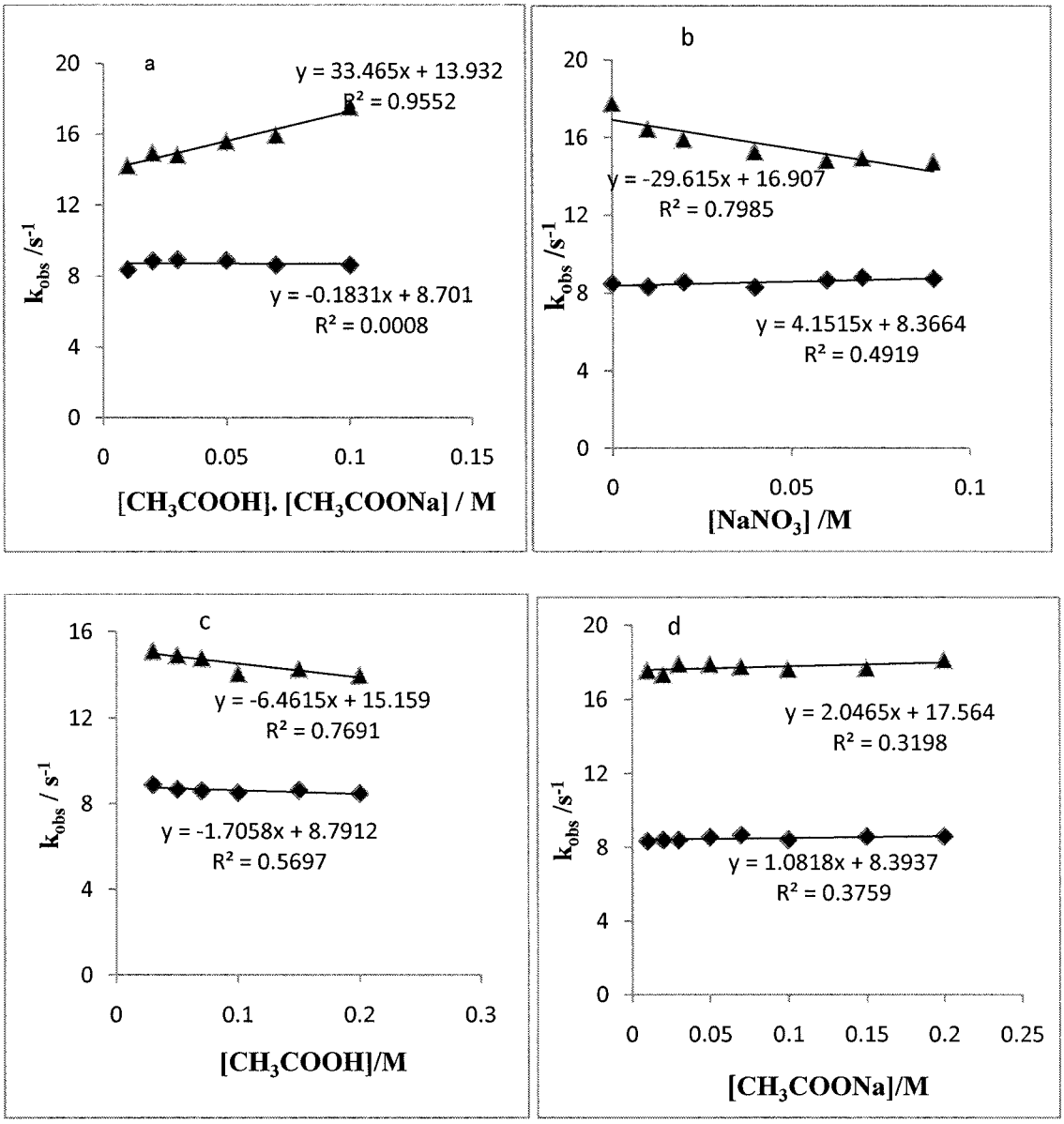

Figure 3.3: Observed rate constant versus buffer component and sodium nitrate concentration. Reaction conditions are 0.0015 M of potassium iodide and 4×10^{-6} M MCPBA at 25° C with zero Brij-35 (filled diamonds), 0.0033 M Brij-35 (filled triangles),

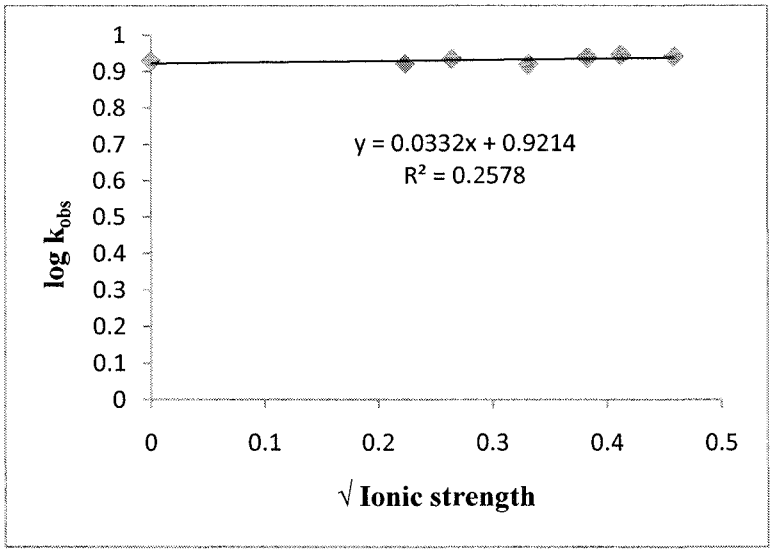

Figure 3.4: The effect of the ionic strength on the reaction between iodide 0.0015 M with 4×10^{-6} M of MCPBA in 0.01 M buffer acetate at 25°C.

3.3.3. The effect of salt concentrations on the rate in the absence of Brij-35 and in the presence of fixed Brij-35 concentration.

The influence of the concentration of added salts, sodium sulfate,sodium perchlorate and sodium chloride, on the reaction in the absence and at a fixed concentration 0.003 M of Brij-35 was investigated with reactant concentration of 0.0015 and 4×10^{-6} M for iodide and MCPBA respectively. The observed rate versus the salt concentration is graphically shown in Figures 3.5a to c. The rate in the absence of surfactants is insensitive to added electrolytes; the same has been found in a previous study [100]. When the effect of salt on the reaction rate was studied in the presence of fixed Brij-35 concentration the observed rate increased in the presence of sulphate (Figure 3.5c), while the effect of increasing the perchlorate had the opposite effect (Figure 3.5a). The sodium chloride seemed to have no effect on the rate of the reaction, as shown in Figure 3.5b.

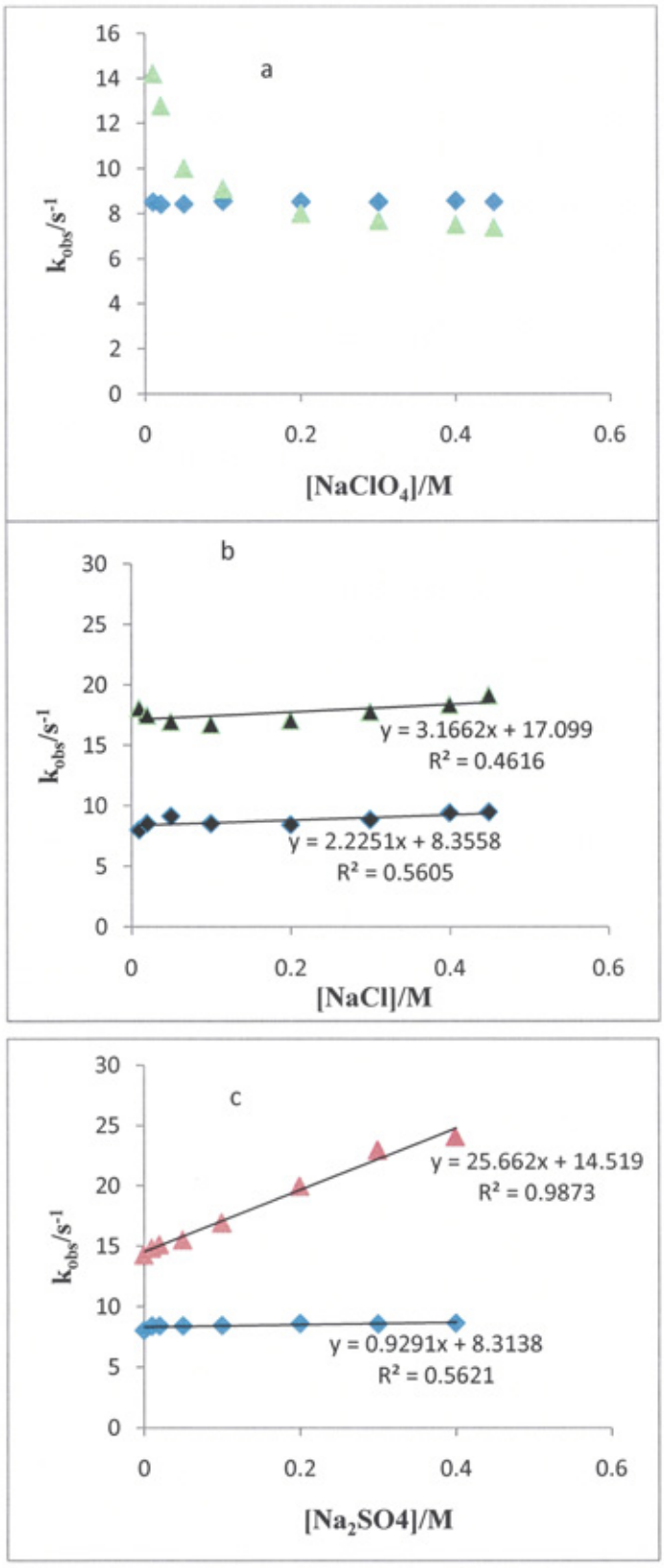

Figure 3.5: Plot of salt concentration against the rate constant for the reaction between 0.0015 M iodide and 4×10^{-6} M MCPBA, with an acetate buffer strength of 0.01M at 25C^{o}. Diamonds and triangles indicate the reaction carried out in the absence and presence of 0.003 M Brij-3.

3.3.4. Effect of $[H^+]$ on $k_{obs.}$

To study the effect of $[H^+]$ on the rate, kinetic runs were carried out using HNO_3 to vary the hydrogen ion concentration. The remaining conditions were kept constant (0.0015 M potassium iodide and 4.6×10^{-6} M MCPBA). The effect of the $[H^+]$ was investigated in the absence and presence of 0.013 M Brij-35. It was observed that the rate is independent of the concentration of acid. The plot of k_{obs} versus $[H^+]$ is shown in Figure 3.6. Thus, nitric acid was chosen as reaction media.

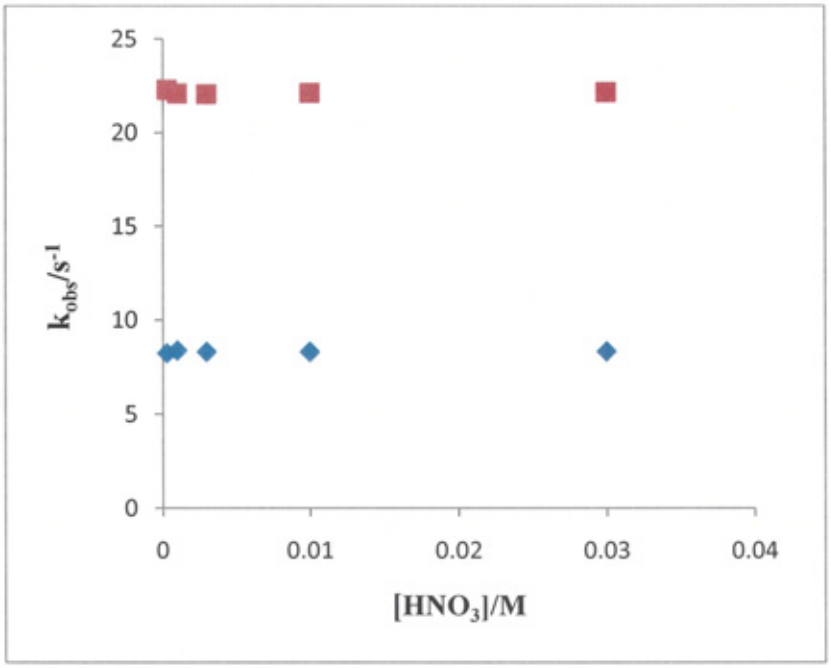

Figure 3.6: The effect for $[H^+]$ on the observed rate constant for the reaction of iodide with MCPBA in the absence of Brij-35 (filled diamonds) and in the presence of 0.013 M Brij-35 (filled squares) at 25°C.

3.3.5. The dependence of the observed rate constant on reactant concentrations in the absence and presence of Brij-35 in 0.003 M nitric acid

In order to investigate whether the reaction remains second order in these acid conditions, a number of runs were carried out in the presence of a fixed concentration of Brij-35, comparing the findings to the reaction in the absence of Brij-35. The data are plotted in Figure 3.7 and Figure 3.8. The results show that increasing the iodide concentration leads to an increase in the observed rate in the absence and presence of Brij-35, which indicates that the reaction follows a similar mechanism to that in acetate buffer; thus, further study can be conducted.

As required for a second order reaction under pseudo first order conditions, k_{obs} (in 1.1 x 10^{-2} M Brij-35) is directly proportional to iodide concentration over the range 7 x 10^{-4} M to 3 x 10^{-3} M. At higher concentrations there is a slight negative deviation from linearity. Also as required, k_{obs} is independent of peracid concentration between 1.8 x 10^{-6} M and 3.7 x 10^{-5} M (in 3.3 x 10^{-3} M Brij-35).

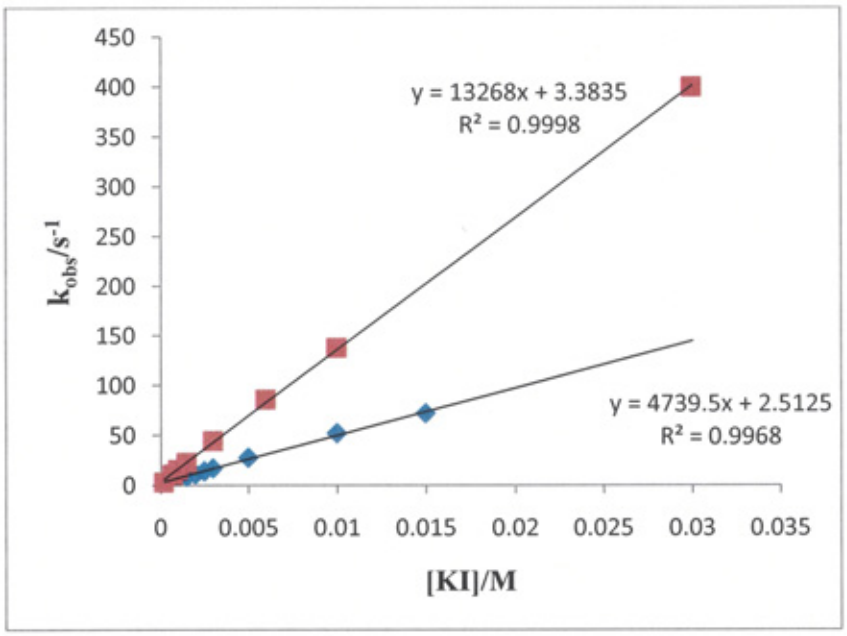

Figure 3.7: Observed rate constant versus iodide. Other conditions are 4×10^{-6} M of MCPBA, 0.003 M nitric acid in the absence of Brij-35 (filled diamonds) and presence of 0.011M Brij-35 (filled squares) at 25°C.

It has been observed that for non-ionic surfactants, CMC decreases with an increase in temperature due to an increase in hydrophobicity caused by the destruction of hydrogen bonds between water molecules and hydrophilic groups. The plot of log CMC against 1/T is almost linear [34], and as the process of micellization is one of the most important characteristics of a surfactant solution [75], this plot is used to derive the thermodynamics of micelle formation, which can help us to understand the nature of thermodynamics and the driving force behind micelle formation.

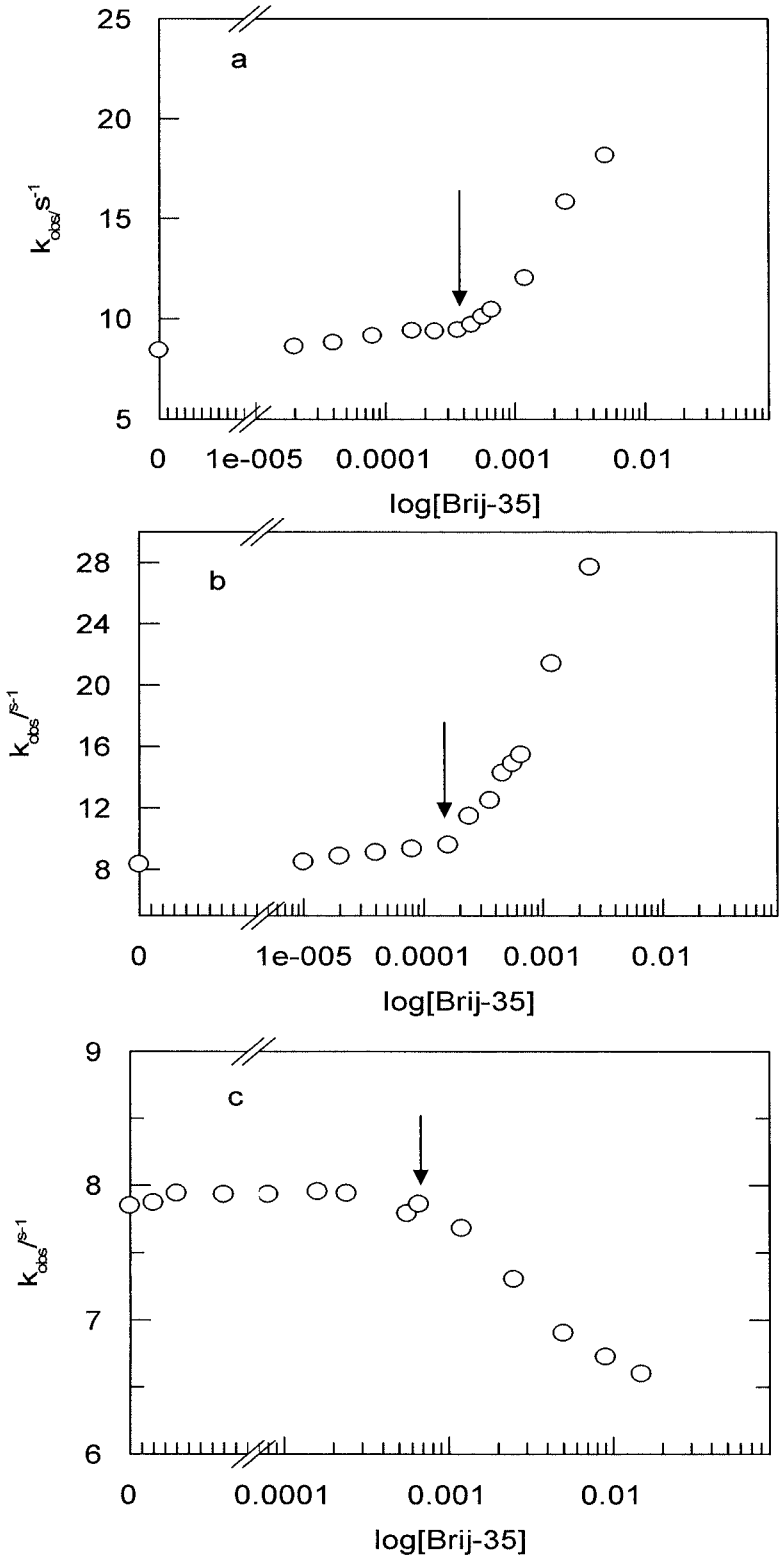

Figure 3.9: Observed rate constant versus logarithm of Brij-35 concentration for the reaction in water (a), 0.35 M sulfate (b), and 1 M perchlorate (c) at 25°C.

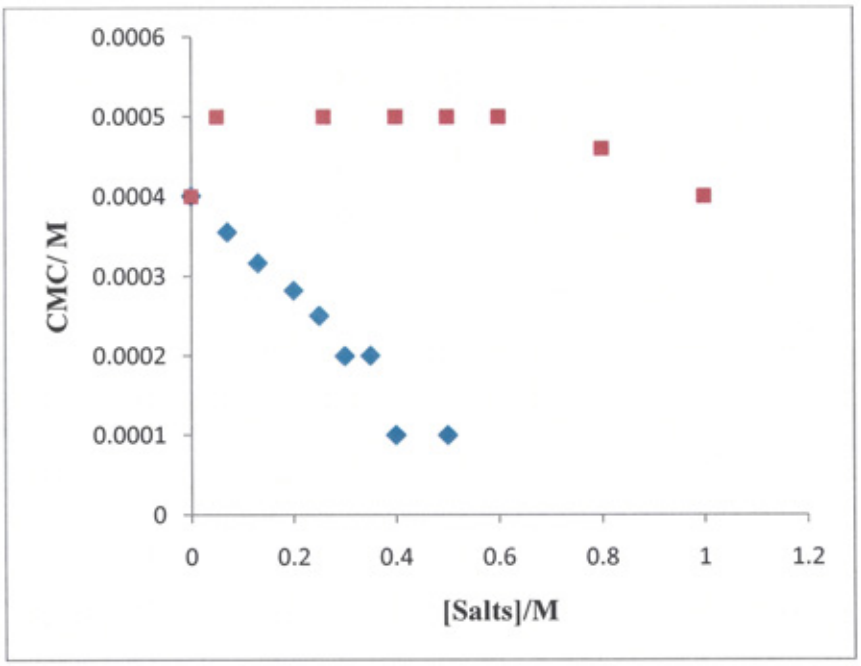

Figure 3.10: Critical micellar concentrations at different added salt concentrations. Squares represent perchlorate and diamonds represent sulfate.

Table 3.1: Effect of sodium sulfate: best fit parameters and their standard deviations, according to Equation 3.6, for the reaction of *ca.* 4×10^{-6} M MCPBA and 1.5×10^{-3} M iodide in 3.0×10^{-3} M nitric acid at 25°C.

$[Na_2SO_4]$, M	$(k_{obs})_o$, s^{-1}	CMC, 10^{-4} M	k_w, s^{-1}	$k_{mic} - k_w \overline{V}_{mic}$, $10^3 M^{-1}s^{-1}$	$K^{PH}_{mic} - \overline{V}_{mic}$, 10^2 M^{-1}	$K^{I}_{mic} - \overline{V}_{mic}$, M^{-1}	K_{TS}, M^{-1}	K_{TS}/K_P
0.07	8.7	3.6	9.3 ± 0.2	8.5 ± 0.6	2.0 ± 0.2	7.1 ± 1.2	977	4.8
0.13	8.4	3.2	10.0 ± 0.1	9.2 ± 0.4	2.0 ± 0.2	8.5 ± 0.8	1095	5.5
0.20	8.4	2.8	8.4 ± 0.4	12.4 ± 1.1	2.6 ± 0.3	6.9 ± 1.4	1476	5.7
0.25	8.3	2.5	10.3 ± 0.2	13.4 ± 0.8	2.6 ± 0.3	8.1 ± 1.2	1614	6.2
0.30	8.7	2.0	10.0 ± 0.3	14.7 ± 1.1	2.5 ± 0.3	12 ± 3	1690	6.8
0.35	8.3	2.0	10.5 ± 0.3	16 ± 1.2	3.2 ± 0.4	4.5 ± 1.4	2108	6.5
0.40	8.8	1.6	10.9 ± 0.2	23.3 ± 1.2	4.1 ±0.3	6.4 ± 1.2	2648	6.5
0.50	8.9	1.0	10.2 ± 0.3	24.0 ± 0.9	3.9 ± 0.2	7.2 ± 0.8	2697	6.9

Table 3.2: Effect of sodium perchlorate: best fit parameters and their standard deviations, according to Equation 3.6, for the reaction of *ca.* 4 x 10^{-6} M MCPBA and 1.5 x 10^{-3} M iodide in 3.0 x 10^{-3} M nitric acid at 25°C.

$[NaClO_4]$, M	$(k_{obs})_o$, s^{-1}	CMC, 10^{-4} M	k_w, s^{-1}	$k_{mic} - k_w\overline{V}_{mic}$, 10^3 M^{-1} s^{-1}	$K^{PH}_{mic}-\overline{V}_{mic}$, 10^2 M^{-1}	$K^{I}_{mic}-\overline{V}_{mic}$, M^{-1}	K_{TS}, M^{-1}	K_{TS}/K_P
0.05	8.5	5.0	9.6 ± 0.2	2.7 ± 0.6	1.4 ± 0.4	2.6 ± 1.6	317	2.2
0.26	8.2	5.0	8.1 ± 0.02	1.0 ± 0.2	1.5 ± 0.3	-0.4 ± 0.2	122	0.8
0.40	7.9	5.0	7.9 ± 0.05	0.9 ± 0.2	1.5 ± 0.4	-1.3 ± 0.3	114	0.76
0.50	8.0	4.5	8.0 ± 0.04	0.8 ± 0.2	1.4 ± 0.3	-1.8 ± 0.5	100	0.7
0.60	8. 1	4.5	7.5 ± 0.03	0.9 ± 0.3	1.5 ± 0.4	-0.9 ± 0.5	111	0.74
0.80	8.1	4.0	7.7 ± 0.02	0.8 ± 0.1	1.4 ± 0.2	-2.1 ± 0.4	99	0.7
1.00	7.8	4.0	7.8 ± 0.06	0.92 ± 0.3	1.6 ± 0.6	-0.73 ± 0.9	118	0.72

3.3.7. Effect of Non-ionic surfactants on the rate of reaction

In this section a variety of Brij surfactants will be used to examine the effect of chain length on the reduction of peracid. The reaction of iodide with MCPBA was carried out in the presence of a non-ionic micelle of polyoxyethylene type. These surfactants were chosen because they have different lengths of hydrophobic chain and head group, and so the influence of the hydrophobic interaction can be investigated. Table 3.3 shows some of the properties of these surfactants. The CMC values in the table were obtained using a surface tension method.

For the four surfactants studied, the variation of k_{obs} in the absence of added salt over the full range of surfactant concentrations above the CMC is shown in Figure 3.11. The data is fitted according to Equation 3.6[101] using non-linear regression. The results are shown in Table 3.4 together with, $(k_{obs})_o$, the independent value of the rate constant in the absence of surfactant.

Table A1 in appendix A lists the kinetic data with their standard error obtained from the stopped flow method for $C_{12}E_{10}$, $C_{16}E_{20}$ and $C_{18}E_{100}$.

Table 3.3: Non-ionic surfactant properties with CMC values measured by surface tension and dye absorption.

Surfactant	Name	(HLB)[178]	N	CMC/ 10^{-5}M Surface tension	CMC/ 10^{-5}M Dye absorption	Chemical formula
$C_{12}E_{10}$	Polyoxyethylene 10 lauryl ether	12	59[177a]	9[177b]		$C_{12}H_{25}(OCH_2CH_2)_{10}OH$
$C_{12}E_{23}$	Brij 35	17	40	5.3[177c] 6.8[180] 6[177b]	3.8[177c]	$C_{12}H_{25}(OCH_2CH_2)_{23}OH$
$C_{16}E_{20}$	Brij 58	16	93[179]	0.9[177c] 1[180]	2.4[177c]	$C_{16}H_{33}(OCH_2CH_2)_{20}OH$
$C_{18}E_{100}$	Brij 700	18				$C_{18}H_{37}(OCH_2CH_2)_{100}OH$

Where HLB and N denote hydrophile-lipophile balance and aggregation number of micelle respectively.

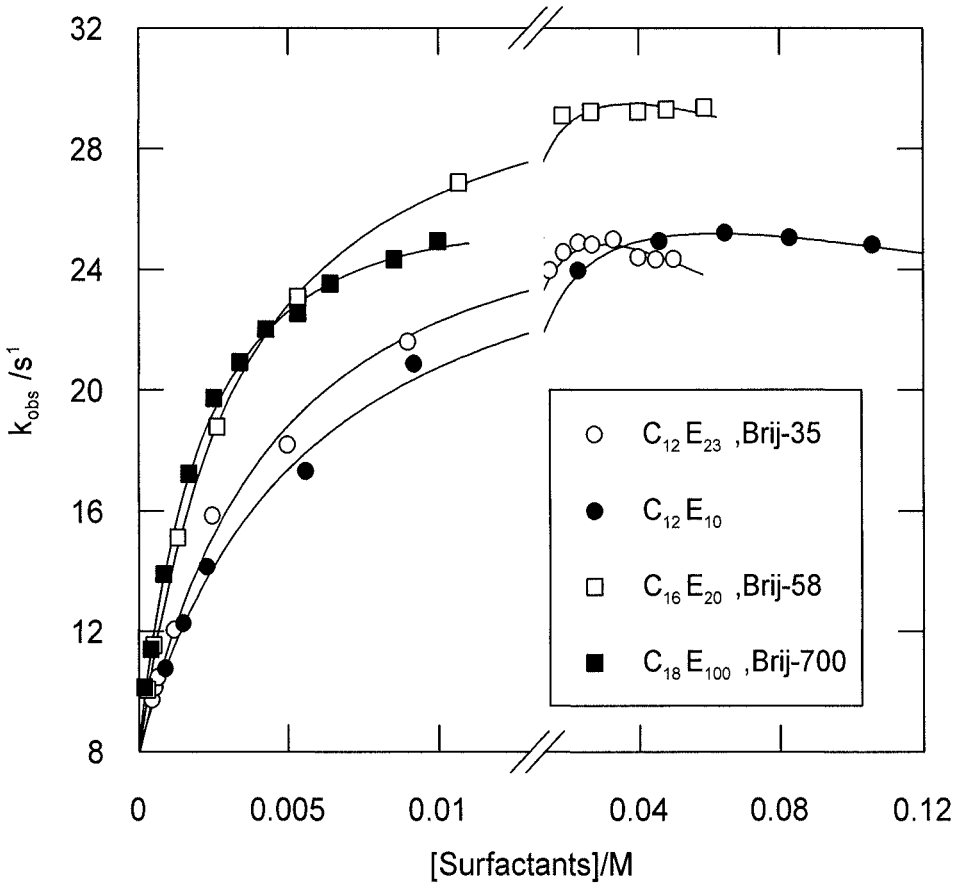

Figure 3.11: Effect of different surfactants on the reaction in 3.0 x 10^{-3} M nitric acid at 25°C. The curves represent the best fit values of Equation 3.6, shown in Table 3.4.

Table 3.4: Effect of different surfactants: best fit parameters and their standard deviations, according to Equation 3.6, for the reaction of *ca.* 4 x 10^{-6} M MCPBA and 1.5 x 10^{-3} M iodide in 3.0 x 10^{-3} M nitric acid at 25°C.

Surfactant	CMC, 10^{-4} M	k_w, s^{-1}	$k_{mic} - k_w \overline{V}_{mic}$, 10^3 M^{-1} s^{-1}	$K^{PH}_{mic} - \overline{V}_{mic}$, 10^2 M^{-1}	$K^{I}_{mic} - \overline{V}_{mic}$, M^{-1}	K_{TS}/M^{-1}	K_{TS}/K_P
$C_{18}E_{100}$	2.0	9.5 ± 0.1	11.5 ± 0.9	3.7 ± 0.5	7.4 ± 5.4	1210	3.27
$C_{16}E_{20}$	3.0	9.6 ± 0.1	8.8 ± 0.4	2.6 ± 0.2	1.8 ± 0.4	920	3.5
$C_{12}E_{23}$	3.8	9.5 ± 0.2	5.4 ± 0.5	1.7 ± 0.4	4± 1.1	631	3.7
$C_{12}E_{10}$	4.0	9.4 ± 0.3	4.5 ± 0.6	1.6 ± 0.3	1.0 ± 0.5	478	2.98

3.3.8. The effect of Brij-35 concentrations on the observed rate in the presence of fixed salt concentration

The reduction of peracid by iodide in the presence of Brij-35 at 25°C has been studied previously, as stated at the beginning of this chapter, and the kinetic data was treated by MMPP so as to obtain the binding constant of the substrates to the micelle. However, there has been no study of the effect of salt on this reaction in the presence of a micelle. Hence, this section deals with the effect of salt concentrations and types on this reaction.

The value of the cmc, shown in Table 3.5 and obtained as shown in Figure 3.9, is substituted into Equation 3.6 and the best fit values of the other parameters are determined using non-linear regression. The results are shown in Table 3.5, together with $(k_{obs})_o$, the value of the rate constant in the absence of the surfactant. It is clear that k_w values are slightly larger than $(k_{obs})_o$ (see Figure 3.14d and Figure 3.15d). The values of $k_{mic} - k_w\overline{V}_{mic}$ and $K_{mic}^{PH} - \overline{V}_{mic}$ are large and determined with reasonable precision, as judged by their standard deviations. The values of $K_{mic}^{I} - \overline{V}_{mic}$ are small and their relative standard deviations are slightly larger than those of the other parameters. This means that they cannot be determined with great accuracy.

The kinetically obtained data for the reaction of 0.0015 M iodide with 4×10^{-6} M MCPBA in the presence of various concentrations of sodium sulfate and Perchlorate at various Brij-35 concentrations are listed in Table A2 and Table A3 in appendix A, and graphically fitted to Equation 3.6 and shown in Figure 3.12 and Figure 3.13. The best fit parameter was obtained by fitting the kinetic data to Equation.3.6, and was then plotted versus the concentration of sulfate and perchlorate in Figure 3.14 and Figure 3.15 respectively.

k_w and k_{mic} are the rates in the aqueous and micellar pseudo phase, K_{mic}^{I} and K_{mic}^{PH} are the binding constants of iodide and MCPBA to the micelle respectively (written in the following text as K_I and K_P), and [S] and CMC represent the concentration of micellized surfactant and the critical micellar concentrations. The binding of the transition state is given by Equation 3.7.

$$K_{TS} = \frac{k_{mic}}{(k_{obs})_o} \qquad 3.7$$

Table 3.5: Effect of different salts: best fit parameters and their standard deviations, according to Equation 3.6, for the reaction of *ca.* 4 x 10^{-6} M MCPBA and 1.5 x 10^{-3} M iodide in 3.0 x 10^{-3} M nitric acid at 25°C.

Salt	*Conc, M*	$(k_{obs})_o$, s^{-1}	CMC, 10^{-4} M	k_w, s^{-1}	$k_{mic} - k_w \overline{V}_{mic}$, 10^3 M^{-1} s^{-1}	$K^{PH}_{mic} - \overline{V}_{mic}$, 10^2 M^{-1}	$K^{I}_{mic} - \overline{V}_{mic}$, M^{-1}
None	0	8.4	4.0	9.4 ± 0.2	5.4 ± 0.5	1.7 ± 0.2	4 ± 1.2
Na_2SO_4	0.5	8.9	1.0	10.2 ± 0.3	24.0 ± 0.9	3.9 ± 0.2	7.2 ± 0.8
$NaClO_4$	1.0	7.9	4.0	7.8 ± 0.1	0.92 ± 0.3	1.6 ± 0.6	-0.73 ± 0.9
NaCl	1.0	9.3	3.0	10.3 ± 0.4	7.4 ± 1.1	1.8 ± 0.4	8.5 ± 2.5

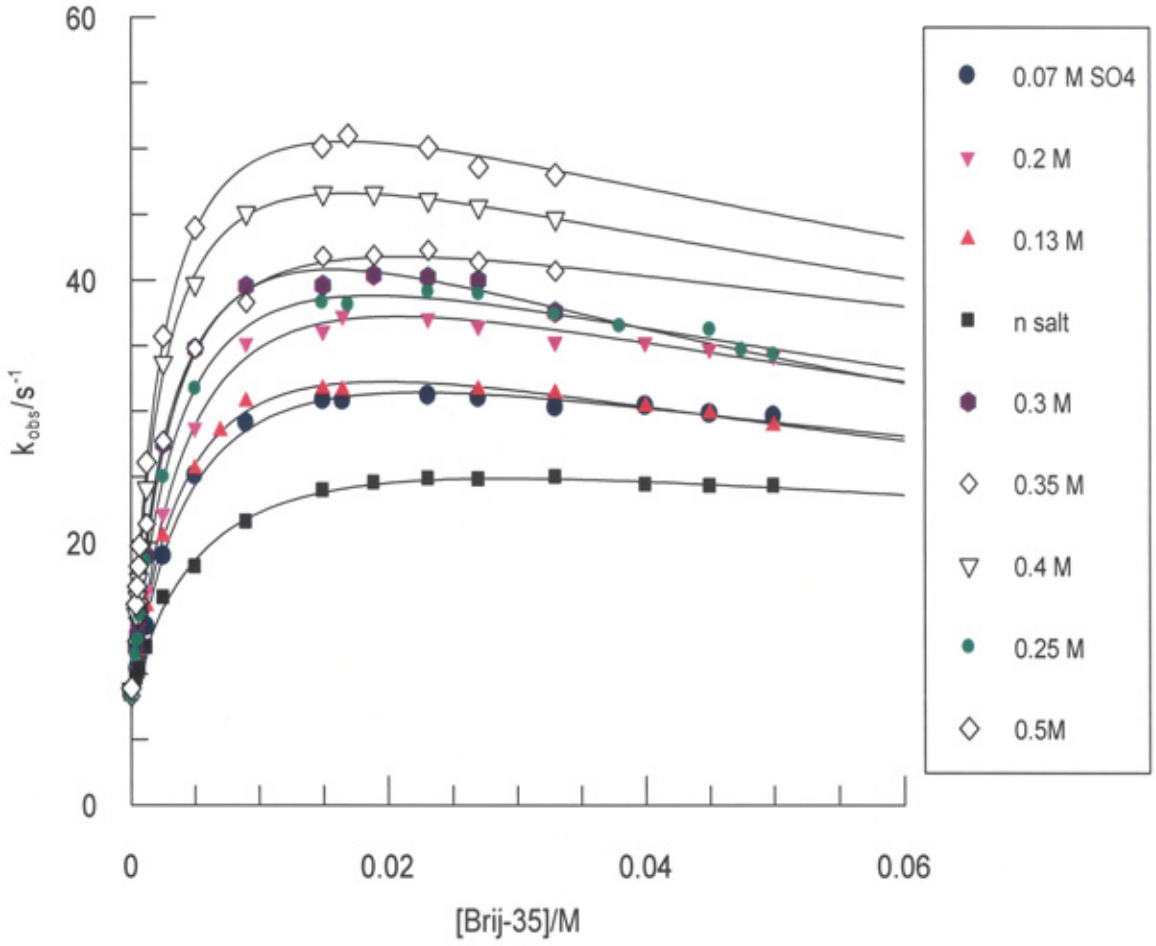

Figure 3.12: The observed rate constant versus [Brij-35] for the reaction of 0.0015 M potassium iodide with 4×10^{-6} M of MCPBA in 0.003 M nitric acid at different sulfate concentrations at 25°C.

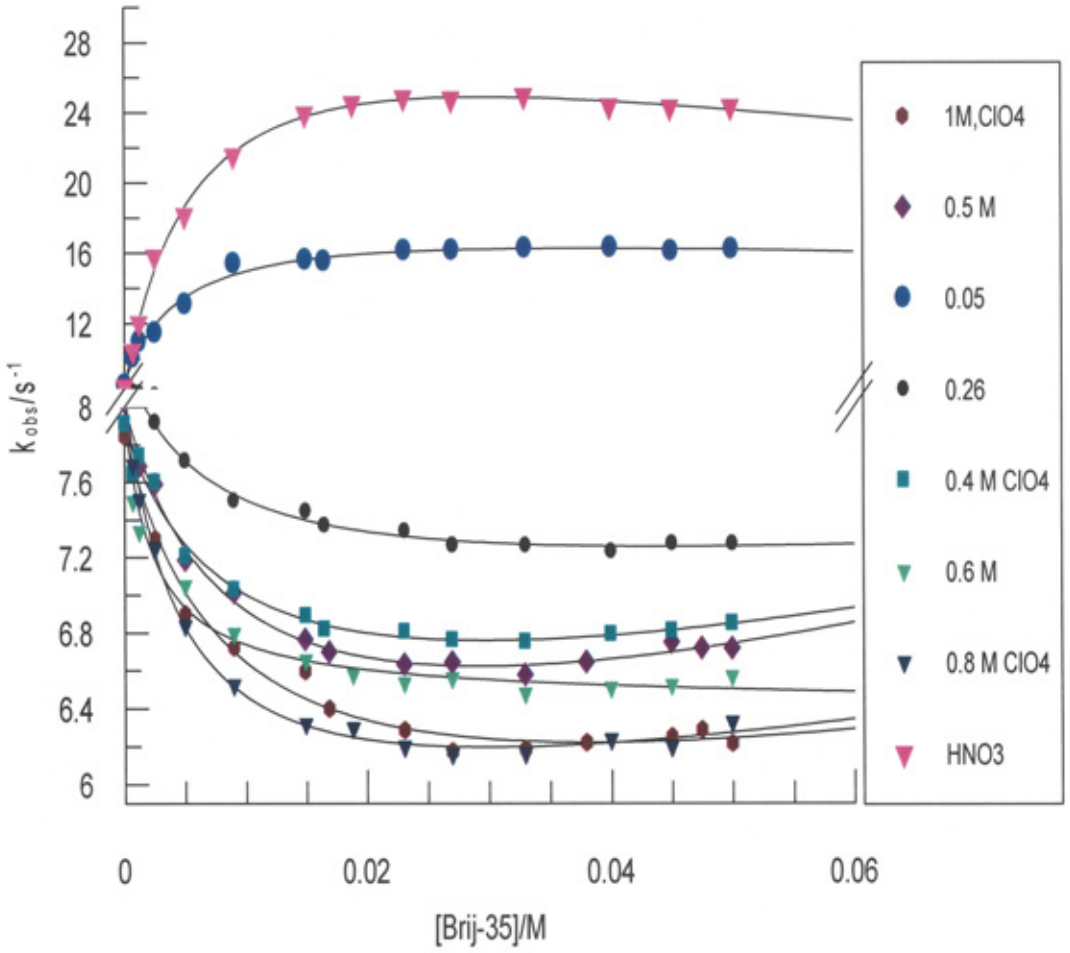

Figure 3.13: The observed rate constant versus [Brij-35] for the reaction of 0.0015 M potassium iodide with 4×10^{-6} M of MCPBA in 0.003 M nitric acid at different perchlorate concentrations at 25°C.

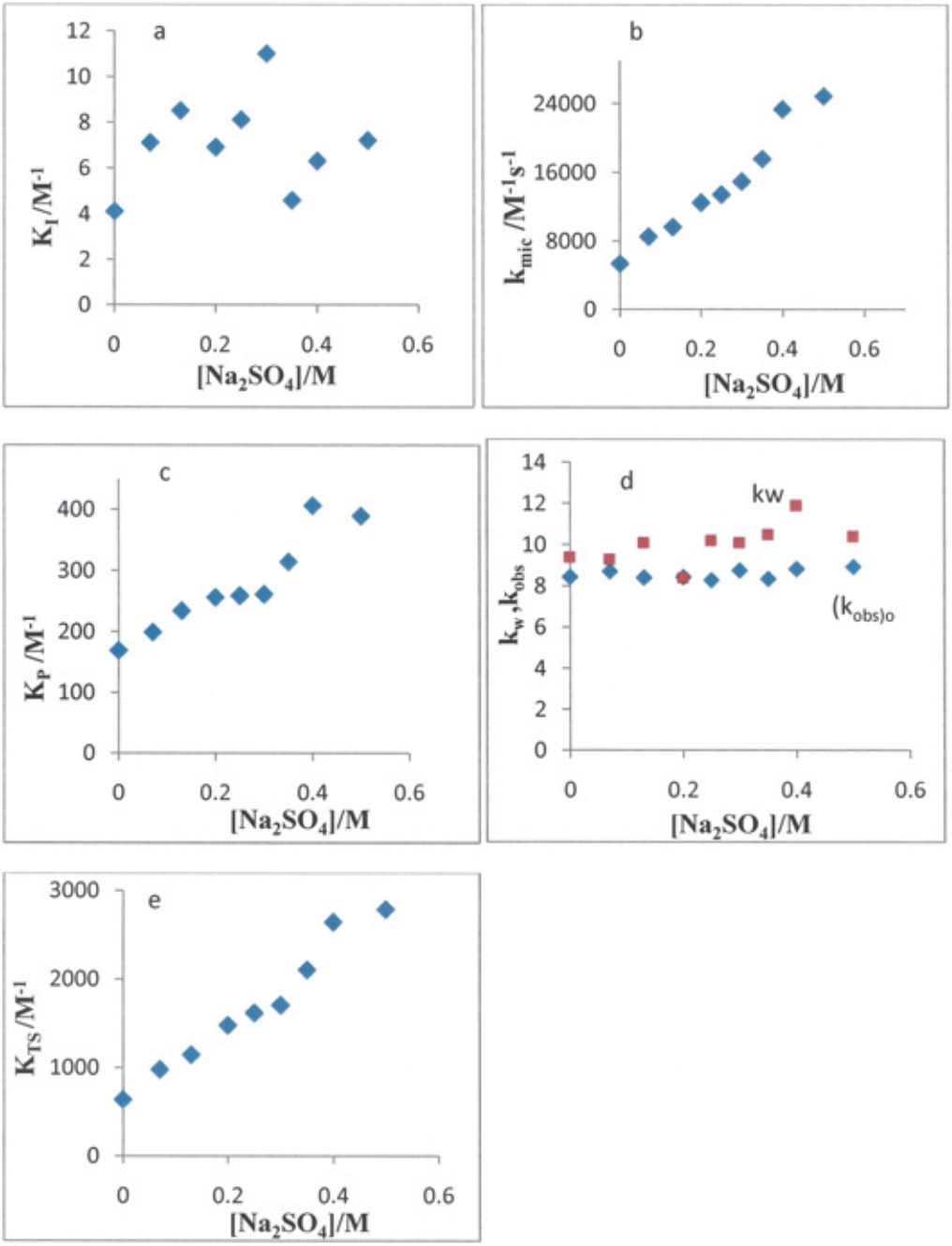

Figure 3.14: Derived kinetic parameters versus sulfate concentrations for the reaction of 0.0015 M KI and 4×10^{-6} M of MCPBA in 0.003 M HNO_3 at 25°C. In plot d, $(k_{obs})_o$ is denoted by diamonds and k_w by squares. The unit for the y axis for each parameter is as in Table 3.5.

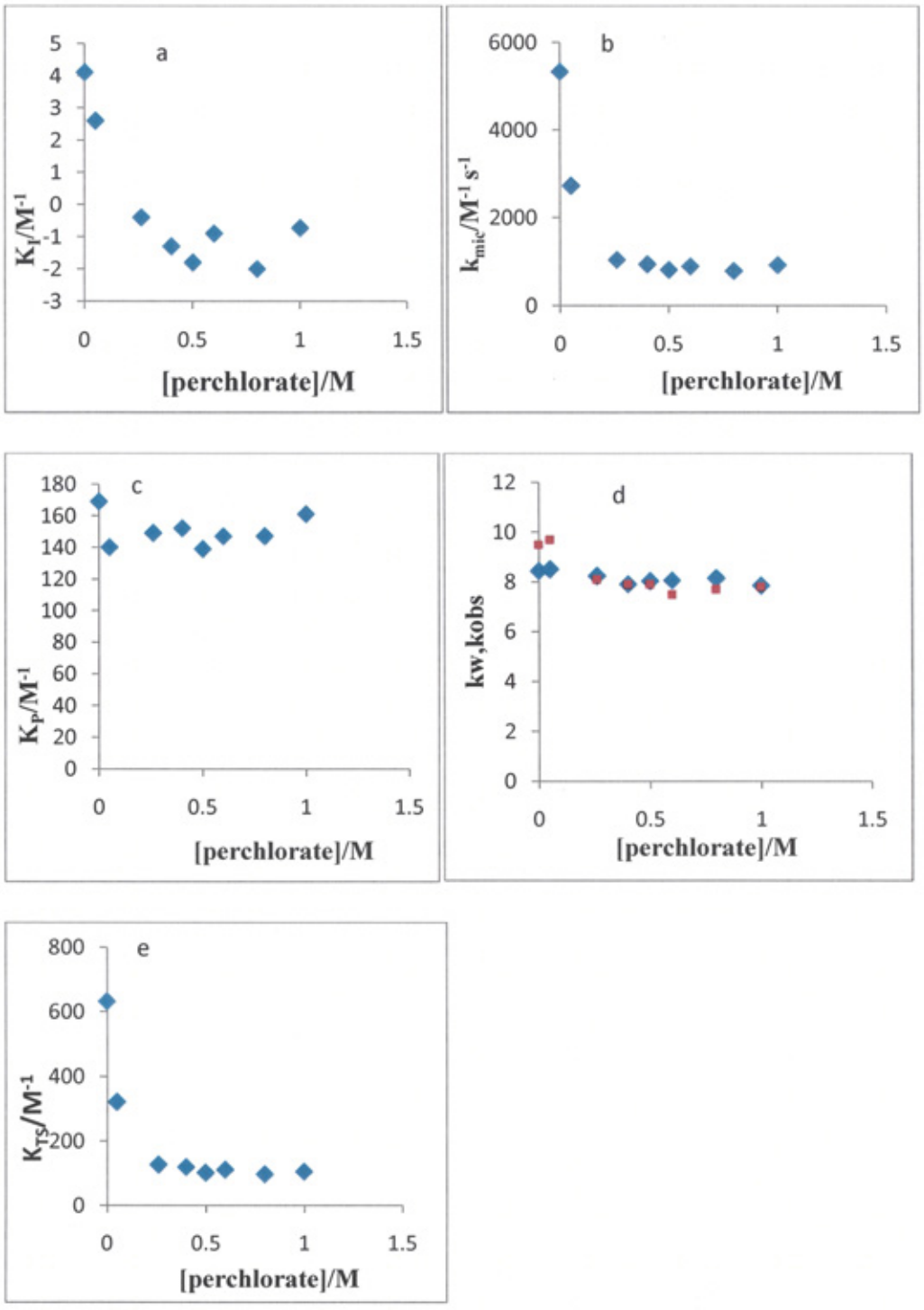

Figure 3.15: The best fit parameters versus perchlorate concentrations for the reaction of 0.0015 M KI and 4×10^{-6} M of MCPBA in 0.003 M HNO_3 at 25°C. In plot d, $(k_{obs})_0$ is denoted by diamonds and k_w by squares. The unit for the y axis for each parameter is as in Table 3.5. The units are as in Figure 3.14.

3.3.9. The effect of temperature on Brij-35 catalysis

Very few studies have investigated the reaction in the micelles when the concentration of surfactants is varied at different temperatures so that the enthalpy and entropy of binding for the reactants can be obtained [147,181]. However, there are many more studies that have looked into the effect of temperature at fixed surfactant concentrations [118, 119].

The reaction of iodide with peracid at different Brij-35 concentrations, and in the absence and presence of 1 M and 0.35 M perchlorate and sulfate respectively, was investigated at various temperatures ranging from 15°C to 35°C. Figure 3.16 to Figure 3.19 show the plots of the observed rate constant versus the [Brij-35] in the absence and presence of 0.35 M and 1 M sulfate and perchlorate respectively at various temperatures ranging from 15°C to 35°C. The raw data are listed in Table A4 to Table A6 in appendix A. The kinetic data were fitted to Equation 3.6 and the results obtained from the best fit include K_{mic}^{I}, K_{mic}^{PH}, k_{mic} and k_w. These best fit parameters are given in Table 3.6a to Table 3.6c below.

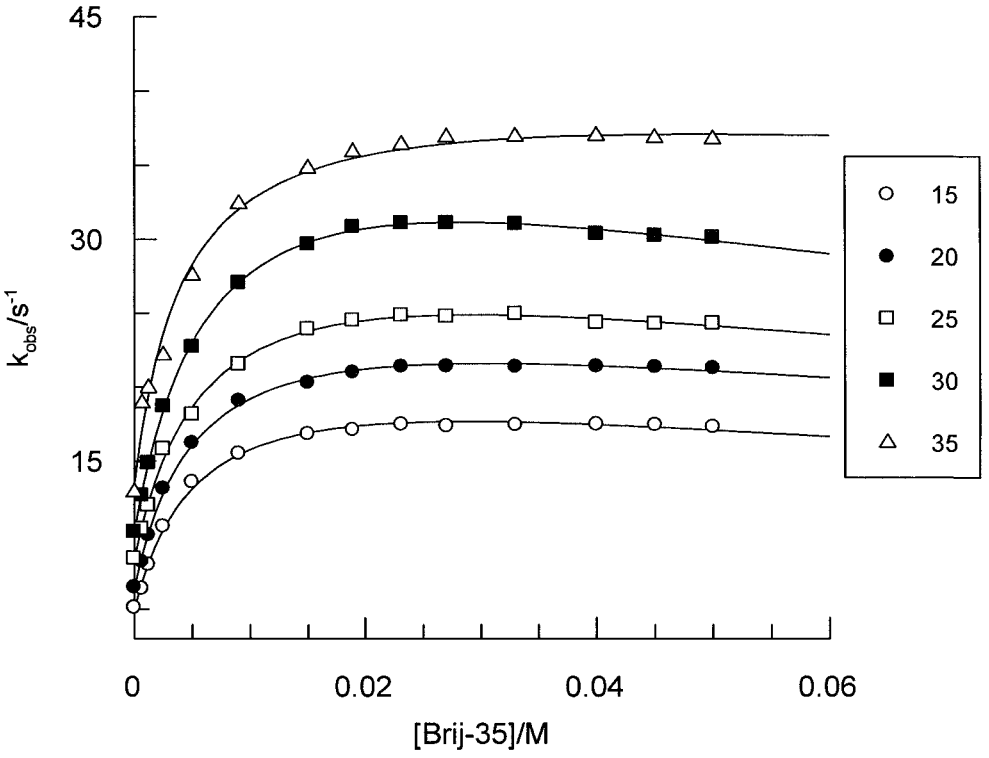

Figure 3.16: Plot of the observed pseudo first order rate constant for the reaction of 3-perchloroperbenzoic acid with iodide in the absence of salt at 0.003 M nitric acid and at different temperatures with non-linear least square best fit line using Equation 3.6.

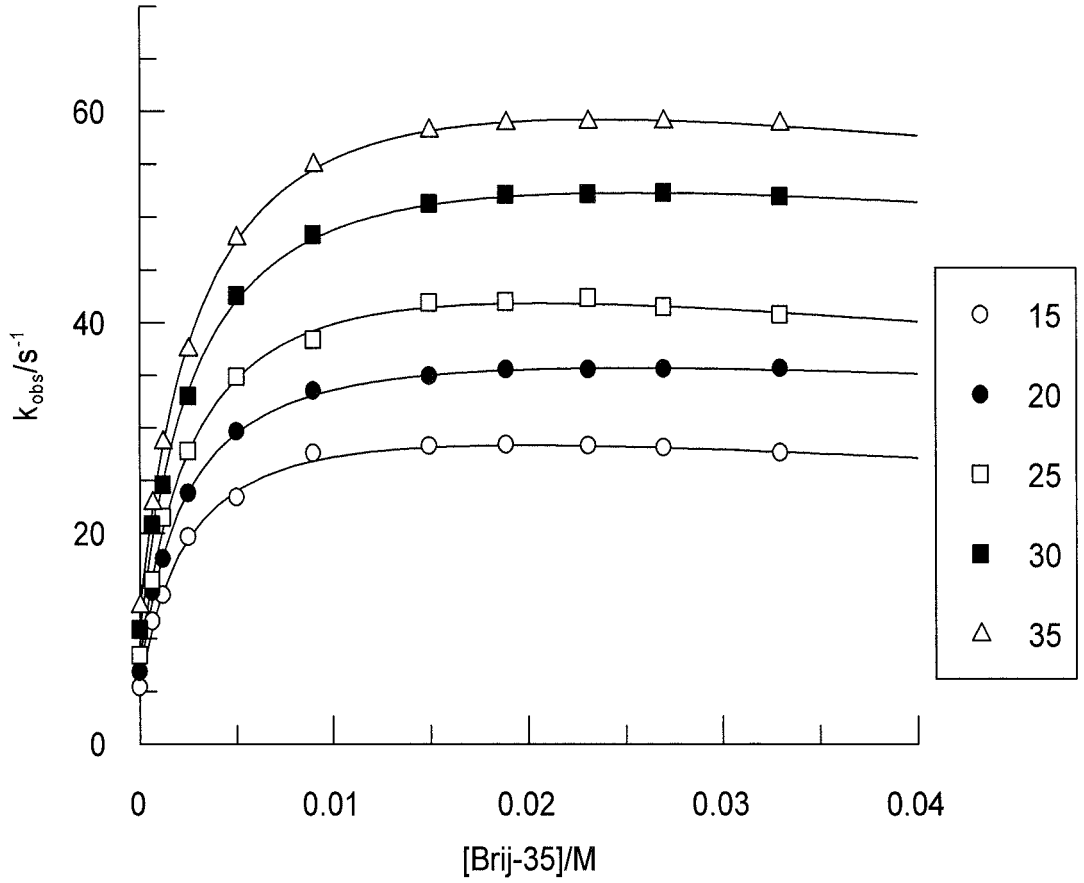

Figure 3.17: Plot of the observed pseudo first order rate constant for the reaction of 3-perchloroperbenzoic acid with iodide at 0.35 M of sulfate at different temperatures with non-linear least square best fit line using Equation 3.6.

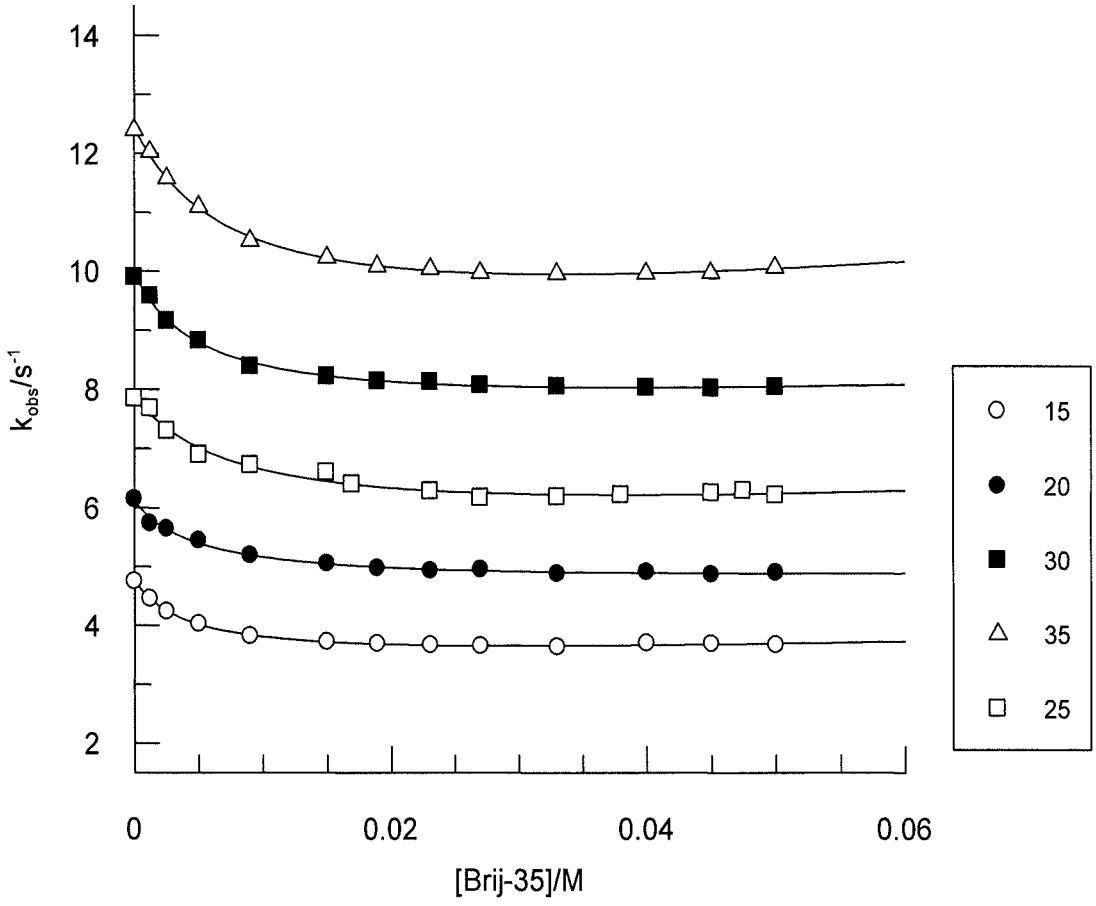

Figure 3.18: Plot of the observed pseudo first order rate constant for the reaction of 3-perchloroperbenzoic acid with iodide at 1 M of perchlorate at different temperatures with non-linear least square best fit line using Equation 3.6.

Table 3.6a: Effect of temperature in the absence of added salt: best fit parameters and their standard deviations, according to Equation 3.6, for the reaction of *ca.* 4×10^{-6} M MCPBA and 1.5×10^{-3} M iodide in 3.0×10^{-3} M nitric acid.

T, °C	$(k_{obs})_o$, s^{-1}	CMC, 10^{-4} M	k_w, s^{-1}	$k_{mic} - k_w \overline{V}_{mic}$, 10^3 M^{-1} s^{-1}	$K_{mic}^{PH} - \overline{V}_{mic}$, 10^2 M^{-1}	$K_{mic}^{I} - \overline{V}_{mic}$, M^{-1}	K_{TS}, M^{-1}	K_{TS}/K_P
15	5.1	5.0	5.8 ± 0.04	5.1 ± 0.1	2.4 ± 0.1	2.7 ± 0.3	1000	4.2
20	6.5	4.3	7.0 ± 0.05	5.7 ± 0.2	2.2 ± 0.1	2.5 ± 0.3	907	3.9
25	8.3	4	9.5 ± 0.02	5.4 ± 0.5	1.7 ± 0.2	4 ± 1.1	631	3.7
30	10.3	3	11.0 ± 0.1	6.5 ± 0.4	1.6 ± 0.1	4.8 ± 0.8	650	4
35	12.9	2.0	15.7 ±0.3	6.5 ± 1.0	1.4 ± 0.3	3.4 ± 1.8	503	3.6

Table 3.6b: Effect of temperature in the presence of 0.35 M sodium sulfate: best fit parameters and their standard deviations, according to Equation 3.6, for the reaction of *ca.* 4 x 10^{-6} M MCPBA and 1.5 x 10^{-3} M iodide in 3.0 x 10^{-3} M nitric acid.

T, °C	$(k_{obs})_o$, s^{-1}	CMC, 10^{-4} M	k_w, s^{-1}	$k_{mic} - k_w \overline{V}_{mic}$, 10^3 M^{-1} s^{-1}	$K^{PH}_{mic} - \overline{V}_{mic}$, 10^2 M^{-1}	$K^{I}_{mic} - \overline{V}_{mic}$, M^{-1}	K_{TS}, M^{-1}	K_{TS}/K_P
15	5.3	4.5	10 ± 0.3	9.2 ± 0.8	2.5 ± 0.3	8 ± 2	1736	6.9
20	6.8	4.0	12.1 ± 0.2	12 ± 0.8	2.7 ± 0.3	4.9 ± 0.5	1764	6.5
25	8.3	2.0	10.3 ± 0.3	16 ± 1.2	3.2 ± 0.4	4.5 ± 1.8	2108	6.5
30	10.8	1.6	12 ± 0.8	21 ± 3	3.3 ± 0.7	3.8 ± 1.2	1944	5.5
35	13.1	1.0	13.4 ± 0.4	22.4 ± 1.5	3.1 ± 0.3	4.0 ± 1	1710	5.5

Table 3.6c: Effect of temperature in the presence of 1.0 M sodium perchlorate: best fit parameters and their standard deviations, according to Equation 3.6, for the reaction of *ca.* 4 x 10^{-6} M MCPBA and 1.5 x 10^{-3} M iodide in 3.0 x 10^{-3} M nitric acid.

T, °C	$(k_{obs})_o$, s^{-1}	CMC, 10^{-4} M	k_w, s^{-1}	$k_{mic} - k_w \bar{V}_{mic}$, 10^3 M^{-1} s^{-1}	$K^{PH}_{mic} - \bar{V}_{mic}$, 10^2 M^{-1}	$K^{I}_{mic} - \bar{V}_{mic}$, M^{-1}	K_{TS}, M^{-1}	K_{TS}/K_P
15	4.77	5.4	4.5 ± 0.02	0.60 ± 0.12	1.9 ± 0.3	-1.4 ± 0.4	126	0.66
20	6.2	4.8	6.0 ± 0.01	0.85 ± 0.28	1.8 ± 0.5	-0.4 ± 0.6	141	0.78
25	7.9	4.0	7.8 ± 0.06	0.92 ± 0.29	1.6 ± 0.6	-0.73 ± 0.9	118	0.72
30	9.9	3.8	9.7 ± 0.03	1.07 ± 0.22	1.5 ± 0.3	-1.0 ± 0.4	108	0.72
35	12.4	3.4	12.3 ± 0.02	1.11 ± 0.09	1.3 ± 0.1	-1.7 ± 0.2	89	0.68

3.3.10. Effect of cations on the catalysed oxidation of iodide by MCPBA

The effect of various cations on the oxidation of iodide by peracid in the presence of Brij35 was investigated using a range of chloride salts (chosen because it is on the border between kosmotropic and chaotropic anions). These cations include large singly charged ions with low charge density (Cs^+ and K^+) exhibiting weaker interactions with water and they are (chaotropes), and small ions with a single or multiple charge with high charge density including Mg^{2+} and Li^+, representing kosmotrope ions according to the Hofmeister series [103]. These cations were chosen to see whether or not they would have the same effect as those obtained in the presence of perchlorate and sulfate. Chaotropes cations were expected to inhibit the reaction while kosmotropes were expected to enhance the rate.

The kinetic data are listed in Table A7 to Table A10 in appendix A. These kinetic data were fitted to Equation 3.6 and are illustrated in Figure A1 to Figure A4, with the best fit line in appendix A. The best fit parameters are listed in Table 3.7, which include the binding constants of iodide (K_{mic}^{I}) and MCPBA (K_{mic}^{PH}) to Brij-35.

Table 3.7: Effect of different cations: best fit parameters and their standard deviations, according to equation 3.6, for the reaction of *ca.* 4 x 10^{-6} M MCPBA and 1.5 x 10^{-3} M iodide in 3.0 x 10^{-3} M nitric acid at 25°C.

Salt	*Conc, M*	$(k_{obs})_o$, s^{-1}	CMC, 10^{-4} M	k_w, s^{-1}	$k_{mic} - k_w \overline{V}_{mic}$, 10^3 M^{-1} s^{-1}	$K^{PH}_{mic} - \overline{V}_{mic}$, 10^2 M^{-1}	$K^{I}_{mic} - \overline{V}_{mic}$, M^{-1}
CsCl	0.2	9.6	3.5	10.4 ± 0.2	5.6 ± 0.5	1.5 ± 0.2	7 ± 2
CsCl	0.5	10.0	2.0	11.3 ± 0.5	7.2 ± 0.8	1.7 ± 0.3	4.7 ± 1.6
CsCl	0.8	11.0	1.8	12.6 ± 0.2	8.0 ± 0.6	1.8 ± 0.2	6.7 ± 1.1
LiCl	0.2	8.8	3.2	10.4 ± 0.1	6.1 ± 0.3	1.9 ± 0.2	4.8 ± 0.6
LiCl	0.5	9.1	2.1	10.6 ± 0.8	7.2 ± 1.3	1.5 ± 0.4	13 ± 3
LiCl	0.8	9.8	1.9	11.0 ± 0.1	8.1 ± 0.4	2.0 ± 0.2	7.6 ± 0.8
$MgCl_2$	0.2	8.9	3.5	10.3 ± 0.4	4.8 ± 0.9	1.6 ± 0.4	4.2 ± 1.8
$MgCl_2$	0.5	10.0	2.4	12.0 ± 0.1	9.1 ± 0.7	2.6 ± 0.3	5.5 ± 0.9
KCl	0.5	8.4	3.0	11.9 ± 0.2	8.5 ± 0.5	1.9 ± 0.2	5.5 ± 1.0
KCl	0.8	9.6	2.5	10.3 ± 0.5	11.8 ± 1.8	2.3 ± 0.6	5.6 ± 2.7

3.3.11. Reduction of MCPBA in the presence of P104 (PEO-PPO-PEO triblock copolymers)

PEO-PPO-PEO is a triblock copolymers which has poly (ethylene oxide), (PEO) as hydrophilic end blocks and PPO (poly propylene) as the hydrophobic middle block. Its structure is (PEO_{27} PPO_{61} PEO_{27}) and it is available under the commercial name P104 with molecular weight 5900 [182]. When present in a solution it aggregates to form a micelle, with the hydrophobic blocks comprising the core and the hydrophilic blocks along with the solvent water forming the exterior. One of the most useful properties of such aggregates is their ability to incorporate hydrophobic substances, thus enhancing dramatically the effective solubility of these (otherwise) practically insoluble molecules in aqueous solutions.

P104 was chosen as it resembles the Brij in its hydrophobic core. Also, it has high solubility, which can facilitate the study of the MCPBA reduction by iodide at high concentrations (which was not possible for Brij), hence the binding of iodide can be estimated.

The effect of pluronic (P104) triblock copolymer on the rate of the reduction of peracid by iodide was investigated by varying the concentration of the reactants and the pluronic concentration. Figures A5, A6 and A7 in appendix A show the absorbance versus time plots for this reaction in different conditions which are indicated in the figures. The data (absorbance versus time) were fitted to double exponential Equation 3.8 and the results are listed in Table 3.8. Other sets of experiments were carried out in the absence of MCPBA and in the presence of iodine and iodide in one syringe and the pluronic in the other one. The data collected are shown in Table 3.9. These values were obtained by fitting the data to double exponential Equation 3.8. The data in Figure 8A to Figure 10A in appendix A are fitted to Equation 3.8 using Grafit software [176].

Figure A11 and Figure A12 in appendix A show the reaction of iodide with MCPBA using pluronic-104 after dialysis.

$A = a + b\,e^{-k1t} + c\,e^{-k2t}$ 3.8

If $t = \infty$ then $A_\infty = a$.

And if $t = 0$ then $A_o = a + b + c$.

$A_{max} = a + c$

Where $a = A_\infty$, $b = A_o - A_{max}$ and $c = A_{max} - A_o$

Table 3.8: The kinetic data obtained for the reaction of iodide with MCPBA in the presence of P104 in various reaction conditions and with a constant temperature of 25°C.

[P 104]/ 10^{-4} M	[KI]/M	[MCPBA]/ 10^{-5}M	k_1, s^{-1}	k_2, M^{-1} s^{-1}
5	0.0015	1	14.3±0.3	0.58±0.004
5	0.0015	2	16.7±0.6	0.67±0.007
2.5	0.0015	1	17.1±0.7	0.79±0.01
10	0.0015	1	16.8±0.18	0.35±0.001
5	0.003	1	24.9±0.6	0.36±-.002
5	0.006	1	44.7±0.13	0.28±0.002

Table 3.9: The kinetic data obtained for the iodine in the presence of P104 in various reaction conditions and with a constant temperature of 25°C.

[P104]/ 10^{-4} M	[I_2]/ 10^{-5} M	[KI]/M	k_1, s^{-1}	k_2, s^{-1}
5.	1	0.0015	1.202±0.03	0.3507±0.021
5	1	0.003	0.5639±0.008	0.184±0.026
5	1	0.006	0.4255±0.01	0.1235±0.018
2.5	1	0.0015	0.886±0.02	0.453±0.009
10	1	0.0015	0.6445±0.04	0.2643±0.01
5	2	0.0015	1.6±0.01	0.3755±0.024

3.4. Discussion

3.4.1. Summary of results and observations from sections 3.3.1-3.3.5.

In the foregoing sections the reduction of MCPBA by iodide was investigated under various conditions. Figure 3.1 and Figure 3.2 show the dependence of the reaction on the reactant concentration in the presence of 0.1 M buffer acetate; increasing the iodide concentrations at fixed MCPBA results in an increase in the rate (doubling the iodide concentration doubles the rate, which means that the rate is first order in iodide). Figure 3.2 shows the effect of varying the MCPBA concentrations on the rate, while keeping the iodide concentrations constant and in excess. The rate in this case is not affected by altering the [MCPBA], which confirms that the reaction is under pseudo first - order conditions.

Figures 3.3 and 3.4 show the effect of buffer components, sodium nitrate and ionic strength on the reduction of MCPBA by iodide in the absence of Brij-35 and in the presence of fixed Brij-35 concentrations. From these results it can be seen that the reaction is not influenced by hydrogen ion concentration, salt effect or ionic strength, as stated previously [18]. However, in the presence of Brij-35 the rate is very slightly increased by increasing the concentration of the buffer component. Figures 3.3 a, c and d are best explained by the acetate anion strengthening the hydrophobic interaction by salting out the organic substrate and concentrating them in the micelle; while nitrate ion decreases the rate in the presence of Brij-35, which may be due to the salting in effect of these ions, thus weakening hydrophobic interaction.

The effect of other salts, sulfate (kosmotrope ion), perchlorate (chaotrope ion) and chloride (which is on the border between kosmotropes and chaotropes) on the reduction of MCPBA by iodide is shown in Figure 3.5. As expected, in the absence of Brij-35 the rate is not affected by varying the salt concentration, while in the presence of Brij-35 the observed rate is increased by increasing the sulfate concentration and decreased by increasing the perchlorate concentration. These results are in accordance with the Hofmeister series, in which salting out anions (sulfate) enhances the concentration of the substrate in the micelle, thus increasing the rate increases. On the other hand, perchlorate has the opposite effect as it salts-in the reactants and hence decreases their effective concentration in the micelle, which might be the cause of the observed rate inhibition. The observed rate is not affected by

increasing chloride concentration, which is in accordance with its position in the Hofmeister series.

3.4.2. Critical micelle concentration

In this section firstly the cmc of the studied surfactants will be discussed and then the Brij-35 system will be discussed in more detail, as the reaction of iodide and peracid in this chapter is investigated intensively in Brij-35. It can be seen that there are differences between the values of CMC found in literature (see Table 3.3) and the values observed in this study for non-ionic surfactants (determined from kinetic measurement (see Table 3.4)). These differences are most probably explained by the fact that literature values were measured by means of the surface tension method; this method is a surface phenomenon and is highly sensitive to surface-active impurities in the surfactant solution, which often significantly reduce the cmc of surfactants,

In general, non-ionic surfactants show much lower CMC values than ionic ones, whose hydrophobic chains are of the same length, due to the absence of electrical repulsion between ionised groups [32]. The critical micelle concentration of non-ionic surfactants is lowered by the addition of salt, but the lowering is always much smaller than that of ionic surfactants [32, 183]. In this study the effect of perchlorate and sulfate is shown in Figure 3.9 and Figure 3.10, which plots CMC versus salt concentration. It is clear that the CMC is lowered as the concentration of sulfate increases. However, the effect of perchlorate is not clear and the CMC might have an effect but to a lesser extent than sulfate. Ray [184] and colleagues have investigated the effect of inorganic salts (which include sulfate and perchlorate) on the cmc of p-tert-Octylphenoxy (polyethoxy) ethanol, OPE_{30} and $OPE_{9\text{-}10}$ in aqueous solution at 25°C. Their findings show that the CMC is lowered by all salts except Lithium iodide, which increases the CMC. By plotting CMC versus salt concentration it was found that the sulphate is the ion most effective at lowering the CMC and has the steepest slope, while the perchlorate has less of an effect that the sulfate. Ray and co-workers [184] concluded that the reduction in the CMC was due to the salting out or in of the hydrocarbon moiety of the detergent.

From Table 3.6 it is clear that temperature enhances micellization in the absence and presence of sulfate salt. Also, the data show that the CMC is lowered by increasing the temperature, which is a well documented finding [32]. Megure [185] has extensively reviewed

the effect of temperature on the CMC of non-ionic surfactants and has compiled CMC dependent temperatures for several non-ionic surfactants of the type ($C_n E_m$), in which n is the number of carbon in the alkyl chain and m is the number of oxyethylene groups in the surfactant. All the CMC temperature data (with temperature ranging from 15°C to 40°C) in his review show that CMC is decreased as temperature is raised, which is a similar finding to what we have observed.

The variation of CMC with temperature can be used to calculate the enthalpy and entropy of micellization, as shown in Figure 3.19a which plots the natural logarithm of CMC as a function 1/T for the reaction in water, 0.35 M sulfate and 1 M perchlorate respectively. From the slope and intercept of this plot the enthalpy and entropy of micellization was calculated. The entropy of micellization versus the enthalpy of micellization is shown in Figure 3.19b. This plot shows that the micellization process exhibits compensation phenomena, as stated in [144] in which an increase in the entropy is compensated by a decrease in enthalpy, the reaction in presence of sulfate which has the highest entropy of micellization due to an increase in the disorder of the system which is opposite to its behaviour based on Hofmeister series (water structure maker). On the other hand, perchlorate decreases the entropy of micellization (become less positive compare to its absence) and this is in not expected based on its effect on water structure (water structure maker) which should increase the entropy and not decreas it. Figure 3.19b shows that the micellization associated with enthalpy-entropy compensation is a universal phenomenon that can be seen in most chemical and biological processes [144].

The calculated thermodynamic parameters of free energy and the enthalpy and entropy of micellization in three conditions (in water, 0.35 M sulfate and 1 M perchlorate) are shown in Table 3.10 with other thermodynamic parameters. These will be discussed in the following sections. The value of standard free energy for Brij-35 in water and sulfate and perchlorate shows that micellization is more spontaneous for all the investigated systems and are similar while the enthalpy and entropy are different.

The significance of these values (enthalpy, entropy and free energy of micellization) is that they give an insight into the force driving the micelle formation. From Table 3.10 it can be seen that the free energy is large and negative, while enthalpy of micellization is positive, indicating that the micelle formation is an endothermic process. In addition, entropy is large

and positive, which suggests that the micellization process results in an increase in entropy. Also, Table 3.10 shows that the value of free energy for the three studied systems is about -20 Kj / mol^{-1} which accounts for the compensation effect illustrated in Figure 3.19.

The large positive entropy ΔS_m^0 is considered to be primarily due to the disruption of the iceberg structure of water during the course of micellization, and the larger positive ΔS_m^0 in sulphate can be due to the contribution of sulfate to dehydration of polyoxyethylene head group of Brij-35. The addition of perchlorate reduces the entropy and this may be due to the fact that perchlorate increases the hydration of hydrophobic group of Brij-35 and thus reduce the number of available water in solution, and this lead to weakening of the hydrophobic interaction, which are the important driving force for micelle formation. As mentioned in Chapter one, these ions prefer to bind to the zwitterionic micelle sulfabetaine, which may actually be happening here; thus, repellence of the monomer causes an increase in the cmc, compared to that which occurs in the absence and presence of sulfate.

Rakshit and co-workers [186] conducted a thermodynamic study into the pure aqueous solution of Brij-35 and also in the presence of different concentrations of polyethylene glycol solvents. Their general conclusion was that cmc is decreased by increasing the temperature from 35 °C to 50° C in an aqueous system and in the presence of the additive PEG. The calculated thermodynamic parameters for the process of micellization show that micelle formation was exothermic in the presence of the additive but endothermic in the pure aqueous solution. Also, the entropy of micellization was positive in all cases. They attributed this high entropy change to phase change, and also to the breakdown of water structure on micellization.

In general, the results obtained in this study are similar to those of Rakshit and co-workers [186], in which the cmc is lowered by increasing the temperature and the entropy and enthalpy of micellization are positive in all conditions.

Tadros [76] has shown that the thermodynamics of non-ionic micelle formation can be calculated from a plot of ln CMC versus 1/T. The results show that the micellization process is associated with positive enthalpy and large positive entropy, as observed in present study for the micellization of Brij-35 (see Table 3.10). These positive values were attributed to an increase in the disorder of the system: even though the aggregation leads to entropy loss, the main reason behind the positive entropy is the desolvation of the ethylene oxide chain and a

release of more water molecules. Another factor contributing to the large positive entropy upon micellization is the increase in flexibility of the hydrocarbon chain upon its transfer from the aqueous phase to hydrocarbon medium in the micelle core; thus the orientation of the organic chain is more restricted in the aqueous phase than in the organic phase [76]. Also, in a non-ionic micelle increasing the polyoxyethylene chain causes an increase in the CMC and decreases the micelle size [32]. This gives the monomer more hydrophilic character and thus higher CMC.

The process of micelle formation has been described as an example of entropy that is driven by the hydrophobic effect; when the micelle is formed the surfactant monomers come close to each other and produce one cavity (before, each monomer has it is own cavity), which is smaller than the sum of the two separated cavities accommodating each monomer. This contraction in the cavity is entropy driven and ΔS become more positive as a result of the release of water and distribution of the solute –solute or solute-solvent interaction [43].

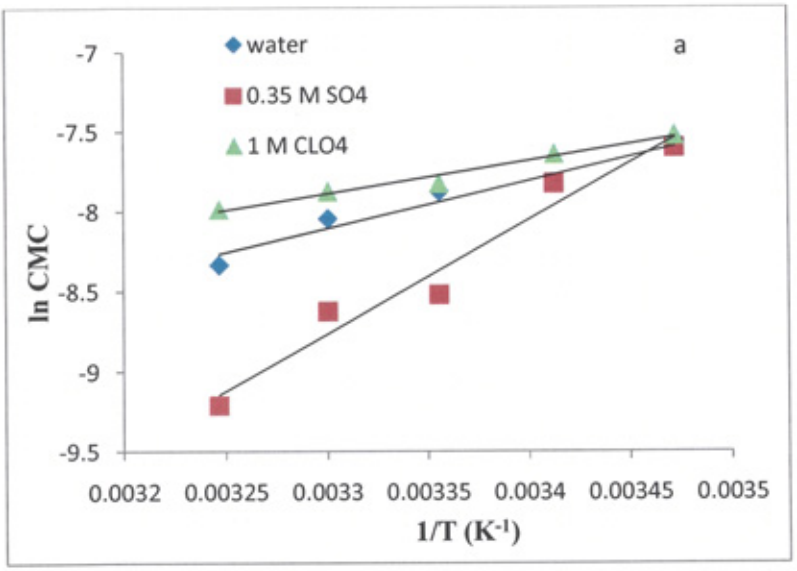

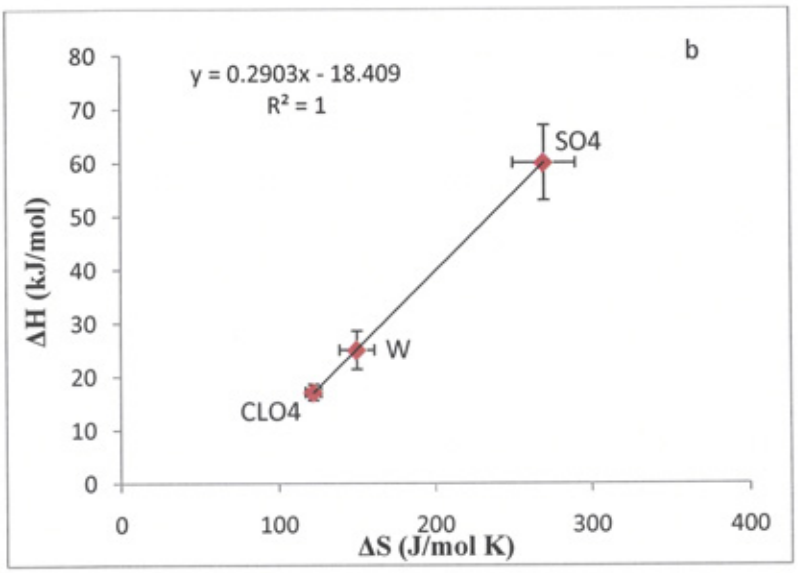

Figure 3.19: Plot of reciprocal of temperature versus natural logarithm of the critical micelle concentration for the reaction of MCPBA 4×10^{-6} M with 0.0015 M potassium iodide in 0.003 M nitric acid in water (w), 0.35 M sulfate and 1 M perchlorate (a), (b) shows the enthalpy versus entropy of micellization data taken from Table 3.10. The isokinetic temperature is 290 K.

Table 3.10: Calculated thermodynamic parameters for the reaction of 0.0015 M potassium iodide and 4×10^{-6} MCPBA in 0.003 M nitric acid.

	Added salt		
	None	0.35 M Na_2SO_4	1.0 M $NaClO_4$
$\Delta H^{\ddagger}(k_{obs})$, kJ mol^{-1}	31.5 ±0.65	30.7 ± 0.7	32.9 ± 0.2
$\Delta S^{\ddagger}(k_{obs}/s^{-1})$, J mol^{-1} K^{-1}	-122 ± 2	-124 ± 2	-117.5 ± 0.6
$\Delta G^{\ddagger}(k_{obs})$, kJ mol^{-1}	67.8 ± 2.1	67.6 ± 2	67.9 ± 0.63
ΔH^{0}(CMC), kJ mol^{-1}	25 ± 4	60 ± 7	17 ± 2
ΔS^{0}(CMC, M), J mol^{-1} K^{-1}	150 ± 10	270 ± 20	122 ± 5
ΔG^{0}(CMC), kJ mol^{-1}	-19.68 ± 4.8	-20 ± 5.3	-19.2 ± 2
$\Delta H^{\ddagger}(k_{mic} - k_w \overline{V}_{mic})$, kJ mol^{-1}	6.4 ± 3.8	32 ± 3.5	17 ± 3
$\Delta S^{\ddagger}(k_{mic} - k_w \overline{V}_{mic}, M^{-1} s^{-1})$, J mol^{-1} K^{-1}	-150 ± 10	-56.5 ± 11	-130± 10
$\Delta G^{\ddagger}(k_{mic} - k_w \overline{V}_{mic})$, kJ mol^{-1}	51 ± 10.7	49 ± 6	55.7 ± 10.4
$\Delta H^{0}(K_{mic}^{PH} - \overline{V}_{mic})$, kJ mol^{-1}	-22 ± 3	10 ± 5	-15.7 ± 1
$\Delta S^{0}(K_{mic}^{PH} - \overline{V}_{mic}, M^{-1})$, J mol^{-1} K^{-1}	-30 ± 10	82 ± 18	-10.6 ± 4
$\Delta G^{0}(K_{mic}^{PH} - \overline{V}_{mic})$, kJ mol^{-1}	-13.1 ± 10	-14 ± 18.6	-12.7 ± 4
$\Delta H^{0}(K_{mic}^{I} - \overline{V}_{mic})$, kJ mol^{-1}	20 ± 10	-25 ± 10	NA[a]
$\Delta S^{0}(K_{mic}^{I} - \overline{V}_{mic}, M^{-1})$, J mol^{-1} K^{-1}	70 ± 40	-71 ± 18	NA[a]
$\Delta H^{0}(K_{mic}^{TS} - \overline{V}_{mic})$, kJ mol^{-1}	-29.3±4.3	1.5 ± 9.7	-15.5±3.8
$\Delta S^{0}(K_{mic}^{TS} - \overline{V}_{mic}, M^{-1})$, J mol^{-1} K^{-1}	-25±14.6	79±2.9	-13.9±12

[a] Not calculable.

ΔG calculated from the following relation: $\Delta G = \Delta H - T\Delta S$, T= 298 K.

3.4.3. Effect of non-ionic surfactants on the rate of reaction

For all the non-ionic surfactants used, the rate of oxidation is increased and reaches a plateau, staying almost unchanged within the concentrations used. The reaction can not be studied at high surfactant concentrations due to the solubility limit.

The results in Table 3.4 show that the binding of iodide to the non-ionic micelle is increased by increasing the size of the head group (polyoxyethylene length), which can give an insight into the location of binding of this substrate to the micelle polyoxyethylene layer. However, for the peracid the binding is affected very little by the EO (ethoxylene group) length. For example, the binding of peracid, K_p, in Brij-35 is 1.7 M^{-1} and for C_{12} E_{10} is 1.6 M^{-1}, which shows that increasing the EO length does not have much of an effect.

As in Table 3.4, the larger value of the observed second-order rate constant in the micellar pseudophase (k_{mic}-$k_w \overline{V}_{mic}$) is obtained for Polyoxyethylene (100) stearyl ether ($C_{18}E_{100}$ or Brij-700), followed by Polyoxyethylene (20) cetyl ether ($C_{16}E_{20}$ or Brin-58), and then Brij-35, and the lower value for Polyoxyethylene (10) lauryl ether ($C_{12}E_{10}$).

Comparisons can be made between $C_{12}E_{23}$ and $C_{12}E_{10}$. They have a similar chain length but different head group length, and it is clear that the longer the head group length the higher the binding of both substrates. This indicates that the reactant especially iodide prefers to bind to the palisade layer of the micellar. It manifests in the higher rate constant at low concentrations of Brij-35 ($C_{12}E_{23}$) compared to $C_{12}E_{10}$. Due to the solubility problem the reaction could not be followed at higher concentrations of micelle.

Table 3.4 compares the micellar association constants of the MCPBA and the micellar association constants of the transition states for the reaction in the four surfactants. In all cases the ratio K_{TS}/K_P is quite constant and larger than one, which indicates that the reaction is micellar catalysed in all cases and the transition state is more stabilised than the reactants. Also, it can be seen from the table that there is a good correlation between the association constant of the peracid and association constant of the transition state for all the micellar systems, which indicates that the same factors stabilise the reactants and transition states, and that the binding of the transition state parallels substrate binding. Figure 3.20 shows a plot of transition state binding versus substrate binding with a correlation coefficient of 0.98, which suggests the similarities between binding of transition state and substrate.

The transition state approach described in Equation 3.7 has been used previously to treat kinetic data for the reduction of peracid by iodide in Brij-35 at 25°C. Values of 575 ± 65 for the micellar association constant of the transition state were obtained, which are quite similar to the values obtained in this work (630 M^{-1}), especially given the difference in conditions.

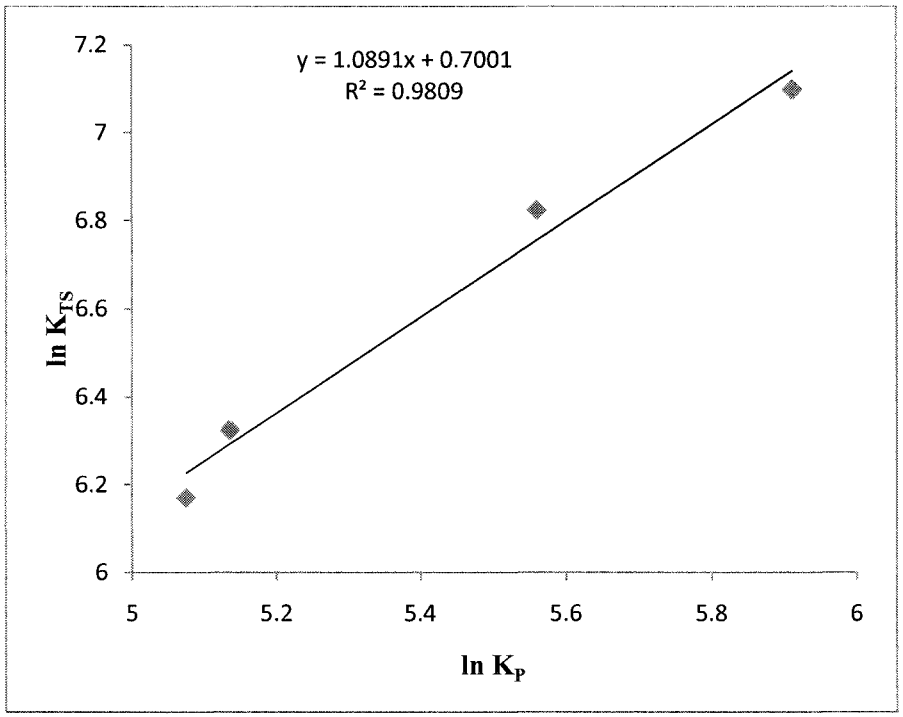

Figure 3.20: Plot of the natural logarithm for the transition state binding constant versus natural logarithm of the binding constant of MCPBA.

3.4.4. Effect of the salting in and salting out agent on the micellar catalysed reaction

It is known that micelles can catalyze a chemical reaction through two dominant factors: electrostatic and/or hydrophobic interactions between the micellar phase and reactants, and transition state and product [39]. The hydrophobic effect is the natural tendency of hydrocarbon-like molecules to form aggregates in aqueous solution so as to minimize the water–hydrocarbon interfacial area. The water–hydrocarbon interactions are modified in the presence of certain additives [105], such as urea, sodium perchlorate, sodium nitrate, sodium sulfate and sodium chloride. Depending upon their nature, the additives are classified as either salting in or salting out agents. Salting in agents are those that have a tendency to

increase the solubility of organic compounds in aqueous solution [105], such as urea and perchlorate. Salting out agents tend to reduce the solubility of organic compounds in water because of their higher solubility in water originating from a polar characteristic, and include sodium chloride and sodium sulfate.

In this study the effect of both salt sodium sulfate and perchlorate on the catalysed micellar reaction are investigated. Figure 3.12 and Figure 3.13 illustrate that sodium sulfate salt tends to enhance the catalysis and this enhancement is increased by increasing the salt concentration; while for perchlorate the reaction is inhibited which may be due to reactant separation. The derived kinetic parameters obtained were plotted versus the concentrations of salt, as shown in Figure 3.14 and Figure 3.15. In the case of sulfate, both the binding constant for MCPBA, K_P, and the micellar rate constant, k_{mic}, increases with increasing the concentration of the salt. Based on this result the rate enhancement can be explained by the salting out of the MCPBA by the sulfate as described in the introduction. The binding of iodide K_I shows apparently random variation with salt concentrations and no correlation is observed. The effect of perchlorate is much less obvious from the parameters obtained; the binding of peracid is not affected by increasing the salt concentration, and micellar association constant for the iodide is too low to be measured and so it is not possible to estimate its association enthalpy and entropy in the presence of perchlorate.

In addition the ratio of K_{TS}/K_P is more than one in the presence of sulfate which indicates micellar catalysis see Table 3.1. While for the reaction in presence of perchlorate the ratio was less than one which indicates micellar inhibition as shown in Table 3.2

As stated in the introduction, there is no clear consensus regarding the effect of salt on the property and structure of water, as many interpretations have been stated. The salt dependence of peracid and iodide binding to the Brij-35 at 25°C shows that as in Figure 3.14 and Figure 3.15, the binding of MCPBA increases with an increase in the sulfate concentration of 0.05 M (due to the limited solubility of this salt it was not possible to exceed this concentration). On the other hand, increasing the perchlorate concentration results in a slight decrease of the binding of MCPBA, and as can be seen from Figure 3.15, increasing the perchlorate concentration attenuates the peracid binding to the micelle until equilibrium come close to saturation at about 0.4 M, where the binding is shown to be stable.

The dependence on the nature of the added salt shows that the highly hydrated and more charged ions, such as sulfate, tend to have a positive effect on the rate; while the more polarisable and less hydrated ions (perchlorate) have an inhibitory influence on the catalysed reaction.

3.4.5. Effect of cation on the oxidation of iodide by MCPBA

Paired with chloride (because it is in the border between the kosmotropic and chaotropic anions), the effect of cations including K^+, Mg^{+2}, Li^+, Cs^+ on the micelle catalysed reaction was investigated. For the given cations, increasing the concentration caused the rate to increase, but not as much as that observed for the sulfate and no inhibitory effect was observed for the cations. The kinetic data obtained were fitted to Equation 3.6 and are listed in Table 3.7. It was found that the order of salting out power of cations follow $K^+ > Na^+ > Li^+$, which differs to the Hofmeister series where the lithium ion precedes the sodium ion also the effect of cation is much less clear than that of the anions [32]. The explanation for this was pointed out by Schott [61a], who stated that this behaviour can be the result of the salting in of non-ionic surfactants due to complex formation between the ether linkage of these surface active agents and lithium ion. The stability of aqueous solutions of non-ionic amphiphiles of the polyoxyethylene type is determined by a special oxyethylene–water interaction in which the ether groups form highly directional hydrogen bonds with the water molecules and the ethylene parts are accommodated in the overall water structure [61b, 62]. The interaction between ether oxygen atoms and water is affected by the presence of ions and the polyoxyethylene moiety of the surfactant acts as a polydentate ligand [62]. The weak binding of cations imparts a slightly cationic character to the non-ionic surfactant micelles, which accounts for the salting in [62]. However, it has also been stated that non-ionic surfactants may also affect the structure of water. As an example, Brij-35 below the cmc is a strong water structure breaker [108].

3.4.6. Effect of temperature on micellar catalysed reaction and compensation effect

Plots of $\ln(k_{obs}/T)$, $\ln\{(k_{mic} - k_w\overline{V}_{mic})/T\}$, $\ln(K^{PH}_{mic} - \overline{V}_{mic})$, and $\ln(K^{I}_{mic} - \overline{V}_{mic})$ against inverse temperature are shown in Figure 3.22. The enthalpy and entropy change from the kinetic parameters are calculated using Equation 3.8. Also from the plot of ln k/T versus 1/T, the activation of entropy and activation of enthalpy were calculated using Equation 3.9. The propagation of error was used in the calculation and the results are summarised in Table 3.10.

$$\ln K = \frac{\Delta S}{R} - \frac{\Delta H}{R} \cdot \frac{1}{T} \qquad 3.8$$

$$\boxed{\ln\left(\frac{k}{T}\right) = \ln\left(\frac{k_B}{h}\right) + \frac{\Delta S^{\ddagger}}{R} - \frac{\Delta H^{\ddagger}}{R} \cdot \frac{1}{T}} \qquad 3.9$$

This equation describes the variation in the rate constant k_{obs} with the thermodynamic parameters, where k_B is the Boltzman constant and h is Planck's constant.

By plotting ln k/T versus 1/T a straight line is obtained, from which the entropy and enthalpy of activation for the reaction can be calculated from the intercept and the slope respectively.

Xiang [144] has stated that the existence of the compensation effect for a series of similar reactions carried out in different conditions can be established by plotting the log of preexponential factors versus activation energy, or enthalpy change versus entropy change, which should give a straight line; while the isoequilibrium relationships can be established by constructing a Van't Hoff plot. All should be on one plot looking for a point of intersection. Based on this statement, Van't Hoff plots were used and can be seen in Figure 3.21, which includes $\ln k_{obs}$, $\ln K_P$, $\ln K_I$, $\ln k_{mic}$ and $\ln K_{TS}$. There is a good linear correlation between these parameters and the lines are parallel to each other. There is no clear common point of intersection within the experimental temperature, but there is still the presence of isokinetic relationships, as stated in reference 144.

From Figure 3.21 it can be seen that the sulfate line is above that of water, and the perchlorate is below that of water. Also, the transition state is more stabilised in the presence of sulfate than perchlorate. For the reactions in perchlorate, binding constant derived for iodide, $K^{I}_{mic}-\overline{V}_{mic}$, were negative and the thermodynamic parameters in this case could not be obtained. Paradis [23] have found small and negative value of binding constants for anions in Brij-35 micelle which attributed to the low permeativity of the mantle regions of the micelle. Thus negative values of binding constants ($K_{mic}-\overline{V}_{mic}$) are not impossible if the contribution of the molar volume of micelle is relatively large which in the case of Brij-35 is 1.2 dm^3 mol^{-1}. Equation 3.6 show that, $\overline{V}_{mic}$, will affect the value of , K_{mic} , if the later is smaller compared to , $\overline{V}_{mic}$,

In addition, by examining these plots (Figure 3.21) the line for the reaction in presence of sulfate and water seems to have a point of intersection for the binding of peracid and iodide, while that for the transition state has no point of intersection, as observed in the experimental temperature range. Generally, from this plot the enhancement of the rate in the presence of sulfate is caused by stabilisation of the transition state, and the inhibition is caused by the perchlorate, which could be due to the destabilisation of the transition state compared to the reactant (see Figure 3.21). This can be inferred from the ratio of K_{TS}/K_P, where values below 1 are an indication of inhibition and values greater than 1 suggest catalysis. The former is observed in the presence of perchlorate, while a greater ratio than that obtained can be observed in the presence of sulfate.

The standard entropy of the binding constant for the peracid shows there is a difference in behaviour in different conditions. The enthalpy of binding of peracid in the absence and presence of perchlorate are quite negative and also associated with negative entropy. On the other hand, the sulfate system shows positive values of enthalpy and high positive entropy, which may be an indication that the rate in such a case is accelerated by entropy gain.

As stated by Xiang [144], the existence of IKR has been analysed by means of linear relationships between ΔS^0 and ΔH^0 which are calculated as above. Based on this a series of plots of the calculated thermodynamic parameters listed in Table 3.10 were used to construct compensation plots (ΔS^0 versus ΔH^0), which are shown in Figure 3.22.

The value of entropy and enthalpy change for the equilibrium process for reactant and transition state plotted in Figure 3.22 with there error bars. There is a straight line with very good correlation coefficient, which shows that there might be a compensation effect, but in the case of transition state there is little deviation of data point from the line.

Analysis of these thermodynamic data values indicate that the reaction in water and perchlorate is driven by favourable enthalpy change, while in the presence of sulfate the reaction is entropy driven. The values of ΔH^{o} and ΔS^{o} for the oxidation of iodide are linearly related (see Figure 3.22 with correlation coefficient above 0.9).

Wenle [187a] has studied the association equilibrium constant and thermodynamic parameters for the complexion between N, N-dimethylindoaniline and p-sulfonated Calixarene in aqueous solution using UV.VIS spectroscopy. The results of this study show there are linear relationships between ΔH^{o} and ΔS^{o}. It was suggested that this correlation can be attributed to the change in the conformation of calixarene and also to host guest desolvation involved in the complexion process. The enthalpy change is affected by many factors including the nature of interaction between reactants (hydrogen bonding, Van der Waals force). Also, the entropy change is affected by loss of ordering of water molecular originally enclosing the organic molecules, and also due to the freezing of the motion as a result of the association between the host and the guest species. Based on this argument, the high entropy change in the presence of sulfate observed for the present study can be due to an increase in the degree of freedom of the system and an increase in the disordering of the water molecules.

The relationships between entropy and enthalpy can be interpreted according to the hypothesis put forward by Grunwald and co-workers [187b], which is based on solvent reorganisation being the major cause of the compensation effect. They conclude that the entropy enthalpy compensation can be accounted for by solvent reorganisation, which means the transfer of molecules between the bulk phase and the adjacent solvation layer of the solute. Generally, Grunwald and co-workers [187b] separate the effect into two parts to account for this compensation process: one is called the environmental equation or part and the other the nominal part. This suggests that if the environmental part (associated with water molecules involved in the salvation and desolvation process upon complex or binding of substrate to host) controls the variation in ΔS_{env} and ΔH_{env}, and the contribution of this part to free energy is zero, then a linear correlation will be obtained with a slope equal to

isokinetic temperature, complete compensation exists and ΔG^{o} should be larger than ΔH^{o}. The nominal part (associated with the complexation of solvated guest with solvated host to form solvated host: guest complex) contributes to the compensation when the reactants form a stable strong complex, which leads to more negative ΔH_{nom} and also more negative ΔS_{nom}. This is considered not to be complete compensation and ΔG^{o} has the same sign as ΔH_{nom}.

For the present study the presence of isokinetic relationships will be tested and verified using the Exner approach [142] see appendix A section S.

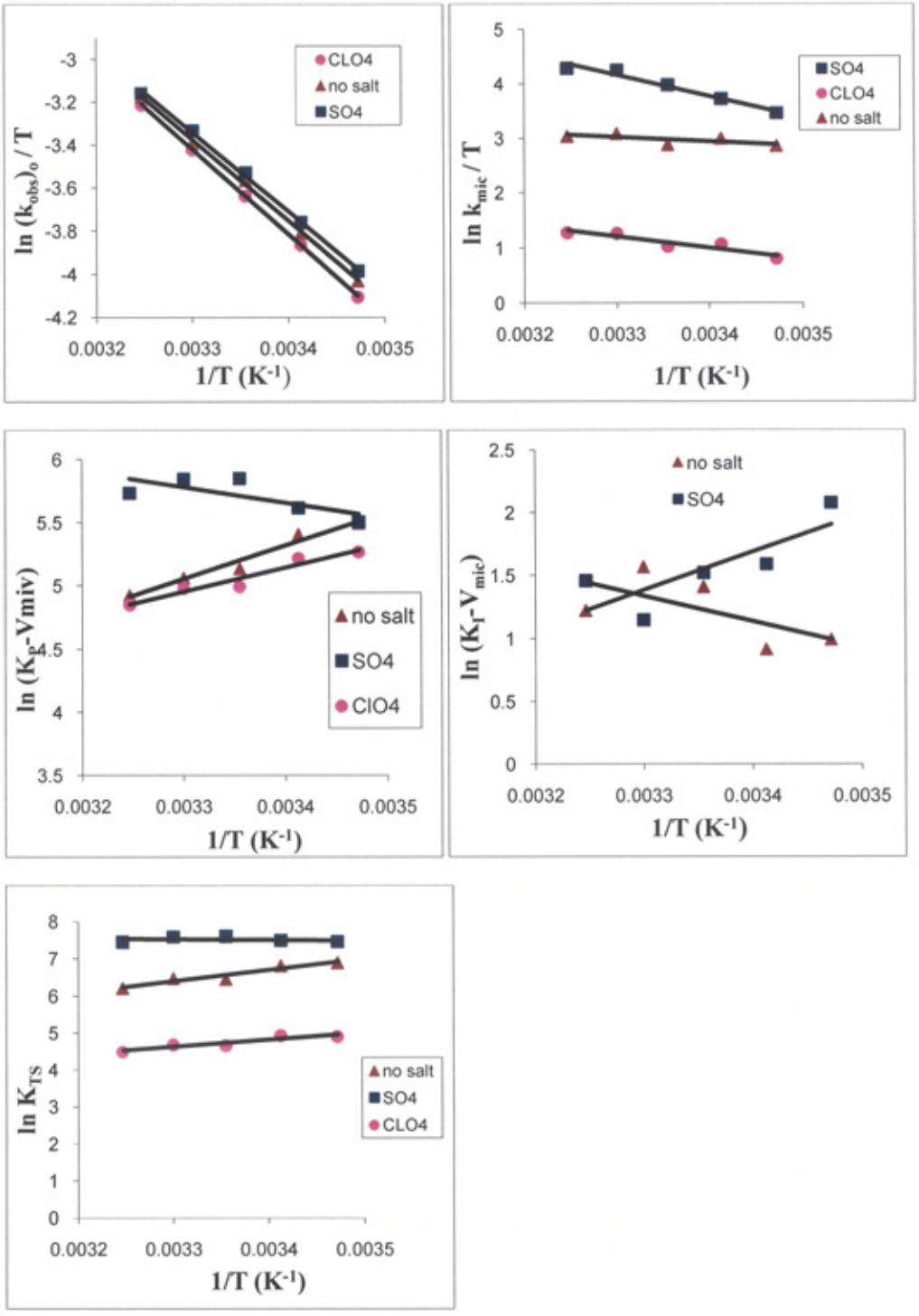

Figure 3.21: Natural logarithm of binding constant versus reciprocal of temperature (Arrhenius plot) for the reaction between 0.0015 M iodide and 5×10^{-6} M of MCPBA in the absence of salt and presence of 0.35 M and 1 M of sodium sulfate and sodium perchlorate respectively.

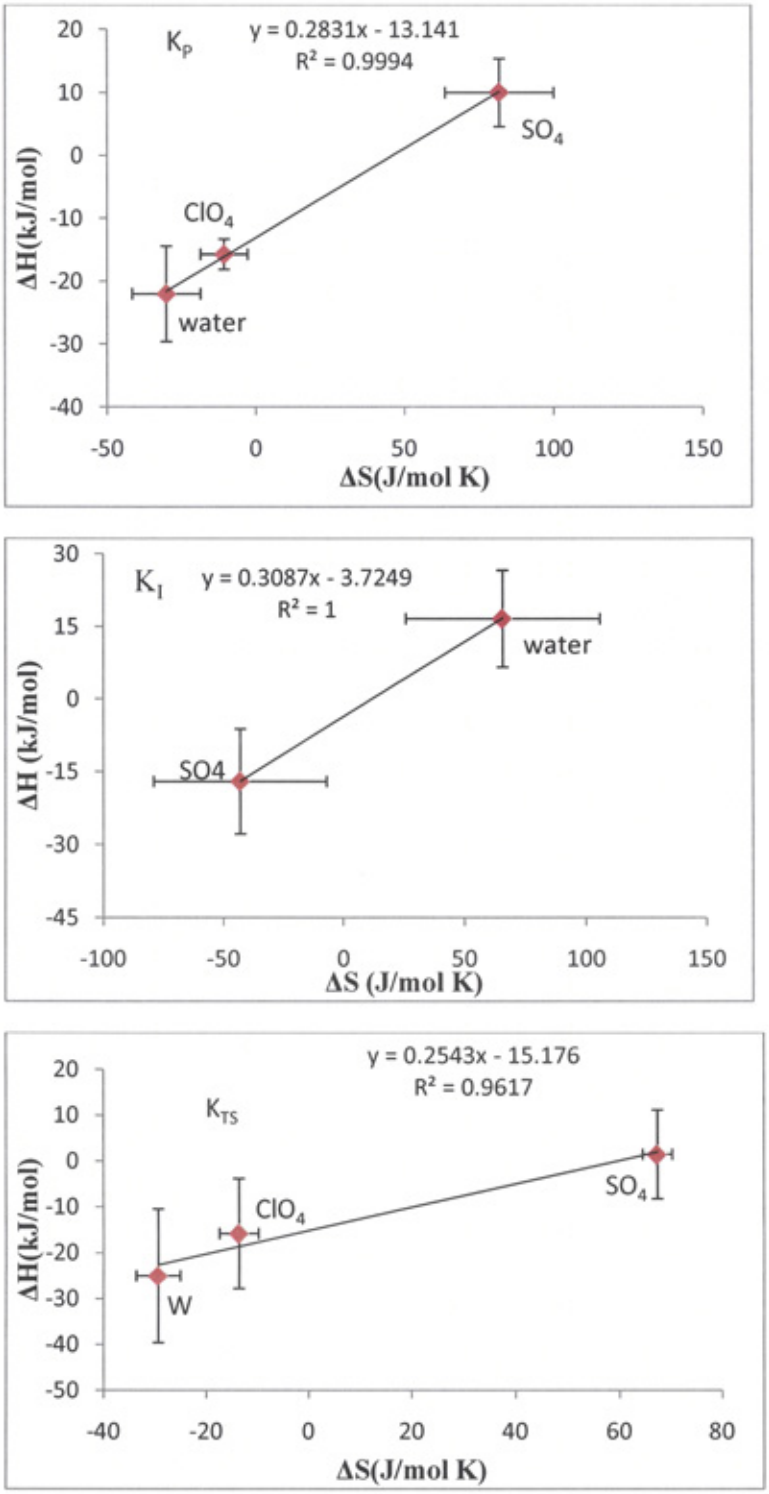

Figure 3.22: Compensation plot of the calculated standard enthalpy and entropy change for the peracid, iodide and transition state from top to bottom respectively. T_{iso} = 288 K, 308 K and 252 K respectively. Sulfate and perchlorate concentrations were 0.35 and 1 M respectively.

3.4.7. Enthalpy and entropy of activation

Activation parameters in aqueous medium for the uncatalysed reaction (Table 3.10), when compared with those obtained in non-ionic micellar in different conditions, show that the presence of non-ionic micelles decreases the enthalpy of activation in the absence and presence of 1 M perchlorate, which can be an indication of more interaction and consequently the entropy becomes more negative due to restriction of motion and reduced disorder of the system. This indicates that the transition state is highly stabilised in the micellar system.

For the reaction in the absence and presence of salts the values of enthalpy of activation is more positive and quite similar, but when the reaction is carried out in micelles $\Delta H^{\ddagger}$ goes from 31.5 to 6.4 respectively for the reaction in absence of salts; while $\Delta S^{\ddagger}$ becomes more negative in the micelle, which may be due to the higher order of the system in the presence of the micelle. The reaction in perchlorate shows the same trend. With the reaction in the presence of sulfate, the entropy of activation becomes less negative and the enthalpy of activation increases. This can be explained by the higher acceleration in the rate in the presence of sulphate due to the entropic effect.

In general, Brij-35 lowers the free energy of activation of the reaction, even in the presence of perchlorate where the inhibition is observed, which is due to the destabilisation of the transition state compared to the reactant in this case, as can be seen from the value of K_{TS}/K_P in Table 3.10c.

Figure 3.23 shows the plot and entropy of activation versus enthalpy of activation for an uncatalysed and catalysed reaction by Brij-35, with error bars for the reaction of peracid with iodide in three different conditions (water, in the presence of 0.35 M sulfate and 1 M perchlorate) showing a linear correlation. This can be explained by the existence of the compensation effect, which means that a loss of entropy due to strong interaction or loss of molecule motion can be compensated by an increase in enthalpy gain. On the other hand, a decrease in the enthalpy as a result of weak interaction can be cancelled out by an increase in the entropy (favourable entropy).

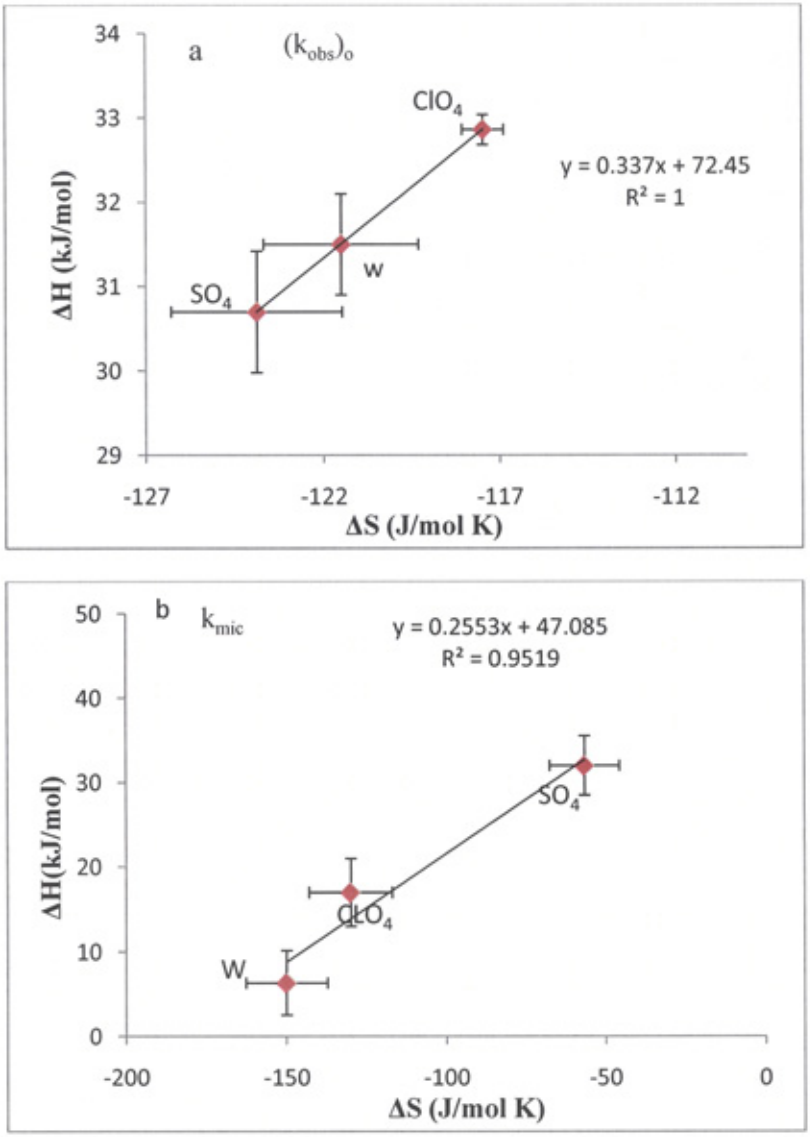

Figure 3.23: Compensation plot of the calculated enthalpy and entropy of activation for the process in bulk water (a) and micellar pseudo phase (b). The activation parameters were derived by using the linear form of the Eyring equation. Isokinetic temperature for the process in water is 337K, and in the micelle is 255 K.

3.4.8. Effect of Pluronic 104 (P 104) on the oxidation of iodide by peracid

This reaction was chosen due to the good solubility of pluronic, which means it can be used in high concentrations and thus better values of the binding of iodide can be obtained. The P104 is a non-ionic Tri-block co-polymer polyoxyethylene – polyoxoyproplyene – polyoxyethylene. Reduction of the peracid by iodide in the presence of P104 proceeded some what differently to that which was observed with Brij-35 and other non-ionic micelles investigated. With P104 the reaction was observed to be biphasic. The triiodide formed was consumed immediately by further reaction, which might have been due to impurity being present in the copolymer used. The solution of P104 was thus dialysed three times using membranes to facilitate removal of low molecular weight molecule impurity if present. After this process the P104 obtained was used in the kinetic study. The same results were found, which could mean that the P104 reacted with the iodide or that it reacted very quickly with the product formed triiodide in this case. Absorbance versus time is shown in Figure A11 and Figure A12 in appendix A. As can be seen, there was an increase at the beginning of the reaction in the absorbance, followed by a decline to almost zero.

Other sets of experiment were carried out using potassium iodide and iodine instead of peracid to eliminate the possibility of the reaction of P104 with peracid. The potassium iodide and iodine was mixed and introduced in one syringe (triiodide is formed by equilibrium), with the P104 in another syringe. The absorbance versus time is shown in Figure A8 to Figure A10 in appendix A, from which it can be concluded that the P104 or other impurities which can not be eliminated by dialysis may react with the triiodide formed, resulting in a decline in absorbance, which was not seen in the reaction of iodide with peracid in Brij-35.

Chapter 4: The effect of Brij-35 on the reaction between series of alkyl aryl sulfides and peracids

4.1. Introduction

In this chapter the oxidation of series of aryl alkyl sulfides by peracids will be investigated in the presence of various concentrations of Brij-35 at five temperatures (for three of the sulfides; the rest will be studied at 25°C). The binding constant of reactants will be obtained by fitting the rate versus [Brij-35] to Equation 4.3 using the Grafit Programme [176]. From these binding constants the thermodynamic parameters of binding will be calculated from Van't Hoff plots. This can provide an insight into the force controlling the binding process and whether the nature of the substituent has an affect on the thermodynamic parameters.

The general characteristics of these reactions are similar to other cases of nucleophilic displacement on peroxidic oxygen. The mechanism for the reaction of sulfur compounds and peroxide involves nucleophilic attack of the outer peroxidic oxygen by sulfur atoms, producing sulfoxide and the leaving groups as in Scheme 4.1. The mechanism also involves a build up of positive charge on the sulfur in the transition state as the electrons are transferred to the peracid [122]. The sulfoxide can react further to from the sulfone (Scheme 4.1) though under these conditions the reaction is extremely slow [2].

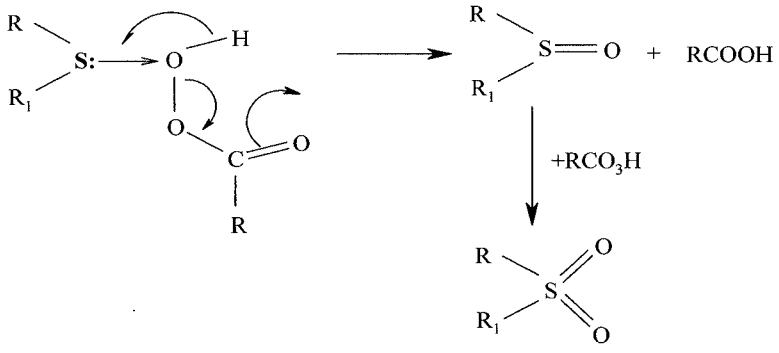

Scheme 4.1

Sulfide oxidation by peroxyacid is speeded up by an electron releasing group at the para position in the sulfide and reduced by an electron withdrawing group [123]. For the peroxide, the reactivity increases as the basicity of the leaving group decreases (i. e as the pKa of the

leaving group is lower [122]). The oxidation of sulfide compounds by peroxides has been studied extensively and it has been concluded that hydrogen peroxide is less reactive than other peroxides. The most reactive peracid has been identified as peroxymonosulfate and the least reactive as peroxoborate [124].

4.2. Experiment

4.2.1. Materials

The chemicals used in this study include organic sulfides (nucleophiles) and all of them were obtained from an Aldrich: their purities are listed in Table 4.1 and they were used without further purification. The solutions of the sulfides were prepared as previously stated[164]: a small amount was weighed and dissolved in distilled water and then stirred for several hours, after which it was filtered with a sintered funnel to remove undissolved materials.

The other chemical compounds used in the study include peroxymonosulfate (PMS 98%), which was purchased from Aldrich and 3-chloroperbenzoic acid (as mentioned in the Chapter 2). All other chemicals used have been mentioned in the previous chapter.

Table 4.1: List of sulfides and their maximum wavelength, at which the kinetic experiments were carried out.

Sulfide and its purity	**Molecular Weight [178]**	**Wavelength / nm**
4-(Methylthio) benzyl alcohol 98%	154.23	255
4-Methoxythioanisole, 97%	154.23	253
4-Chlorothioanisole, 98%,	158.65	358
2-Chlorothioanisole, 96%	158.65	250
4-Bromothioanisole 97%	203.1	259
4-Nitrothioanisole, 96%	169.2	251
Methyl *p*-tolyl sulfide, 99%,	138.23	252
3-chlorothioanisole, 98%,	158.65	254
Methyl phenyl sulfide, 99%	124.2	253

4.2.2. Methods

4.2.2.1. UV visible measurement

Prior to each kinetic study the concentration of the sulfide was determined by measuring the absorbance of stock solution, which was prepared with a weight of about 0.1g of sulfide and stirred for several hours. Then its absorbance was taken and from its molar absorpitivty (which is known [164]) the concentration was calculated. Concentrations were calculated from the Beers Lambert Law equation (Equation 4.1), as shown below:

$$A = c\, l\, \varepsilon \qquad 4.1$$

Where A is the absorbance, c, l and ε are the concentration, path length and extinction coefficient respectively.

4.2.2.2. Kinetic measurement and determination of the pseudo first order rate constant k_{obs}

Solutions of the reagents were prepared immediately before the kinetic measurements. The reactions were made on an Applied Photophysics SX17 MV stopped-flow spectrophotometer. The temperature was maintained at 25°C, unless otherwise stated, by circulating water from a thermostated bath around the injection syringes and the reaction chamber. The oxidation of sulphides was monitored spectrophometrically under pseudo first order conditions using a large excess of peracid, about twenty times more than the sulfides.

A typical run was carried out by filling one of the injection syringes with a solution containing the peracid and the surfactant and another with the sulfides and 0.003 M nitric acid. The reaction was followed by monitoring the decrease in the absorbance of the sulfides at values listed in Table 4.1 for each one. The decrease in the absorbance is due to the disappearance of the sulphide as it is oxidised by the peracid. Pseudo first order rate constants were evaluated from the nonlinear plots of absorbance versus time using the following exponential equation (Equation 4.2) below:

$$A_\infty - A_t = (A_\infty - A_o)\, e^{-kobs} \qquad 4.2$$

The terms in the equation are defined in Chapter 3.

4.2.3. Curve fitting

All the kinetic data were fitted universally to Equation 4.3 using nonlinear regression and the Grafit version 6.05 statistic computer programme [176].

$$k_{obs} = \frac{k_w + (k_{mic} - k_w\bar{V}_{mic})([S] - CMC)}{\{1 + (K_{mic}^{PH} - \bar{V}_{mic})([S] - CMC)\}\{1 + (K_{mic}^{S} - \bar{V}_{mic})([S] - CMC)\}} \qquad 4.3$$

In this Equation, k_w, $k_{mic} - k_w\overline{V}_{mic}$ (as defined previously) are the observed first order rate constant in water and the micelle respectively, $K^{s}_{mic}-\overline{V}_{mic}$ is the binding constant of sulfides and is sometimes written as K_S, and $K^{PH}_{mic}-\overline{V}_{mic}$ is the peracid binding constant written as K_P. $\overline{V}_{mic}$ is the partial molar volume of the micelle. The other terms are defined in Chapter 3.

In general, nonlinear regression to find best fit parameters of a model is carried out by minimizing the sum of the squares of the vertical distances between the data points and curve line. For universal nonlinear regression several data sets are fitted at once with common parameters.

For universal fitting all data sets for the oxidation of sulfides by MCPBA and PMS were fitted at once at each temperature and by setting the $K^{PH}_{mic}-\overline{V}_{mic}$ and $k_{mic} - k_w\overline{V}_{mic}$ for PMS to zero; while $K^{PH}_{mic}-\overline{V}_{mic}$ for MCPBA was kept common for all sulfides at each temperature, assuming that the binding of this peracid was not affected by changing the sulfide. The binding constant of sulfides to the micelle, $K^{s}_{mic}-\overline{V}_{mic}$ was determined from the curve fitting for each reaction of the sulfides with MCPBA and PMS. For example, the data for the reactions of methyl p-tolyl sulfide, 4-Bromothioanisole and 4-(methythio) benzyl alcohol with MCPBA and PMS at a single temperature were fitted universally to obtain the binding constant of MCPBA as a common parameter.

4.3. Results

4.3.1. Oxidation of methyl-p-tolyl sulfide in the absence and presence of Brij-35

4.3.1.1. Dependence of rate on sulfide and peracid concentrations

Some kinetic runs were carried out to confirm the pseudo first order rate. They showed that by changing the concentration of methyl *p*-tolyl sulfide from 2 x 10^{-6} to 1.5 x 10^{-5}, and at a constant concentration of MCPBA 2×10^{-4} M in the presence of 0.0113 M Brij-35, there was no effect on the observed pseudo first order rate and it was found that the rate is independent of sulfide concentration. The data are collected in Table 1B in appendix B and plotted in Figure 4.1. Also, the reactions were carried out at a fixed methyl *p*-tolyl sulfide concentration of 1×10^{-5} M in the absence and presence of 0.0113 M Brij-35, as shown in Figure 4.2 and Figure 4.3. The peracid concentration was varied and as expected for a second order reaction conducted under pseudo first order conditions, the observed first order rate was directly proportional to substrate with excess concentration; in this case the MCPBA was over the range 4x 10^{-5} M to 4 x 10^{-3} M. Figure 4.2 shows the observed first order rate versus the [MCPBA], with intercept almost equal to zero. The second order rate constant is equal to the quotient (k_{obs})/ [peracid]. Figure 4.2 also shows the observed rate constants versus [MCPBA] for the reaction in 0.0113 M Brij-35. The data are listed in Table B2 in appendix B. Overall the findings confirm that the reaction is first order with respect to both MCPBA and sulfide concentrations, in the presence and absence of Brij-35.

Some runs were also conducted in the presence of fixed 1×10^{-5} M methyl *p*-tolyl sulfide at various PMS concentrations. It was found that the rate is proportional to the peracid concentration, as shown in Figure 4.3. The data are listed in Table B3 in appendix B.

Table 4.2 compares the second order rate constant for the reaction of meta-chloroperbenzoic acid with series of aryl alkyl sulfide obtained in this study with that obtained in previous work [162] (measured in acetic acid-acetate buffer pH = 4.6). Excellent agreement was found.

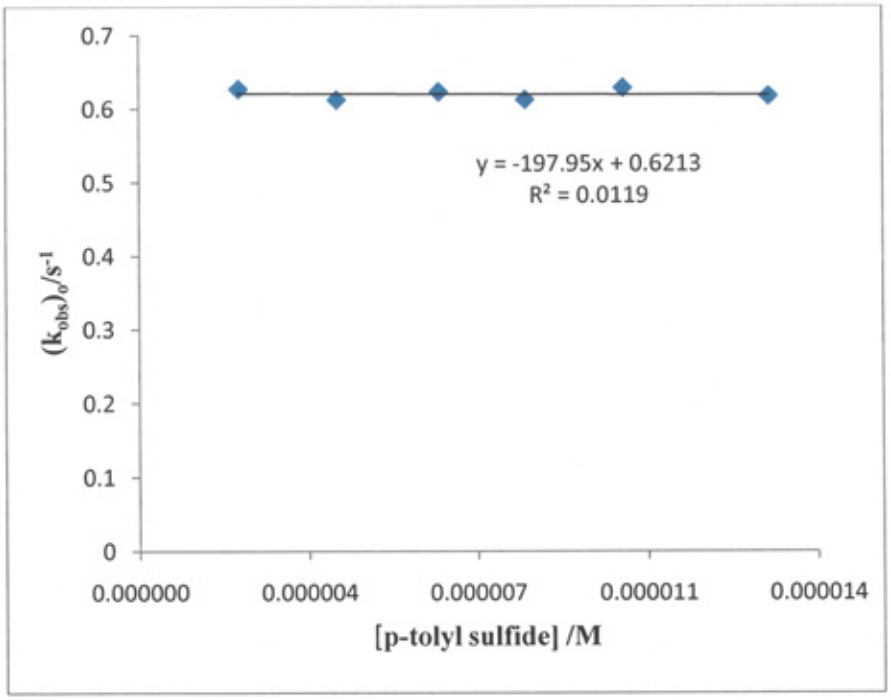

Figure 4.1: The observed pseudo first order rate constant as a function of the concentration of methyl *p*-tolyl sulfide at 2×10^{-4} M MCPBA and in 0.003 M nitric acid at 25°C.

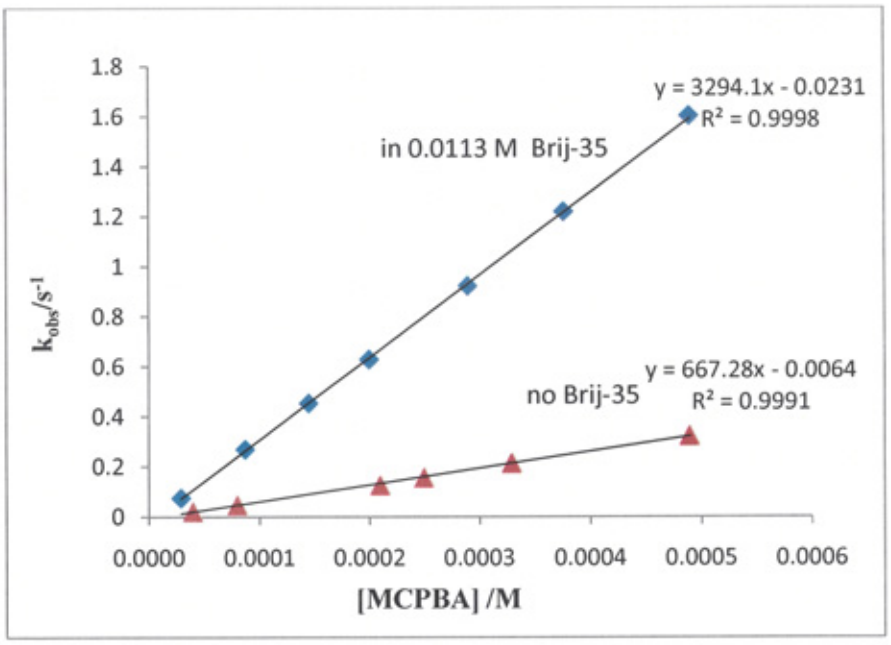

Figure 4.2: The observed rate constant against concentration of MCPBA at 1×10^{-5} M of methyl p- tolyl sulfide in the absence and presence of 0.0113 M Brij-35 and in 0.003 M nitric acid at 25°C.

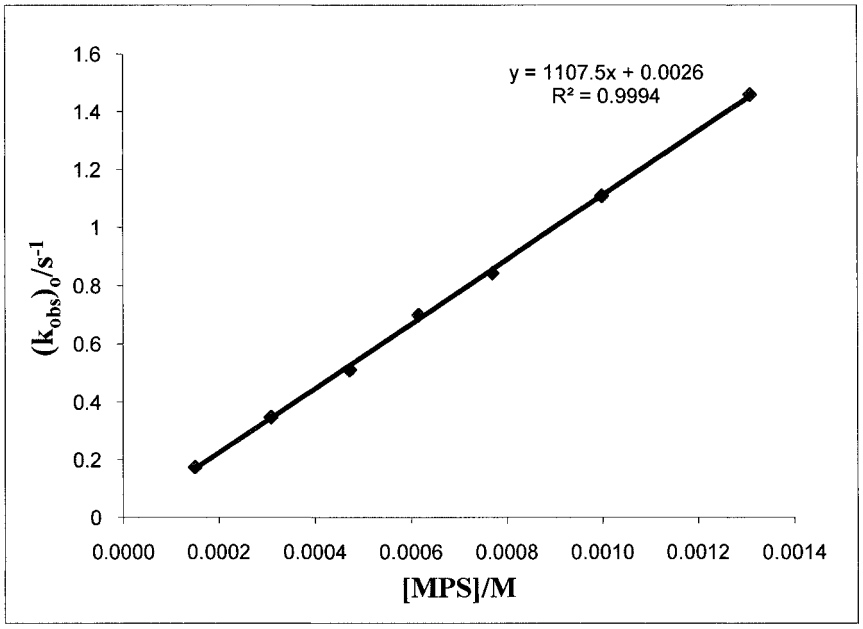

Figure 4.3: The observed first order rate constant versus the [PMS] reaction condition methyl p-tolyl sulfide 1×10^{-5} M and 0.003 M nitric acid at 25°C.

Table 4.2: comparison of second order rate constants for the reaction of aryl alkyl sulfide with MCPBA.

[Sulfides]/M	k / M^{-1} s^{-1} this work	k/ M^{-1} s^{-1}, Ref [162]	Hammett sigma constant σ_p [188]
4-CH_3	699.5	701	-0.17
4-OCH_3	1006	1002	-0.27
4-Br	332.5	333	0.23
4-Cl	390	312	0.23
2-Cl	119	nd	
4-CH_2OH	509	nd	0
4-NO_2	45.5	52.7	0.78
3-Cl	255.7	nd	0.37
Phenyl methyl sulfide	507.5	nd	0

4.3.1.2. The effect of Brij-35 concentrations on the observed rate for the oxidation of series of alkyl phenyl sulfides by PMS and MCPBA

The reaction of series of aryl alkyl sulfides with PMS and MCPBA were conducted at different Brij-35 concentrations below the CMC and up to 0.05 M, with the substrate concentration being maintained at a constant 5×10^{-4} M of PMS or 2×10^{-4} M of MCPBA with 1×10^{-5} of sulfides at 25°C. The kinetic data for the reaction of series of aryl alkyl sulfides with MCPBA acid and PMS at 25°C are collected in Table B4 to Table B10 in appendix B. Table 4.3 and Table 4.4 show the best fit parameters obtained by fitting the kinetic data for the oxidation of sulfides by MCPBA and PMS respectively to Equation 4.3 universally using the Grafit software programme. For the reactions of PMS with aryl alkyl sulfides, Equation 4.3 was also used to obtain the binding of sulfides ($K^{s}_{mic}-\overline{V}_{mic}$) to the micelle, assuming that the PMS does not bind to the micelle and setting both $k_{mic}-k_{w}\overline{V}_{mic}$ and $K^{PH}_{mic}-\overline{V}_{mic}$ to zero. It has been shown previously using a potentiometric study that this compound has zero binding to cyclodextrin due to the unfavourable desolvation required for the inclusion of this charged compound into the α-cyclodextrin [164]. In addition, the assumption made of setting $k_{mic}-k_{w}\overline{V}_{mic}$ and $K^{PH}_{mic}-\overline{V}_{mic}$ to zero for fitting the kinetic data in the presence of PMS was validated by fitting the same data to the same equation but leaving $K^{PH}_{mic}-\overline{V}_{mic}$ and $k_{mic}-k_{w}\overline{V}_{mic}$ parameters for the PMS system to 'float'. The results show that values of $k_{mic}-k_{w}\overline{V}_{mic}$ and $K^{PH}_{mic}-\overline{V}_{mic}$ turn out to be close to zero, which can confirm and validate the assumption made.

Figure 4.4 shows the observed rate constant for the reaction of PMS with series of alkyl sulfide. Figure 4.5 shows the plot of k_{obs} versus Brij-35 concentration for the reaction of alkyl aryl sulfide, with 2×10^{-4} M of MCPBA. For clarity, the data are plotted separately in Figure 4.6 to Figure 4.9 for some of the sulfides to show the effect of Brij-35 on the observed first order rate constant for MCPBA and PMS respectively. The line going through the data represents the best fit to Equation 4.3 using the Grafit programme [176].

It is clear from Figures 4.4 to 4.9 that for all sulfides increasing the Brij-35 concentration result in a decrease in k_{obs} when the oxidant is PMS, whereas for MCPBA there is an increase in k_{obs} at lower Brij concentration (catalysis) followed by a gradual decline in k_{obs} at

higher Brij concentrations. The magnitude of the increases in k_{obs} at lower concentrations for the reaction with MCPBA shows variations that are dependent on the sulfides.

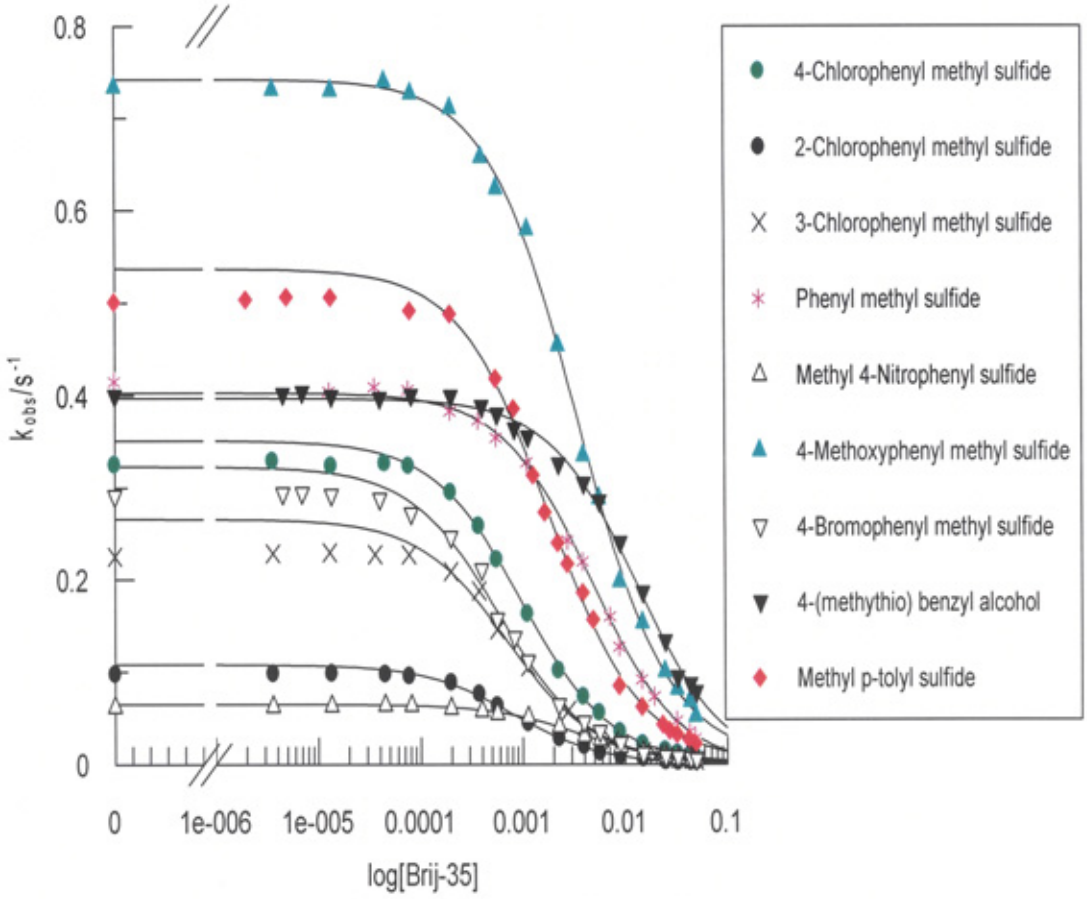

Figure 4.4: The observed rate constant as a function of log [Brij-35] for the reaction of 5×10^{-4} M PMS with 1×10^{-5} M sulfide in 0.003 M nitric acid at 25°C.

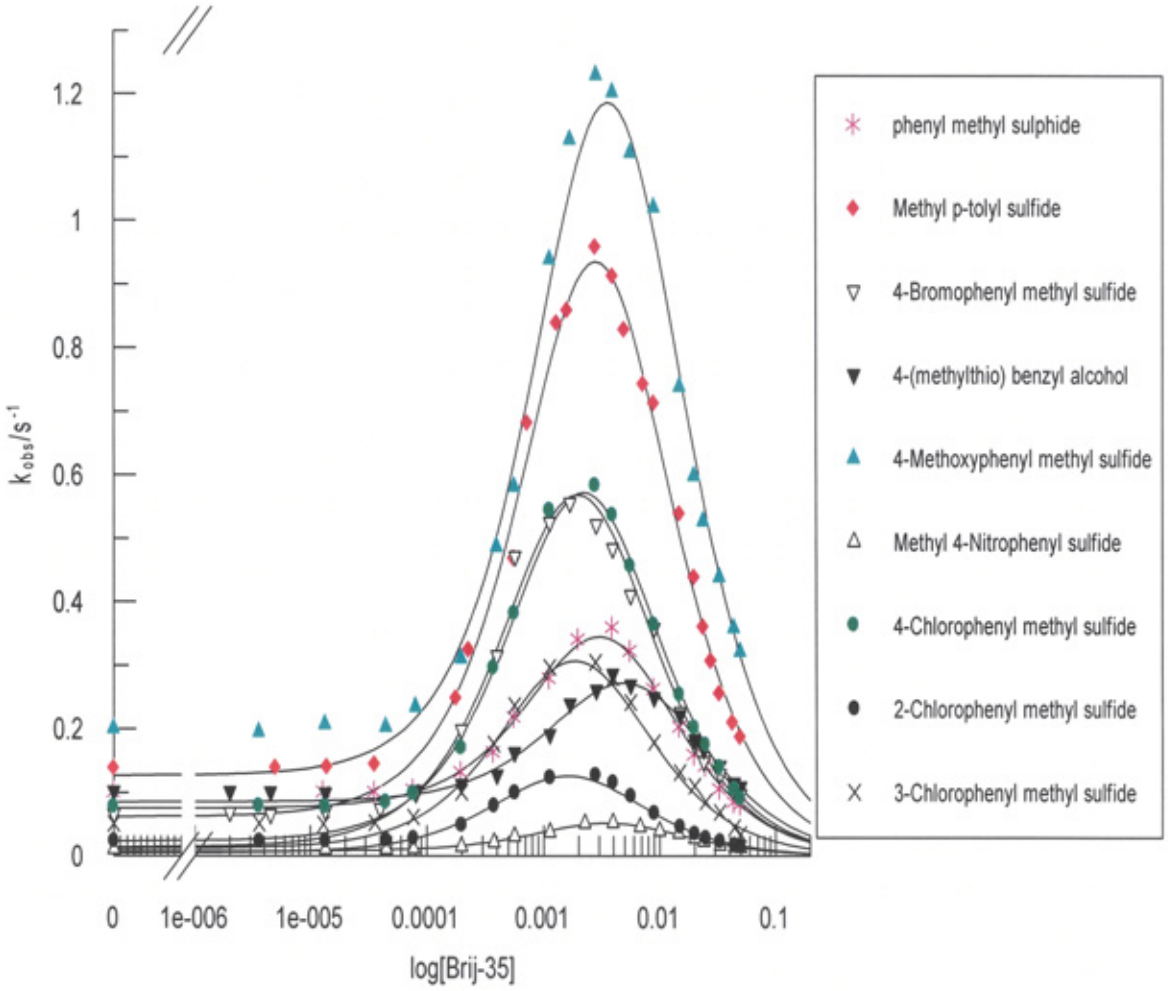

Figure 4.5: The observed rate constant as a function of log [Brij-35] for the reaction of 5×10^{-4} M MCPBA with 1×10^{-5} M sulfide in 0.003 M nitric acid at 25°C.

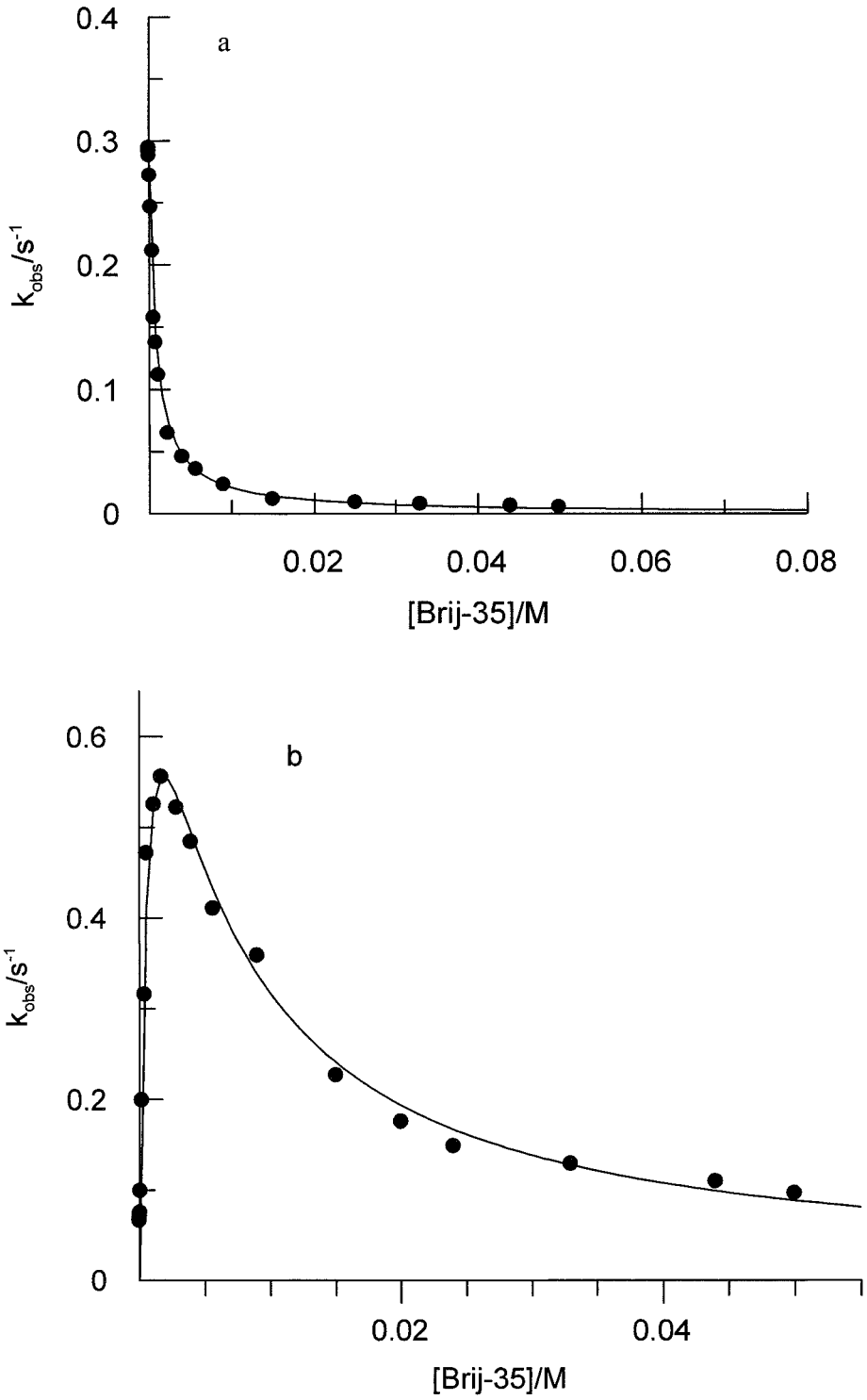

Figure 4.6: The observed rate constant versus [Brij-35] for the reaction of 1×10^{-5} M 4-bromothioanisole with 5×10^{-4} M of PMS (a) and 2×10^{-4} M of MCPBA (b) in 0.003 M nitric acid at 25° C.

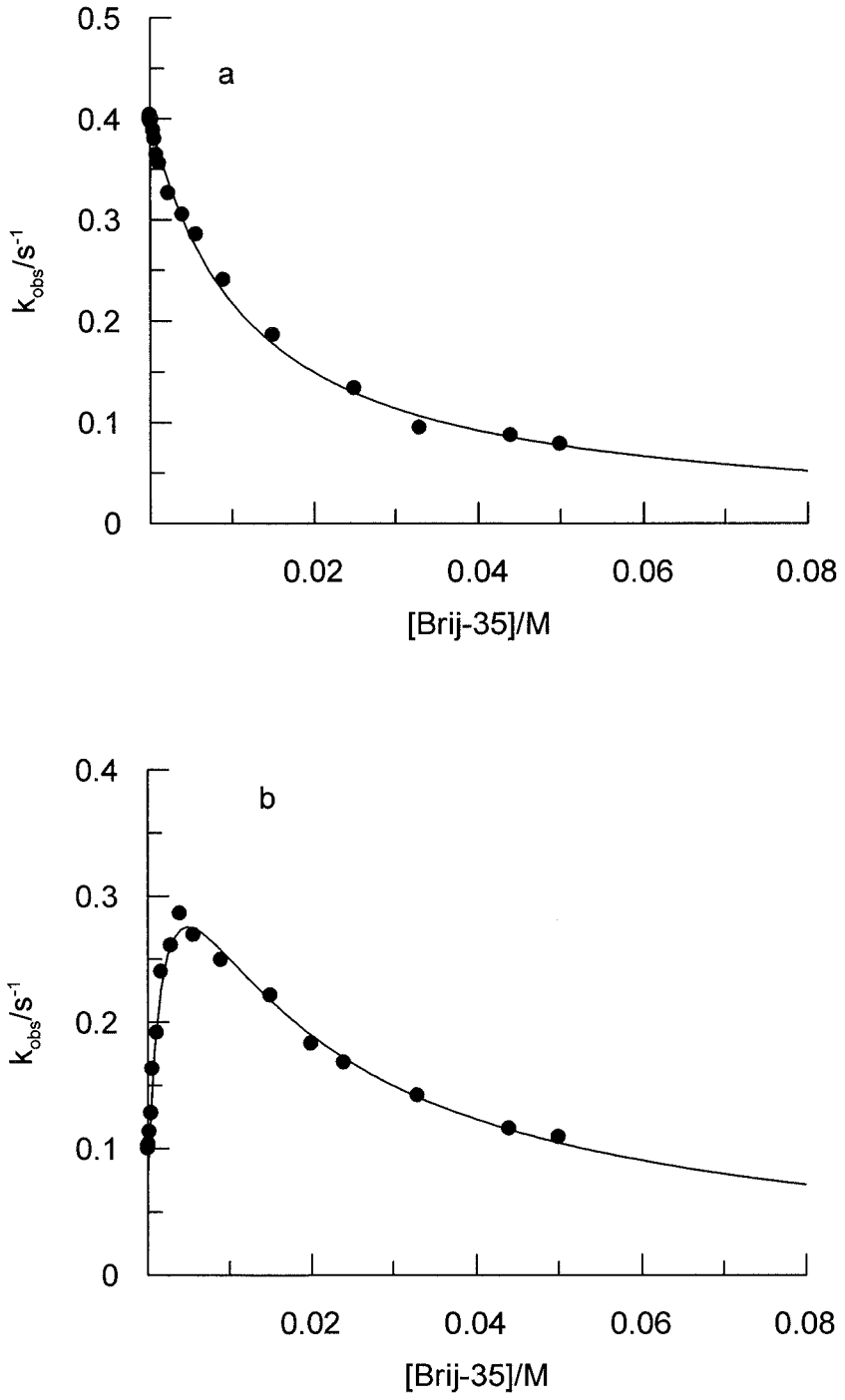

Figure 4.7: The observed rate constant versus [Brij-35] for the reaction of 1×10^{-5} M 4-(methylthio) benzyl alcohol with 5×10^{-4} M of PMS (a) and 2×10^{-4} M of MCPBA (b) in 0.003 M nitric acid at 25° C.

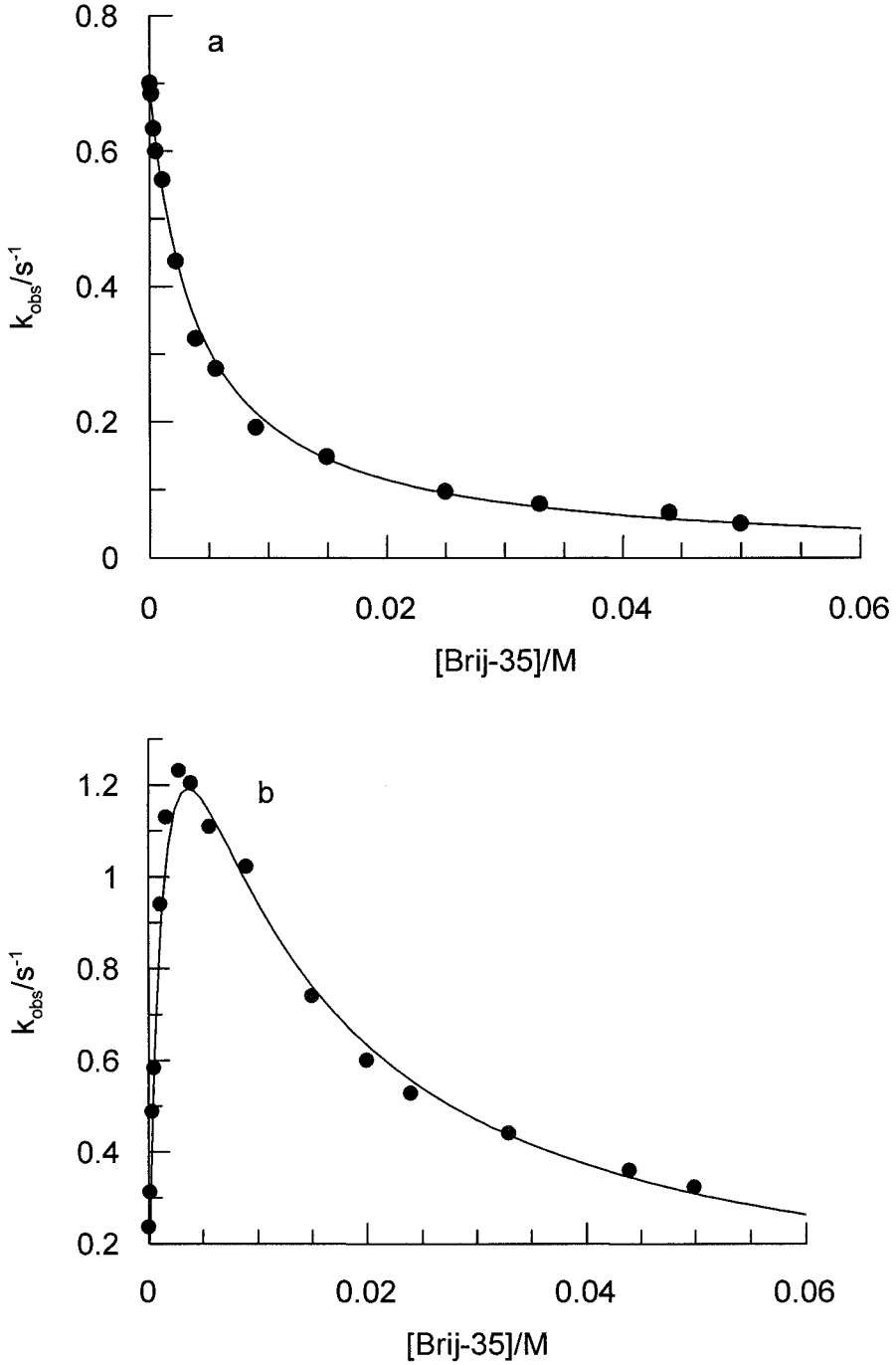

Figure 4.8: The observed rate constant versus [Brij-35] for the reaction of 1×10^{-5} M 4-methoxythioanisole with 5×10^{-4} M of PMS (a) and 2×10^{-4} M of MCPBA (b) in 0.003 M nitric acid at 25° C.

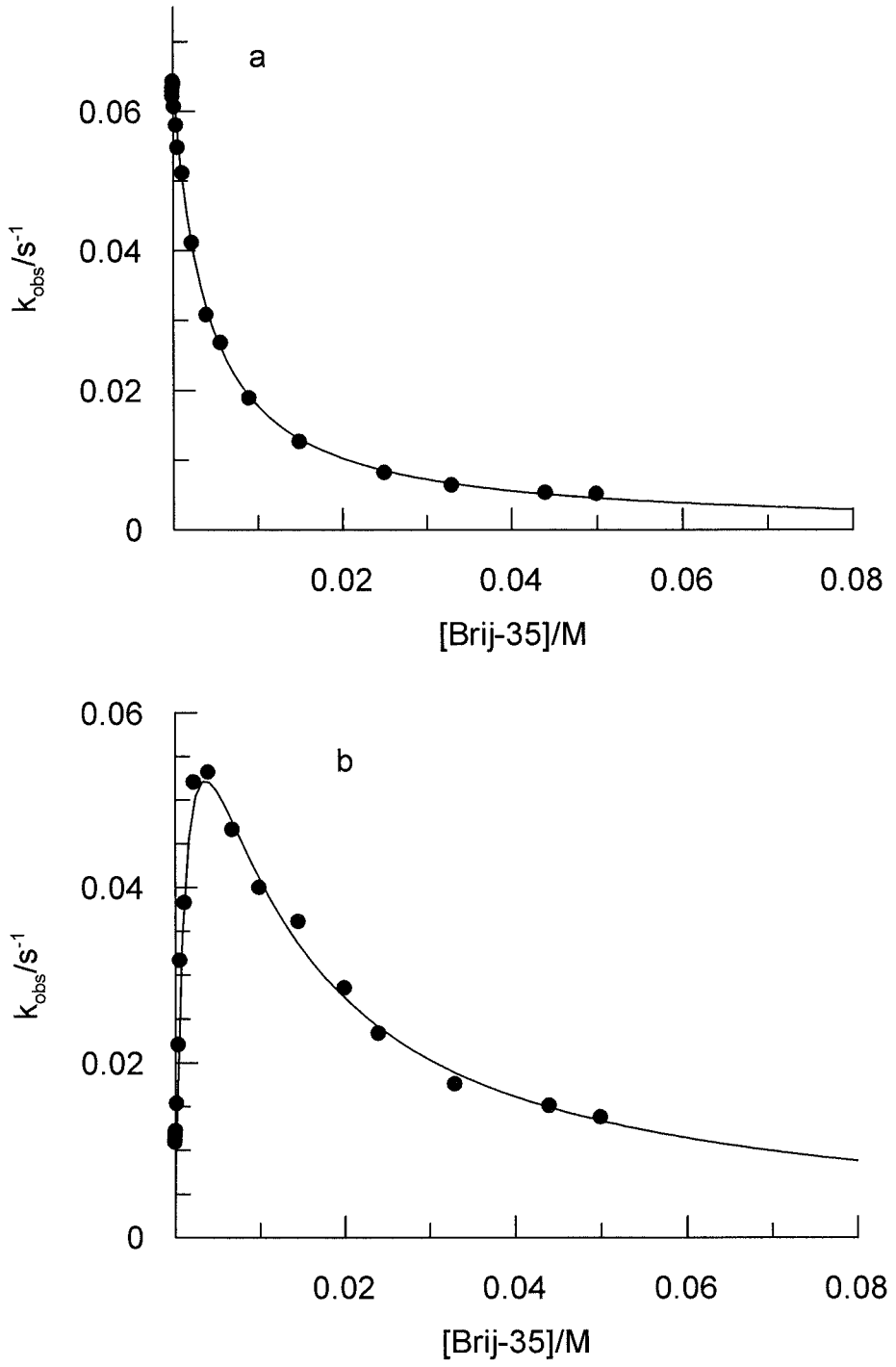

Figure 4.9: The observed rate constant versus [Brij-35] for the reaction of 1×10^{-5} M 4-nitrothioanisole with 5×10^{-4} M of PMS (a) and 2×10^{-4} M of MCPBA (b) in 0.003 M nitric acid at 25° C.

Table 4.3: Best fit parameters and their standard deviations, according to Equation 4.3, for the reaction of *ca.* 2 x 10^{-4} M MCPBA and 5 x 10^{-4} M PMS with 1 x 10^{-5} M alkyl aryl sulfide in 3.0 x 10^{-3} M nitric acid at 25°C. The CMC was fixed to 6 x 10^{-5} M.

[sulfides]/M	$(k_{obs})_o$, s^{-1} in MCPBA	$k_{mic} - k_w$ $\overline{V}_{mic}$, M^{-1} s^{-1}	$K_{mic}^{PH} - \overline{V}_{mic}$, M^{-1}	$(K_{TS})^{MCPBA}$, M^{-1}	K_{TS}/K_S
4-CH_3	0.1399±0.001	1170 ± 68	244± 15	8357	18.4
4-CH_2OH	0.1019±0.005	151± 9	-	1472	17.5
4-OCH_3	0.2012±0.004	1162 ± 53	-	5775	23.3
Phenyl	0.1015±0.001	367±18	-	3616	15.5
4-Cl	0.078±0.0004	1057 ± 43	-	13551	16.4
3-Cl	0.05115±0.0002	718±63	-	14037	12.4
2-Cl	0.0238±0.0002	315 ± 15	-	13235	12.4
2-NO_2	0.01095±0.0003	50 ± 2	-	4566	17.9
4-Br	0.06649±0.0005	1314 ± 69	-	19567	17

Table 4.4: Best fit parameters and their standard deviations, according to Equation 4.3, for the reaction of *ca.* 5 x 10^{-4} M PMS with 1 x 10^{-5} M alkyl aryl sulfide in 3.0 x 10^{-3} M nitric acid at 25°C. The cmc was fixed to 6 x 10^{-5} M.

[sulfides]/M	$(k_{obs})_o$, s^{-1} IN MPS	k_w, s^{-1}	$K_{mic}^{s} - \overline{V}_{mic}$, M^{-1}
4-CH_3	0.501±.002	0.494 ± .016	452 ± 26
4-CH_2OH	0.4±0.0014	0.3968± 0.01	87 ± 6
4-OCH_3	0.734±0.013	0.708 ±0.02	247 ± 11.6
Phenyl methyl sulfide	0.4155±.002	0.4±0.01	232±9
4-Cl	0.3249±0.0015	0.3077± 0.01	827 ± 38
3-Cl	0.225 ± 0.0012	0.23±0.012	1130±76
2-Cl	0.0976±0.0005	0.096 ± 0.004	1065 ±58
4-NO_2	0.062±0.0002	0.063 ± 0.001	254± 8
4-Br	0.2955±0.003	0.26± 0.02	1142 ± 71

4.3.1.3 Steric effects

The effect of substituent position on the catalysed oxidation of alkyl aryl sulfides at various Brij-35 concentrations has been studied by employing *p*-, o- and *m*-substituted phenyl methyl sulfides. Figure 4.10 shows the observed rate constant versus the Brij-35 concentrations for the reaction of three substituted chloro phenyl methyl sulfides with both MCPBA and PMS.

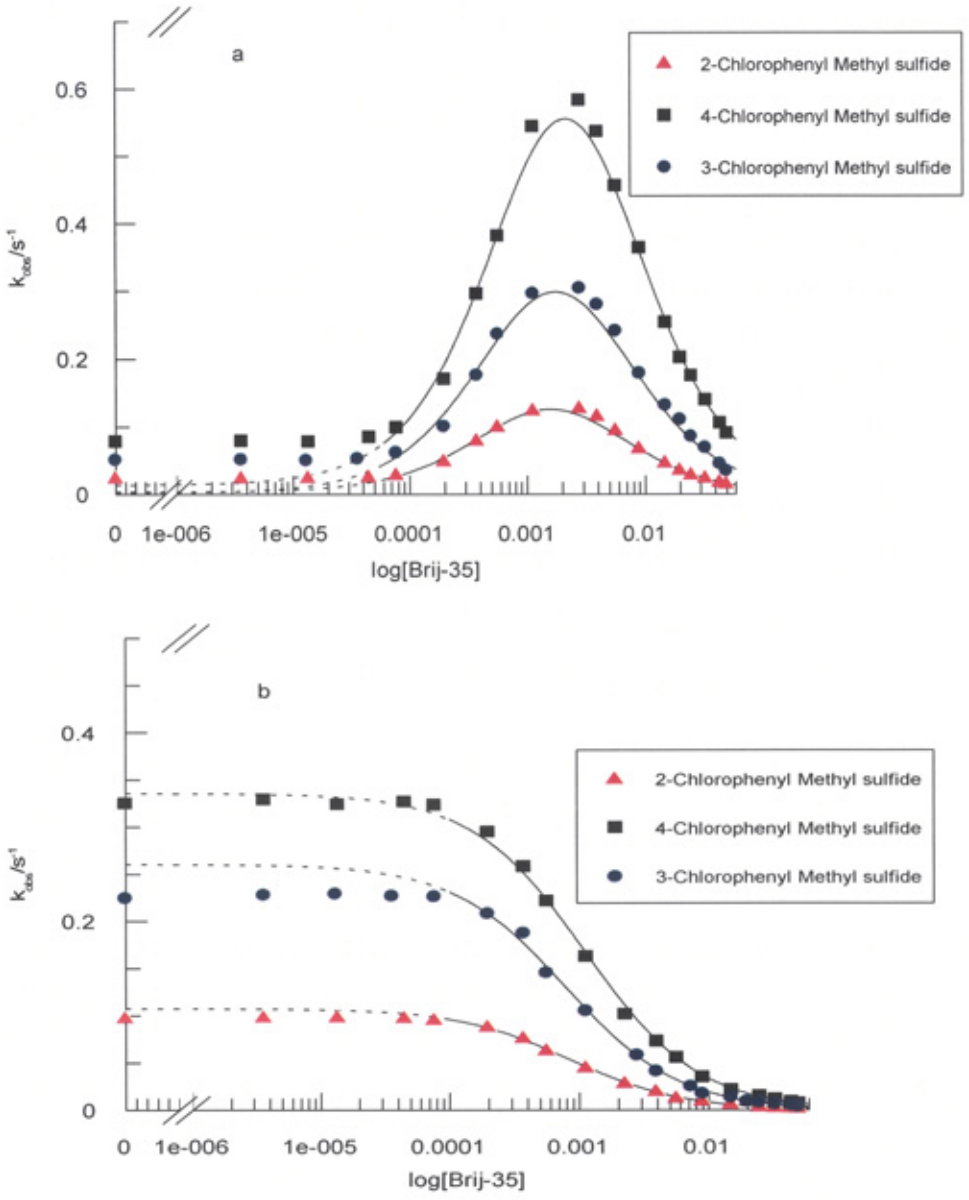

Figure 4.10: The observed rate constant versus [Brij-35] for the reaction of 1×10^{-5} M 4-Chlorothioanisole with 5×10^{-4} M of PMS (a) and 2×10^{-4} M of MCPBA (b) in 0.003 M nitric acid at 25 C^{o}.

4.3.2. The effect of Temperature on Brij-35 catalysis of aryl alkyl sulfide oxidation

No thermodynamic parameters are available for the binding of aryl alkyl sulfides to Brij-35, which would have given an insight into the binding process. Thus, an investigation is carried out to try to determine the effect of temperature on this reaction in Brij-35.

The effect of temperature on the reaction of methyl p-tolyl sulfide, 4-bromothioanisole and 4-(methylthio) benzyl alcohol concentrations (1×10^{-5} M) with both 5×10^{-4} M PMS and 2×10^{-4} M of MCPBA acid was studied at a temperature range from 15°C to 35°C. Figures 4.11 to 4.25 show the corresponding plots of the observed rate constant versus the [Brij-35] for both MCPBA and PMS respectively at various temperatures. The data were fitted universally to Equation 4.3 and the solid line on the figures represents the best fit line. The observed rate constants at different temperatures for the three compounds methyl-p-tolyl sulfide, 4-bromothioanisole and 4-(methylthio) benzyl alcohol are listed in Table B11 to Table B13 in appendix B. The best fit parameters obtained are given in Tables 4.5, 4.6 and 4.7.

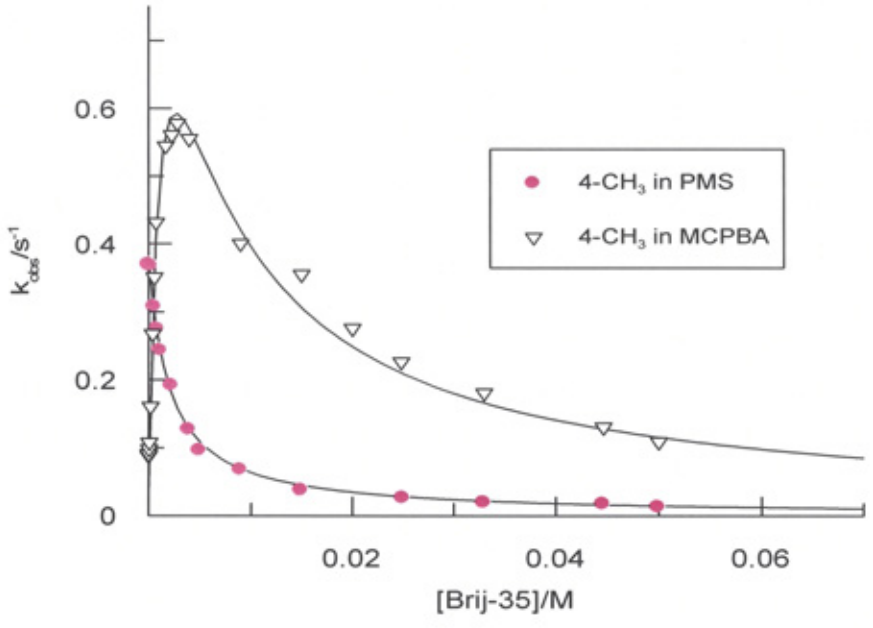

Figure 4.11: The oxidation of methyl *p*-tolyl sulfide by PMS (circle) and MCPBA (inverted triangular) at various Brij-35 concentrations and in 3.0 x 10^{-3} M nitric acid at 15°C. The curves represent the best fit line obtained by fitting the data to Equation 4.3 using universal fitting.

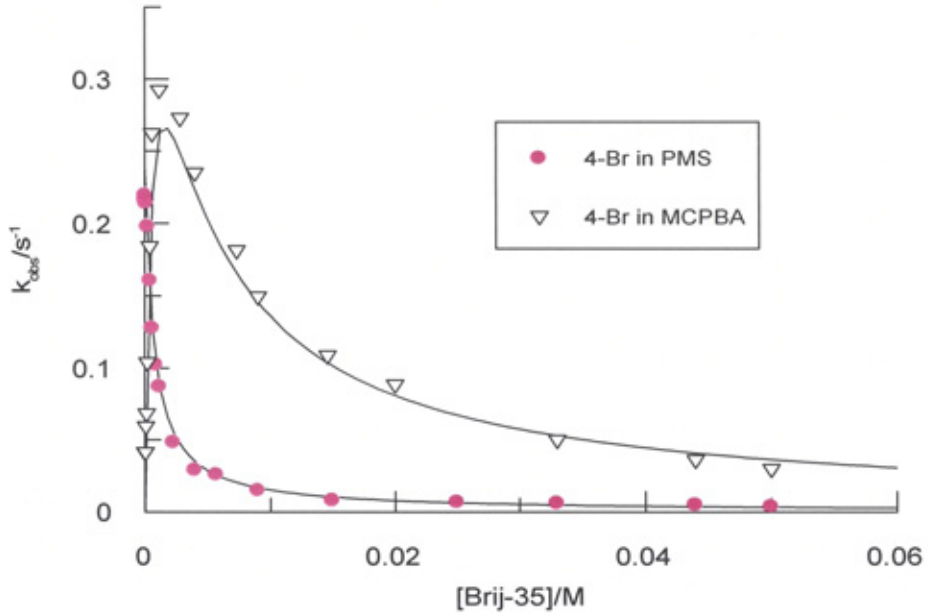

Figure 4.12: The oxidation of 4-bromothioanisole by PMS (circle) and MCPBA (inverted triangular) at various Brij-35 concentrations and in 3.0 x 10^{-3} M nitric acid at 15°C. The curves represent the best fit line obtained by fitting the data to Equation 4.3 using universal fitting.

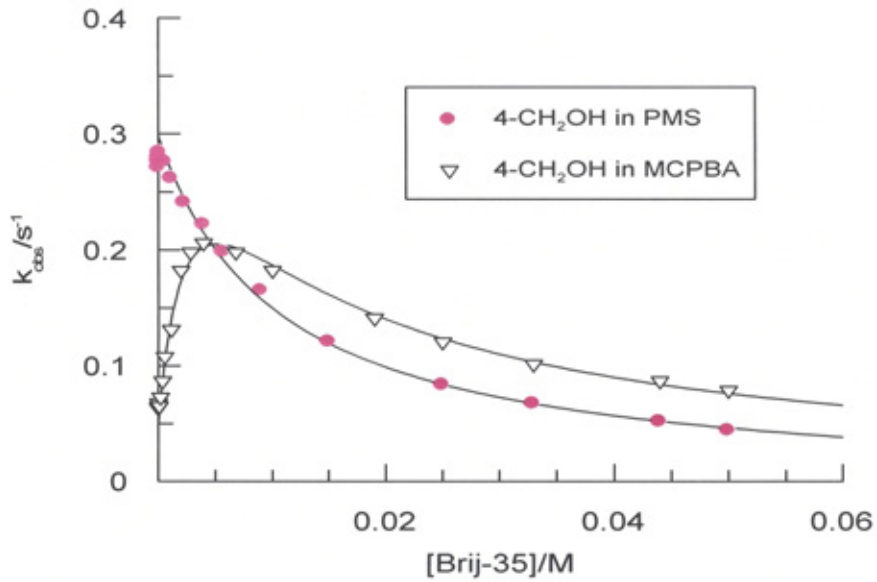

Figure 4.13: The oxidation of 4-(methylthio) benzyl alcohol by PMS (circle) and MCPBA (inverted triangular) at various Brij-35 concentrations and in 3.0 x 10^{-3} M nitric acid at 15°C. The curves represent the best fit line obtained by fitting the data to Equation 4.3 using universal fitting.

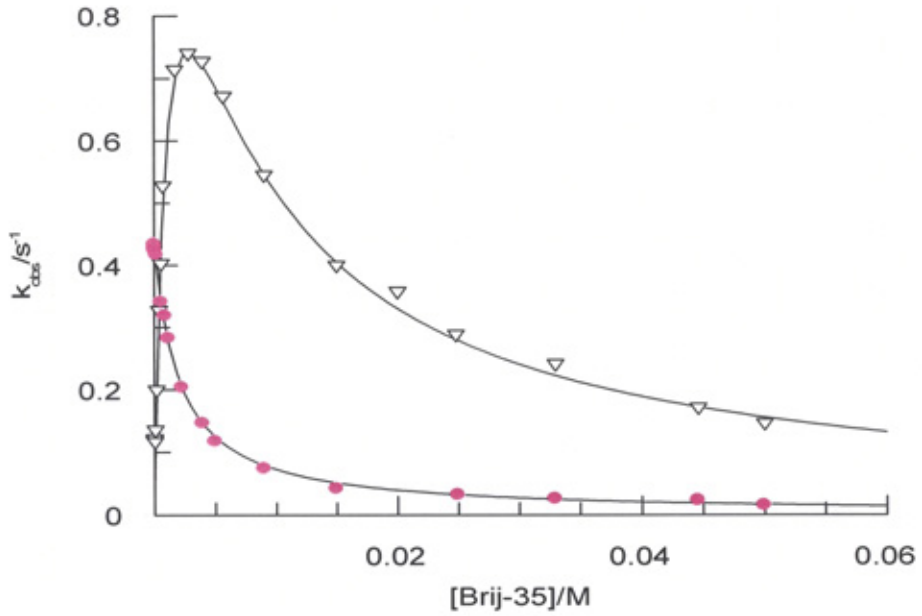

Figure 4.14: The oxidation of methyl *p*-tolyl sulfide by PMS (circle) and MCPBA (inverted triangular) at various Brij-35 concentrations and in 3.0 x 10^{-3} M nitric acid at 20°C. The curves represent the best fit line obtained by fitting the data to Equation 4.3 using universal fitting.

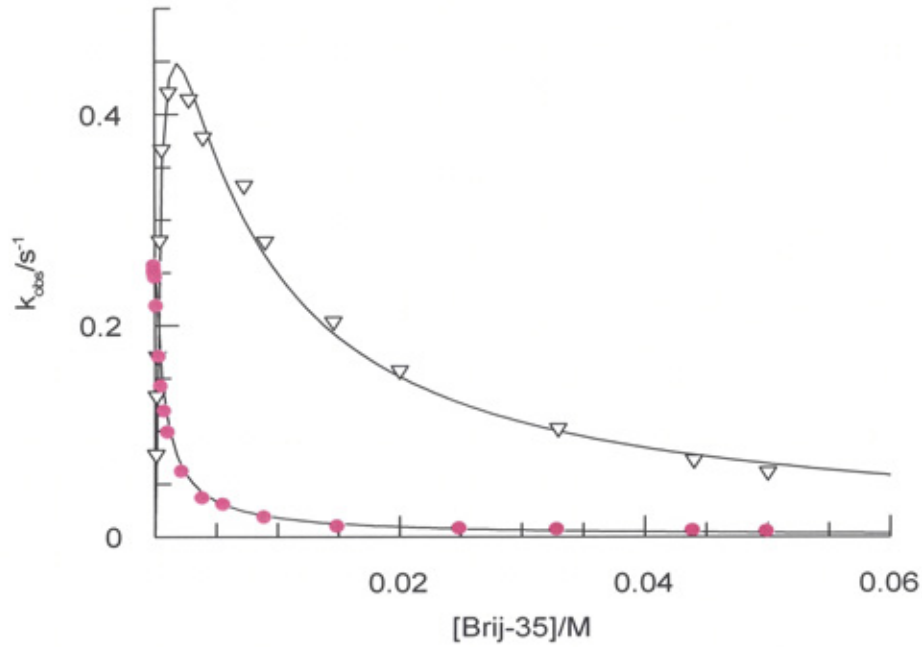

Figure 4.15: The oxidation of 4-bromothioanisole by PMS (circle) and MCPBA (inverted triangular) at various Brij-35 concentrations and in 3.0 x 10^{-3} M nitric acid at 20°C. The curves represent the best fit line obtained by fitting the data to Equation 4.3 using universal fitting.

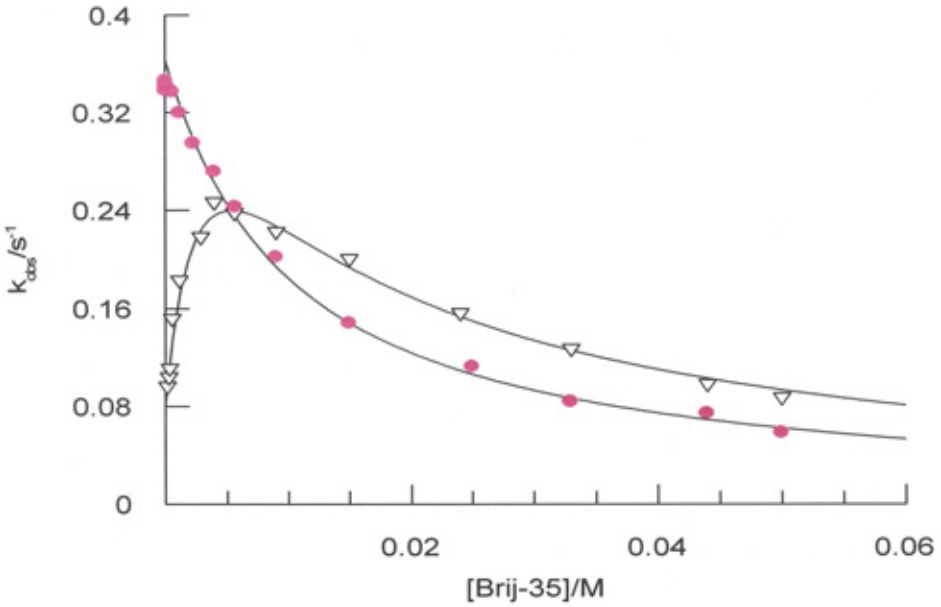

Figure 4.16: The oxidation of 4-(methylthio) benzyl alcohol by PMS (circle) and MCPBA (inverted triangular) at various Brij-35 concentrations and in 3.0 x 10^{-3} M nitric acid at 20°C. The curves represent the best fit line obtained by fitting the data to Equation 4.3 using universal fitting.

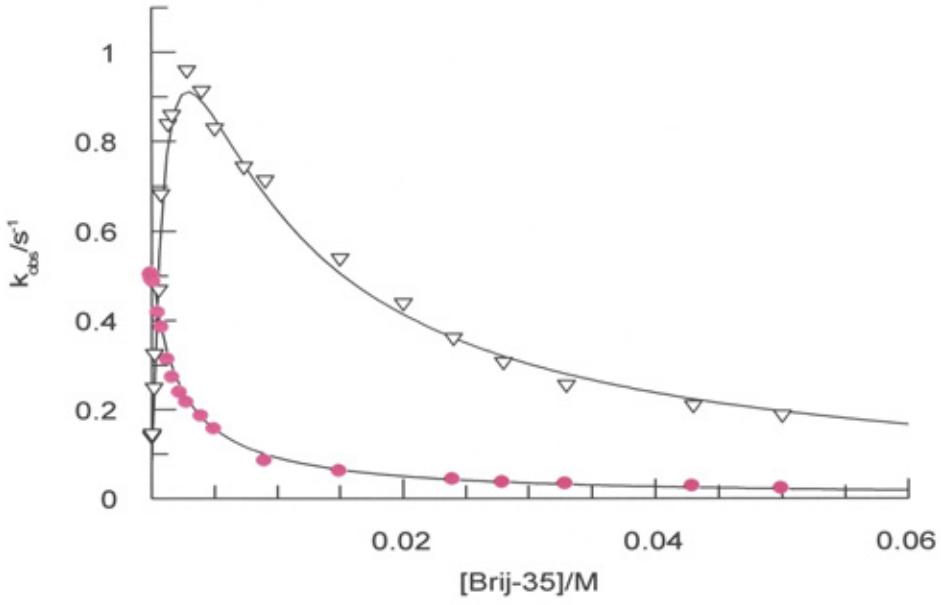

Figure 4.17: The oxidation of methyl *p*-tolyl sulfide by PMS (circle) and MCPBA (inverted triangular) at various Brij-35 concentrations and in 3.0 x 10^{-3} M nitric acid at 25°C. The curves represent the best fit line obtained by fitting the data to Equation 4.3 using universal fitting.

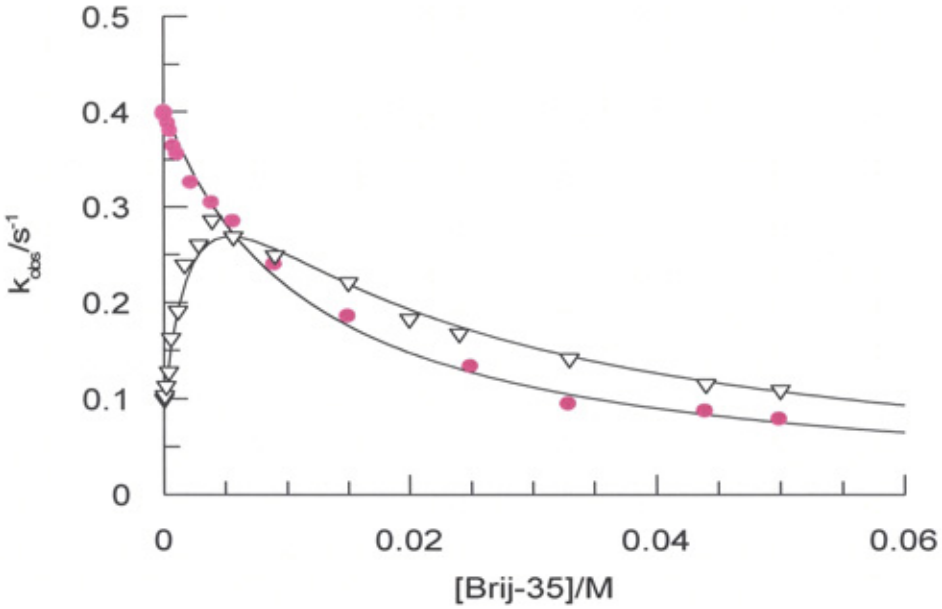

Figure 4.18: The oxidation of 4-(methylthio) benzyl alcohol by PMS (circle) and MCPBA (inverted triangular) at various Brij-35 concentrations and in 3.0 x 10^{-3} M nitric acid at 25°C. The curves represent the best fit line obtained by fitting the data to Equation 4.3 using universal fitting.

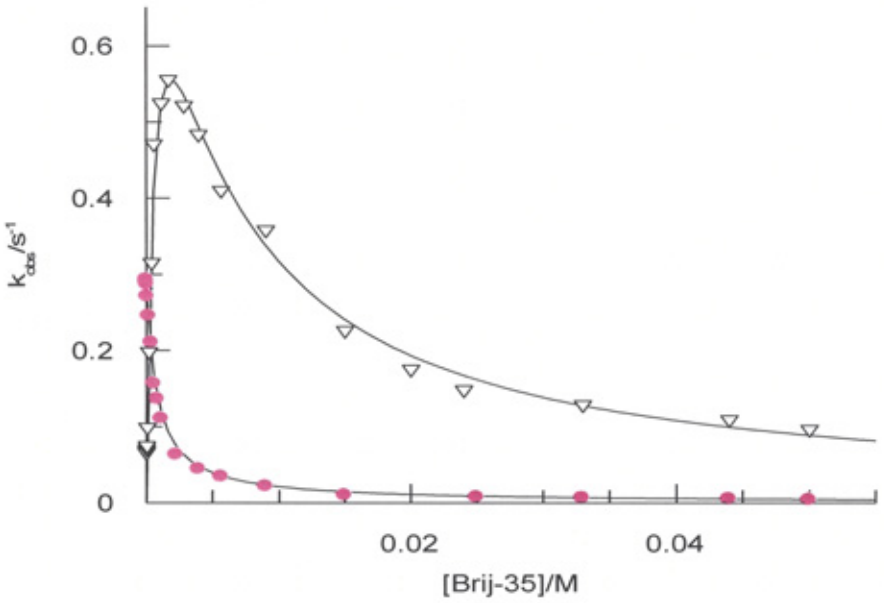

Figure 4.19: The oxidation of 4-bromothioanisole by PMS (circle) and MCPBA (inverted triangular) at various Brij-35 concentrations and in 3.0 x 10^{-3} M nitric acid at 25°C. The curves represent the best fit line obtained by fitting the data to Equation 4.3 using universal fitting.

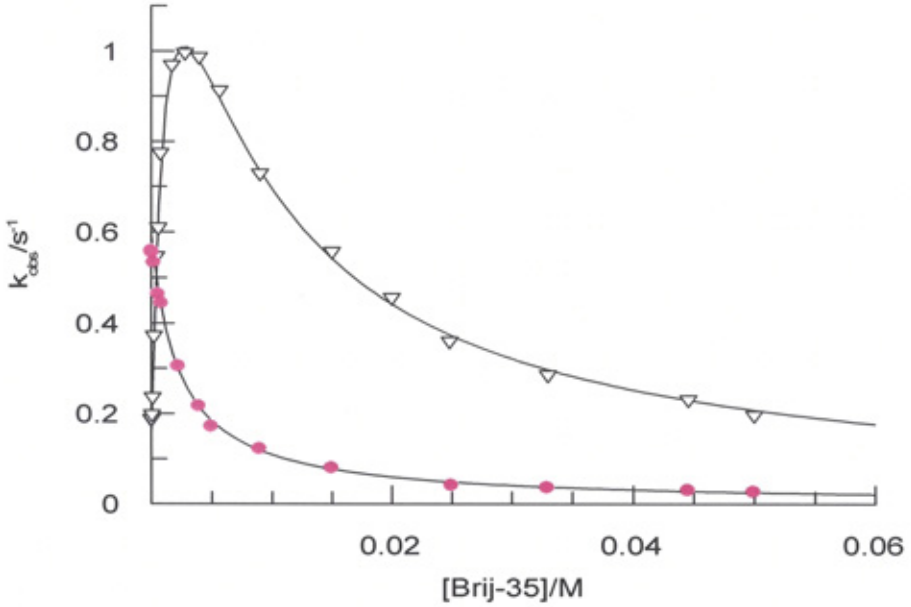

Figure 4.20: The oxidation of methyl *p*-tolyl sulfide by PMS (circle) and MCPBA (inverted triangular) at various Brij-35 concentrations and in 3.0 x 10^{-3} M nitric acid at 30°C. The curves represent the best fit line obtained by fitting the data to Equation 4.3 using universal fitting.

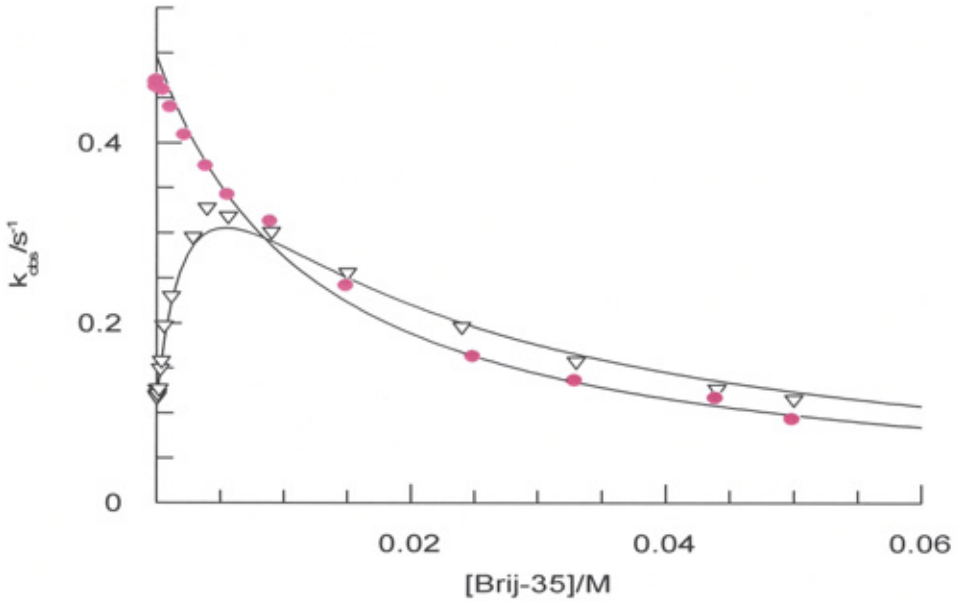

Figure 4.21: The oxidation of 4-(methylthio) benzyl alcohol by PMS (circle) and MCPBA (inverted triangular) at various Brij-35 concentrations and in 3.0 x 10^{-3} M nitric acid at 30°C. The curves represent the best fit line obtained by fitting the data to Equation 4.3 using universal fitting.

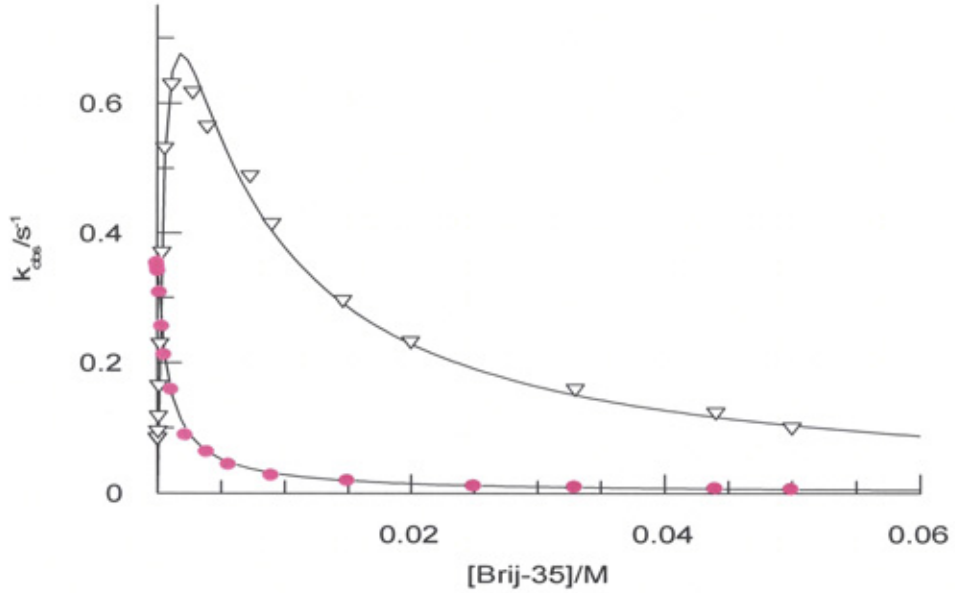

Figure 4.22: The oxidation of 4-bromothioanisole by PMS (circle) and MCPBA (inverted triangular), at various Brij-35 concentrations and in 3.0 x 10^{-3} M nitric acid at 30°C. The curves represent the best fit line obtained by fitting the data to Equation 4.3 using universal fitting.

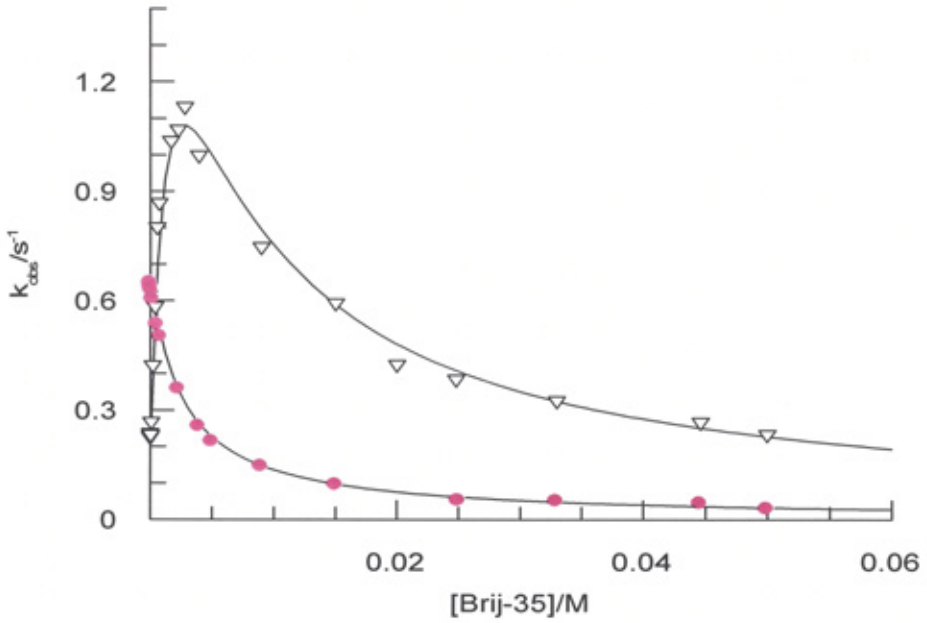

Figure 4.23: The oxidation of methyl *p*-tolyl sulfide by PMS (circle) and MCPBA (inverted triangular) at various Brij-35 concentrations and in 3.0 x 10^{-3} M nitric acid at 35°C. The curves represent the best fit line obtained by fitting the data to Equation 4.3 using universal fitting.

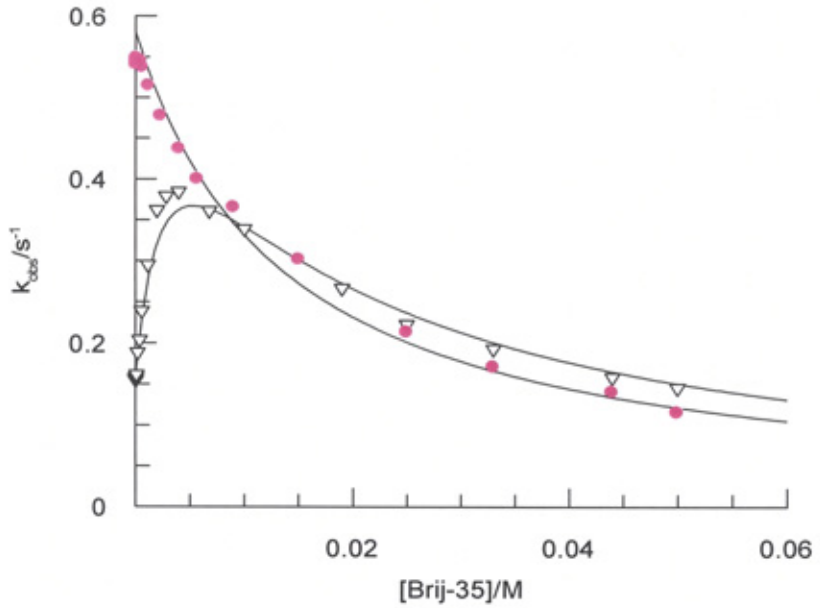

Figure 4.24: The oxidation of 4-(methylthio) benzyl alcohol by PMS (circle) and MCPBA (inverted triangular) at various Brij-35 concentrations and in 3.0 x 10^{-3} M nitric acid at 35°C. The curves represent the best fit line obtained by fitting the data to Equation 4.3 using universal fitting.

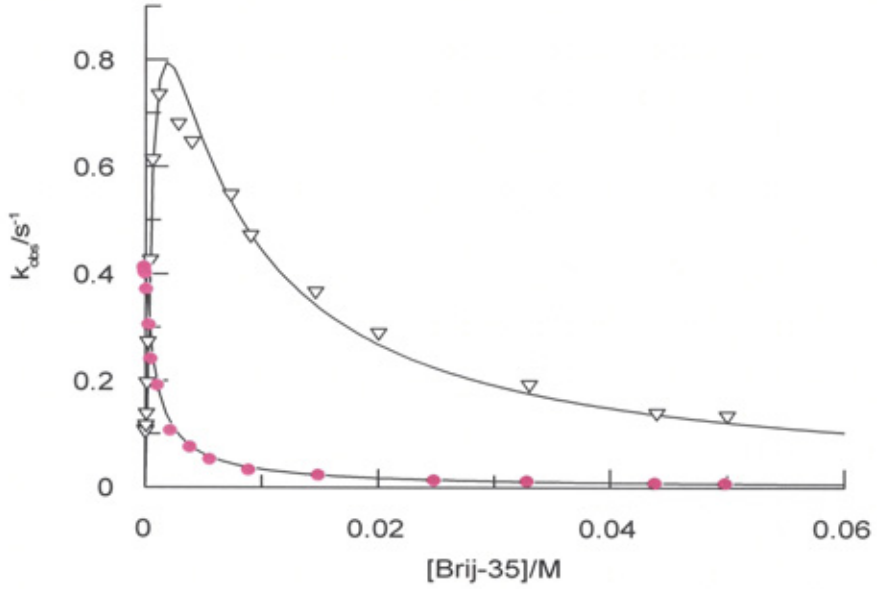

Figure 4.25: The oxidation of 4-bromothioanisole by PMS (circle) and MCPBA (inverted triangular) at various Brij-35 concentrations and in 3.0 x 10^{-3} M nitric acid at 35°C. The curves represent the best fit line obtained by fitting the data to Equation 4.3 using universal fitting.

Table 4.5: Best fit parameters and their standard deviations, obtained by fitting the data to Equation 4.3 for the reaction of *ca.* 2 x 10^{-4} M MCPBA and 5 x 10^{-4} M PMS with 1 x 10^{-5} M methyl *p*-tolyl sulfide in 3.0 x 10^{-3} M nitric acid at different temperatures.

T, °C	$(k_{obs})_o$, s^{-1} (MCPBA)	$(k_{obs})_o$, s^{-1} (PMS)	$k_{mic} - k_w \overline{V}_{mic}$, M^{-1} s^{-1}	$K^{PH}_{mic} - \overline{V}_{mic}$, M^{-1}	$K^{S}_{mic} - \overline{V}_{mic}$, M^{-1}	K_{TS}, M^{-1}
15	0.0882±.001	0.37 ± .007	842 ± 52	274 ± 21	474 ± 33	9546
20	0.1198±.0013	0.43 ± 0.007	994 ± 54	235± 16	481 ± 29	8359
25	0.14±.001	0.501 ± 0.02	1174 ± 64	244 ± 15	452± 26	8357
30	0.1867 ±.002	0.55± 0.007	1291± 52	255± 12	433 ± 18	6881
35	0.23±.0035	0.65 ±0.017	1304± 67	262± 16	389± 20	5502

Table 4.6: Best fit parameters and their standard deviations, obtained by fitting the data to Equation 4.3 for the reaction of *ca.* 2 x 10^{-4} M MCPBA and 5 x 10^{-4} M PMS with 1 x 10^{-5} M 4-(methylthio) benzyl alcohol in 3.0 x 10^{-3} M nitric acid at different temperatures.

T, °C	$(k_{obs})_o$, s^{-1} (PMS)	$(k_{obs})_o$, s^{-1} (MCPBA)	$k_{mic} - k_w \overline{V}_{mic}$, M^{-1} s^{-1}	$K^{PH}_{mic} - \overline{V}_{mic}$, M^{-1}	$K^{S}_{mic} - \overline{V}_{mic}$, M^{-1}	K_{TS}, M^{-1}
15	0.271±.006	0.064 ± 0.01	133 ± 6.5	274 ± 21	101± 7	2084
20	0.338±.007	0.0826± 0.003	137 ±9	235± 16	95± 6	1659
25	0.4±.0086	0.101± 0.005	151 ± 9	244 ± 15	87± 5.4	1472
30	0.46±.01	0.127± 0.0027	169± 8	255± 12	81 ± 3	1334
35	0.54±.01	0.155±0.002	198± 12	262± 16	74± 4	1276

Table 4.7: Best fit parameters and their standard deviations, obtained by fitting the data to Equation 4.3 for the reaction of *ca.* 2 x 10^{-4} M MCPBA and 5 x 10^{-4} M PMS with 1 x 10^{-5} M 4-Bromothioanisole in 3.0 x 10^{-3} M nitric acid at different temperatures.

T, °C	$(k_{obs})_o$, s^{-1} (PMS)	$(k_{obs})_o$, s^{-1} (MCPBA)	$k_{mic} - k_w \overline{V}_{mic}$, M^{-1} s^{-1}	$K^{PH}_{mic} - \overline{V}_{mic}$, M^{-1}	$K^{S}_{mic} - \overline{V}_{mic}$, M^{-1}	K_{TS}, M^{-1}
15	0.217±.025	0.0413± 0.2	736± 56	274 ± 21	1356 ± 104	18475
20	0.25±.02	0.0518 ± 0.02	1106 ± 66	235± 16	1235± 79	21351
25	0.291±.02	0.066 ± 0.02	1314± 69	244 ± 15	1142± 71	19567
30	0.345 ±.01	0.085± 0.01	1554± 65	255± 12	1068± 46	18154
35	0.41±.016	0.107 ±0.015	1799± 89	262± 16	1031± 56	16595

4.4. Discussion

4.4.1. Oxidation of p-tolyl methyl sulfide in the absence and presence of fixed concentrations of Brij-35

The reaction of aryl alkyl sulfide with peracid is a second order reaction overall, first order in the sulfide and first order in peracid. In general, the plot of k_{obs} versus the concentration of the peracid (which is about twenty times more concentrated than the sulfide) in the absence and presence of Brij-35 is linear, with intercept close to zero, and indication of first order rate dependence as shown in Figure 4.2 and Figure 4.3. Thus, the presence of Brij-35 does not affect the order of the reaction and so Brij-35 dependence can be carried out.

Table 4.2 compares the second order rate constant for the reaction of MCPBA with series of aryl alkyl sulfide obtained in this study with that of previous work [162]. There is excellent agreement between these values, even though the previous work [162] was carried out in acetate buffer of pH = 4.8.

The reaction rates of sulfides with peracid are sensitive to the influence of the type of substituent, and both reactions with peracids (MCPBA and PMS) conform to the Hammett equation, $\log (k/k_o) = \sigma\rho$, where k_o is the value of the rate constant when there is no substituent, k is the rate constant for the substituted compounds, σ is a constant dependent only on the properties of the ring substituent, and ρ is the reaction constant which does not depend on the type of substituent but on the reaction, as shown in Figure 4.26 which shows log of the rate constant for the oxidation of alkyl aryl sulfide with MCPBA and PMS versus the Hammett sigma values obtained from reference [188]. The negative values of ρ, which depend only on the reaction and the experimental conditions, show that the reactions are favoured by an increase in electron availability at the sulphur atom. The reactions of 3-chloroperbenzoic acid show the most negative values of ρ, revealing a greater sensitivity to electron availability at the sulfur atom.

Figure 4.26 shows a log of the rate constant for the oxidation of alkyl aryl sulfide with MCPBA and PMS versus the Hammett sigma values with a slope equal to ρ values of -1 $\pm$ 0.11 and -0.9 $\pm$ 0.1 respectively. These negative values indicate that the reaction is accelerated by an electron donating group and it follows the same pathway for both peroxyacids.

4.4.2. The oxidation of alkyl sulfide in the presence of various Brij-35 concentrations

As can be seen from Figure 4.4 and Figure 4.5, which show the plot of k_{obs} versus [Brij-35] for the reaction between PMS and MCPBA with alkyl aryl sulfide respectively, the rate of the reaction in the case of MCPBA initially increases (when the CMC is reached at about 6×10^{-5} M in Brij-35) toward a maximum level of around 0.002 M Brij-35, after which point the rate decreases with an increase in surfactant concentration. This is characteristic of micellar catalysis, when both reagents bind to the micelle [101]. Also, it is clear that there is a difference between the shape of the curves in the figure for different sulfides. A greater enhancement of the rate was seen for 4-methoxythioanisole (electron donor substituent) which exhibited a sharp peak. This is due to an increase in the nucleophilicity of the sulfur atom as the methoxy group pushes electrons toward this reaction centre; while for 4-nitrothioanisole, which includes the electron attracting group (nitro group), the rate is lower. This is due to the fact that the nitro group reduces the electron density at the sulfur atom and consequently its nucleophility. Also, the curve is characterised by its broadness.

The oxidation of all alkyl aryl sulfides by PMS in the presence of Brij-35 was observed to be inhibited without exception. The decrease in the rate of oxidation of sulfides by PMS in presence of [Brij-35] starts at value of 6×10^{-5} M which corresponds to the value of the critical micelle concentration. This is an indication that the reactants are partitioning between the phases, and as observed before, the PMS prefers to stay in the aqueous phase due to unfavourable desolvation [164].

A log of the binding constant of the substituted sulfide was plotted as a function of the Hammett sigma constant, as shown in Figure 4.27. And in Figure 4.28, a log plot of the association constant of the transition state for the reaction in MCPBA was plotted as a function of Hammett values (the K_{TS} was calculated from the ratio of the $k_{mic}/(k_{obs})_o$ as described in chapter 3 for the reaction with iodide).

It is worth noting that the binding constant of MCPBA is not sensitive to p-substituent of sulfides and thus $K_{mic}^{PH}-\overline{V}_{mic}$ was kept common for all systems when fitting the data to Equation 4.3.

From both Figure 4.27 and Figure 4.28 it can be seen that there is no correlation between the electron withdrawing or donating group of the substituent and the binding constant of the sulfides and transition state. It can also be seen from these figures that there are

variations and no clear relationships exist. This implies that the binding is not controlled by the electronic nature of the substituents, and similar variations in both figures suggest that the same factor that stabilises the transition state also stabilises the sulfides.

In Figure 4.29 the values of log $(k_{obs})_o$ the observed rate constant for the reaction of MCPBA acid with various alkyl aryl sulfides have been plotted against log $(k_{obs})_o$ values for the reaction of PMS with the same series of alkyl aryl sulfides. The correlation coefficient values of ($r = 0.99$) indicate that the mechanism of the reaction is common in both peracids for the oxidation of sulfides.

The steric effect on reaction rate is investigated by varying the chloride atom position on the aromatic ring of the sulphide. From Figure 4.10 reaction is faster in the case of para followed by meta and a low rate is observed for the o- Chlorothioanisole. This clearly indicates that the reaction is quite sensitive to steric congestion around the reaction site. The large chloride atom in the ortho position makes the attack of peracid on the sulfur centre less as a result of its presence in this position, and hence the rate observed is lower than other chlorothioanisoles.

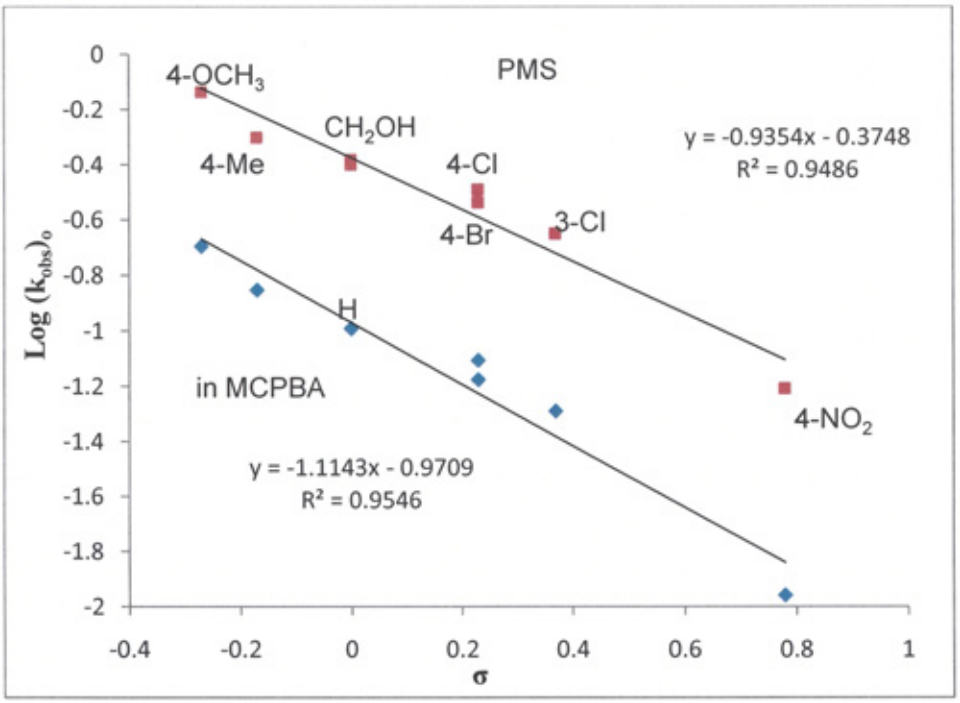

Figure 4.26: Hammett plots for the oxidation of series of alkyl aryl sulfide with MCPBA and PMS at 25°C. The standard error for the slope of MCPBA and MPS are ±0.11 and 0.1 respectively.

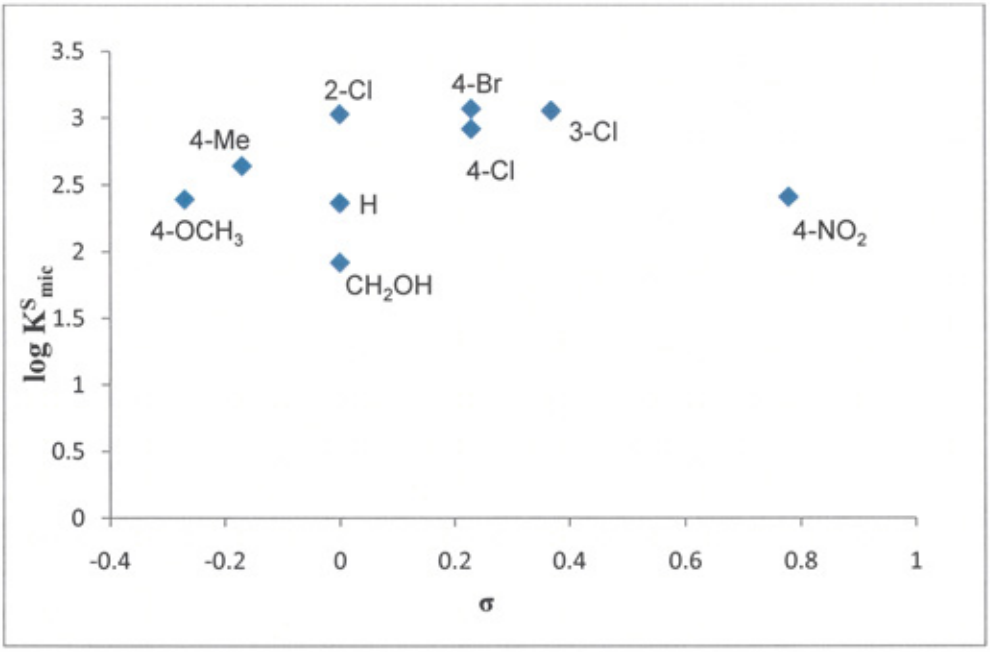

Figure 4.27: The Hammett sigma constant versus the binding constant of the sulfide, obtained from fitting the kinetic data to Equation 4.3.

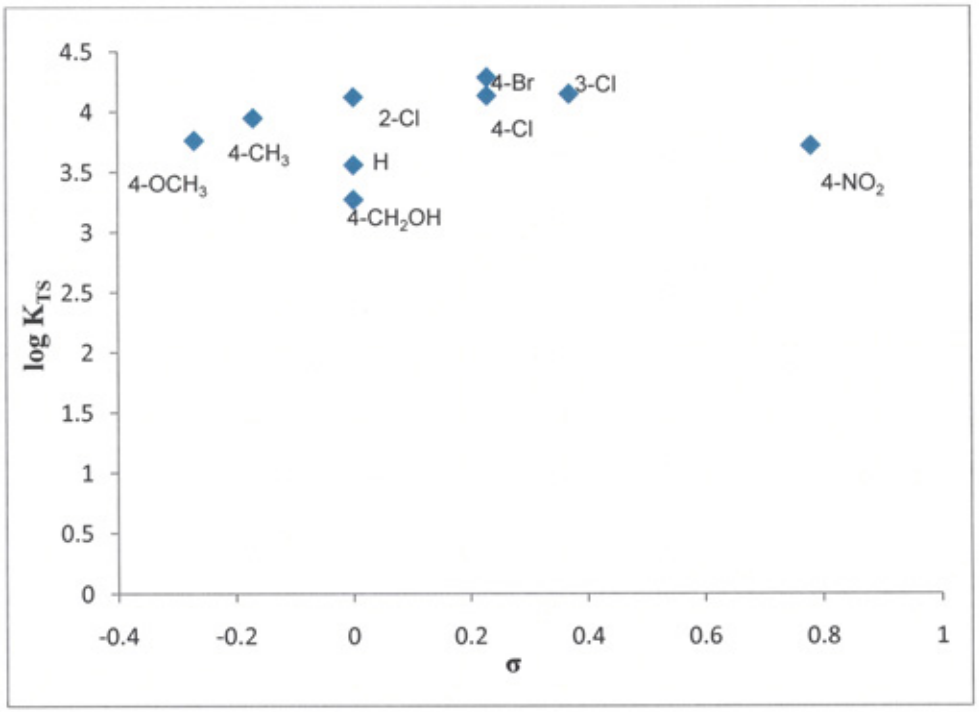

Figure 4.28: The natural log of the binding constant of the transition state plotted as a function of Hammett sigma values for the oxidation of sulfides by MCPBA at 25°C.

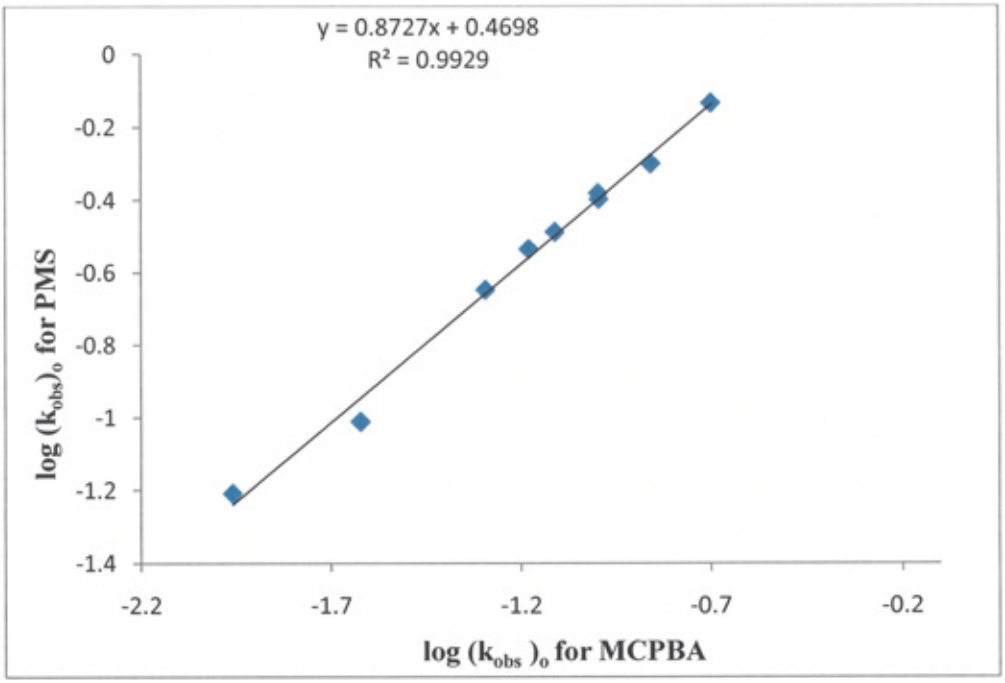

Figure 4.29: Free energy relationships correlation of log k_{obs} of MCPBA oxidation with log k_{obs} of PMS for the oxidation of aryl alkyl sulfides in the absence of Brij-35.

4.4.3. Discussion of the binding constant of sulfides and peracid, and the relationship with transition state K_{TS}

Two peracids were investigated in these studies: the anionic PMS and the neutral MCPBA. In the case of PMS, inhibition is a result of the trivial separation of the reagents, where one of them (the hydrophobic substrate) is bonded to the micelles, while the anionic oxidant (HSO_5^-) is found predominantly in the aqueous phase.

For the MCPBA the rate goes to maximum and then starts to decline at concentrations of about 0.002 M of Brij-35. The shape of the peak is different for different sulfides. In general, the degree of binding of sulfides to the micelles is increased by a change in substrate structure; it is higher for sulfides with halide moiety and a lower value of binding constant is observed for 4-(methylthio) benzyl alcohol, possibly due to hydrogen bonding with water in the bulk phase which leads to a small binding constant of about 80 M^{-1}.

Figure 4.30 shows that there is a good correlation between the association constant for the stabilisation of transition state and that of the sulfides. Transition state binding K_{TS} and substrate binding K_S are strongly correlated with each other, with a correlation coefficient of 0.95. They exhibit the same sensitivity to Brij-35, and the binding of both sulfides and transition state are governed by the same factor. In all cases for the reaction of MCPBA with sulfides, the ratio of K_{TS}/K_S is more than one, which indicates micellar catalysis. The highest ratio K_{TS}/K_S is for the 4-methoxy phenyl sulfide, which shows the greatest micellar catalysis. A similar parallel correlation between the pseudo association constant of the transition state and that of the reactant has been found for the ester cleavage by hydroxide ion in CTAB micelles [189], and for thiolysis of p-nitrophenyl alkanoate in the same cationic micelle, where the relative stabilisation of transition states and esters remains constant. This is explained by the fact that the same factors are responsible for the stabilisation [190].

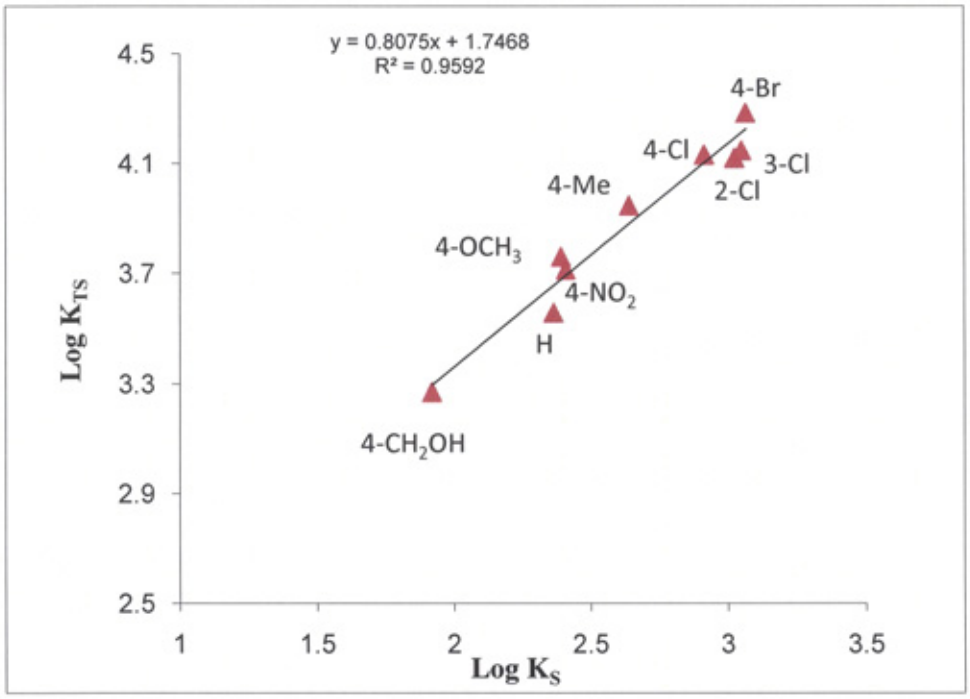

Figure 4.30: log plot of the of transition state binding constant versus sulfides binding constant for the reaction of peracids with sulfides in Brij-35 at 25°C

4.4.4. Discussion on the thermodynamic parameters for the oxidation of alkyl aryl sulfides

The kinetics of the oxidation reaction of sulfide substrates 4-Br, 4-Me and 4-CH_2OH in micellar solutions of Brij-35 were measured at different temperatures. Plots of ln (k_{obs}/T), ln{($k_{mic} - k_w \overline{V}_{mic}$)/T}, ln ($K^{PH}_{mic} - \overline{V}_{mic}$), and ln ($K^{s}_{mic} - \overline{V}_{mic}$) against inverse temperature in Kelvin for the reactions of 4-bromothioanisole, methyl p-tolyl sulfide, and 4-(methylthio) benzyl alcohol are shown in Figure 4.31 to Figure 4.33. These plots enable the calculation of thermodynamic parameters which will be used in the next section.

The enthalpy and entropy of activation from the kinetic parameters are calculated using the Eyring Equation, with h and k_B Planck's and Boltzmann's constants respectively, and the enthalpy and entropy of the association parameters from the linear form (assuming the parameters are independent of temperature) of the Van't Hoff Equation. These quantities are shown in Table 4.8.

The activation parameters of the reaction activation enthalpy and activation entropy were calculated both in the absence of a surfactant and in the micellar pseudophase, as shown in Table 4.8. It is clear that the values of activation of enthalpy in the absence of Brij-35 are higher than those when the reaction occurs in the micelle, which indicates that the

micelle catalyses the reaction by decreasing the energy requirement. For the entropy of activation the values of three substituted sulfides become less negative (entropy gain) in the presence of the micelle, which shows that the system becomes less ordered.

Table 4.8 shows that the Gibbs free energy for the activation process is almost constant and positive for all three sulfides, even though the enthalpy and entropy are varied. This confirms that both parameters compensate for each other so that the values of $\Delta G^{\ddagger}$ are almost constant and the positive free energy indicates that the reaction is not spontaneous.

The small binding of 4-(methylthio) benzyl alcohol can be attributed to the presence of the hydroxyl group, which may favour hydrogen binding to the solvent water rather than incorporation into the Brij-35. However, the binding of this sulfide has small negative values of ΔH^{o} as with the other two, which is an indication of weak interaction. Notwithstanding, it is associated with entropy loss which is indicated by a small negative value; while for the other two sulfides (methyl p- tolyl sulfide and 4-(methylthio) benzyl alcohol) the entropy is more positive. So, it can be said that the binding of sulfide is enthalpy driven for the 4-CH_2OH and entropy driven in the two other sulfides. Also, these three substrates have negative values of ΔG^{o}, which may indicate that the binding is a favourable process.

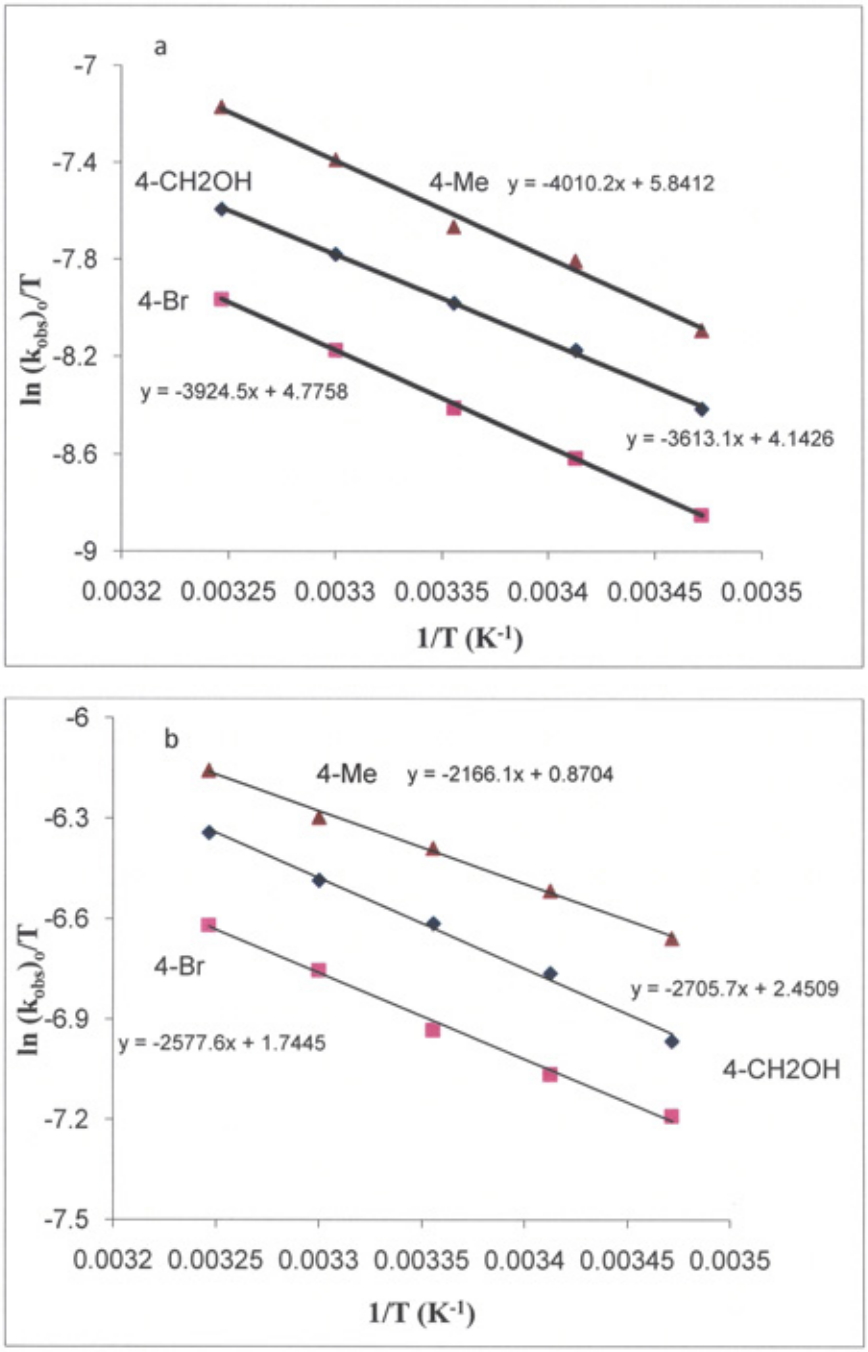

Figure 4.31: The Eyring plot for the reaction of MCPBA (a) and PMS (b) with methyl-p-tolyl sulfides, 4-bromothioanisole and 4-(methylthio) benzyl alcohol in the absence of Brij-35.

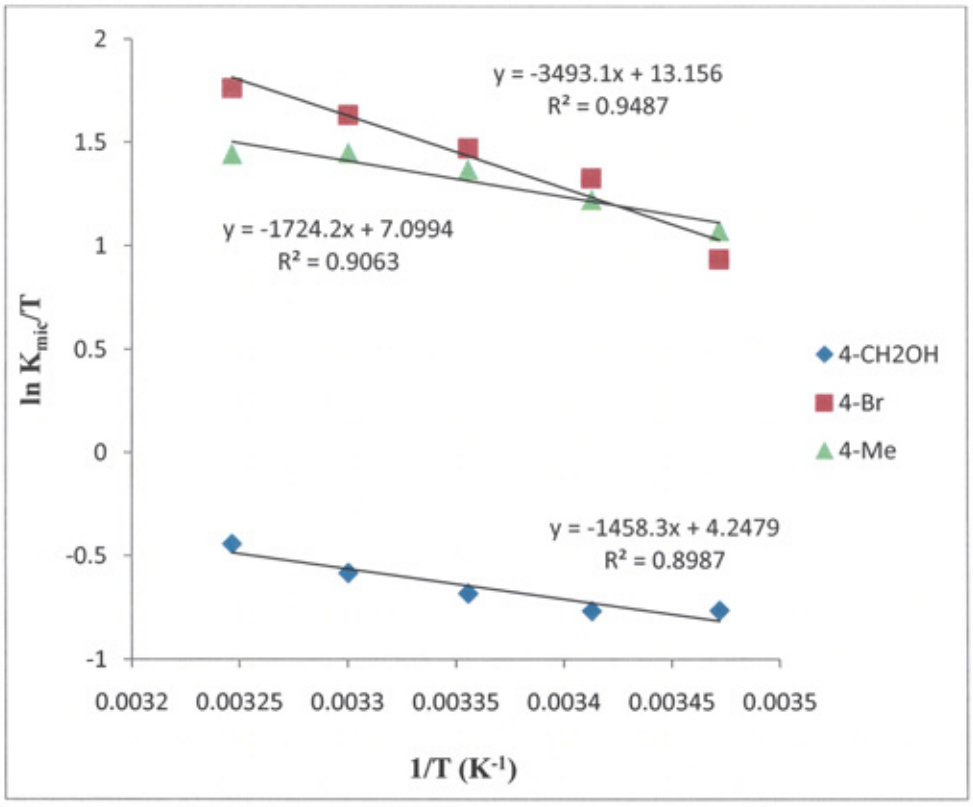

Figure 4.32: The Eyring plot for the reaction of 4-Br, 4-Me, and 4-CH_2OH sulfide with MCPBA at different temperatures in presence of Brij-35.

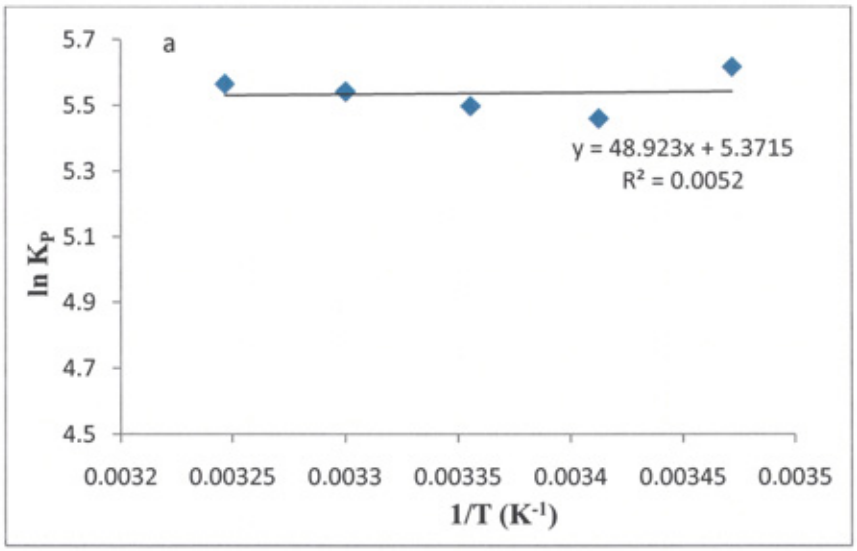

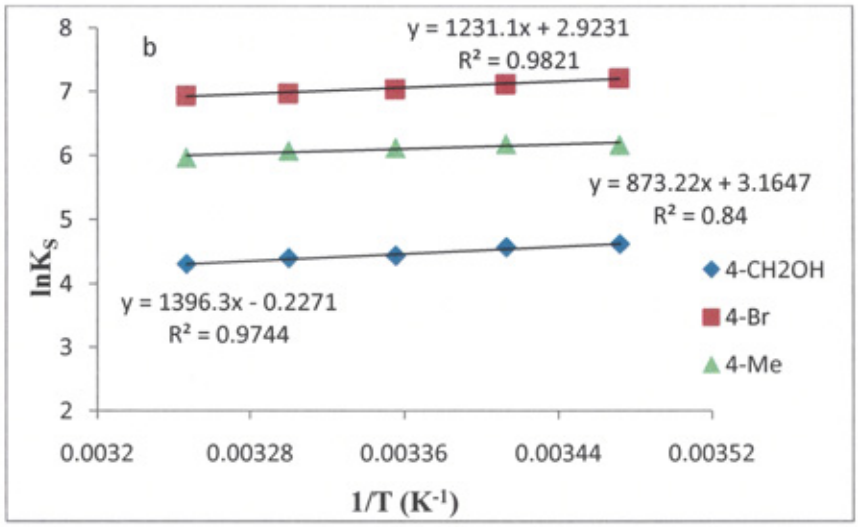

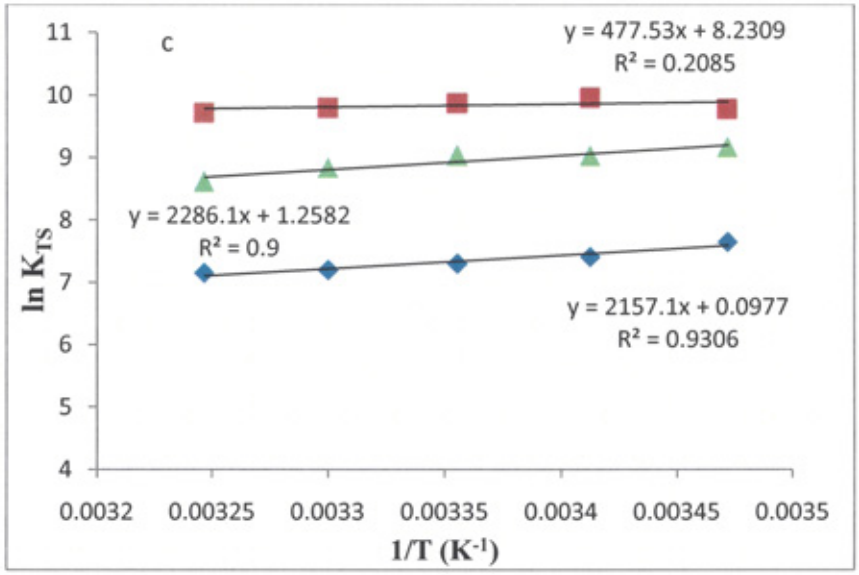

Figure 4.33: Arrhenius plot for the binding constant of: (a) MCPBA, (b) sulfides and(c) transition state for the reaction of 4-Br, 4-Me, and 4-CH_2OH sulfides at different temperatures in the presence of Brij-35.

Table 4.8: The calculated thermodynamic parameters for the reaction of *ca.* 2 x 10^{-4} M MCPBA and 5 x 10^{-4} M PMS with 1 x 10^{-5} M methyl *p*-tolyl sulfide, 4-(methylthio) benzyl alcohol and 4-bromothioanisole in 3.0 x 10^{-3} M nitric acid.

Parameters	4-CH_3	4-CH_2OH	4-Br
$\Delta H^{\ddagger}(k_{obs})_o$, kJ mol^{-1} (MCPBA)	33.3 ± 1.7	30± 0.55	32.6 ± 0.42
$\Delta H^{\ddagger}(k_{obs})_o$, kJ mol^{-1} (PMS)	18 ± 0.64	22.5 ± 0.95	21.9 ± 0.72
$\Delta S^{\ddagger}((k_{obs})_o/s^{-1})$, J mol^{-1} K^{-1} (MCPBA)	-148.9 ± 5.7	-163 ± 1.8	-157.8 ± 1.4
$\Delta S^{\ddagger}((k_{obs})_o/s^{-1})$, J mol^{-1} K^{-1} (PMS)	-190 ± 2.2	-177.2 ± 3.2	-181.4 ± 2.4
$\Delta H^{\ddagger}(k_{mic} - k_w\overline{V}_{mic})$, kJ mol^{-1}	21.6 ± 2.9	28.7 ± 2	23.5 ± 3.8
$\Delta S^{\ddagger}(k_{mic} - k_w\overline{V}_{mic}, M^{-1} s^{-1})$, J mol^{-1}	-113.9 ± 9.9	-104.5 ± 6.6	-107 ± 12.9
$\Delta G^{\ddagger}(k_{obs})_o$, kJ mol^{-1} (MCPBA)	77±3.8	85±1.9	79±1.5
$\Delta G^{\ddagger}(k_{obs})_o$, kJ mol^{-1} (PMS)	74.6±2.3	75±3.3	75.9±3.9
$\Delta H^0(K^S_{mic} - \overline{V}_{mic})$, kJ mol^{-1}	-7±1.8	-11.5±1.1	-10.2±0.77
$\Delta S^0(K^S_{mic} - \overline{V}_{mic}, M^{-1})$, J mol^{-1} K^{-1}	26.4±6	-1.8±3.7	23.5±2.6
$\Delta G^0(K^S_{mic} - \overline{V}_{mic})$, kJ mol^{-1}	-14.8±6	-10.9±3.8	-17±2.7
$\Delta H^0(K^{PH}_{mic} - \overline{V}_{mic})$, kJ mol^{-1}	-0.41±3.6	-0.41±3.6	-0.41±3.6
$\Delta S^0(K^{PH}_{mic} - \overline{V}_{mic}, M^{-1})$, J mol^{-1} K^{-1}	44.6±12.6	44.6±12.6	44.6±12.6
$\Delta G^0(K^{PH}_{mic} - \overline{V}_{mic})$, kJ mol^{-1}	-12.8±13	-12.8±13	-12.8±13
$\Delta H^0(K^{TS}_{mic} - \overline{V}_{mic})$, kJ mol^{-1}	-19±3.6	-17.9±2.8	-3.9±4.4
$\Delta S^0(K^{TS}_{mic} - \overline{V}_{mic}, M^{-1})$, J mol^{-1} K^{-1}	10±12	0.8±9	68.4±14.9

4.4.5. Compensation effect and isokinetic relationships for the reaction of peracids with the three substituted sulfides

It is well known that for a structurally-related series of compounds undergoing a defined chemical reaction, parallel changes in enthalpy and entropy are usually found [143, 144]. The existence of a linear enthalpy-entropy compensation effect (isokinetic relationships) phenomenon has been greatly investigated and shown to occur in almost every biological and chemical process [141, 144]. However, its origin and meaning is still controversial [144]. Guo and colleagues [161] have recently suggested that solvent reorganisation should be the main source of the observed compensation. Therefore, this section will investigate the compensation phenomenon for the reaction of peracid with three sulfides (4-bromothioanisole, methyl *p*-tolyl sulfide and 4-(methylthio) benzyl alcohol) to see whether such a relationship exists.

The enthalpy of activation is plotted as a function of entropy of activation for the $(k_{obs})_o$ of the process in the aqueous phase in MCPBA and PMS in Figure 4.34. It is clear that there is a correlation between these two parameters, and this relationship (as stated in Chapter 1) may be due to the interdependence of these two parameters for a series of related reactions. The compensation temperature for the MPS system is 444 K and for MCPBA it is 393 K; this is obtained from the slope.

The enthalpy-entropy plot for the process in the micelle is plotted in Figure 4.35. It can be seen that there is a linear correlation with (R^2 =0.95) and the slope ×1000 gives the isokinetic temperature.

Figure 4.36a shows the enthalpy-entropy compensation plot of the binding constant of sulfides with an error bar. The plot shows there is a poor correlation, which suggests that compensation in this case does not exist. Figure 4.36b shows the corresponding plot for the association constant of the transition state. The data are associated with a large error bar for the entropy of association. In general R^2 are close to 1 which indicates good correlation between enthalpy and entropy of transition state association.

The presence of a straight line in an enthalpy-entropy plot is an indication of the compensation phenomenon, and as mentioned in Chapter 1, for series of related reactions with only different substituents or conditions, compensation relationships are observed. This can be thought of as an energy exchange, as stated in the first law of thermodynamic energy, which can not be created or destroyed but can change from one form to another. However, it should be noted that in Figure 4.34 to Figure 4.36 some points of the data

fall out of the fitting line (most significantly in Figure 4.36), and this may be due to the error associated with the calculation of the interdependent thermodynamics parameters. However, this does not rule out the existence of such compensation.

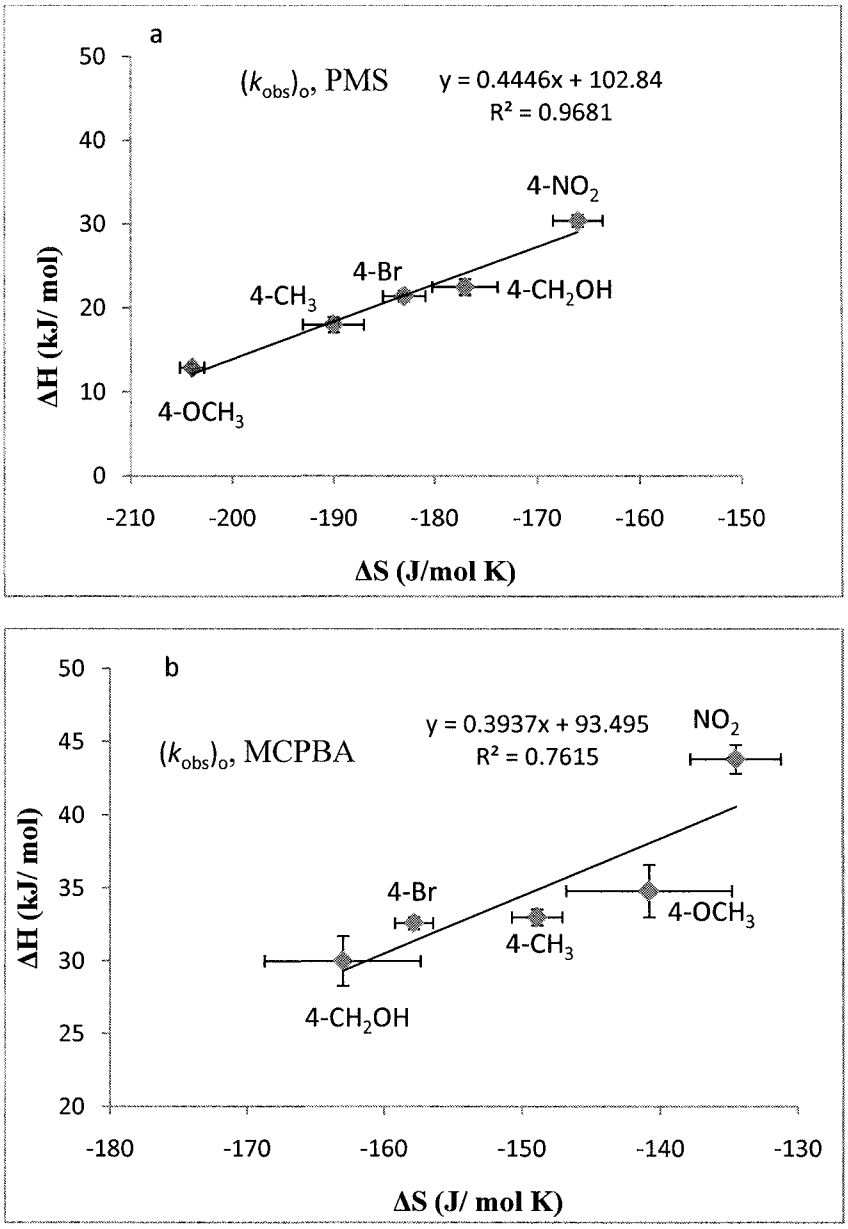

Figure 4.34: The entropy–enthalpy compensation for the oxidation of alkyl aryl sulfides by PMS (a) and MCPBA (b) in water.

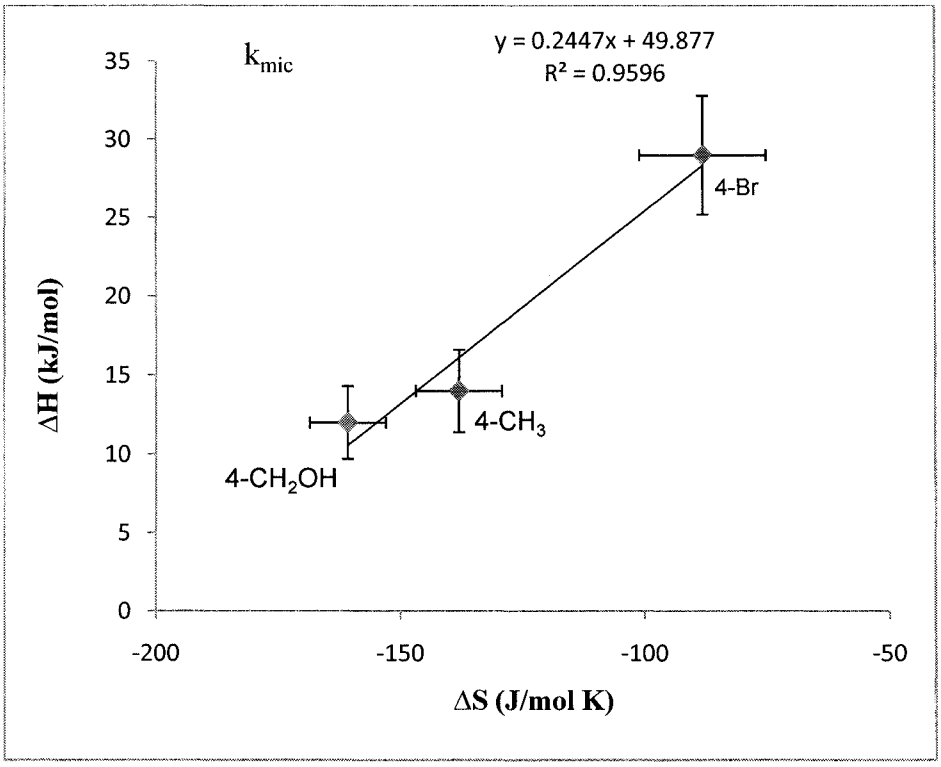

Figure 4.35: The enthalpy–entropy compensation plot for the process in micelle

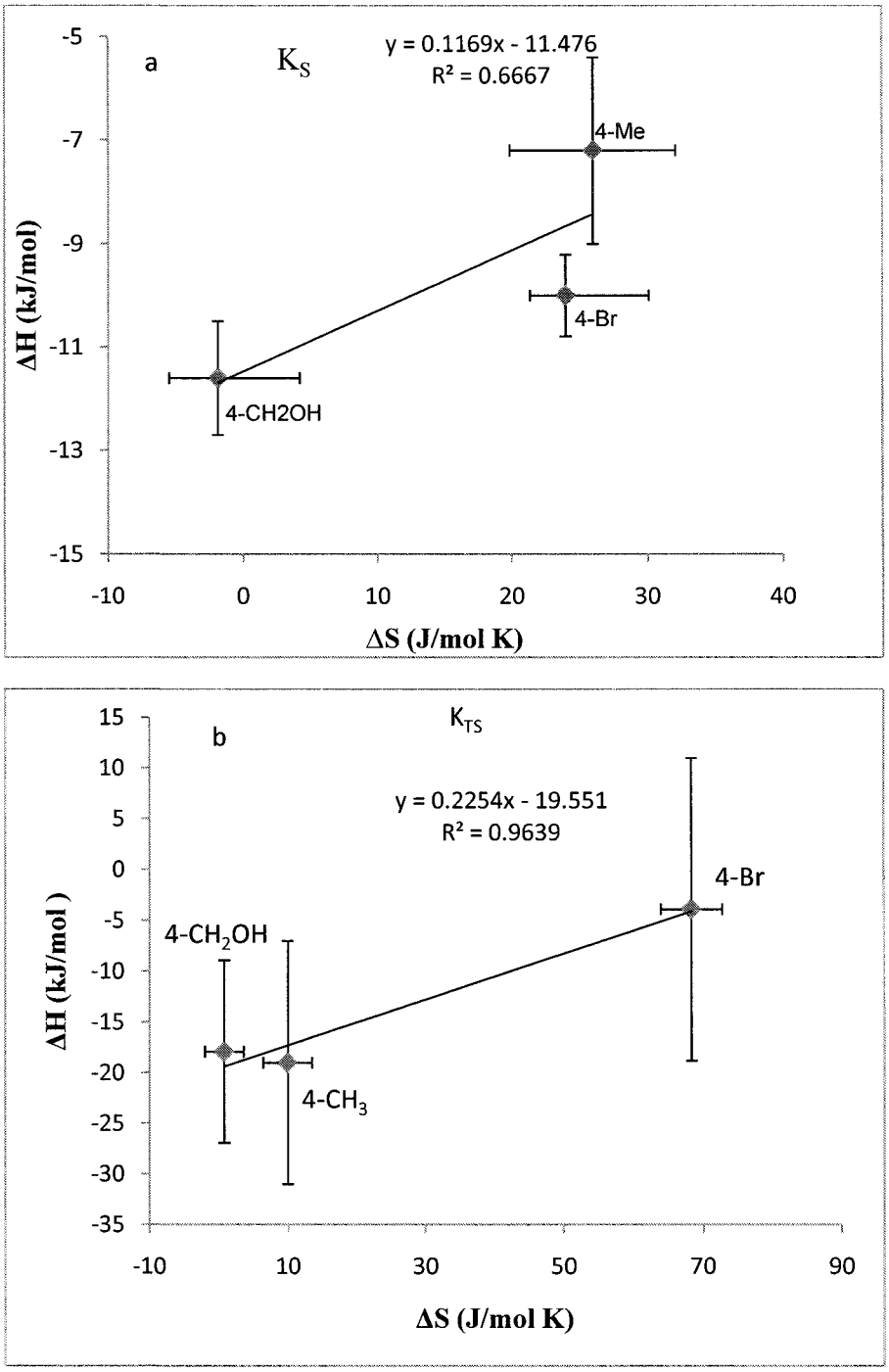

Figure 4.36: The enthalpy–entropy compensation plot for the binding of sulfides (a) and the apparent association constant of transition state (b) to Brij-35.

4.4.6. Testing the existence of the compensation effect

At the isokinetic temperature all the compounds of the reaction series react at an equal rate, which means that variation of the substituent at this temperature has no effect on the free energy of activation. The existence of such relationships needs to be viewed with scepticism, as the parameters ΔH and ΔS are mutually interdependent [141, 142].

Exner [142] suggests that if linear double logarithm relationships between rates at two different temperatures exist then it confirms there is an isokinetic relationship and reveals that the series undergoes the same mechanism. From the slope the compensation temperature can be calculated using Equation 4.4.

$$T_{ios} = T_1 T_2 (b-1)/ bT_2 - T_1 \qquad 4.4$$

Where b is the slope obtained from the plot of ln k_2 or ln K_2 at T_2 versus ln k_1 or ln K_1 at T_1 respectively with $T_2 > T_1$, and T_{iso} is the compensation temperature.

Using this method, Figure 4.37 shows the corresponding plot with compensation temperature calculated using Equation 4.4. The compensation temperature shown in Figure 4.37 is out of the experimental temperature range. Exner [140] has shown that T_{iso} may be positive or negative and experimentally unattainable.

It is clear from the plot that isokinetic or compensation relationships exist and that for the binding of sulfides all the data fall on the best fit line. In addition, it is better than that in Figure 4.36 using enthalpy and entropy compensation plot.

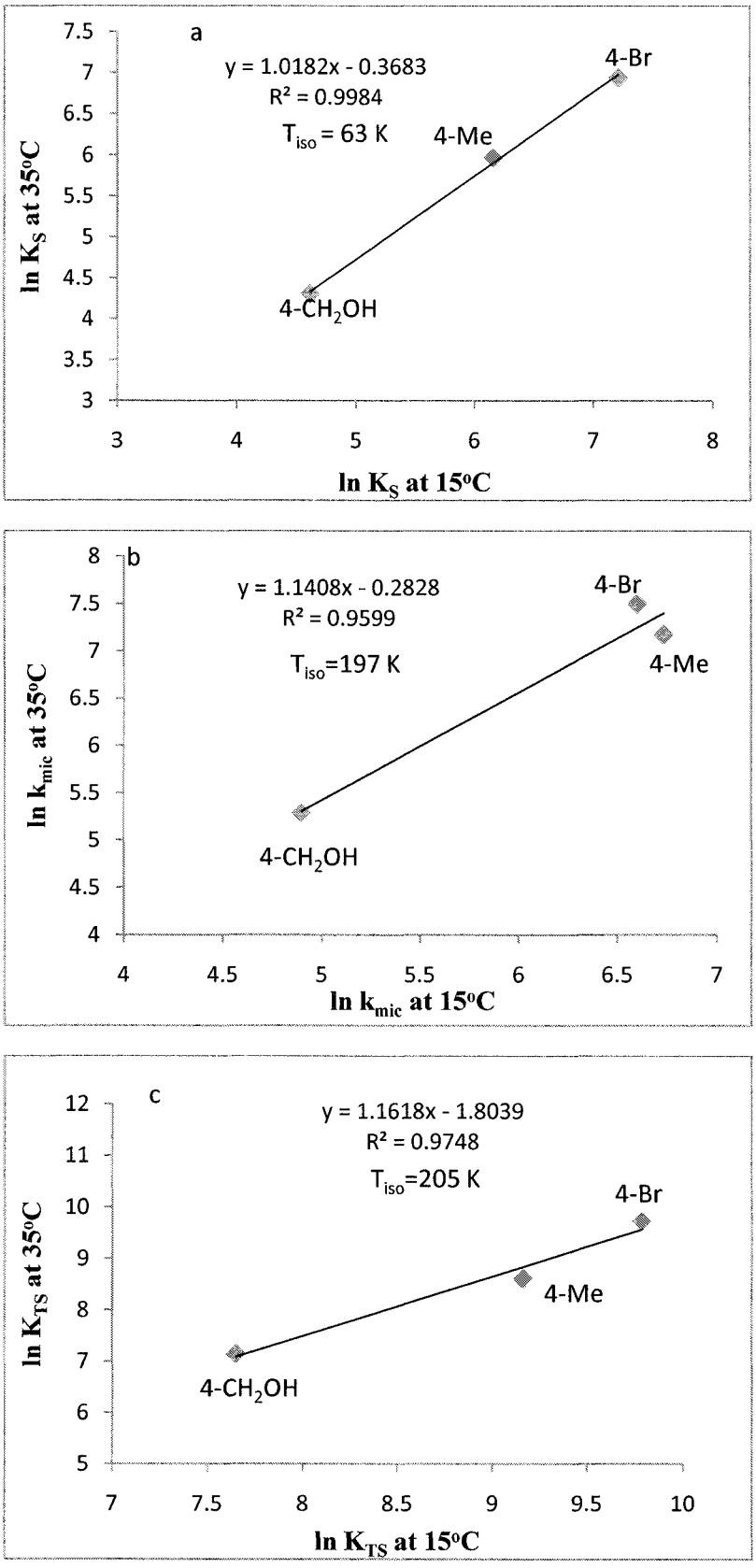

Figure 4.37: Plot of ln k_2 and ln K_2 against ln $k_1$and ln K_2 respectively; (a) for the binding constant of sulfides; (b) for the observed first order rate constant in the micelle; and (c) for the binding of transition state to the micelle.

4.4.7. Comparison of the critical micelle concentration for iodide reaction and sulfide

As stated previously, the value for CMC of Brij-35 reported in literature is about 6×10^{-5} M[177b] (measured from surface tension in water). However, a value of 0.0002 M [101] has also been reported as well, so there is confusion about the true value of CMC. However, Patist and co-workers [180] have confirmed that the CMC for series of commercial non-ionic surfactants, including Brij-35, is very low when measured by the surface tension compared to the dye micellization method. They attributed low values to the presence of impurity and state that low CMC is a result of the saturation of the air/liquid interface by the active material before the CMC is reached. After the removal of an impurity present, the CMC for both methods are matched and equal to the CMC of the mono dispersed non-ionic surfactant.

In general, for this work the CMC obtained for the reaction in iodide is about 4×10^{-4} M, compared to 6×10^{-5} M in the presence of sulfide. This higher value in the presence of iodide is specific to iodide, and to confirm this, reaction of iodide with MCPBA in the presence of 4-methyl phenyl sulfoxide 1×10^{-5} M was carried out to see whether the sulfide compounds actually lower the CMC or not. This result showed that the CMC is still the same: about 4×10^{-4} M. It is possible that the iodide may in some way interact with the monomers of the micelle and repel them at lower concentrations of iodide. It should be noted that in the iodide-MCPBA reaction, iodide was in excess (unlike MCPBA – sulfide reaction). The results are plotted in Figure 4.38.

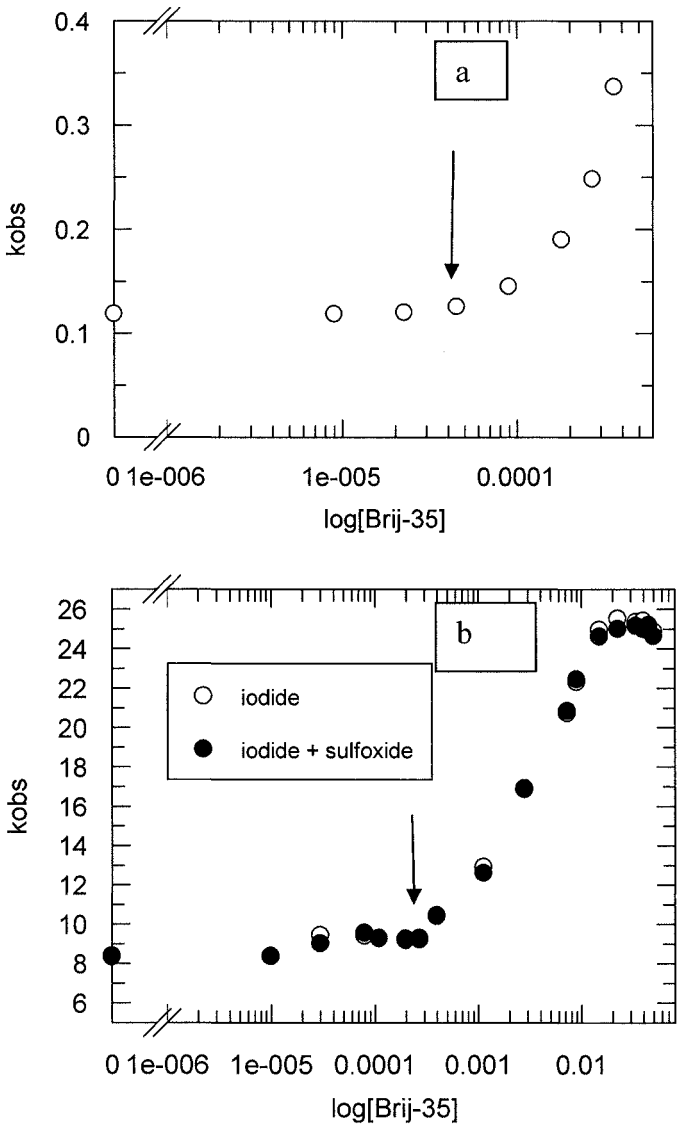

Figure 4.38: The observed rate constant versus natural logarithm of Brij-35 for sulfide oxidation by MCPBA (a) and for the reaction of iodide with MCPBA (b) in the presence of sulfoxide.

Chapter 5 Temperature dependence study of the oxidation of aryl alkyl sulfides by peroxyacids in the presence of α-cyclodextrin.

5.1. Introduction

The mechanism for the uncatalysed reaction of sulfur compounds and peroxide involves nucleophilic attack on the outer peroxidic oxygen by the sulfur atom of the sulfides, which react as reducing agents producing sulfoxide and the leaving group YOH [2] (see Scheme 4.1 in Chapter 4). The rate of reaction is second order; first order each in peracid and nucleophile. Also, the reaction rate is increased by inserting an electron donating group at the para position of the aryl alkyl sulfide, and reduced by an electron withdrawing group which reduces the nucleophility of the sulfur. The uncatalysed reaction has been observed to be associated with negative $\Delta S^{\ddagger}$ due to the definite orientation of the reactants in the transition state [2].

The binding of α-cyclodextrin with the investigated aryl alkyl sulfides has been studied previously at a temperature of 25°C in 0.05 mol dm^{-3} ionic strength acetate buffer at pH 4.6 by means of UV-visible spectrophotometry. It was found that all these compounds, except two charged ones, form complexes having 1:1 and 1:2 (guest: host) stoichiometric ratios [164]. The results also suggested that for 4-substituted aryl alkyl sulfides, an orientation is taken up within the cyclodextrin whereby the sulfur containing group always protrudes from the wider, secondary, rim of the cavity, irrespective of the nature of the substituent. This suggestion was made on the basis that significant steric hindrance would be caused by the interaction of S-CH_3 group with 5H-protons of the cyclodextrin, as shown in Structure 5.1, causing displacement of the benzene ring from its most favourable position; consequently it was likely that the non-sterically hindered *p*-substituent would be located at the narrow end of the cavity even if the dipole-dipole interactions were unfavourable.

The importance of dipole-dipole interactions between host and guest, along with the molar refractivity, R_m, of the included substituent, have been shown by Davies and co-workers [165] to be significant factors in predicting association constants of α-cyclodextrin with 1,4-disubstituted benzenes. A model developed by these authors assumed that for these compounds the most electron withdrawing group is always orientated towards the narrow, primary, positive dipole end of the cyclodextrin cavity. Deviations from this model were observed to occur when one of the *p*-substituents, which on consideration of

the dipole-dipole interactions, should have included at the narrow end of the cavity, was prevented from doing so on either steric grounds (methyl sulfides[164]) or where the substituent was an ion, such as carboxylate, thus requiring significant desolvation energy. For cases where significant steric hindrance was likely, a much better fit to the model was predicted when the assumption was made that it was the non-sterically hindered substituent that included at the narrow end of the cavity, i.e. the molecule was 'flipped' from the orientation predicted purely on the grounds of dipole-dipole interactions.

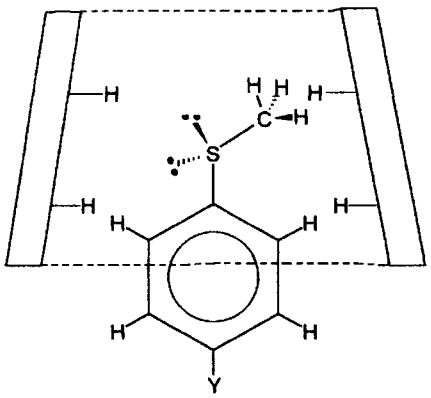

Structure 5.1 (taken from [164]; see text for detail).

Probably the most remarkable aspect of α-cyclodextrin complexation of 4-substituted aryl alkyl sulfides is the observed cooperative binding, whereby the binding constant for the 1:2 (guest: CD) complex is significantly higher than that for the 1:1 complex. For example, in the case of methyl-p-tolyl sulfide, the K_{11} and K_{12} values were 41 and 1000 $dm^3\ mol^{-1}$ respectively, i.e. the second step is 25 times greater than the first. At first sight it is difficult to reconcile this observation to how we might expect the second cyclodextrin to associate with the 1:1 complex: with the guest fully included in the cavity of the first cyclodextrin, only the $-S-CH_3$ group will protrude, and so the question is how this might result in such an energetically favourable association for the second binding step? However, there is evidence that the driving force for such interactions is through substrate promoted dipole-dipole interactions between cyclodextrins, i.e. that the process of binding results in the development of a significant dipole within the cyclodextrin cavity, and that the dipole-dipole interaction between the two cyclodextrins is the driving force for the second binding step. This is supported by the work of Sakurai et al [191] who have generated CNDO (complete neglect of differential overlap) electrical potential maps

and dipole moments for cyclodextrin and have shown that electrostatic properties within the cavity are highly dependent on the conformation of the macrocyclic ring. For cyclodextrin-water complexes the water molecules are hydrogen bonded between the primary hydroxyl groups causing one of the glucosidic residues to be tilted. The consequent distortion to the macrocyclic ring results in a dipole moment (ca. 8 D) which is not only reduced compared to other inclusion compounds, but which is also directed away from the axis of the cyclodextrin cavity. The inclusion of a tight fitting disubstituted benzene within the cavity, however, changes the conformation of the cyclodextrin in such a way as to maximise the electrostatic interaction between the host and guest. The dipole moment of the cyclodextrin increases markedly and the direction of the dipole becomes almost parallel with the longitudinal axis (13.5 D for p-nitrophenol, 16 D for p-iodoaniline[191]). Whilst induced dipole effects undoubtedly play a part in this change, the fact that the inclusion of krypton (no dipole) within the cavity gives a similar directional and magnitudinal change in dipole (ca. 18 D) implies that conformational changes alone are highly significant [191].

Whilst these molecular modelling studies were based on crystallographic data, it has been suggested that similar conformational and electrostatic changes may occur in solution and that the driving force in the formation of a 1:2 complex is the enhanced interaction between the opposite dipoles of the primary and secondary hydroxyl rims as a result of substrate inclusion. For this to occur the protruding substituent of the guest in the 1:1 complex must penetrate the primary hydroxyl rim of a second 'empty' cyclodextrin molecule, breaking the hydrogen bonded interaction between water molecules and the primary hydroxyls, thus reducing the distortion of the macrocycle. The dipole moment of the second cyclodextrin molecule is then likely to approach the magnitude and direction of the first. Depending on the orientation of the second molecule of cyclodextrin, hydrogen bonding interactions may also occur. Clearly, this substrate promoted dipole-dipole interaction between cyclodextrins affords a mechanism whereby cooperative binding could occur, as shown in Structure 5.2

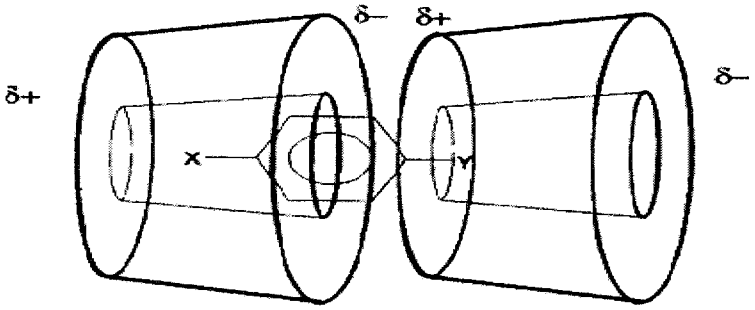

Structure 5.2: 'Head to tail' 1:2 complex (taken from reference 164)

Davies and Deary [162] have kinetically investigated the reaction of peracids with a series of aryl alkyl sulfides in α-cyclodextrin, observing that for strong binding peracids such as m-chloroperbenzoic acid the reaction is catalysed by cyclodextrin at low cyclodextrin concentrations, but at successively higher concentrations the rate then declines. The likely reason for this is that at low cyclodextrin concentration the predominant reaction is between the bound peracid and the unbound aryl alkyl sulfide, with catalysis possibly being effected by facilitating the internally bonded hydrogen bonded structure of the peracid transition state for these reactions that has been proposed by Curci and co-workers [2] (Structure 5.3)

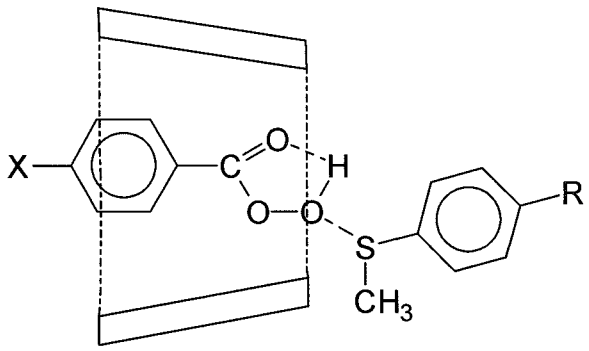

Structure 5.3: Transition state involving one molecule of cyclodextrin

There is strong evidence from linear free energy studies, correlating transition state stabilisation with binding constants of both sulfides and peracids, that the transition state resembles the bound peracid, and, moreover, that the peracid binds with the peroxy group at the narrow end on the cyclodextrin cavity. At higher cyclodextrin concentrations

significant proportions of the sulfide are bound in 1:1 and, as discussed previously, the cooperatively formed 1:2 guest: CD complexes. On the other hand, for weakly binding peracids, the rate merely declines with cyclodextrin concentration [162] as a result of the predominant non-productive binding of the sulfides.

There are, of course, other important factors that determine binding strength in addition to those discussed above, including: desolvation of the guest, desolvation of the host cavity, and reorganisation of the solvent around and inside the cavity. Thermodynamic studies of binding suggest that in most cases these processes are enthalpy driven[160].

In this chapter the thermodynamic parameters of the binding of α-cyclodextrin with five aryl alkyl sulfides will be studied and compared. Binding of such compounds at different temperatures with cyclodextrin has not been reported in literature and there is also no information available on the thermodynamics of this class of compounds in α-cyclodextrin. As mentioned above, the binding constant was determined at 25°C. However, the binding constant by itself does not provide a complete understanding of the binding phenomena and does not give any information about the driving force behind the complexation process. The aim of carrying out this work is to find out if any additional information about the complexation process can be ascertained from enthalpy-entropy plots. Whilst there is much debate about the physical meaning of enthalpy-entropy compensation, as discussed in previous chapters, one interesting interpretation is that the observation of compensation for a series of related rate or equilibrium processes results from the reorganisation of water molecules around the host and guest during the process of complexation. For hydrophobic guest molecules, where there is minimal interaction with the solvent, then very good correlations are seen, whereas guests that interact with the solvent molecules through hydrogen bond formation appear as outliers on these plots because the energy from this interaction cannot be compensated.

For the study presented in this Chapter, the substrates investigated include two types of sulfides that have electron withdrawing substituents, namely 4- nitrothioanisole and 4-bromothioanisole. The other three sulfides contain electron donating groups and are 4-methoxythioanisole, methyl *p*-tolyl sulfide and 4-(methythio) benzyl alcohol. The binding constants were determined by means of kinetic data obtained from the reaction between the sulfides and the oxidants 3-chloroperbenzoic acid (MCPBA) and peroxomonosulfate (PMS). The kinetic data are then fitted to a suitable equation as described earlier in order to generate the binding parameters, which are then analysed using a Van't Hoff plot to determine the thermodynamics parameters.

5.2. Experimental

5.2.1 Materials

The peracid preparation is described in the previous chapter. The alpha-cyclodextrin hydrate was purchased from the Avocado Company and the sample was used as received. The stock solution of cyclodextrin was prepared by dissolving the required amount of cyclodextrin in distilled water, which was then filtered through a sintered glass funnel. A series of dilutions were made for the kinetic runs.

5.2.2. Kinetics

The reaction of peracid with sulfides in 0.003 M nitric acid was followed by measuring the decrease in absorbance due to the disappearance of the sulfides. The wave length at which the measurement was carried out is listed in Table 3. The reaction was carried out using an SX-17 Applied Photophysics stopped flow spectrophotometer. The concentration of the sulfides and MCPBA and PMS were 1×10^{-5}, 2×10^{-4} and 4.8×10^{-4} M respectively. The measurements were performed in 0.003 M nitric acid at pH = 2.5, which is below the pK_a of the MCPBA. This was to ensure the peracid was in a completely protonated form and to get a strong binding for the neutral form.

5.3. Results

5.3.1. The equilibria and the reactions of sulfides with peracid

As discussed earlier in this Chapter, the equilibria and the reaction of aryl alkyl sulfides with peracid in α-cyclodextrin have previously been studied previously at 25°C [162]. The results show that sulfides form inclusion complexes with cyclodextrin with stoichiometric ratios of 1:1 and 1:2 (substrate: CD), while MCPBA forms 1:1 complex. Equations 5.1 to 5.9 describe the equilibria and reactions related to this system. The stability constants of reactants are described in Equation 5.10 and Equation 5.11. The variation of k_{obs} pseudo first order rate with [CD] is described in Equation 5.12.

Peracid- cyclodextrin complex

$$P + CD \overset{K_p}{\rightleftharpoons} CD,P \qquad 5.1$$

sulfides- cyclodextrin complexes

$$S + CD \overset{K_{S11}}{\rightleftharpoons} CD,S \qquad 5.2$$

$$S,CD + CD \overset{K_{S12}}{\rightleftharpoons} S,(CD)_2 \qquad 5.3$$

Reactions

$$P + S \xrightarrow{k_o} \text{Products} \qquad 5.4$$

$$CD, P + S \xrightarrow{k_{1a}} \text{Products} \qquad 5.5$$

$$P + CD, S \xrightarrow{k_{1b}} \text{Products} \qquad 5.6$$

$$CD, P + CD, S \xrightarrow{k_{2a}} \text{Products} \qquad 5.7$$

$$(CD)_2, P + S \xrightarrow{k_{2b}} \text{Products} \qquad 5.8$$

$$(CD)_2, S + P \xrightarrow{k_{2c}} \text{Products} \qquad 5.9$$

$$Kp = \frac{[CD,P]}{[CD][P]} \qquad 5.10$$

$$K_S = \frac{[CD,S]}{[CD][S]} \qquad 5.11$$

The reaction scheme leads to the rate law given in Equation 5.12 below:

$$k_{obs} = \frac{k_o + k_{1obs}[CD] + k_{2obs}[CD]^2}{(1 + K_{S11}[CD] + K_{S11}K_{S12}[CD]^2)} \times \frac{1}{(1 + K_P[CD])} \qquad 5.12$$

Here k_o denotes the pseudo first order rate constant for the uncatalysed reaction, K_{S11} and K_{S12} are the association constants of sulfides for the complex (guest: host) 1:1 and 1:2 respectively, and K_P is the binding constant of the peracid. k_{1obs} and k_{2obs} are defined in Equation 5.13 and Equation 5.14.

$$k_{1obs} = k_{1a}K_P + k_{1b}K_{s11} \qquad 5.13$$

$$k_{2obs} = k_2K_{P11}K_{s11} + k_{2c}K_{s11}K_{s21} \qquad 5.14$$

k_{1obs} *and* k_{2obs} are first and second order rate constants in cyclodextrin and [CD] is the total cyclodextrin concentration. And for the k_{2obs} the term k_{2b} is negligible and hence it cancelled in the Equation 5.14

5.3.2. Determination of the rate constant

Kinetic results ± standard deviations obtained for the reaction of MCPBA and PMS with series of alkyl aryl sulfides, including 4-bromothioanisole, methyl *p*-tolyl sulfide, 4-nitrothioanisole, 4-methoxythioanisole and 4-(methylthio) benzyl alcohol, at several temperatures (15°C, 20°C, 25°C, 30°C and 35°C) are listed in Tables 5.1c to Table 5.10c in Appendix C. The observed pseudo first order rate constants are obtained by fitting the change of absorbance versus time to a single mono exponential equation (see Chapter 2). The second order rate constant for an uncatalysed reaction was calculated from the quotient of the observed pseudo first order rate constant and the concentration of peracid in the absence of α-cyclodextrin. The results are collected in Table 4.4 in Chapter 4, obtained for the previously described study of the effect of surfactants on these reactions.

5.3.3. Curve fitting

To obtain the best fit parameters, the stability constant of the sulfides and MCPBA, k_{1obs} (the first order dependence on cyclodextrin obtained at 25°C from previous work [162]), and the observed first order rate constant k_{obs} (the observed zero order rate in cyclodextrin values) that was determined experimentally were all substituted in Equation 5.12.

Plots of pseudo first order rate constant against the cyclodextrin concentrations for the reaction of methyl *p*-tolyl sulfide, 4-nitrothioanisole, 4-methoxythioanisole 4-(methylthio) benzyl alcohol and 4-bromothioanisole at different temperatures are shown in Figure 5.1 to Figure 5.5. The line going through the data points is the best fit to Equation 5.12. Using universal fitting, all the reactions for the sulfides with both peracids at one temperature are fitted simultaneously with the association constant for the MCPBA kept as a common parameter. The association constant for PMS was set to zero; k_{2obs} was also set to zero, as poor fitting for all data was obtained when k_{2obs} was left to 'float' (not shown).

The stability constant parameters for the α-cyclodextrin complexes of peracid and aryl alkyl sulfides obtained from such fitting include the K_{S11} and K_{S12}, which are the binding

constants of sulfides with one and two α-cyclodextrin respectively, and K_P, the binding of peracid; these are listed in Tables 5.1 to Table 5.5.

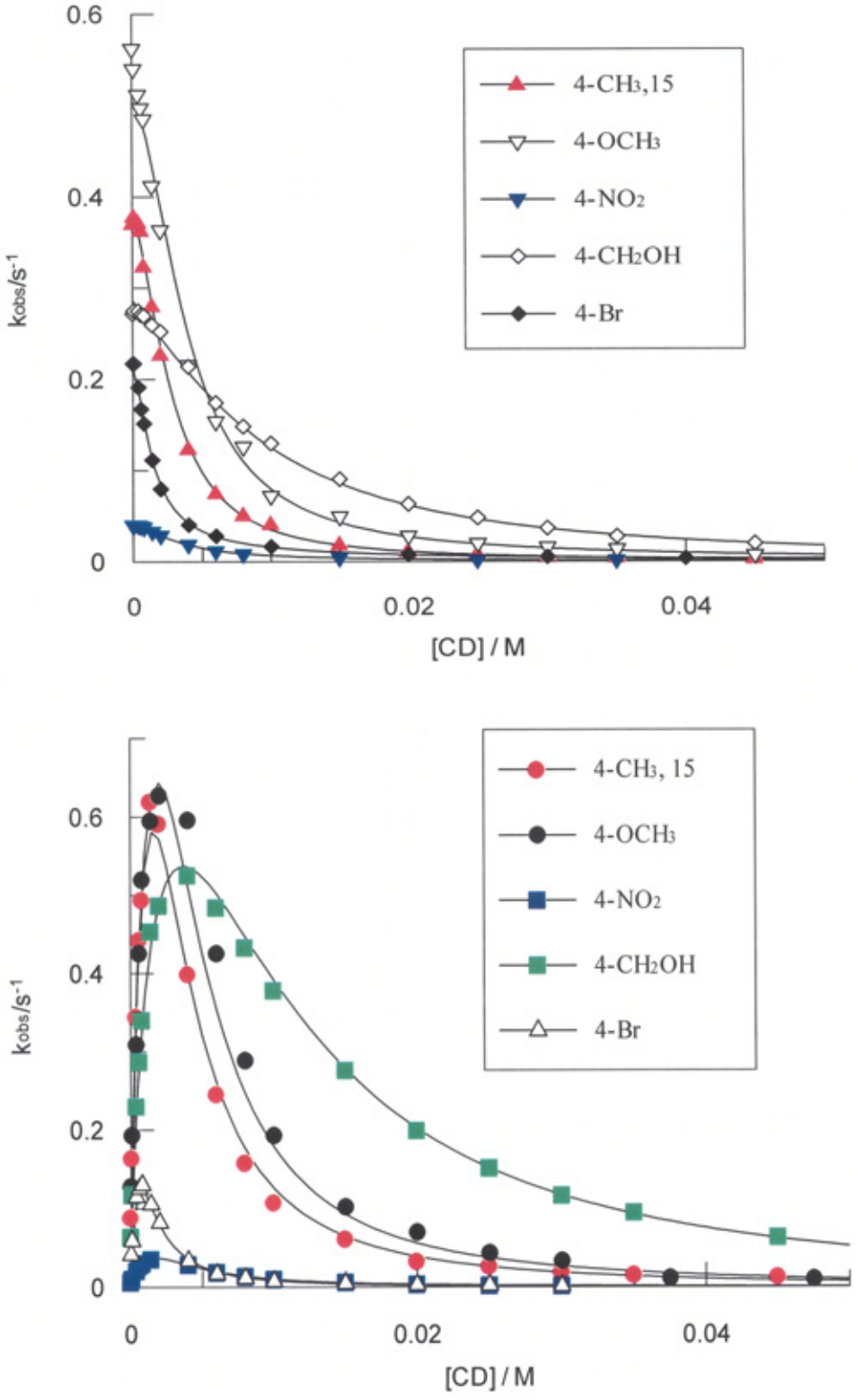

Figure 5.1: Plots showing the different effects of α- cyclodextrin on the reaction between a series of sulfides and PMS (top plot) and MCPBA (lower plot) at 15°C in 0.003 M nitric acid.

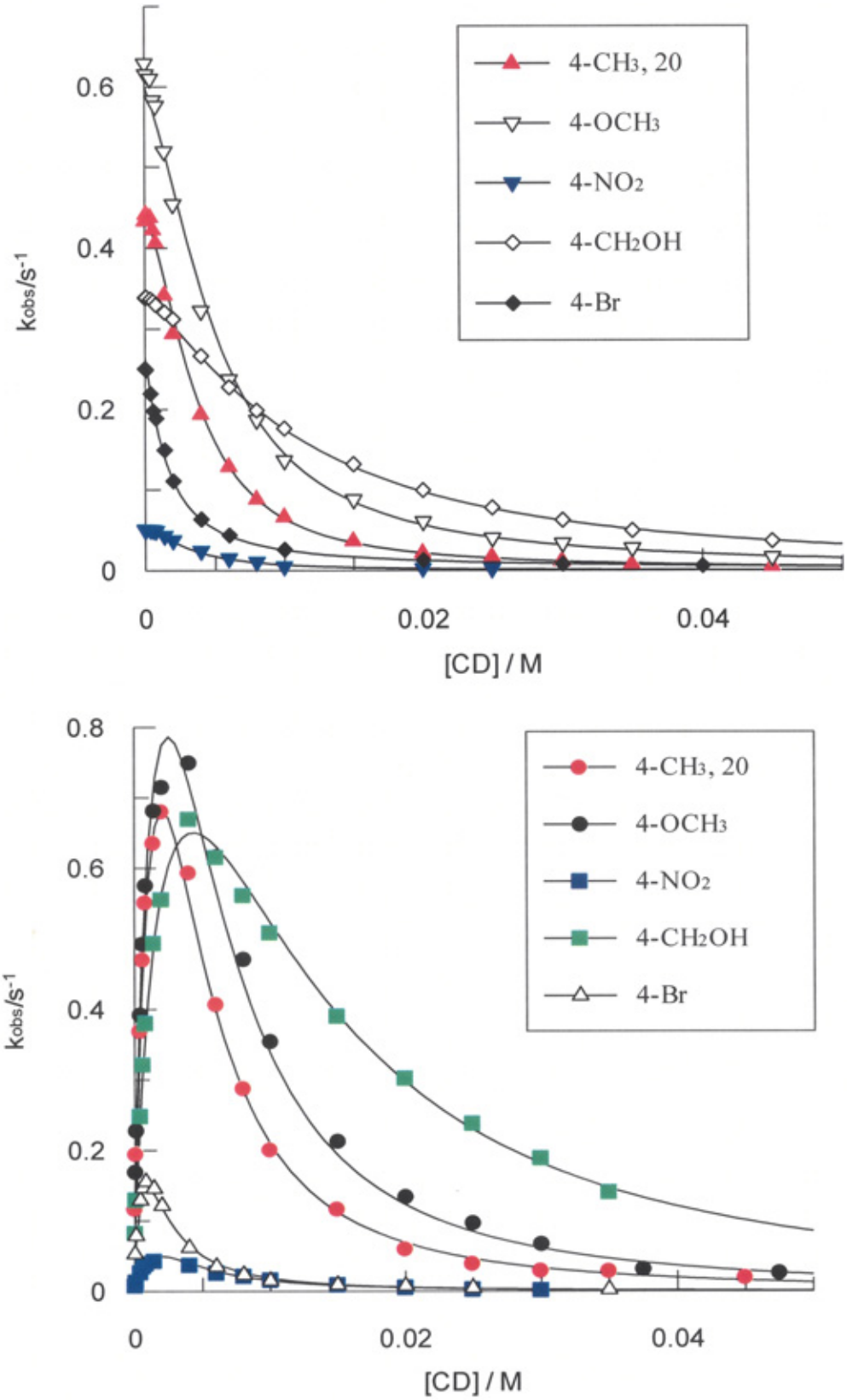

Figure 5.2: Plots showing the different effects of α- cyclodextrin on the reaction between series of sulfides and PMS (top plot) and MCPBA (lower plot) at 20 °C in 0.003 M nitric acid.

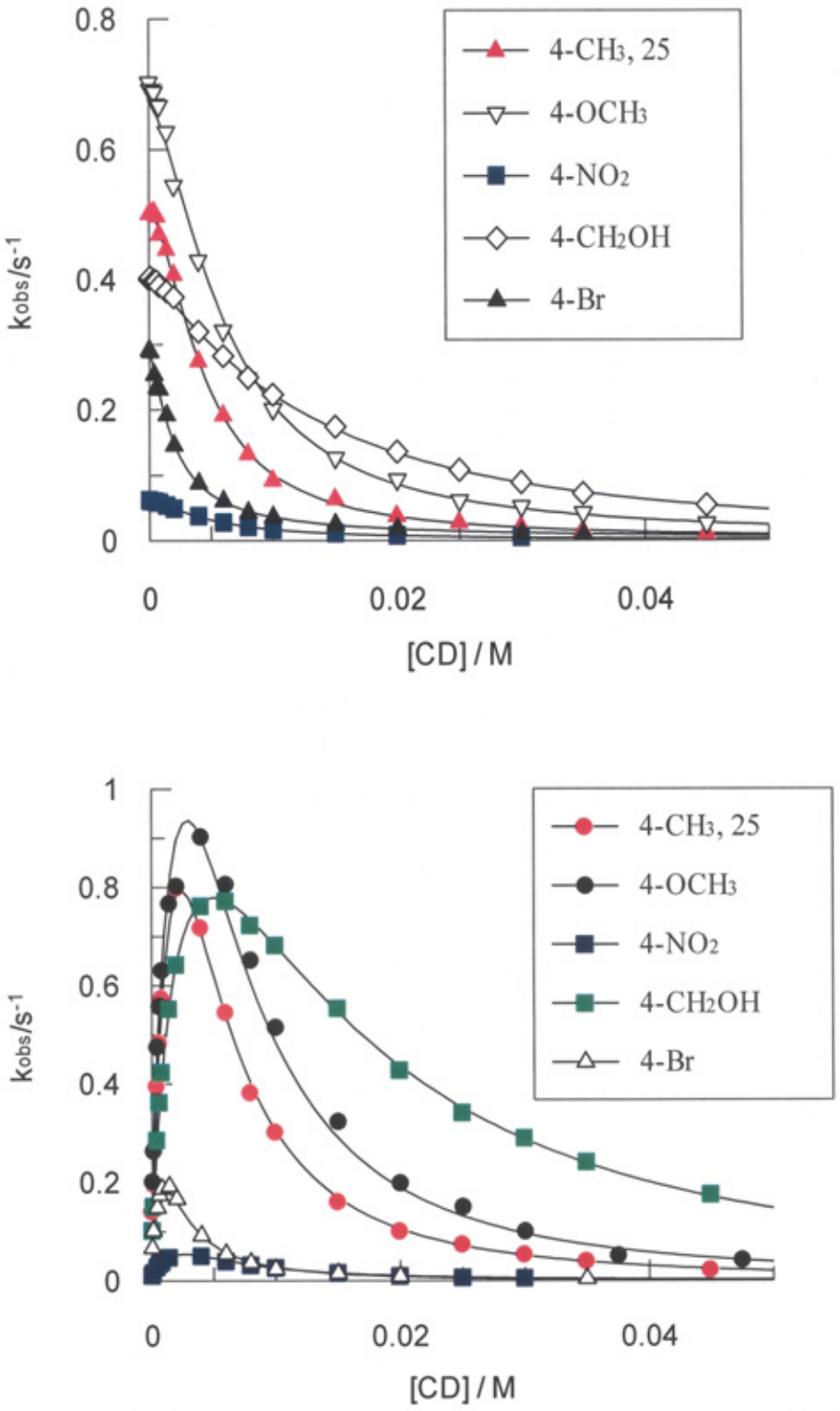

Figure 5.3: Plots showing the different effects of α- cyclodextrin on the reaction between series of sulfides and PMS (top plot) and MCPBA (lower plot) at 25 °C in 0.003 M nitric acid.

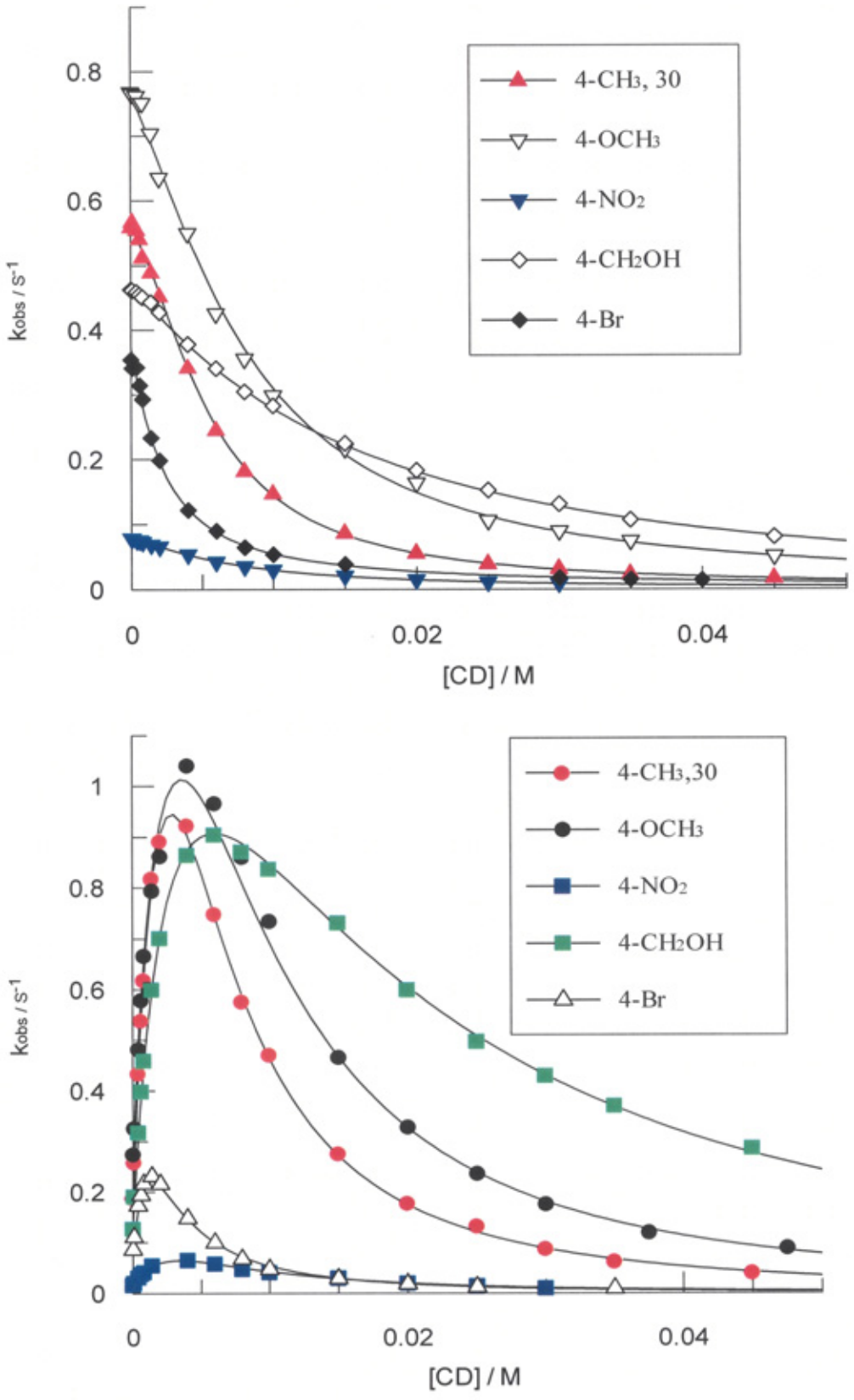

Figure 5.4: Plots showing the different effects of α- cyclodextrin on the reaction between series of sulfides and PMS (top plot) and MCPBA (lower plot) at 30 °C in 0.003 M^{-1} nitric acid.

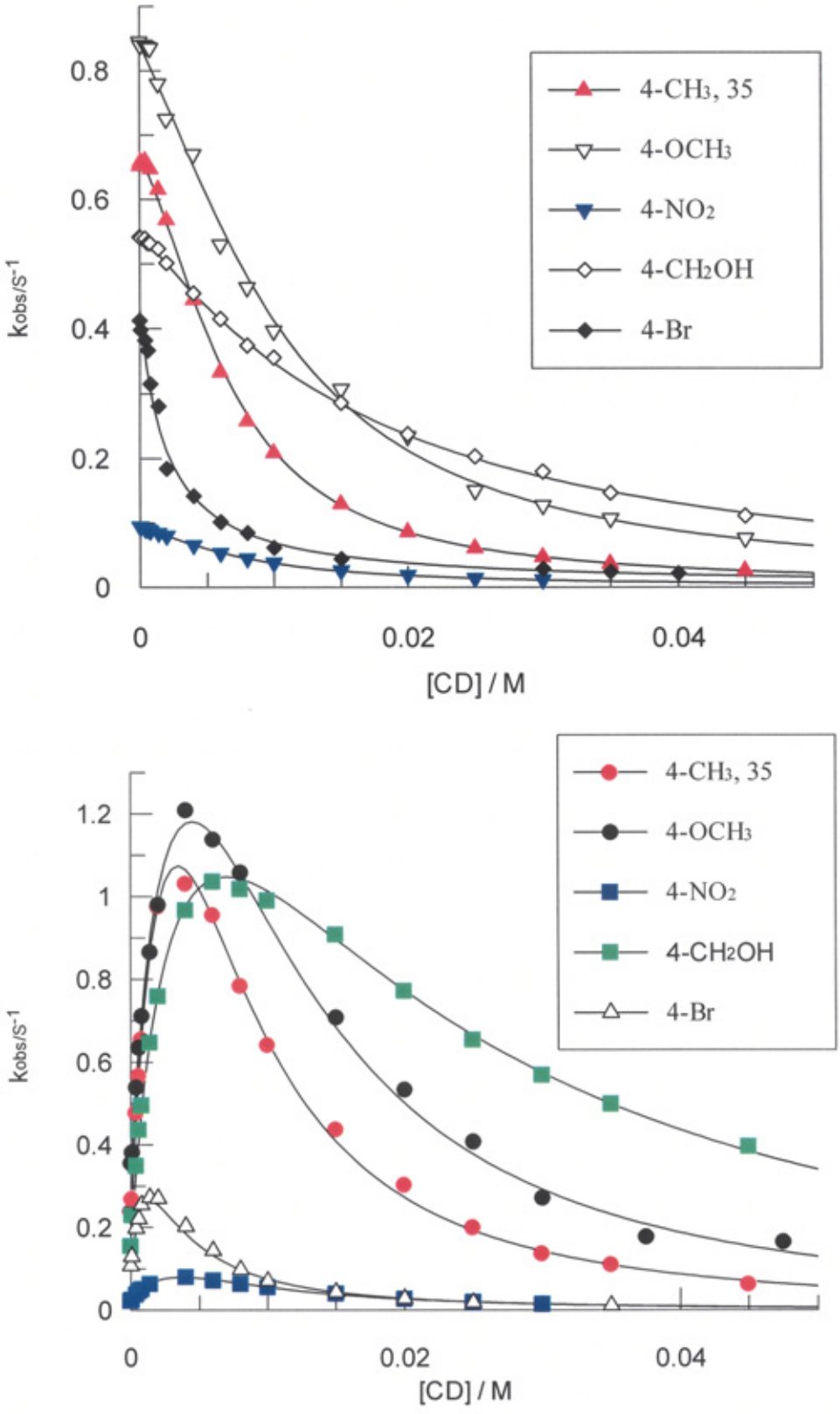

Figure 5.5: Plots showing the different effects of α- cyclodextrin on the reaction between series of sulfides and PMS (top plot) and MCPBA (lower plot) at 35 °C in 0.003 M nitric acid.

Table 5.1: The stability constant parameters for α-cyclodextrin complexes of peracid and methyl *p*-tolyl sulfide using Equation 5.12.

T/°C	K_{S11}/M^{-1}	K_{S12}/M^{-1}	K_P/M^{-1}
15	133±19	762±136	460±36
20	105±35	582±217	378±42
25	84±17	509.6±120	341±28
30	75±10.8	380±62	284±19
35	69.6±11	270±49	234±21

Table 5.2: The stability constant parameters for α-cyclodextrin complexes of peracid and 4-methoxythioanisole using Equation 5.12.

T/°C	K_{S11}/M^{-1}	K_{S12}/M^{-1}	K_P/M^{-1}
15	51.7±7	1226±209	460
20	94±25	333±79	378
25	79±13	218±52	341
30	82.6±8	128±15	284
35	60.5±8	111±17	234

Table 5.3: The stability constant parameters for α-cyclodextrin complexes of peracid and 4-nitrothioanisole using Equation 5.12.

T/°C	K_{S11}/M^{-1}	K_{S12}/M^{-1}	K_P/M^{-1}
15	172.6±29	398±78	460
20	157±42	396±124	378
25	133±19	197±33	341
30	106±10	110±14	284
35	92±13	120±20	234

Table 5.4: The stability constant parameters for α-cyclodextrin complexes of peracid 4-(methylthio) benzyl alcohol using Equation 5.12.

T/°C	K_{S11}/M^{-1}	K_{S12}/M^{-1}	K_P/M^{-1}
15	75±12	85±17	460
20	71±14	61±4.8	378
25	68±8	37±6	341
30	61.7±5.6	22.6±3.7	284
35	54±6	18.7±4	234

Table 5.5: The stability constant parameters for α-cyclodextrin complexes of peracid and 4-bromothioanisole using Equation 5.12.

T/°C	K_{S11}/M^{-1}	K_{S12}/M^{-1}	K_P/M^{-1}
15	569±84	1245±205	460
20	747±133	452±77	378
25	530±66	470.5±57	341
30	536±40	238±19	284
35	741±67	162±15	234

5.4. Discussion

5.4.1. Discussion on the binding constant of substrates to α-cyclodextrin

As mentioned in previous work and in the introduction to this Chapter, it is likely that the p-substituted aryl alkyl sulfides include in the cyclodextrin cavity with the sulfur containing substitutes directed toward the host secondary rim (wider end). The peracid is likely to be incorporated into the CD with its peroxycarboxilic group directed into the narrow end of the cyclodextrin [192].

Figures 5.1 to 5.5 show that for the reaction of sulfides with MCPBA the rate increases to a maximum and then declines with increasing cyclodextrin concentration, which indicates there is strong binding between CD and peracid; while for PMS the rate shows only a decline with an increase in cyclodextrin concentration, indicating weak binding of the peracid, as might be expected for this charged species. The effect of the complex formation between cyclodextrin and sulfides is illustrated in the shape and the height of the curve: for the strongly binding 4-bromothioanisole the curve is very sharp and small, while for 4-(methythio) benzyl alcohol, which bind less, the peak is large and broad.

This is similar to the results observed previously in the Brij-35 system; in the present case the effect is due to the sulfide being protected from reaction by inclusion into two cyclodextrin molecules as a result of cooperative binding.

Tables 5.1 to 5.5 list the values of the association constants K_{S11}, K_{S12} and the binding constant of peracid at 25°C. Figure 5.6 compares binding constants K_{S11} and K_{S12} obtained from this study and those obtained in reference[162]. It can be seen that for the binding constant type 1:1 a good correlation was obtained with a correlation coefficient of 0.93; while for K_{S12} a fair correlation was obtained. However, it should be mentioned that the binding constants obtained previously were carried out at pH 4.6 and ionic strength 0.05 M^{-1} using a spectrophotometric technique; whereas ours was a kinetic study, conducted with a pH of 2.5 and an ionic strength of 0.003 M.

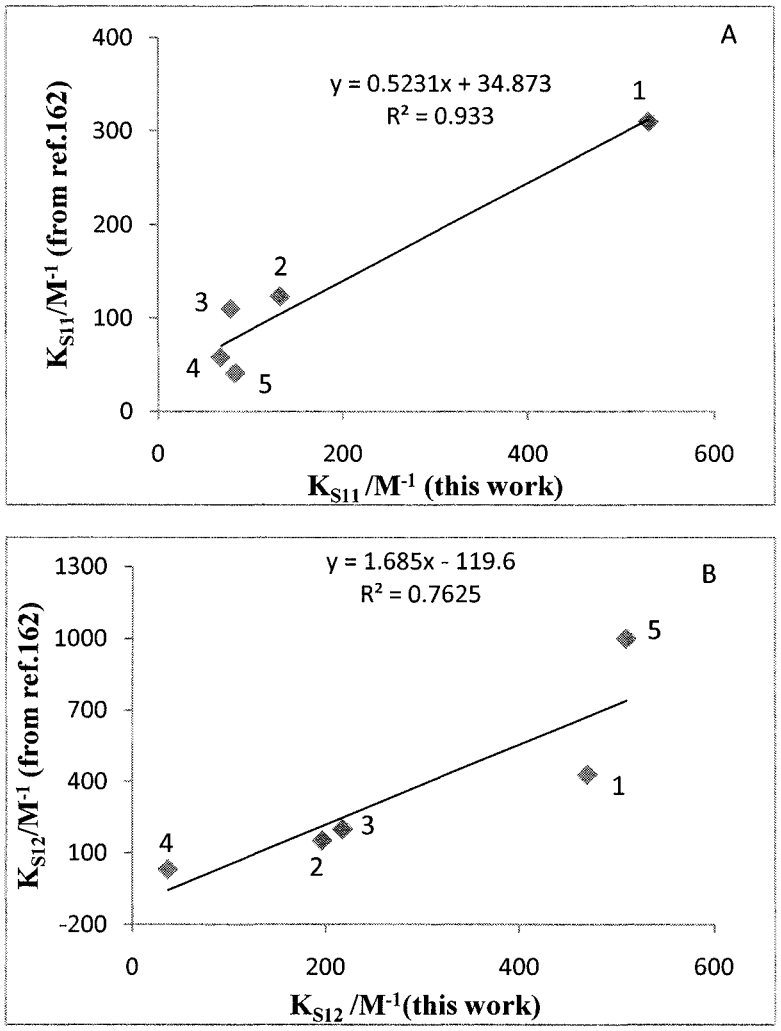

Figure 5.6: Plot of K_{11} obtained from reference 2 versus that of our study. Plot A for K_{S11} and plot B for K_{S12}, 1 = 4-Br, 2=4-NO_2, 3 = 4-OCH_3, 4= 4-CH_2OH and 5= 4-CH_3.

Table 5.6: Best fit parameters for the reaction of sulfides with MCPBA. The values between parentheses are from reference[162].

Compound	K_{S11}/dm^3 mol^{-1}	K_{S12}/dm^3 mol^{-1}	K_P/dm^3 mol^{-1}
Methyl *p*-tolyl sulfide	(41), 84	(1000),510	
4-Methoxythioanisole	(110), 79	(200), 218	
4-Nitrothioanisole	(123), 133	(153), 197	
4-(Methylthio) benzyl alcohol	(58), 68	(32), 37	
4-Bromothioanisole	(310), 530	(430), 470	
3-Chloroperbenzoic acid			(439), 341

5.4.2. Effect of temperature on the complexation process

The host–guest complexation is an equilibrium process where the force of the binding is affected by temperature. Tables 5.1 to 5.5 show that K_{S11}, K_{S12} and K_P all decreased with increasing temperature, with the result that the shape of the curves observed in Figures 5.1 to 5.5 remained relatively unaffected by temperature. These observations are in agreement with literature cases, for example the association constant for naproxen molecule with beta-cyclodextrin decreases from 1379 to 975 to 788 as the temperature increases from 25°C to 35°C to 45°C respectively [167].

The rate of sulfide oxidation by PMS decreases with increasing α-CD concentration as a result of the partition of the reactant between phases. The charged PMS prefers to stay in the aqueous phase while the sulfides are incorporated in the complexes containing one and two molecules of cyclodextrin (as we have discussed, because of cooperative binding, the 1:2 complex is formed at low cyclodextrin concentrations). Increasing the temperature does not affect the shape of the curve, but it does increase the rate as the temperature increases. On the other hand, the rate constant of the oxidation of sulfides by MCPBA shows an initial increase with increasing CD concentration to a certain point; there is then a decline due to the protection of the sulfide by the cyclodextrin(s).

5.4.3. Thermodynamic parameters of the inclusion complexation

The binding constant can be clarified more in terms of the enthalpy and entropy of binding which can give some physical insight into the nature of binding interactions. Table 5.7 shows the entropy and enthalpy of binding constants for aryl alkyl sulfides and peracid. On the basis of the association constants listed in Table, one can easily find that linear relationships exist between ln K_{S11} and ln K_{S12} with inverse temperature. The variations in the binding constants with temperature are represented in the form of Van't Hoff plots; ln *K* versus the inverse of absolute temperature $1/T$, as given in Figure 5.7. The plots, as described in Chapter 1, are used for calculation of the thermodynamic parameters: standard free energy $\Delta G°$, enthalpy $\Delta H°$, and entropy $\Delta S°$ for the 1:1 and 1:2 inclusion complexation of the studied sulfide compounds with α-cyclodextrin, as presented in Table 5.7. All calculated thermodynamic parameters for the complex formation exhibit negative values, except for 4-methoxythioanisole and 4-Bromothioanisole which have a small positive value. Usually, complex formation is associated with large negative values of thermodynamic parameters [157], where predominantly hydrophobic interactions, such as in micelle formation, are usually associated with small positive values of ΔH^o and large positive ΔS^o; thus the hydrophobic interaction is entropy driven [43]. The force controlling the complex formation in this case is not likely to be consistently hydrophobic because for three of the sulfides there were large negative enthalpies and entropies of association, the exceptions being 4-bromothioanisole and 4-methoxythioanisole which have positive entropy of association, though there is considerable scatter in the plots for these compounds compared to the others.

From Table 5.7 it can be seen that the complexation process is generally enthalpy driven. It is thought that during complex formation water molecules inside the cavity release energy which lowers the energy of the system [157, 170]. However, giving more consideration to the binding K_{11}based on the entropy variation can provide a clearer picture. If the interaction between guests and α-CD host results in a more rigid situation, then small differences should be observed when comparing the guest with similar aromatic moiety. This will be different in the substituent at the para position in the aromatic ring. This is in agreement with the values shown in Table 5.7. So, the interaction between the guest and the α-CD 1:1 ratio are different for each aryl alkyl sulfide, suggesting that interaction takes place in which the S-CH_3 group is always directed out of the cavity and the substituent is in the cavity of the α-CD. This way there

is a good relationship between enthalpy and entropy for the K_{S12} binding, as shown in Figure 5.14, which could mean that the second cyclodextrin in all cases interacts with the SCH_3 group protruding from the cavity, and that is where there is a good linear compensation effect in this case.

Negative ΔG^o values strongly imply that the inclusion processes progress spontaneously, while negative ΔH^o and ΔS^o values indicate that the inclusion complexation is exothermic and enthalpy-controlled, but not entropy-driven. This is the common situation concerning the formation of inclusion complexes between cyclodextrins and various guest molecules. It is usually accepted that negative entropy change is due to the steric barrier caused by molecular geometrical shape and the limit of α -CD cavity to the freedom and rotation of guest molecules. It should also be pointed out here that the replacement of one or more water molecules existing in the α-cyclodextrin cavity by a certain guest molecule will cause positive ΔS^o; however, this effect is usually not predominant [157]. For the interactions between sulfide molecules and α-CD, the negative ΔS^o values shown in Table 5.7 for most of the sulfides for the K_{S11} may be an indication of the binding of substrate to α-cyclodextrin and the subsequent restriction of their motion. It may also be due to the small size of the cavity which may hold the guest more tightly and reduce its configurational and hence lower the entropy. This unfavourable effect is overcome by the more negative values of ΔH^o, leading to energetically favourable negative values of ΔG^o.

For the 2:1 host: guest ratio, Table 5.7 shows that the inclusion complexation is associated with a large negative enthalpy and also very large negative entropy. Taken as a whole, the thermodynamic parameters for the K_{S12} values are consistent with the idea of substrate-promoted dipole-dipole interactions between cyclodextrins in 'head to tail' complexes, as previously discussed. There will be a large enthalpic gain through dislodgement of the water molecules from the second cyclodextrin cavity, together with the favourable dipole-dipole interactions between the cyclodextrins; however unfavourable entropy effects are likely to result from the reconfiguration of the cyclodextrin and through the likely formation of hydrogen bonds between the hydroxyls of the primary and secondary rims of the 1:2 complex. Overall, however, the process is enthalpy driven.

In general, the results are for 1:1 and 1:2 complexations are consistent with many complexation processes involving CD and small organic molecules, in which both the enthalpy and entropy of complexation are found to be negative as a result of binding of substrate to cyclodextrin, which leads to a less disorderly system [193]. This is opposite to hydrophobic interaction, which is associated with slightly positive enthalpy and large positive entropy [43] as a result of the exclusion of non-polar molecules from the bulk phase. On the other hand, complexation by CD involves introduction of the less-polar part of the guest into the CD cavity. As the size and shape of the CD cavity are defined by the covalently bonded glucose units, therefore the cavity will give more marked van der Waals interactions than nonpolar organic media, which can be used as an indication of the force controlling the complex formation [161, 194]. From the results it is difficult to estimate the contribution of van der Waals interaction and hydrophobic interaction to the complexation process, but it can be assumed that both are important and responsible for inclusion. Connors [193] has shown that correlation between the logarithms of the stability constant of cyclodextrin inclusion complex of substituted and 1,4-disubstituted benzene derivatives and Hammett sigma values of the substituents can prove the presence of dipolar interaction. However, Connors has also stated that the most nonpolar site of the guest's molecule is enclosed in the cyclodextrin cavity and therefore hydrophobic interaction is important in many cyclodextrin complexations [157].

Table 5.7: Calculated thermodynamic parameters for the reaction of *ca.* 2 x 10^{-4} M MCPBA and 4 x 10^{-4} M PMS with 1 x 10^{-5} M methyl *p*-tolyl sulfide, 4-(methylthio) benzyl alcohol, 4-nitrothioanisole and 4-methoxythioanisole in 3.0 x 10^{-3} M nitric acid at different temperatures.

Parameters	4-CH_3	4-CH_2OH	4-NO_2	4-OCH_3	4-Br
$\Delta H^0(K_{11})$, kJ mol^{-1}	-24 ± 2.9	-11.7 ± 1.7	-24.3± 1.9	3.1 ± 13	2.8 ± 9
$\Delta S^0(K_{11}, M^{-1})$, J mol^{-1} K^{-1}	-43.6 ± 9.7	-4.5 ± 5.7	-41 ± 6.6	46 ± 43	64.7 ± 30.7
$\Delta G^0(k_{11})$, kJ mol^{-1}	-11	-10.3	-12	-10.6	-17.8
$\Delta H^0(K_{12})$, kJ mol^{-1}	-36.8± 3.3	-53 ± 8	-51.7 ± 9.2	-85.4±16.5	-69.7 ± 11.4
$\Delta S^0(K_{12}, M^{-1})$, J mol^{-1} K^{-1}	-72.4± 11	-149.2 ± 26	-129.2 ± 30	-240±54	-184 ± 38
$\Delta G^0(k_{12})$, kJ mol^{-1}	-15.3	-8.5	-13	-13.8	-12

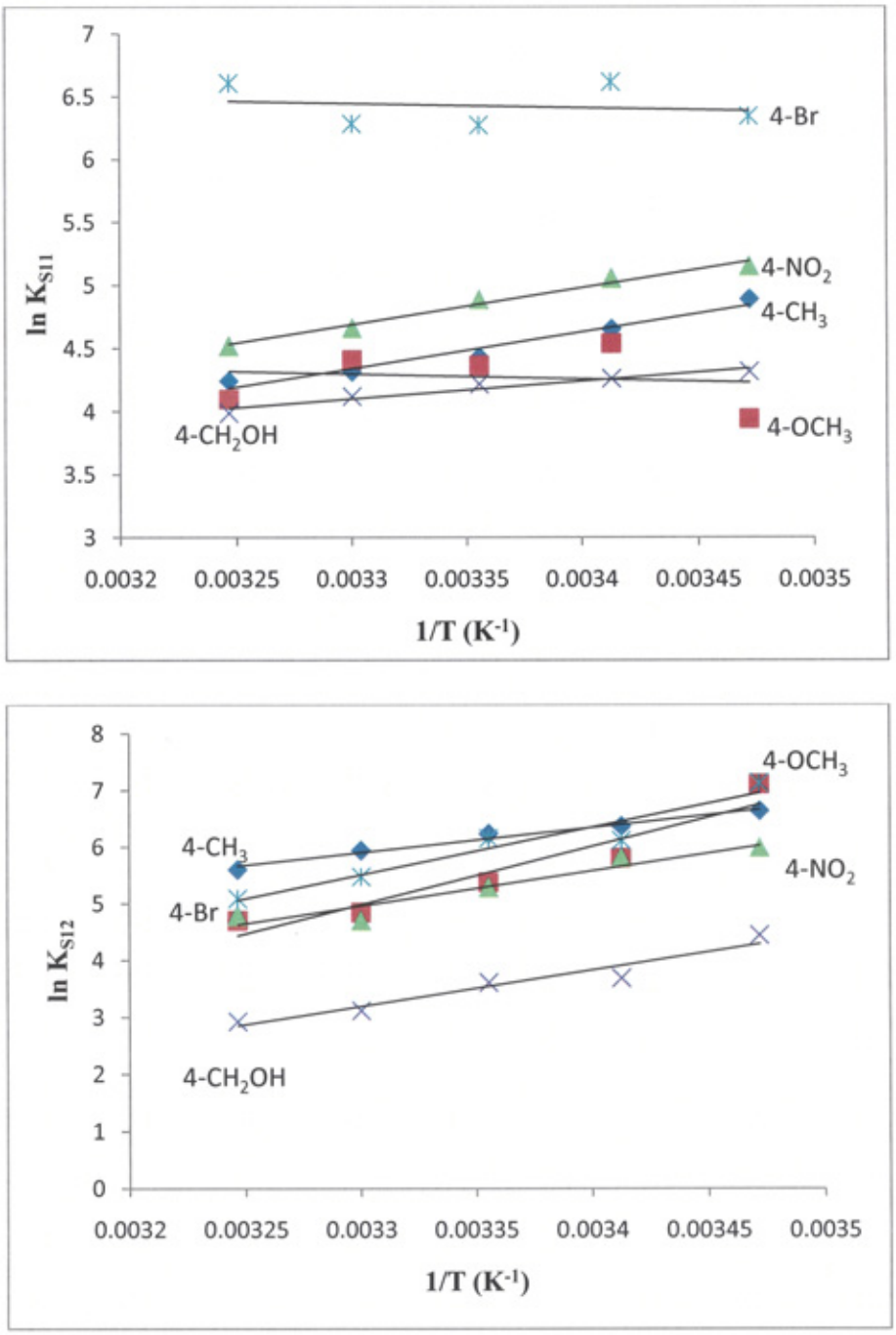

Figure 5.7: Van't Hoff plot of the sulfide association constant K_{S11} and K_{S12}.

5.4.4. Transition state binding K_{TS}

Tee has suggested an approach for quantifying the stabilization of the transition state by cyclodextrin [174]. Tee uses the variation in K_{TS} with the structure to probe the transition state binding to cyclodextrin. Stabilization of the transition state by one molecule of α-cyclodextrin can be described by Equation 5.15.

$$K_{TS1} = \frac{k_{1obs}}{(k_{obs})_o} \qquad 5.15$$

K_{TS} can be used as a measure for the inhibition or catalysis by cyclodextrin using the ratio K_{TS}/K_S, where K_S is the binding of the substrate. In addition, the logarithm of the K_{TS} can give a direct measure of the binding constant energy of the transition state to the catalyst, regardless of the actual pathway from reactant to product, which can be compared with other free energy parameters, such as Hammett values so as to get information about the structure of the transition state [174].

This approach was also used by Davies [162] for the reaction of peracid with sulfides and iodide [163]. Davies used a plot of ln K_{TS1} versus ln K_{S11} and ln K_P to gain an insight into the mode of binding in the activated complex. The results showed there was a good correlation between lnK_{TS1} and natural logarithm of the binding of peracid, but a poor correlation was observed between K_{TS1} and K_{S11} (the binding constant of sulfides), indicating that the transition state resembled the 1:1 cyclodextrin:peracid complex, as previously discussed.

Tables 5.8 to 5.12 show the rate constants and transition state binding constants for the reactions of PMS and MCPBA with aryl alkyl sulfides in the presence of α-cyclodextrin at various temperatures in 0.003 M nitric acid. Table 5.14 compares the values obtained for the transition state binding constant from reference [162] with those found in the present study. There is good agreement between the results, even though the conditions in which the measurements were carried out were different (as mentioned above).

Figure 5.8 shows the Van't Hoff plot for ln K_{TS1} versus inverse temperature, from which the thermodynamic parameters for the binding of the transition state are calculated (listed in Table 5.15).

Looking at the values obtained at 25°C for the reaction between sulfides and MCPBA, Figure 5.9 shows the correlation between complex stability of the transition state ln K_{TS1}, and the sulfide-cyclodextrin complex, ln K_{S11}. The figure shows that there is a small

positive slope (0.09), which may be an indication that the degree of transition state stabilisation is not dependent on the sulfides–cyclodextrin complex. This result is similar to that previously found by Davies [162] who found that the same plot gives a negative small slope of -0.1±0.05. The slight difference in the slope may be due to the large number of sulfides used in the previous study (see Figure 5.10). This poor dependence of K_{TS1} on K_{S11} confirms previous observations that the transition state for these reactions does not resemble the cyclodextrin-sulfide complex (otherwise the same factors that would contribute to the stabilisation of the sulfide-CD complex would also contribute towards the stability of the transition state).

Similar inferences can be made from Figure 5.11, which shows the free energy relationship plot for the binding constant of transition state versus Hammett substituent constant. It can be seen from the figure and from Table 5.13 that the degree of transition state stabilization is virtually independent of the sulfide and the associated electron withdrawing or donating properties of the substituent group, as denoted by the Hammett substituent constant. This is further strong evidence that catalysis is due to the bound peracid reacting with unbound sulfide. It should be noted that this argument does not imply that the substituent effects are unimportant in the reaction; it is just that these effects influence the reaction to the same extent for the uncatalysed reaction as they do for the catalysed reaction, therefore K_{TS1} shows no dependence on them.

Figure 5.12 shows the Van't Hoff plot for the binding of peracid to α-cyclodextrin.Table 5.16 includes the enthalpy and entropy for the kinetic data; all the enthalpy of activation for the reactions of MCPBA and PMS are positive when the reactions are associated with large negative entropy. As stated in the introduction, this is due to the definite orientation of the reactants in the transition state [2].

Table 5.9: Best fit parameters for the oxidation of methyl *p*-tolyl sulfide with peracids using Equation 5.12.

T/ °C	$k_o/^{PMS}$	$k_{1obs}/^{MCPBA}$	$k_{1obs}/^{PMS}$	$k_o/^{MCPBA}$	$K_{TS1}{}^{MCPBA}$	$K_{TS1}{}^{PMS}$	$(K_{TS1}/K_{S11})^{MCPBA}$	$(K_{TS1}/K_{S11})^{PMS}$
15	0.37	872	5.2	0.09	9688	14	72.8	0.1
20	0.43	810	7.8	0.12	6750	18	64	0.6
25	0.509	812	10.6	0.14	5800	20.8	69	0.24
30	0.55	799	10.3	0.19	4205	18.7	56	0.24
35	0.66	758	8.9	0.23	3295	13.4	47	0.19

Table 5.10: Best fit parameters for the oxidation of 4-methoxythioanisole by peracid using Equation 5.12.

T/°C	$k_o/^{PMS}$	$k_{1obs}/^{MCPBA}$	$k_{1obs}/^{PMS}$	$k_o/^{MCPBA}$	$K_{TS1}{}^{MCPBA}$	$K_{TS1}{}^{PMS}$	$(K_{TS1}/K_{S11})^{MCPBA}$	$(K_{TS1}/K_{S11})^{PMS}$
15	0.51	872	12	0.126	6920	23.5	133	0.45
20	0.6	811	14	0.17	4770	23.3	50	0.24
25	0.69	840	15	0.2	4200	21.7	53	0.27
30	0.76	741	12.9	0.27	2744	16.9	33.2	0.2
35	0.84	684	10	0.34	2011	11.9	33	0.19

Table 5.11: Best fit parameters for the oxidation of 4-nitrothioanisole by peracid using Equation 5.12.

T/ °C	k_o/ PMS	k_{1obs}/ MCPBA	k_{1obs}/ PMS	k_o/ MCPBA	K_{TS1} MCPBA	K_{TS1} PMS	(K_{TS1}/K_{S11}) MCPBA	(K_{TS1}/K_{S11}) PMS
15	0.041	54	2	0.0066	8181	48.7	47	0.28
20	0.054	63.7	0.85	0.0087	7321	15.8	46	0.1
25	0.062	55	2	0.011	5000	32.2	37	0.24
30	0.077	50.8	1.6	0.016	3175	20.7	30	0.2
35	0.093	54	1.9	0.021	2571	20.4	28	0.3

Table 5.12: Best fit parameters for the oxidation of 4-(methylthio) benzyl alcohol by peracid using Equation 5.12.

T/ °C	k_o/ PMS	k_{1obs}/ MCPBA	k_{1obs}/ PMS	k_o/ MCPBA	K_{TS1} MCPBA	K_{TS1} PMS	(K_{TS1}/K_{S11}) MCPBA	(K_{TS1}/K_{S11}) PMS
15	0.28	517	1.2	0.068	7602.9	4.3	101	0.05
20	0.34	531	3	0.085	6247	8.8	87.9	0.12
25	0.41	569	1.8	0.1	5690	4.4	83.6	0.06
30	0.46	558	1.6	0.134	4164	3.5	67	0.056
35	0.55	542	1.8	0.168	3226	3.3	59	0.06

Table 5.13: Best fit parameters for the oxidation of 4-bromothioanisole by peracid using Equation 5.12.

T/K	k_o/PMS	k_{1obs}/MCPBA	k_{1obs}/PMS	k_o/MCPBA	K_{TS1} MCPBA	K_{TS1} PMS	(K_{TS1}/K_{S11}) MCPBA	(K_{TS1}/K_{S11}) PMS
15	0.21	357	101	0.039	9153	480.9	16	0.8
20	0.26	370	80	0.054	6851	307.6	9	0.4
25	0.29	375	79	0.06	6250	272.4	11.7	0.5
30	0.37	382	66	0.086	4441	178.3	8.2	0.33
35	0.42	501	98	0.1	5010	233	6.7	0.31

Terms and units used are observed first order rate (uncatalysed reaction) k_o/ S^{-1}, first order rate in cyclodextrin k_{obs1}/ dm^3 mol^{-1} s^{-1}, and second order rate in cyclodextrin k_{obs2}/dm^6 mol^{-2} s^{-1}. PMS and MCPBA represent the peroxymonosulfate and MCPBA respectively.

Table 5.14: The transition state association constant for the sulfide reaction with MCPBA at 25°C (taken from this work and also [162]).

Compounds	K_{TS1}/ dm^3 mol^{-1}, for MCPBA from[162]	K_{TS1}/ dm^3 mol^{-1}, this work	K_{TS1}/ dm^3 mol^{-1},for PMS from[162]	K_{TS1}/ dm^3 mol^{-1}, this work
Methyl *p*-tolyl sulfide	5183 ± 56	5800 ±363		20.8
4-Methoxythioanisole	5067±214	4200 ±250		21.7
4-Nitrothioanisole	5186± 82	5000 ±290	17.2±2.6	32
4-(Methylthio) benzyl alcohol	nd	5690 ± 323		4.3
4-Bromothioanisole	4192	6250		727

Table 5.15: The calculated thermodynamic parameters for the reaction of *ca.* 2 x 10^{-4} M MCPBA and 4 x 10^{-4} M PMS with 1 x 10^{-5} M p-tolyl methyl sulfide, 4-(methylthio)benzyl alcohol, 4-nitrothioanisole and 4-methoxythioanisole, and 4-Bromothioanisole in 3.0 x 10^{-3} M nitric acid at different temperatures.

Parameters	4-CH_3	4-CH_2OH	4-NO_2	4-OCH_3	4-Br
$\Delta H^0(K_{TS1})$, kJ mol^{-1} (MCPBA)	-38.8± 2.3	-31± 3.4	-46.5 ± 5	-44.5±3.7	-24 ± 5.8
$\Delta S^0(K_{TS1})$, J mol^{-1} K^{-1} (MCPBA)	-58.6± 7.7	-33.6 ± 11.3	-85.3 ± 16.8	-81± 12.4	-9 ± 19
$\Delta G^0(K_{TS1})$, kJ mol^{-1} (MCPBA)	-21.3	-21.4	-20.6	-20.3	-21.3
$\Delta H^0(K_{TS1})$, kJ mol^{-1} (PMS)	-0.4 ± 10	-21.4 ± 17	-21.8± 20	-24.6± 6.6	-29.6 ± 9.8
$\Delta S^0(K_{TS1})$, J mol^{-1} K^{-1} (PMS)	22 ± 34	-59.3 ± 58	-46± 68	-58± 22	-52.7 ± 33
$\Delta G^0(K_{TS1})$, kJ mol^{-1} (PMS)	-6.9	-3.3	-5.3	-7.1	-13.8
$\Delta H^0(K_P)$, kJ mol^{-1}	-25.5±0.98				
$\Delta S^0(K_P)$, kJ mol^{-1}	-37.2±3.3				

PMS denotes peroxymonosulfate.

Table 5.16: Enthalpy and entropy of activation for the reaction of sulfides with peracids in 0.003 M^{-1} nitric acid.

Parameters	4-CH_3	4-CH_2OH	4-NO_2	4-OCH_3	4-Br
$\Delta H^{\ddagger}(k_{obs})_o$, kJ mol^{-1} (MCPBA)	33.3 ± 1.7	30± 0.55	43.8 ± 0.99	34.8±1.8	32.6 ± 0.42
$\Delta H^{\ddagger}(k_{obs})_o$, kJ mol^{-1} (PMS)	18 ± 0.64	22.5 ± 0.95	30.4 ± 2.4	12.9 ±1.2	21.9 ± 0.72
$\Delta S^{\ddagger}(k_{obs})_o$, J mol^{-1} K^{-1} (MCPBA)	-148.9 ± 5.7	-163 ± 1.8	-134.5 ± 3.3	-140.8±6	-157.8 ± 1.4
$\Delta S^{\ddagger}(k_{obs})_o$, J mol^{-1} K^{-1} (PMS)	-190 ± 2.2	-177.2 ± 3.2	-166 ± 0.7	-204±0.4	-181.4 ± 2.4
$\Delta G^{\ddagger}(k_{obs})_o$ kJ mol^{-1} (MCPBA)	77.6	78.5	83.8	85.7	79.6

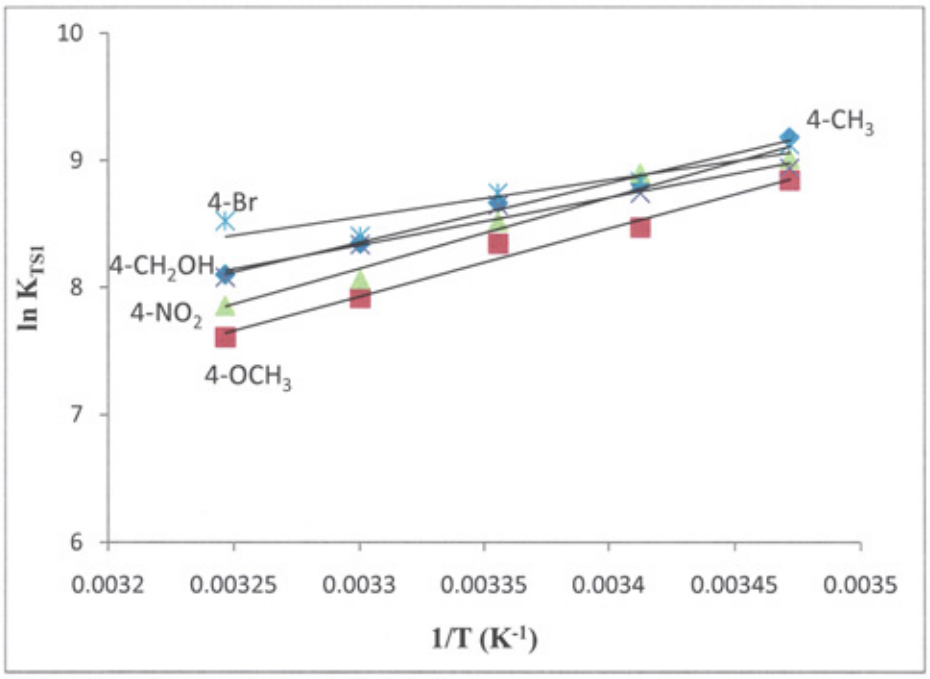

Figure 5.8: Van't Hoff plot for apparent transition state binding constant for the reaction of sulfides with MCPBA.

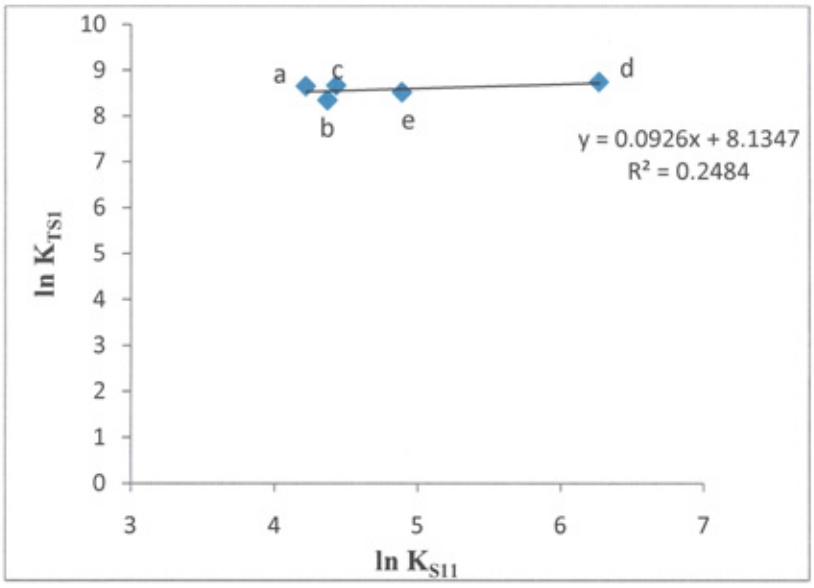

Figure 5.9: Linear free energy relationships and correlation between ln K_{TS1} and Ln K_{S11} for the reaction of m-chloroperbenzoic acid with series of alkyl aryl sulfides; (a) 4-CH_2OH, (b) 4-OCH_3, (c) 4-CH_3, (d) 4-Br, and (e) 4-NO_2.

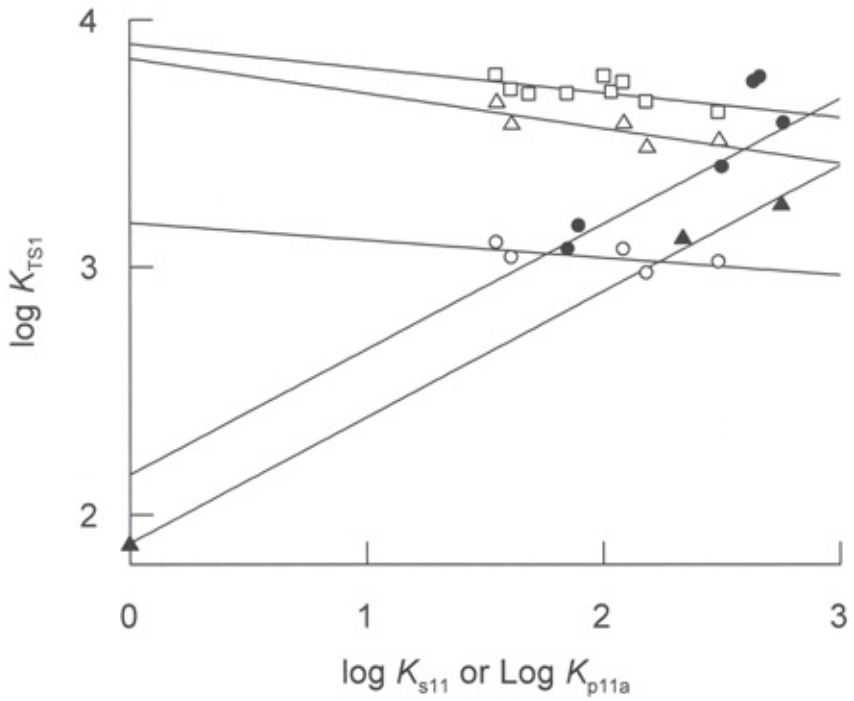

Figure 5.10: Linear free energy relationships between log K_{TS1} versus log K_{S11} (open symbol) and logK_{P11} (filled symbol). The open squares are for the reaction of MCPBA with a range of aryl alkyl sulfides and the triangles are for the reaction of 4-methylperbenzoic acid with a range of alkyl aryl sulfides. For full details about the symbols refer to reference [162]

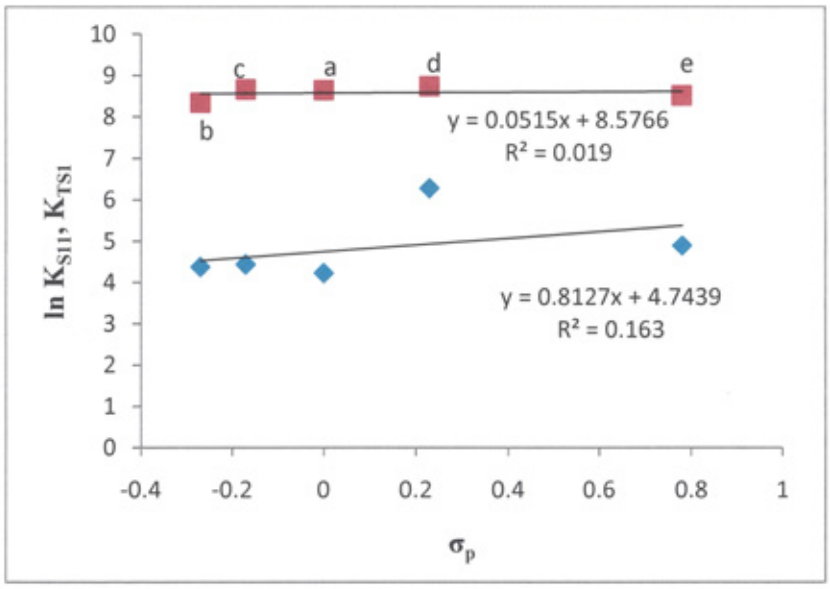

Figure 5.11: Plot of free energy relationships between Hammett substituent constant and binding constant of sulfides. The squares represent K_{TS1}, diamonds denote K_{S11}, a = CH_2OH, b= OCH_3, c= CH_3, d= 4-Br, and e = NO_2.

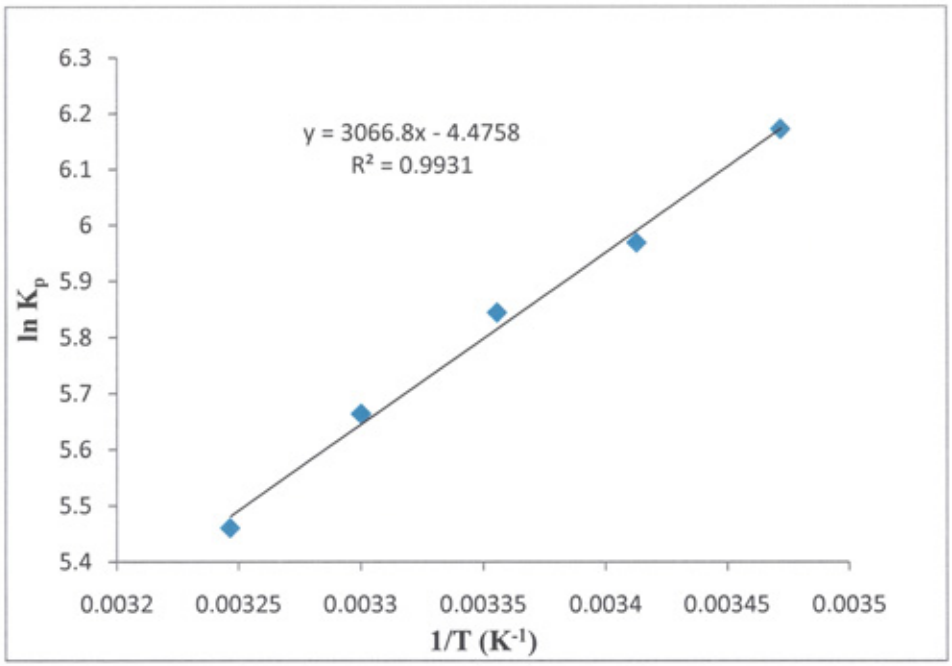

Figure 5.12: Natural logarithm of stability constant of MCPBA versus 1/T for the reaction of sulfides with MCPBA in cyclodextrin.

5.4.5. Testing the presence of the compensation effect with Arrhenius and Van't Hoff plots

5.4.5.1 Compensation effects for K_{S11} and K_{S12}

From the thermodynamic values in Table 5.7 it can be seen that most ΔG^o values, except those for 4-Bromothioanisole, are restricted in a range of about 3 k J/mol. However, ΔH^o is more varied and approximately spans 20 for K_{S11} and 15 for K_{S12}; thus, a comparison can not be made on the basis of an equilibrium constant alone which is equal to $\Delta G^o = -RT \ln K$, but the other thermodynamic parameters ΔH^o and ΔS^o which are varied can be discussed. The presence of the compensation effect, which is a linear correlation between enthalpy and entropy in the cyclodextrin complexation, has been observed [194, 161]. However, its origin and meaning are still controversial [144]. In general, a plot of $T\Delta S^o$ vs ΔH^o generates slope α and intercepts $T\Delta S_o^0$ based on Equation 5.16.

$$T\Delta S^o = \alpha \Delta H^o + T\Delta S_o^0 \qquad 5.16$$

The slope and intercept $T\Delta S_o^0$, which denotes the values of complex stability in the absence of any enthalpy contribution ($\Delta H^o = 0$), have been used as a measure of the host–guest conformational change which contributes to the enthalpy gain, and the intercept is measure of the extent of the host-guest desolvation caused upon inclusion [153]. Inoue [153]

has studied the inclusion of naphthalenesulfonate with α-cyclodextrin and found a linear correlation between $T\Delta S^{o}$ and ΔH^{o} with slope = 0.9 and intercept = 12.5 kJ/mol. Inoue states that the high value of the slope indicates that the cyclodextrin experiences large conformational change upon complexation, which means that the cyclodextrin are flexible and not rigid in aqueous solution. While the intercept of 12.5 indicates fairly extensive desolvation of both the host and the guest accompanying the complexation. This plot will be utilised in the present study to show how much of the enthalpy gain is cancelled by entropy loss, and vice versa.

Figures 5.13 and 5.14 show the compensation plot for the 1:1 and 1:2 complexation process. The isokinetic temperatures obtained from the slope are 240 and 295 K respectively. This slope in the plot is used to calculate compensation temperature. Figure 5.13 shows that the points for both the 4-bromo and 4-methoxy substituents show a deviation from the fitting line as stated in section 5.4.3, and inspection of the data in Table 5.14 suggest that the inclusion 1:1 for these two substrates are entropy driven as opposed to the other sulfides (though one should exercise caution in reaching this conclusion due to the scatter observed in the Van't Hoff plots for these two compounds). Despite the small positive values of enthalpy for 4-bromothioanisole (values of 2.7 k J/ mole) it is associated with the highest entropy, which should be seen for 4-methoxythioanisole due to its positive values of enthalpy. Thus, this deviation from other data may be a result of the fact that enthalpy has become larger and so the less favourable gain in entropy does not compensate well with enthalpy, and vice versa. Also, the large values of entropy in the case of 4-bromothioanisole result in more negative free energy (-17 J / mol K) compared to others sulfides, which are about -11 J / mol K.

In order to compare the results with those obtained by Inoue [153] the data was also plotted according to the method described above, which is used for interpreting the compensation effect, as shown in Figure 5.15 and Figure 5.16 (these plots will be used to get $T\Delta S_o^0$ and the slope as mentioned above) The plots give good linear correlation (correlation coefficients of 0.98 and 0.97) with a slope of 1.06 and 0.98 for 1:1 and 1:2 binding processes respectively, which indicates that both binding processes involve similar high degrees of conformational change upon complexation. Moreover, the positive intercept of about 12 kJ/mol for both 1:1 and 1:2 complexation is similar to that obtained in literature studies, where such values have been taken to imply significant desolvation during the complexation process [153].

It is possible to interpret the enthalpy-entropy compensation plots so as to gain some insight into the binding and orientation of the sulfides. Liu and co-workers [171] have proposed that reorganisation of water molecules during the complexation process is the cause of the enthalpy-entropy compensation. Their theoretical model assumes that the free energy of association can be broken down into a non-compensatable portion related to the interaction between the host, guest and their environment, and a compensatable portion related to water molecular reorganisation. If all of the guests in a series are hydrophobic and do not interact with the water solvent then good compensation will be observed, however, for guests that show strong interaction with water, they will be observed as outliers since no enthalpy–entropy compensation is possible [171]

It is clear from the two similar plots shown in Figures 5.14 and 5.16 that there is a very good linear relationship between entropy and enthalpy for the 1:2 binding constants for the sulfides; the relationship is not so good for the 1:1 complexes, as shown in Figures 5.13 and 5.15. Considering this further, and making the assumption that the methyl sulfide group always protrudes from the wide end of the cyclodextrin cavity, one can see that formation of the 1:2 complex involves essentially the same participants, *irrespective of the sulfide that is included*, i.e. a cyclodextrin with a methyl sulfide group protruding and an unbound cyclodextrin. The *p*-substituent that is buried within the cyclodextrin cavity is 'unseen' by the solvent molecules that reorganise during complexation[172], though clearly it does still affect the strength of the K_{S12} binding. It should be no surprise, therefore, that there is very good enthalpy-entropy compensation for five such similar complexation processes, and this can be taken as good evidence that our assumption of sulfide orientation is correct.

However for the formation of 1:1 complexes, the participants in the complexation process differ by the extent of the *p* -substituent groups and, as Liu and co-workers[171] have pointed out, the substituents may interact with the reorganising solvent molecules to different extents. Where significant interaction takes place, then poor enthalpy-entropy compensation will be observed. The relatively poor correlation observed in the present case for the five sulfides implies that some of the substituents may be interacting with the solvent.

5.4.5.2 Compensation effects for K_{TS11}

In a similar fashion to the work on K_{S11} and K_{S12} discussed in the preceding section, compensation plots might also be useful in gaining insights into the nature of the transition state for the catalysed reaction. Remember that for MCPBA the assumption, based on linear free energy studies, was that the transition state involving one molecule of cyclodextrin comprises the bound peracid with the unbound sulfide. In contrast, for the charged PMS species, which does not bind, the transition state involving one molecule of cyclodextrin comprises the bound sulfide reacting with the unbound peracid; this results largely in inhibition of the reaction, as seen from the K_{TS11}/K_{S11} values shown in Tables 5.9 to 5.13.

Considering the MCPBA reaction one might expect a very good enthalpy-entropy compensation plot, since the peracid is the bound moiety in each case, and so the solvent reorganisation processes will be very similar in each case. For PMS, where the sulfide is the bound moiety then a good correlation is nor necessarily expected for exactly the same arguments as made in Section 5.4.5.1 above.

These predictions are borne out by the compensation plots for the transition state binding constant K_{TS11} for both MCPBA and PMS that are shown in Figure 5.17. Very good relationships can be observed for the transition state association constant for the MCPBA system, with a correlation coefficient of 0.99 whereas for the PMS system a relatively poor correlation is observed.

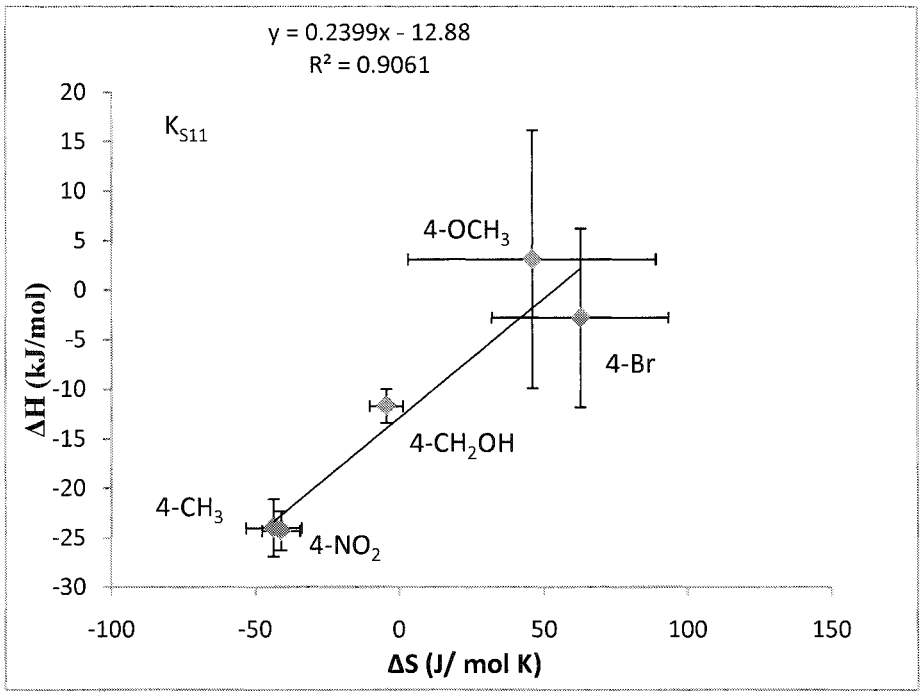

Figure 5.13: enthalpy-entropy compensation plot for the inclusion complexation of α-cyclodextrin with aryl alkyl sulfides type 1:1.

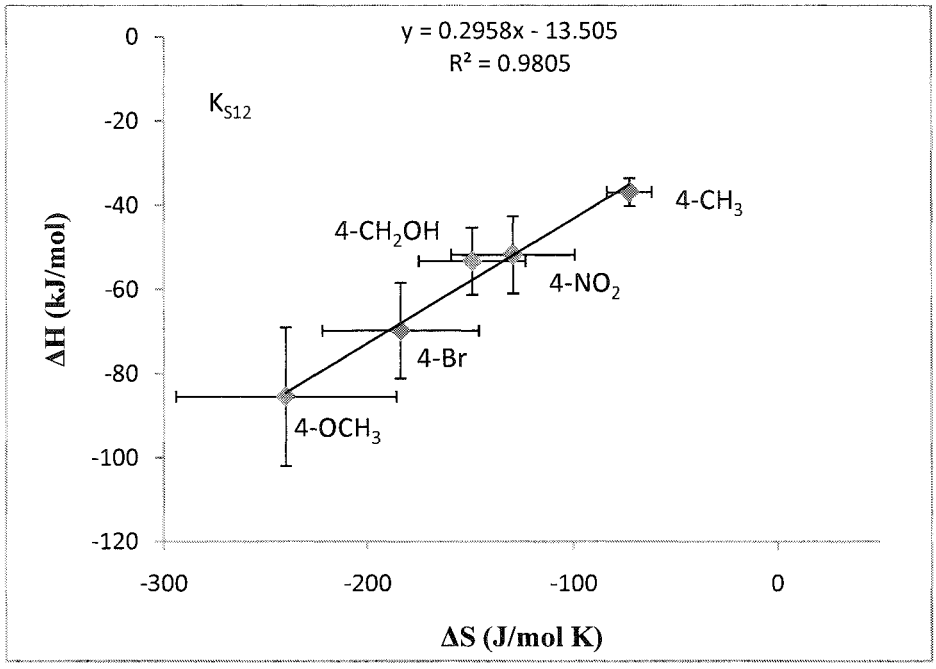

Figure 5.14: Enthalpy-entropy compensation plot for the inclusion complexation of α-cyclodextrin with 4-susbtitued sulfides type 2:1 host: guest.

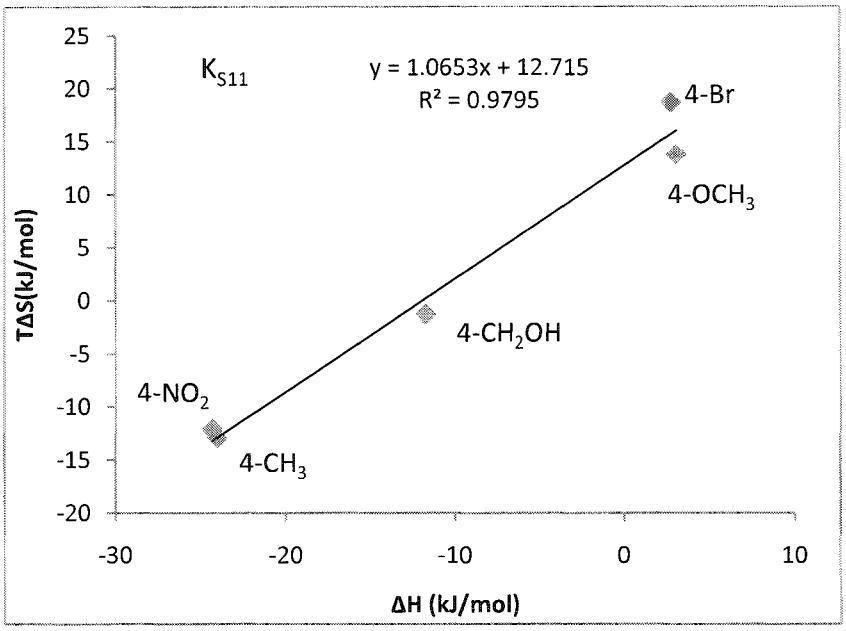

Figure 5.15: Enthalpy-entropy compensation plot for the inclusion complexation of α-cyclodextrin with 4-susbtitued sulfides type 1:1 host: guest.

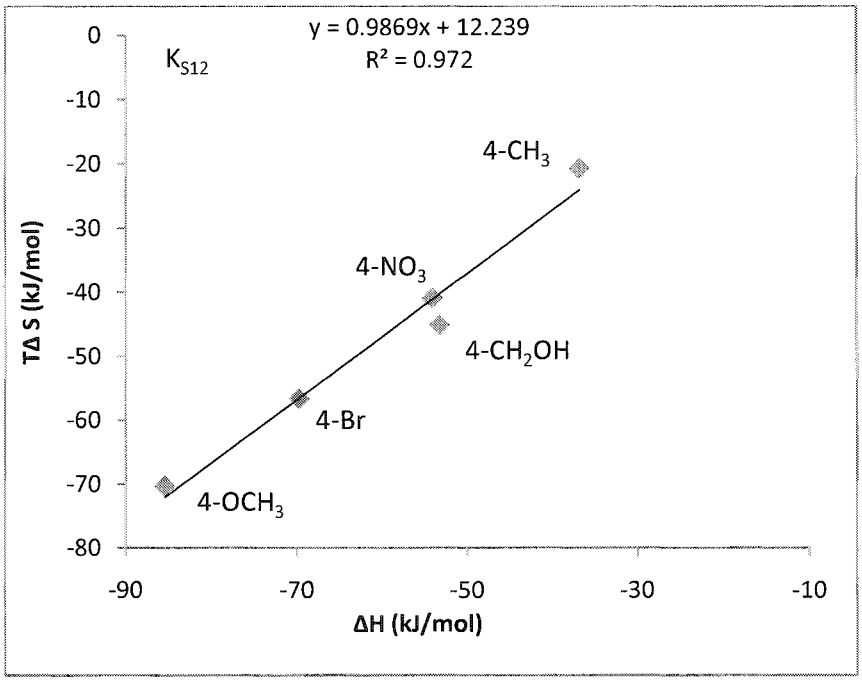

Figure 5.16: Enthalpy-entropy compensation plot for the inclusion complexation of α-cyclodextrin with 4-susbtitued sulfides type 2:1 host: guest.

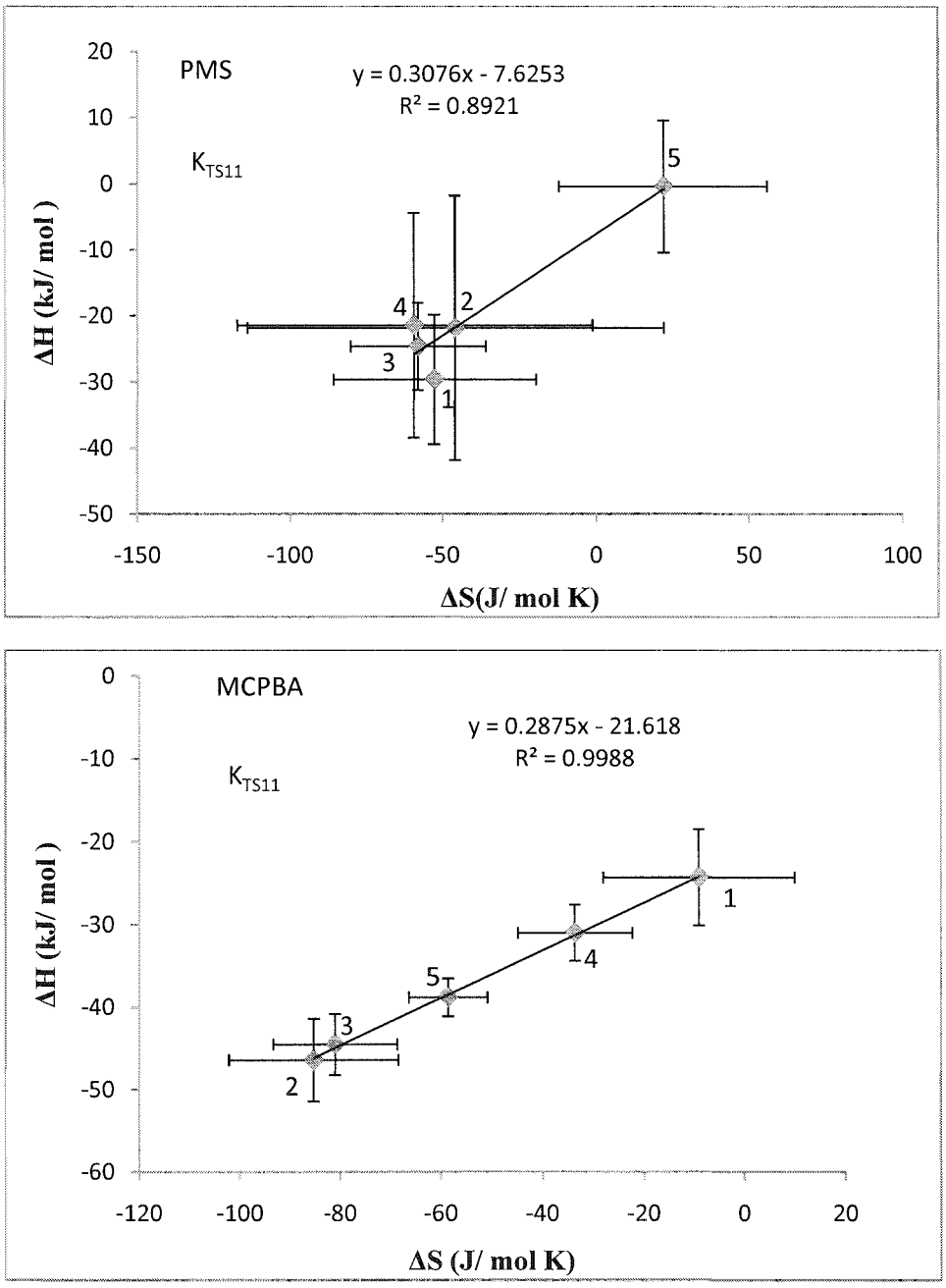

Figure 5.17: Enthalpy-entropy compensation plot for the inclusion complexation of α-cyclodextrin with transition state of aryl alkyl sulfides type 1:1 host: guest, with peroxoymonosulfate (top plot) and MCPBA (lower plot). The numbers denote 1 = 4-Br, 2=4-NO_2, 3 = 4-OCH_3, 4= 4-CH_2OH and 5= 4-CH_3

Chapter 6 Effect of temperature on the reaction of iodide with MCPBA in α-cyclodextrin in different conditions

6.1. Introduction

Literature studies suggest that for a range of electrophilic oxidation reactions involving perbenzoic acids in the presence of α-cyclodextrin, including those of aryl alkyl sulfides and iodide, the catalytic species the is the 1:1 cyclodextrin : peracid complex, with the peroxo group located at the narrow (primary) end of the cyclodextrin cavity. This was confirmed in Chapter 5, where the correlation between Ln K_{TS1} and Ln K_P indicated that the same factors that contribute towards the stabilisation of the peracid, also contribute towards the stabilisation of the transition state.

Reasons for the transition state stabilisation of the α-cyclodextrin mediated reaction of peracids with aryl alkyl sulfides include the intra-molecular hydrogen bonded perbenzoic acid structure discussed in Chapter 5 that serves to minimise charge development in the transition state; however, there are other possible mechanisms for catalysis that should not be overlooked, for example acid-base catalytic effects by the relatively conformationally free primary OH groups,[163] and activation of the peroxide by dipole-dipole effects[162].

In this chapter the reduction of MCPBA with iodide will be investigated at different temperatures in the presence of fixed salt concentrations and in the presence of α-cyclodextrin, which consists of the same hydrophobic core and hydrophilic exterior as Brij-35, except for the latter there is a fast exchange between the monomer in the micelle and that in the bulk aqueous phase. The temperature and salt concentrations will be exactly the same as for the Brij-35 results reported on in Chapter 3, thus allowing the factors governing the complexation process for substrate to the catalyst to be compared for both systems by utilizing the thermodynamic parameters and entropy-enthalpy compensation plots.

6.2. Experiment

6.2.1. Kinetic measurements

All the kinetic measurements have been carried out on a stopped flow instrument, as described previously in Chapter 2.

6.3. Results

6.3.1. Determination of the rate constant

The rate constant was measured under pseudo first order rate conditions using a concentration of iodide (0.0015 M) over the MCPBA (5×10^{-6} M). Figures 6.1 to 6.5 show the effect of cyclodextrin concentration on k_{obs}. The equilibria and reaction of the system are shown in Equation 6.1 to Equation 6.6, and the stability constant of peracid and iodide is described by Equation 6.7 and Equation 6.8, as described previously [164].

$$CD + P \overset{K_P}{\rightleftharpoons} CD,P \qquad 6.1$$

$$CD + I^- \overset{K_I}{\rightleftharpoons} CD,I^- \qquad 6.2$$

$$P + I^- \xrightarrow{k_o} \text{Products} \qquad 6.3$$

$$CD,P + I^- \xrightarrow{k_{1a}} \text{Products} \qquad 6.4$$

$$P + CD,I^- \xrightarrow{k_{1b}} \text{Products} \qquad 6.5$$

$$CD,P + CD,I^- \xrightarrow{k_2} \text{Products} \qquad 6.6$$

$$Kp = \frac{[CD,P]}{[CD][P]} \qquad 6.7$$

$$K_I = \frac{[CD,I]}{[CD][I^-]} \qquad 6.8$$

The reaction scheme leads to the rate law given in Equation 6.9

$$k_{obs} = \frac{k_o + k_{1obs}[CD]_o + k_{2obs}[CD]_o^2}{1 + (K_P + K_I)[CD]_o + K_P K_I [CD]_o^2} \qquad 6.9$$

Where k_{1obs} and k_{2obs} are defined by Equation 6.10 and Equation 6.11

$$k_{1obs} = k_{1a}K_P + k_{1b}K_I \quad 6.10$$

$$k_{2obs} = k_2K_PK_I \quad 6.11$$

k_{1obs} *and* k_{2obs} are the first and second order in α-cyclodextrin, and $[CD]_o$ is the total cyclodextrin concentration.

6.3.2. Curve fitting

For the reactions carried out in Brij-35 in chapter 3, it was necessary to fit the data separately at each condition; this was because for surfactants such as Brij-35, changes in salt and temperature were found to have a great effect on cmc as well as aggregation number; hence, the nature of the micelle is affected in each condition, with consequent affects on binding and reaction rates.

For cyclodextrin, where the macro-structure is covalently bonded, such considerations do not apply and so, at each different temperature, the kinetic data for the different conditions were fitted universally to Equation 6.9, with K_P and K_I kept as common parameters assuming the absence of a salt effect on the binding.

One complication for this system, however, is the fact that some of the anions used will bind with α-cyclodextrin. The complexation of α-cyclodextrin with SO_4^{-2}, NO_3^-, ClO_4^- and I^- anions has been measure measured using conductance methods in literature studies[195]. The binding constant for nitrate is negligible, however those for sulfate and perchlorate, whilst the relatively small, do need to be accounted for because of the high concentrations used in these experiments. This is done by including in the binding isotherm values for K_{ClO4} and K_{SO4}.the binding constants for perchlorate and sulfate respectively. Moreover, the high concentrations used for perchlorate (1 M and 0.2 M) meant that it could not be assumed that the $[CD]_o = [CD]$, where the former is the total and the latter is the free α-cyclodextrin concentration, as a significant amount of CD is complexed by the perchlorate. Therefore, the concentrations of free α-cyclodextrin, for runs using perchlorate, has to be calculated using the bisection method listed in Appendix C (programme 1c) was used for the fitting. In The best fit parameters obtained are listed in Table 6.1 to Table 6.4.

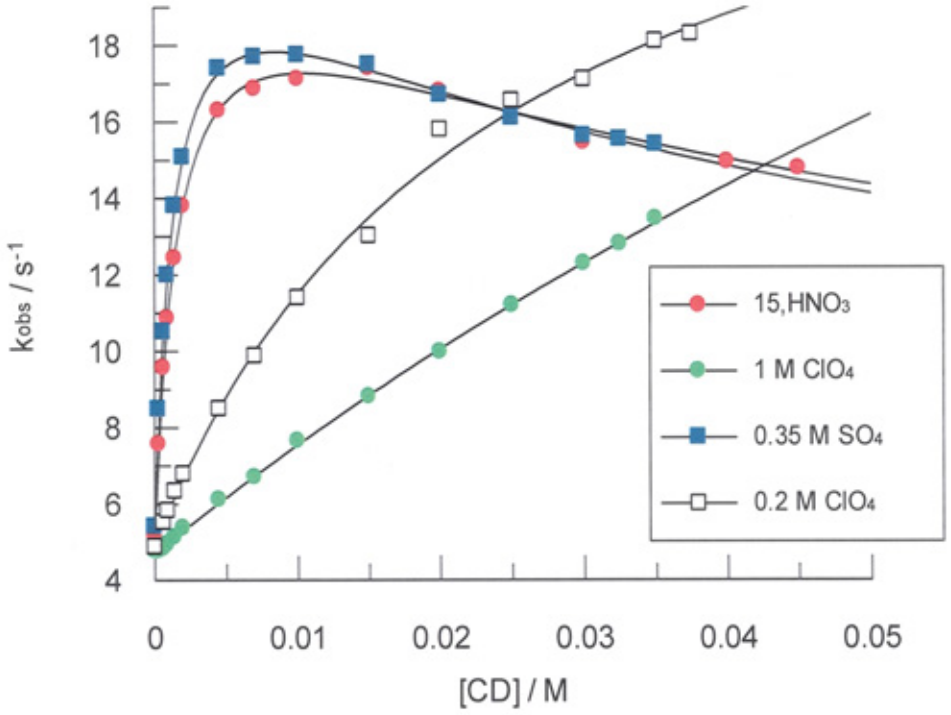

Figure 6.1: Observed rate constant versus α-cyclodextrin concentration for the reaction of 0.0015 M iodide with 5×10^{-6} M of MCPBA in 0.003 M nitric acid, 0.35 M sulfate, and 1 M and 0.2 M perchlorate at 15°C.

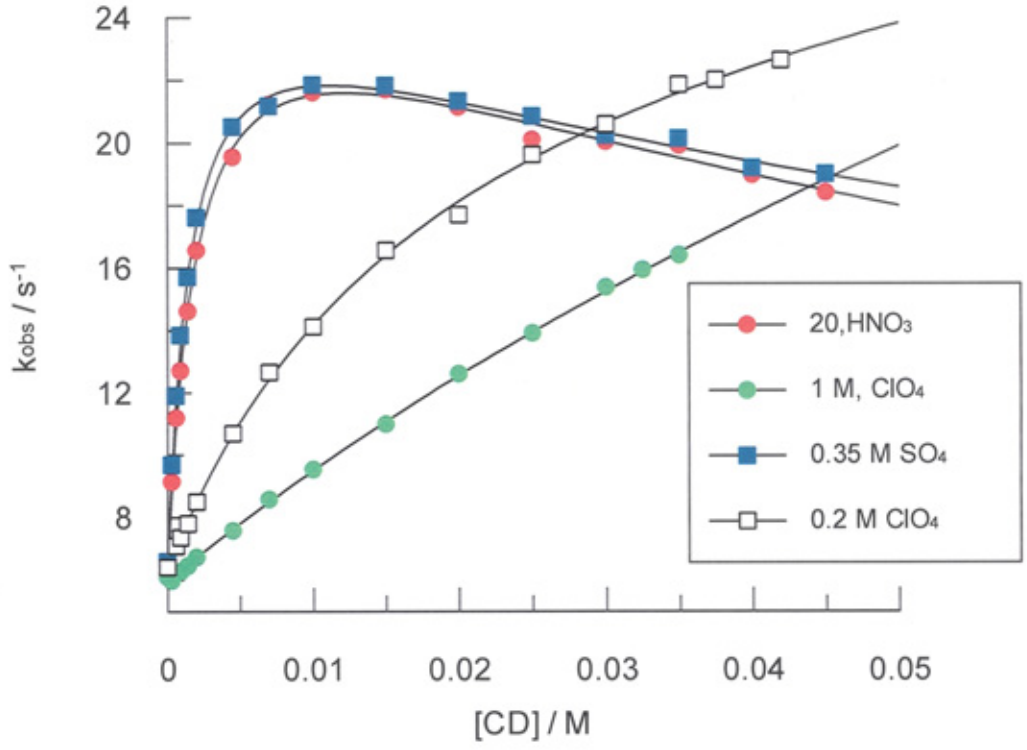

Figure 6.2: Observed rate constant versus α-cyclodextrin concentration for the reaction of 0.0015 M iodide with 5×10^{-6} M of MCPBA in 0.003 M nitric acid, 0.35 M sulfate, and 1 M and 0.2 M perchlorate at 20°C.

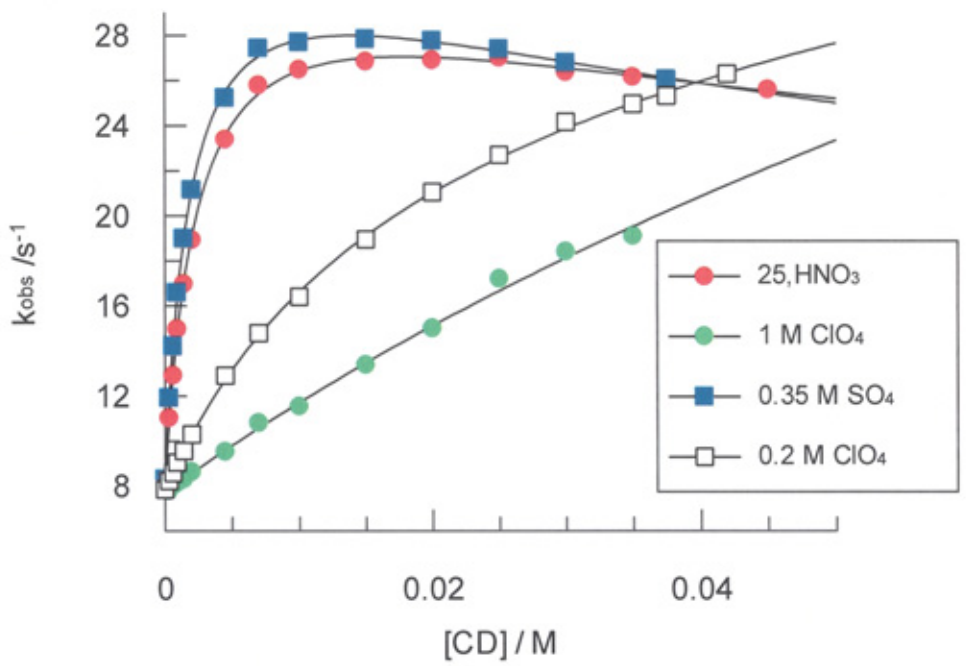

Figure 6.3: Observed rate constant versus α-cyclodextrin concentration for the reaction of 0.0015 M iodide with 5×10^{-6} M of MCPBA in 0.003 M nitric acid, 0.35 M sulfate, and 1 M and 0.2 M perchlorate at 25°C.

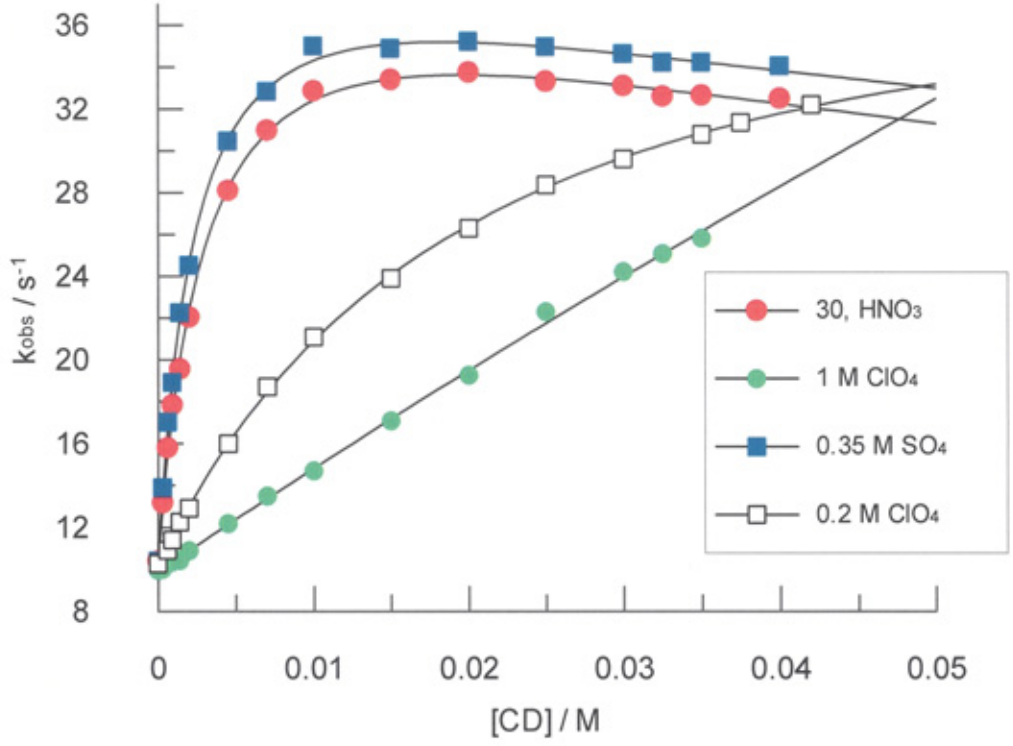

Figure 6.4: Observed rate constant versus α-cyclodextrin concentration for the reaction of 0.0015 M iodide with 5×10^{-6} M of MCPBA in 0.003 M nitric acid, 0.35 M sulfate, and 1 M and 0.2 M perchlorate at 30°C.

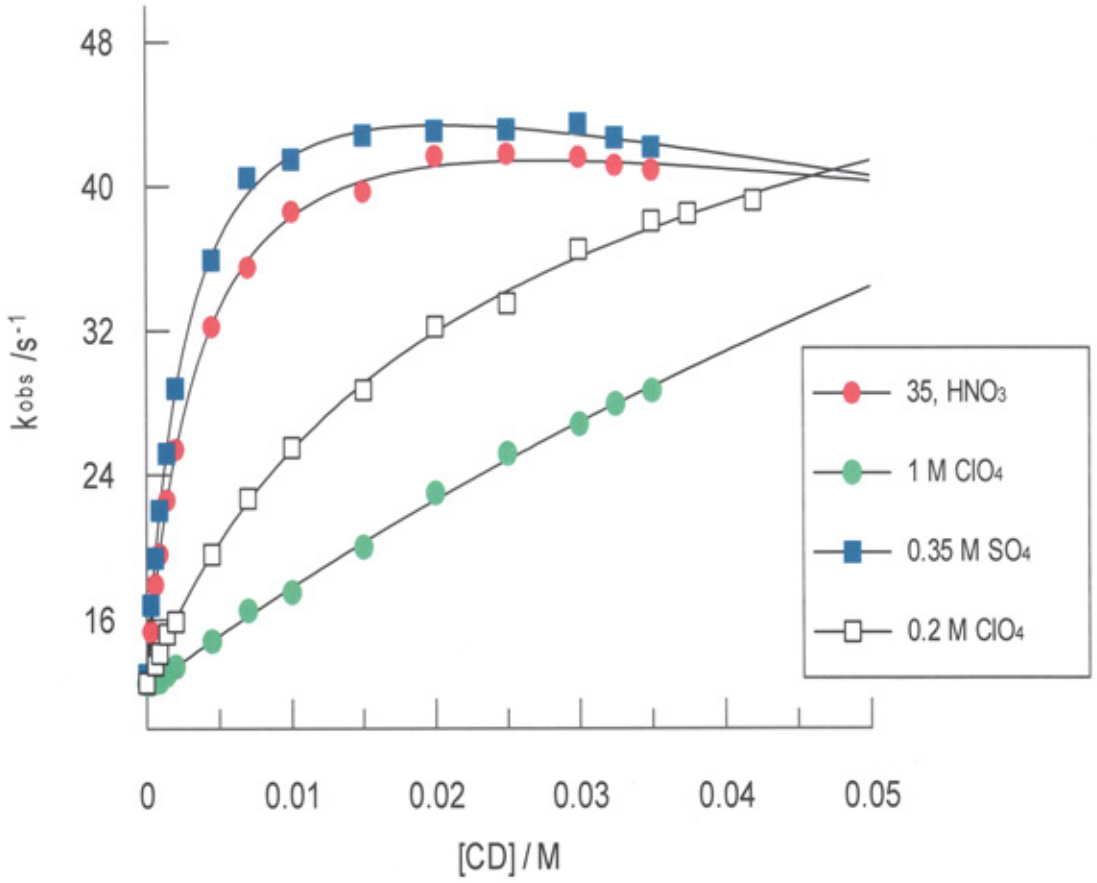

Figure 6.5: Observed rate constant versus α-cyclodextrin concentration for the reaction of 0.0015 M iodide with 5×10^{-6} M of MCPBA in 0.003 M nitric acid, 0.35 M sulfate, and 1 M and 0.2 M perchlorate at 35°C.

Table 6.1: Best fit parameters obtained from fitting Equation 6.9 to kinetic data for the reaction of iodide with MCPBA in nitric acid.

T/°C	k_{obs} /s^{-1}	k_{1obs}/ 10^3 dm^3 mol^{-1} s^{-1}	k_{2obs}/ 10^3 dm^6 mol^{-2} s^{-1}	K_P/M^{-1}	K_I/M^{-1}	K_{ClO4}	K_{SO4}	K_{TS1}/M^{-1}	K_{TS2}/M^{-1}
15	5.1	13	86	603	19	62	-0.54	2563	6.6
20	6.5	13	25	481	12	38	-0.65	2019	1.9
25	8.3	13.5	62	411	10.9	28	-0.6	1632	4.6
30	10.3	13.4	30	320	8.4	30	-0.66	1305	2.2
35	12.9	12.6	15	250	5.1	17	-0.65	983	1.2

Table 6.2: Best fit parameters obtained from fitting Equation 6.9 to kinetic data for the reaction of iodide with MCPBA in 1 M $NaClO_4$.

T/°C	k_{obs}	k_{1obs} / 10^3	k_{2obs} /10^5	K_P	K_I	K_{ClO4}	K_{SO4}	K_{TS1}	K_{TS2}
15	4.77	22	33	603	19	62	-0.54	4659	144
20	6.2	18	23	481	12	38	-0.65	2886	128
25	7.9	16	19	411	10.9	28	-0.6	1998	119
30	9.9	19	37	320	8.4	30	-0.66	1962	191
35	12.4	14	10	250	5.1	17	-0.65	1128	74

Table 6.3: Best fit parameters obtained from fitting Equation 6.9 to kinetic data for the reaction of iodide with MCPBA in 0.35 M Na_2SO_4.

T/°C	k_{obs}	$k_{1obs} / 10^3$	$k_{2obs} / 10^3$	K_P	K_I	K_{ClO4}	K_{SO4}	K_{TS1}	K_{TS2}
15	5.3	13	88	603	19	62	-0.54	2545	6.5
20	6.8	13	54	481	12	38	-0.65	1896	4.2
25	8.4	14	61	411	10.9	28	-0.6	1677	4.3
30	10.8	14	51	320	8.4	30	-0.66	1265	3.8
35	13.1	13	12	250	5.1	17	-0.65	1023	0.9

Table 6.4: Best fit parameters obtained from fitting Equation 6.9 to kinetic data for the reaction of iodide with MCPBA in 0.2 M $NaClO_4$.

T/°C	k_{obs}	$k_{1obs} / 10^3$	$k_{2obs}/10^4$	K_P	K_I	K_{ClO4}	K_{SO4}	K_{TS1}	K_{TS2}
15	5.1	16	42	603	19	62	-0.54	3086	27
20	6.5	13	38	481	12	38	-0.65	2059	28
25	8	12	38	411	10.9	28	-0.6	1544	31
30	10.3	15	2	320	8.4	30	-0.66	1427	1.6
35	12.9	12	16	250	5.1	17	-0.65	920	14

6.4. Discussion

6.4.1. Binding of perchlorate to α- CD and its influence on the observed rate constant

Figure 6.6 shows the observed rate constant versus ClO_4 concentrations in the absence and presence of fixed concentrations of 0.007 and 0.02 M α-CD at 25 °C. It can be seen that the rate observed decreases with an increase in perchlorate concentration in the presence of cyclodextrin; however, no effect on the rate is observed in the absence of CD.

The reason behind this decrease is that the ClO_4^- ions compete for the cyclodextrin binding sites, significantly reducing the free cyclodextrin concentration that is available to complex with the iodide and MCPBA. Nevertheless, this competitive binding is taken into account during the curve fitting by the use of the bisection method to calculate the free cyclodextrin, and the inclusion of binding constants for perchlorate and sulfate as fitting parameters. Our results gave a value of 28 M^{-1} for K_{ClO4} which is close to the literature value of 28.9 M^{-1} [195]. The good agreement of K_{ClO4} value with literature confirms the validity of the fitting.

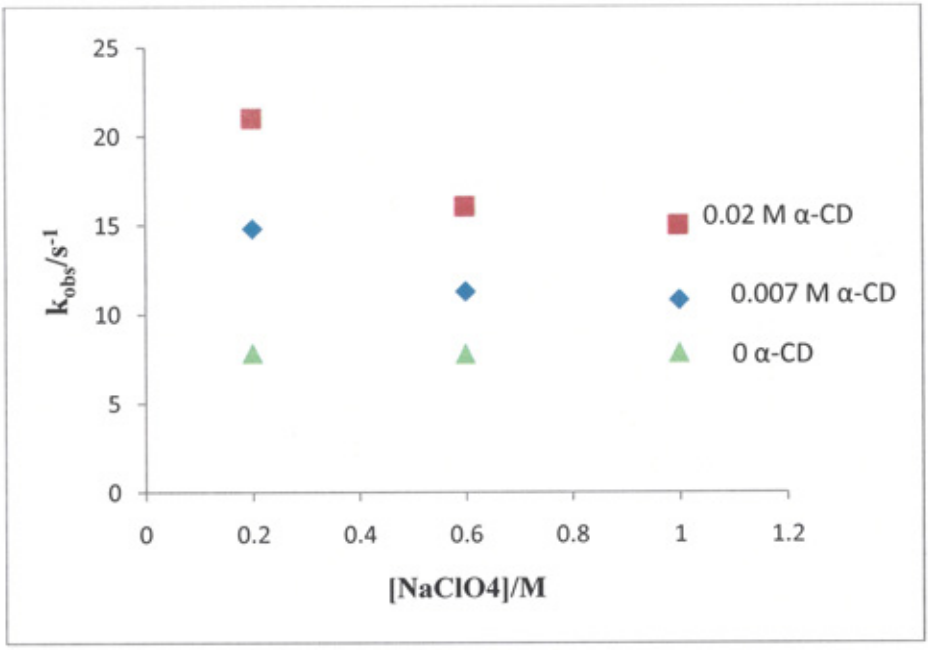

Figure 6.6: Observed rate constant versus perchlorate concentration for the reaction of 0.0015 M iodide with 5×10^{-6} M at 25°C. Other conditions are shown on the figure.

6.4.2. Effect of temperature on binding of substrate to α-cyclodextrin

Literature values for the binding constants of both MCPBA (439 M^{-1})[163] and iodide (12.4 M^{-1})[195] have been reported at 25°C. The values obtained in this present study at the same temperature are very similar (411 and 10.9 M^{-1} for K_{MCPBA} and K_I respectively), which suggests that the approach we have taken to fitting the data, as described in section 6.3.2 is valid.

Turning to the relationship between the value of the binding constants and temperature, it can be seen from Table 6.3 that stability constants for both iodide and MCPBA decrease as temperature increases. Figure 6.7 shows a plot of the logarithm of binding of both substrates versus inverse temperature. In addition, the association constant of perchlorate ions with α-cyclodextrin decreases with an increase in temperature, as shown by the Van't Hoff plot in Figure 6.8; while for the sulfate ions negative values of binding constant close to zero are obtained, which is in agreement with values found in literature [195]. These small values may be due to the large amount of desolvation energy needed to desolvate ions highly charged as SO_4^{-2}.

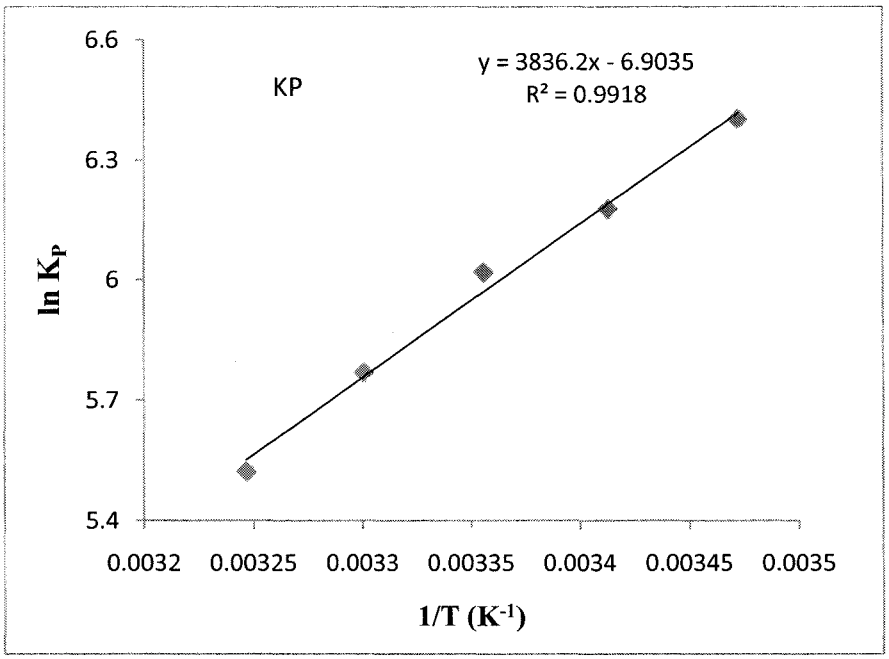

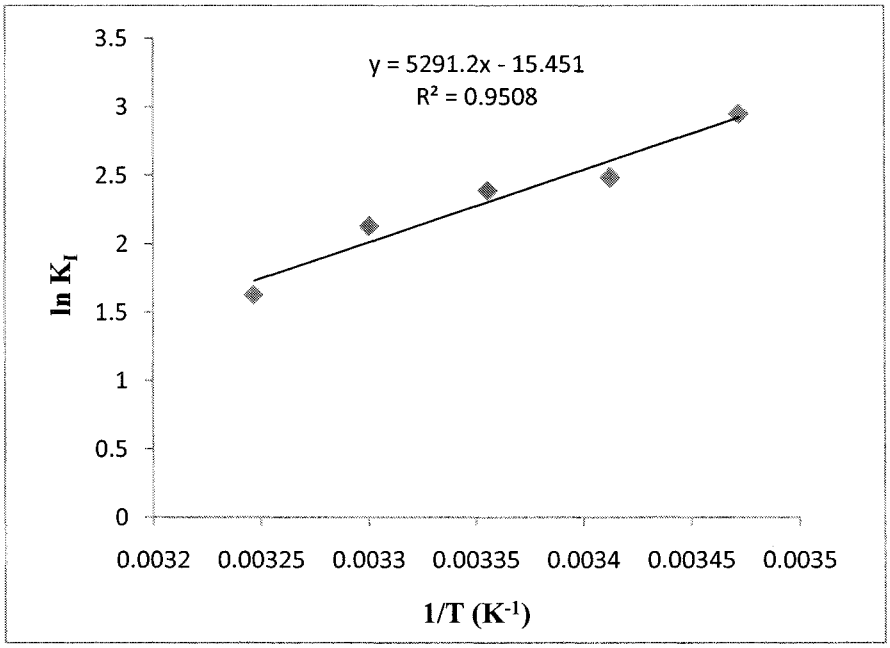

Figure 6.7: plot of the logarithm of binding of both substrates versus inverse temperature for the reaction of *ca.* 5 x 10^{-6} M MCPBA with 1.5 x 10^{-3} M potassium iodide in 3.0 x 10^{-3} M nitric acid, 0.35 M Na_2SO4, 1M $NaClO_4$, and 0.2 M $NaClO_4$ at different temperatures.

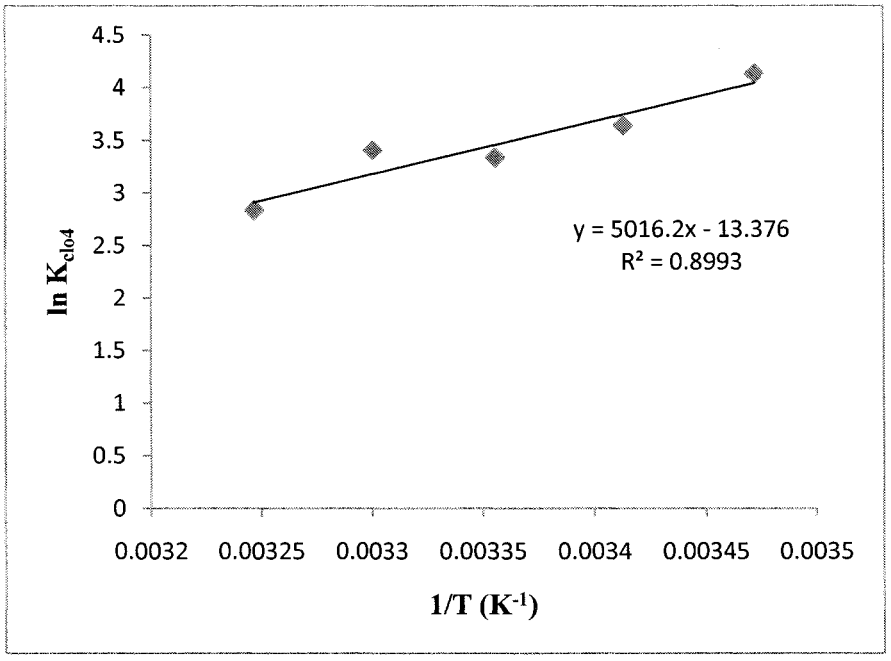

Figure 6.8: Natural logarithm of perchlorate association constant versus 1/T for the reaction of 0.0015 M iodide with 5×10^{-6} M^{-1} MCPBA.

6.4.3. Thermodynamic parameters and enthalpy–entropy compensation

Standard thermodynamic parameters for the encapsulation of MCPBA and iodide, as well as the transition state to the α-cyclodextrin, were calculated from the slope and intercept of the Van't Hoff plot. From this plot the enthalpy and entropy of binding for MCPBA are -31.9 kJ/ mol and -57 J/ mol K respectively, and for the iodide are -44 kJ / mol and -128 J / mol K respectively. From these values it can be seen that the binding of iodide is more enthalpy driven than peracid. Figure 6.9 shows the natural association constant of transition state K_{TS1} versus 1/T. From this slope and intercept the thermodynamic parameters for the transition state binding were calculated. Table 6.5 lists the parameters for the transition state binding constant in the various conditions studied. The trend observed in the thermodynamic parameters for the investigated system is unlikely to be controlled by a hydrophobic effect because of the negative values for entropy of binding. Also, the inclusion is not driven by desolvation, as this process is entropically favourable as a result of the release of more solvent molecules in bulk solvent. Also, the enthalpy is unfavourable as more bonds break; but negative values are observed for many processes involved in the complexation with cyclodextrin and this has been shown to be controlled by non-covalent weak interactions, including van der Waals interaction and dipole-dipole interaction.

Table 6.5 shows that the free energy change ΔG^{o} are quite comparable for all conditions, indicating that the binding process is spontaneous. However, the enthalpy and entropy of substrates binding can provide significant information about the physical force behind the interaction. From these values it can be seen that as the complexation process becomes more driven by enthalpy there is more loss in the entropy which is why good linear relationships occur between ΔH^{o} and ΔS^{o} for complexation of the transition state in different conditions, as shown in Figure 6.10a. Binding of the transition state is more enthalpy driven in the presence of perchlorate, especially at 1 M.

Graph 6.10a shows enthalpy versus entropy for the binding of the transition state with a slope that has a unit of temperature called the compensation temperature; a value of 314±9.6 K is obtained. At this temperature any change in the enthalpy for a similar reaction in a different condition is balanced by compensating the change in entropy which makes the total free energy ΔG^{o} of binding remain constant, as can be seen in Table 6.5. Figure 6.10b shows a plot of ln k at 35°C versus ln k at 25°C for the binding constant of the transition state from which the isokinetic temperature is 342 ± 0.12 K, which is quite different from that calculated from plot 6.10a. The different values of T_{iso} obtained by the two methods used may be a result of the differences between these plots. Also, the isokinetic relationships are not the same as the compensation effects: the former is observed using kinetic data while the latter is obtained from equilibria. This can also be due to the calculations used for both methods; in plot 6.10b the values used are those obtained directly from the experiments, while for plot 6.10a the parameters used are those obtained from fitting the kinetic data to an appropriate equation. The binding constant results are also plotted using the Van't Hoff method, which is used to calculate the thermodynamic parameters. So, the parameters in Figure 6.10a are not obtained directly from the experiment. However, lewis and co-workers [196] have calculated the thermodynamic parameters for the perchlotate-α-cyclodextrin complex using calorimetric titration, values of -41.6 kJ/ mol and -97 J/ mol K for the enthalpy and entropy change was obtained for perchlorate inclusion, which are similar to those obtained in this study see Table 6.5.

Table 6.5: Thermodynamic parameters for the association constant of transition state for the reaction of MCPBA with iodide in different conditions.

Parameters	Nitric acid	0.35 M, Na_2SO_4	1 M, $NaClO_4$	0.2 M, $NaClO_4$
$\Delta H^o(K_{TS1})$, kJ mol^{-1}	-34.7 ± 1.2	-32.9 ± 9.5	-47.6 ± 1.9	-41±6.9
$\Delta S^o(K_{TS1})$, J mol^{-1} K^{-1}	-55 ± 4.4	-49 ± 6.5	-95.4 ± 31	-76.5±23
$\Delta G^o(k_{TS1})$, kJ mol^{-1}	-18.3 ±4.5	-18.2 ± 11	-19 ± 31	-18.2±24
$\Delta H^o(K_{ClO4})$, kJ mol^{-1}	-41.7 ± 8			
$\Delta S^o(K_{ClO4})$, J mol^{-1} K^{-1}	-111± 27			
$\Delta G^o(K_{ClO4})$, kJ mol^{-1}	-8.6±28			
$\Delta H^{o\ (MC\ BAP)}$, kJ mol^{-1}	-31.9± 1.4			
$\Delta S^{o\ (MC\ BAP)}$, J mol^{-1}	-57±4.6			
$\Delta H^{o\ (I)}$, kJ mol^{-1}	-44±5.8			
$\Delta S^{o\ (I)}$, J mol^{-1}	-128±19.3			

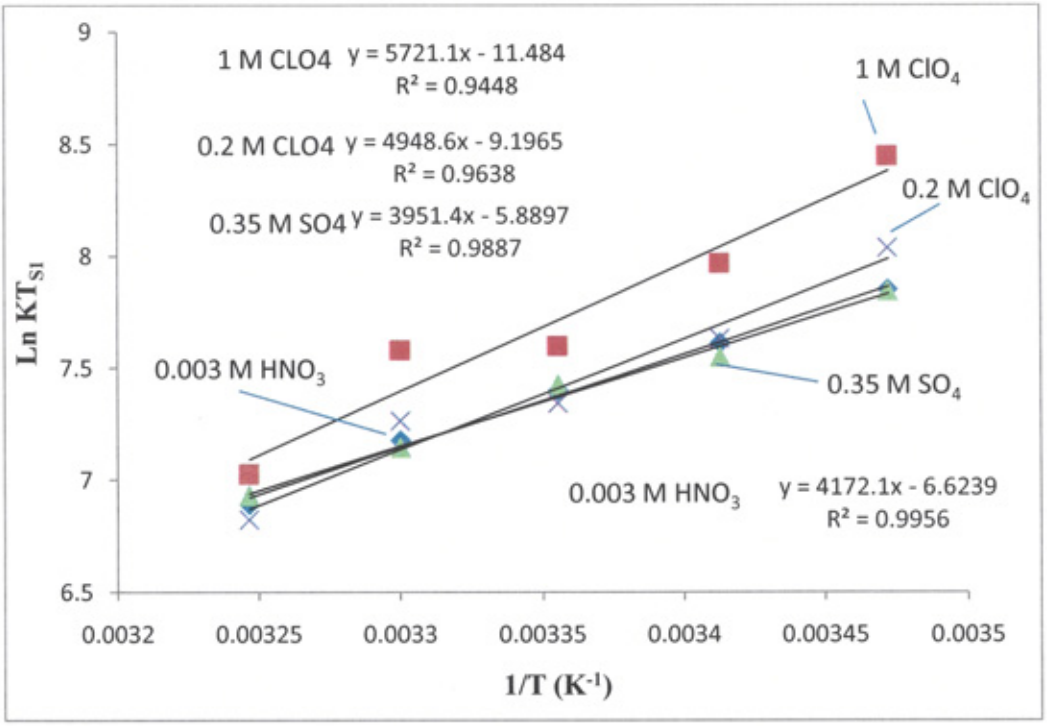

Figure 6.9: Natural logarithm of transition state association constant versus 1/T for the reaction of 0.0015 M iodide with 5×10^{-6} M of MCPBA. The reaction conditions are as follows: filled squares represent 1M ClO_4^-, crosses represent 0.2 M ClO_4^-, filled triangles represent 0.35 M SO_4^-, and diamonds represent reactions without added salt.

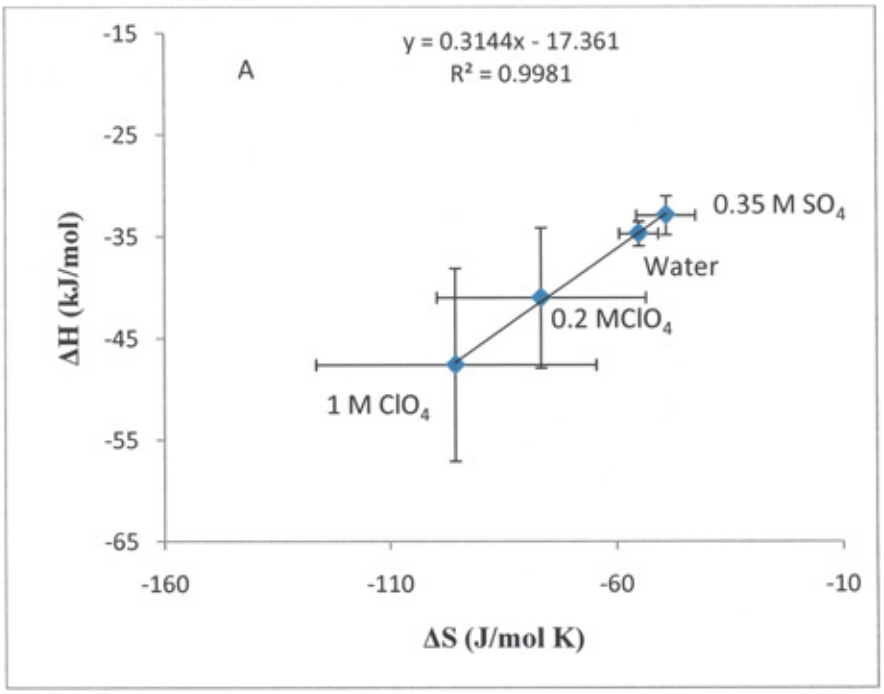

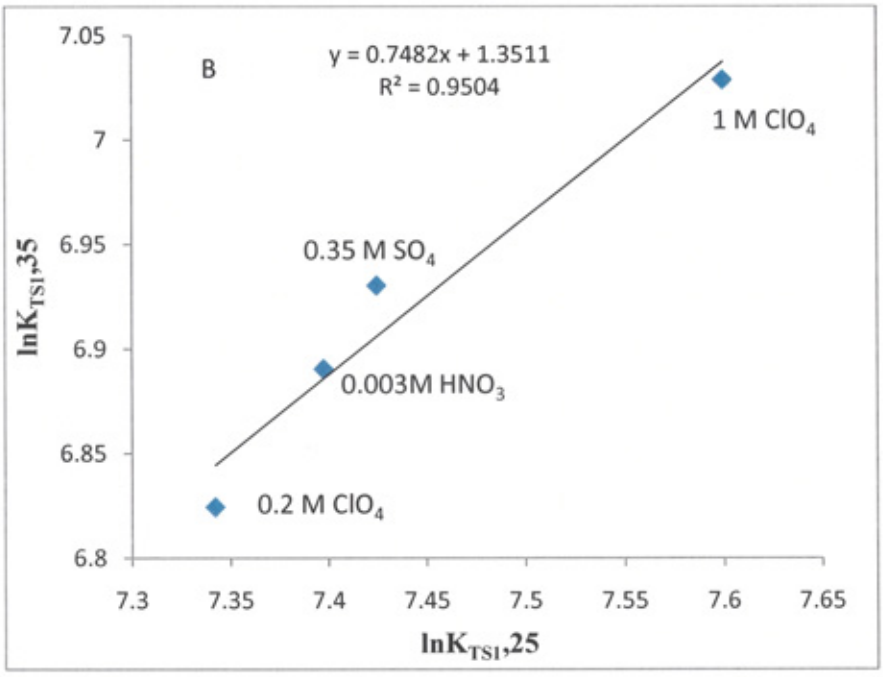

Figure 6.10: (A) Enthalpy entropy compensation plot for the association constants of transition state for the reaction of iodide with MCPBA in different conditions in α-cyclodextrin, (B) is isokinetic plot for the binding constant of transition state for the same condition in (A).

6.4.4. A comparison between the binding of substrate in Brij-35 and α-cyclodextrin

Figures 6.11 and 6.12 below show a compensation plot (for peracid and iodide binding) for the reaction of iodide with peracid in two different catalysts, namely Brij-35 and α-cyclodextrin. From both figures it can be seen that the stability constant of the reactant with cyclodextrin is located in the region of high negative enthalpy and entropy, as opposed to it in Brij-35. So, the complexation process in cyclodextrin is driven by enthalpy, the large negative values of entropy may be due to the restriction imposed on the reactants in the small cavity of cyclodextrin. And the negative enthalpy might result from non-covalent interaction between the substrate and cyclodextrin. Also others factors responsible for these negative values as discussed in [158, 194].

Figure 6.13 shows a compensation plot for the transition state association constant for all the systems studied, i.e. for the reaction of MCPBA with iodide and aryl alkyl sulfides in the presence of α-cyclodextrin and Brij-35 at 25°C. The first thing to state is that these plots are a good way of giving an overview of the relative entropic and enthalpic contributions for different reaction systems. The blue oval superimposed on Figure 6.13 encompasses all of Brij-35 results for the reaction with sulfides (crosses) and iodide (triangles: note that these represent the different conditions, i.e. sulfate, nitric acid and two perchlorate concentrations). It is clear from the figure that the binding process of the transition state to cyclodextrin is enthalpy driven, as opposed to it in Brij-35 for the same reaction.

The second point is to remark on the fact that for these different media and different reactions the values lie on the same line, albeit grouped into different regions depending on whether Brij-35 or α-cyclodextrin is the catalyst. In the previous chapter it was argued on the basis linearity observed for entropy-enthalpy compensation plots for K_{S12} values for sulfide binding to α-cyclodextrin that some information about orientation of substrates within the cyclodextrin cavity could be ascertained, i.e. that the sulfide group always protruded from the cyclodextrin cavity. This inference was based on Guo and co-workers interpretation of these types of plots whereby compensation is due to reorganisation of the water molecules; effectively the water molecules are acting as 'probes'[171]. For the results shown in Figure 6.13 it is more difficult to attempt this type of interpretation; i.e to evaluate what the linear relationship means in terms of similarity of the transition states, both between the two different reactions and the two different catalysts. Whilst at one level all of the transition states involve a bound peracid

(MCPBA bound into either the cyclodextrin or the micelle), at another level there are major differences in the transition states: for example in the α-cyclodextrin system the substrate (iodide or sulfide) is located in the bulk solvent in the transition state, as discussed in Chapter 5, whereas in the Brij-35 system *both* reactants are located within the micelle. This should have major implications for the way in which solvent molecules reorganise.

Perhaps a more intuitive approach to comparing similarities between transition states between the α-cyclodextrin and Brij-35 systems is to correlate the K_{TS1} values obtained for sulfides and iodide in each system. This plot is shown in Figure 6.14 together with a line with a slope of unity; points on or close to the line indicate similar degrees of transition state stabilisation for the same reaction carried out in the two systems, perhaps also indicating similar mechanisms of catalysis. The first point to make is that the sulfides form a horizontal distribution that straddles the line. This is because, as shown by Davies and Deary[162], the extent of transition state stabilisation by α-cyclodextrin is due to the nature of the peracid and is independent of the sulfide; i.e. it is the bound peracid that is the catalytic species. Clearly in Brij-35, there is variable transition state stabilisation that is dependent, to some extent, on the nature of the sulfide; this should not be unexpected since in Brij the sulfide is bound to the micelle in addition to the peracid, and we might expect the position and extent of binding to be dependent on structure. Nevertheless, for three of the sulfides (4-CH_3, 4-CH_3O and 4-NO_2), there is good correlation between K_{TS1} values and it is tempting to suppose overall that the mechanism of catalysis is similar in both systems; perhaps with the peracid in both resembling the structure shown in Structure 5.3.

For the reaction of iodide with peracid under different experimental conditions (the point next to the line is in the presence of 0.35M sulfate) , the degree of transition state stabilisation is independent of salt type or concentration in α-cyclodextrin, but clearly shows a great deal of variability in Brij-35. There is less evidence of a commonality between catalytic mechanisms in the two systems for this reaction.

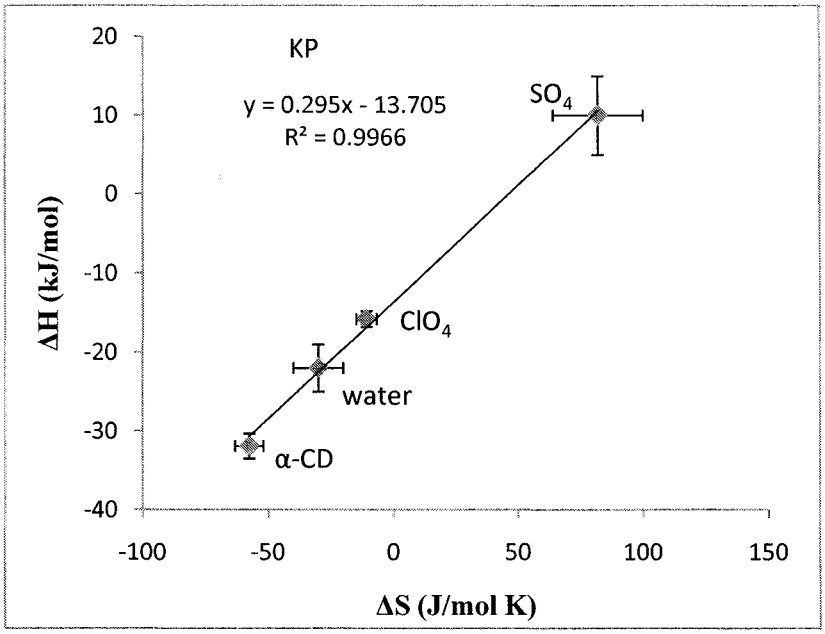

Figure 6.11: Compensation plot for the binding of MCPBA to Brij-35 and α-CD.

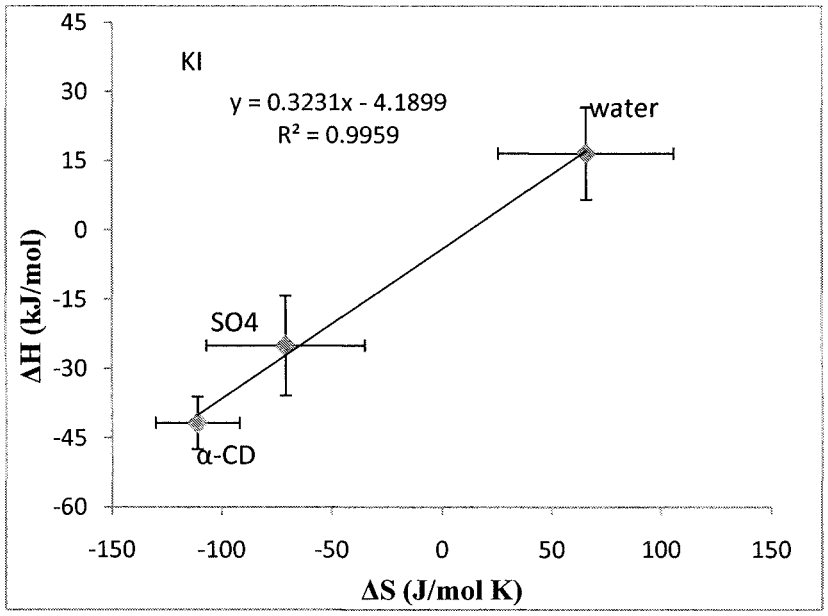

Figure 6.12: Compensation plot for the binding of iodide to Brij-35 and α-CD.

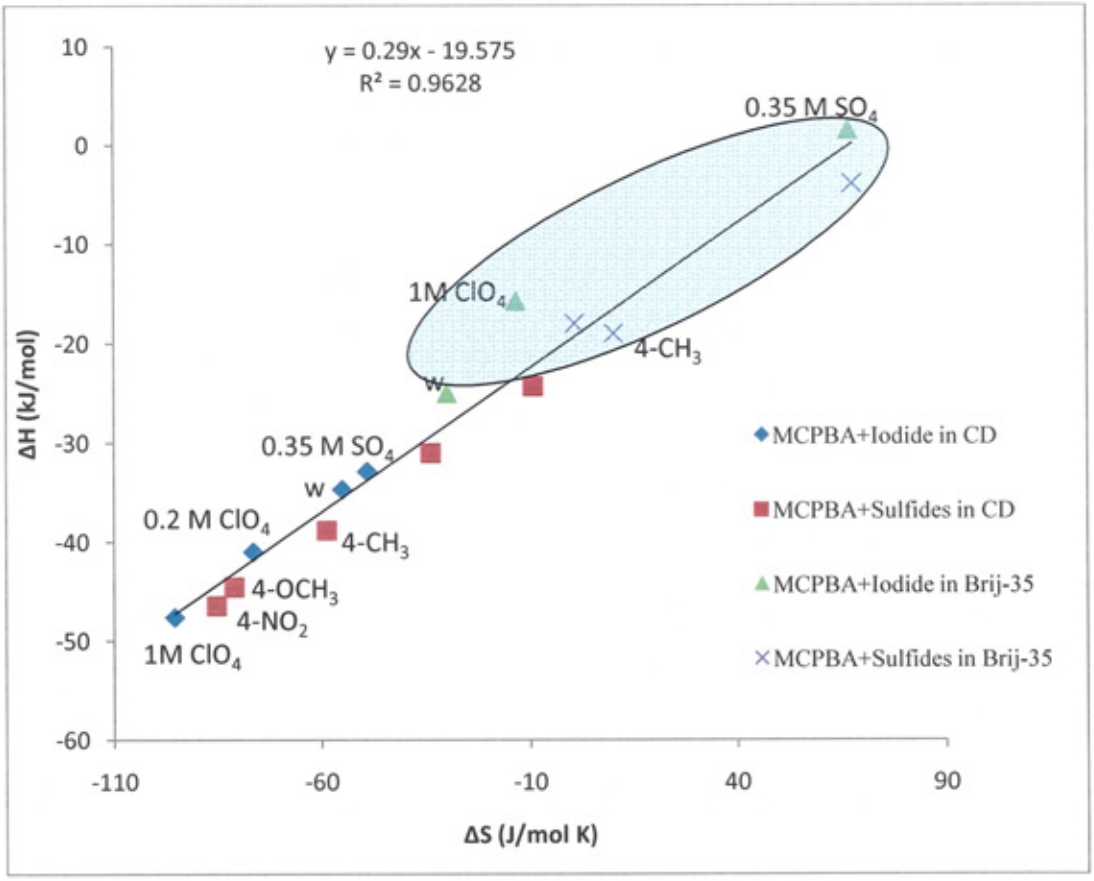

Figure 6.13: Enthalpy-entropy plot for the transition state for an oxidation of iodide reaction by MCPBA in Brij-35 (triangles). The squares and crosses represent sulfide oxidation in α-cyclodextrin and Brij-35 respectively, and the circles represent oxidation of iodide by MCPBA in α-cyclodextrin.

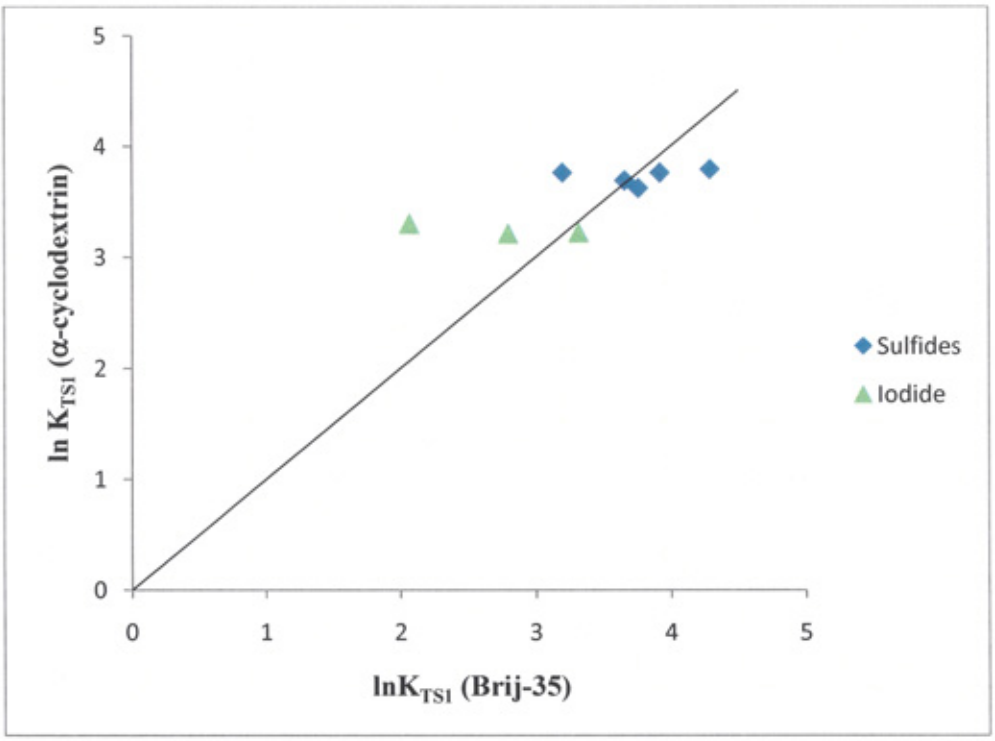

Figure 6.14: Correlation plot between the association constant of transition state for the reduction of MCPBA by iodide and sulfides in Brij-35 and α-cyclodextrin.

Chapter 7 Conclusions and recommendations

7.1 Main findings

The critical micelle concentration (CMC) was determined kinetically under several different conditions. Increasing the temperature was found to cause a decrease in the CMC for the MCPBA-iodide reaction; an increase in the sulfate concentration was also found to decrease the CMC, though the presence of perchlorate has limited affect on the CMC. The value of CMC for the peracid-sulfides reaction is lower than that for iodide-MCPBA even the temperature has no effect on the CMC for the former case.

The oxidation of iodide by MCPBA was shown to be catalysed by the non-ionic micelles studied; the surfactant concentration-rate profile shows an increase in the rate to maximum and then a subsequent levelling off with further increases in surfactant concentration. The association constant of iodide (K_I) and peracid (K_P) in a solution of a non-ionic surfactant strongly depends on the structure of the non-ionic surfactant. The lowest values of K_P and K_I were observed for $C_{12}E_{10}$ surfactants, with the highest values obtained for $C_{18}E_{100}$. Brij 700 has a large K_P and it achieves maximal catalytic efficiency at a low substrate concentration followed by Brij 58, with the large K_P suggesting that the substrate is held. On the other hand, the lower chain length non-ionics, Brij 35 and $C_{12}E_{10}$, have small K_P which means that the substrate is held weakly to these surfactants (low affinity); the rate, therefore, reaches a plateau at high Brij concentrations.

The surfactant (Brij-35) concentration-rate profile for the reaction of iodide with peracid in the absence and presence of 0.35 M sulfate shows an increase in the rate to maximum and then a levelling off with increasing the surfactant concentrations, the rate is enhanced by adding the sulfate compared to that in the absence of salt. In presence of 1 M perchlorate the rate is decreased and this inhibitory effect increases with increasing surfactant concentration. The kinetic data was fitted universally and treated on the basis of multi micelle pseudo phase model.

For the same Brij-35 system, the binding constant of MCPBA is increased by increasing the sulfate concentration, but decreased in the presence of perchlorate. The binding constant of iodide in the absence of salt, $4\pm1\ M^{-1}$ is comparable to the reported literature value of $3.6\pm2\ M^{-1}$ [101] even though the latter was obtained in acetate buffer at pH= 4.8.

Negative values of K_I were obtained in the presence of perchlorate; it was not possible to estimate the association enthalpy and entropy in these cases.

The effect of temperature on the oxidation of iodide by MCPBA at different Brij-35 concentrations has not been studied before, therefore reaction at various temperatures was conducted and the kinetic data obtained treated by multi micelle model and the parameters obtained from this model used to investigate the compensation phenomena, by utilising Erying and vant' Hoff plots to calculate the thermodynamic parameters. The enthalpy-entropy plot for this reaction showed a good correlation, also the Exner[142] method showed that an isokinetic relationship also exists.

The values of $\Delta H^{\ddagger}(k_{obs})$ for the reaction of MCPBA with iodide at the three conditions presented in Table 3.10 shows that these values (in the absence of non-ionic surfactants) are much higher than those of $\Delta H^{\ddagger}(k_{mic} - k_w \overline{V}_{mic})$ for the reaction in 1 M perchlorate and in the aqueous system in the presence of non-ionic surfactants. Moreover, the entropy of activation is more negative compared to the reaction in the aqueous phase. On the other hand the reaction in the presence of sulfate showed the opposite trend, with the enthalpy of activation showing a slight increase in the presence of the non-ionic Brij-35 compared to its absence; the entropy of activation decreased by half in the presence of micelles. From these results it can be inferred that the factor governing the catalysis is not the decrease in the activation energy, but the entropy factor and that the concentration effect is possibly the reason for the catalysis.

In addition to iodide, the oxidations of nine alkyl aryl sulfides by peracids in 0.003 M nitric acid were studied. Those sulfides containing electron-releasing groups in the benzene ring accelerate the rate while those with electron-attracting groups retard the rate. A good correlation is found to exist between log k_{obs} and the Hammett sigma constants for both peracids. An excellent correlation was also obtained between log k_{obs} of peroxymonosulfate and log k_{obs} of MCPBA for the oxidation of all sulfides. It was also found that the oxidation is susceptible to steric congestion at the reaction centre (sulfur atom) as shown for three sulfides having chloro atom at meta, para and ortho position relative to reaction centre.

The oxidation of sulfides by peracid in the presence of Brij-35 at various temperatures has not previously been reported. For MCPBA the reaction with sulfides exhibits initial catalysis at low brij-35 concentration and then there is decline with increasing the brij-35

concentration, while reaction of peroxymonosulfate with sulfides is inhibited in presence of micelles due to separation of reactants, this peracid is charged and so will preferentially partition into the aqueous phase due to high energy of desolvation.

The oxidation of sulfides by peracid was also investigated in α-cyclodextrin at various temperatures, allowing binding and kinetic parameters to be determined and thus allowing a comparison to be made with the same parameters in Brij-35; there are similarities between the Brij micelle and cyclodextrin, i.e. that both have hydrophobic interiors and hydrophilic exteriors. Thermodynamic parameters for the binding of sulfides to Brij-35 and α-cyclodextrin are depicted in Figure 7.1. The results demonstrate that the values of ΔH^{o} for peracid binding to micelles are less negative than peracid complex formations with α-cyclodextrin which are more negative, indicating strong interaction between the peracid and α-cyclodextrin; the entropy of binding of MCPBA is highly negative as a result of the restriction imposed on the reactant in the small cavity of α-cyclodextrin compared to those obtained for the binding to micelle, where the entropies that are high and positive in presence of sodium sulfate, less negative in sodium perchlorate and quite negative in absence of salt; the gain in entropy for the binding of peracid in micelle suggests that the system is less ordered and this could be due to the dynamic nature of micelle as stated in Chapter 1. In addition, this positive value of ΔS^{o} especially in presence SO_4 is the consequence of a disruption of the hydrophobically structured water molecules around the substrate and surfactant molecules as this ion is a strong dehydrating agent; the positive ΔS^{o} value seen here indicates that hydrophobic interactions play the main role for the substrate interactions in the presence of a non-ionic surfactant, and that these interactions are much less important in complex formation. This result can be more visually observed in Figure 7.2 which shows the enthalpy entropy compensation plot for binding of MCPBA in all the studied systems. This example of an enthalpy-entropy compensation plot also illustrates the usefulness of this type of plot in visualising relative enthalpic and entropic contributions for different reaction systems.

Figure 7.3 show a further compensation plot for the reaction of iodide with MCPBA at various conditions and it is clear that the binding is enthalpy driven in the presence of α-cyclodextrin compared to that in micelles. It should be stressed that by using the Van't Hoff and Erying equations, the values of ΔH and ΔS were determined indirectly, which could have lead to some experiment error. But regardless of this, the results presented here reveal that altering the reaction condition (for the same reaction) either by change in

the solvent as in chapter 3 and 6 or altering one of the substrate (aryl alkyl sulfides) as in chapter 4 and 5 significantly influenced the thermodynamic values and result in the compensation effect.

Finally, it was found that there was a very good linear relationship between entropy and enthalpy for 1:2 binding constants for sulfides with α-cyclodextrin, though not for the 1:1 complexes. It was proposed that this was good evidence for aryl alkyl sulfides taking up an orientation within the cyclodextrin cavity where the methyl sulfide group always protrudes from the wide end of the cyclodextrin cavity; formation of 1:2 complexes thus involves very similar reactants.

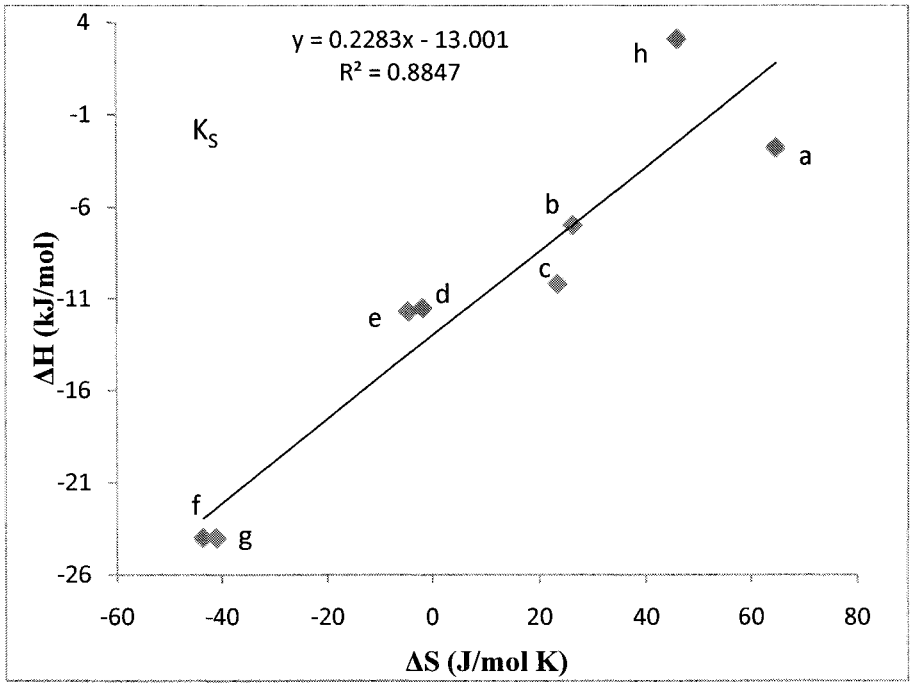

Figure.7.1 enthaply-entropy plot for the binding of sulfides to (a) 4-Br to α-CD, (b) 4-CH_3 in Brij, (c) 4-Br in Brij-35, (d) 4-CH_2OH in Brij-35, (e) 4-CH_2OH in α-CD, (F) 4-CH_3 in α-CD, (g) 4-NO_3 in α-CD and (h) 4-OCH_3 in α-CD

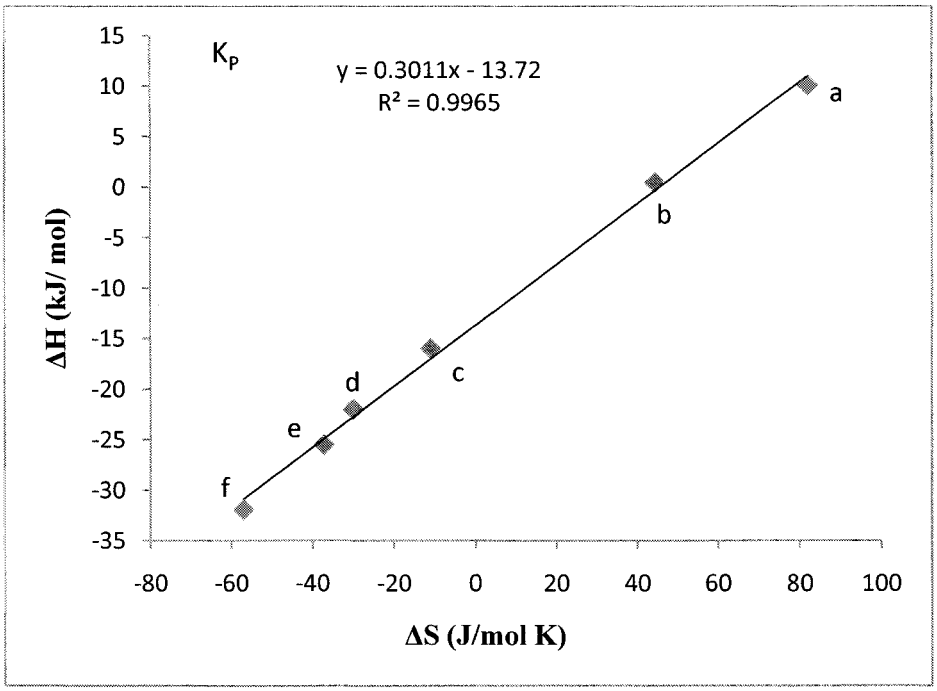

Figure 7.2 enthalpy entropy compensation plot for the binding constant of MCPBA to Brij-35 and α-cyclodextrin at various conditions, the data point represent (a) for reaction of MCPBA with iodide in brij-35 in 0.35 M Na_2SO_4, (b) reaction of MCPBA with sulfides in brij-35, (c) for reaction of MCPBA with iodide in brij-35 in 1 M $NaClO_4$, (d) for reaction of MCPBA with iodide in brij-35 and no added salt, (e) reaction of MCPBA with sulfides in α-cyclodextrin and (f) for reaction of MCPBA with iodide in a α-cyclodextrin

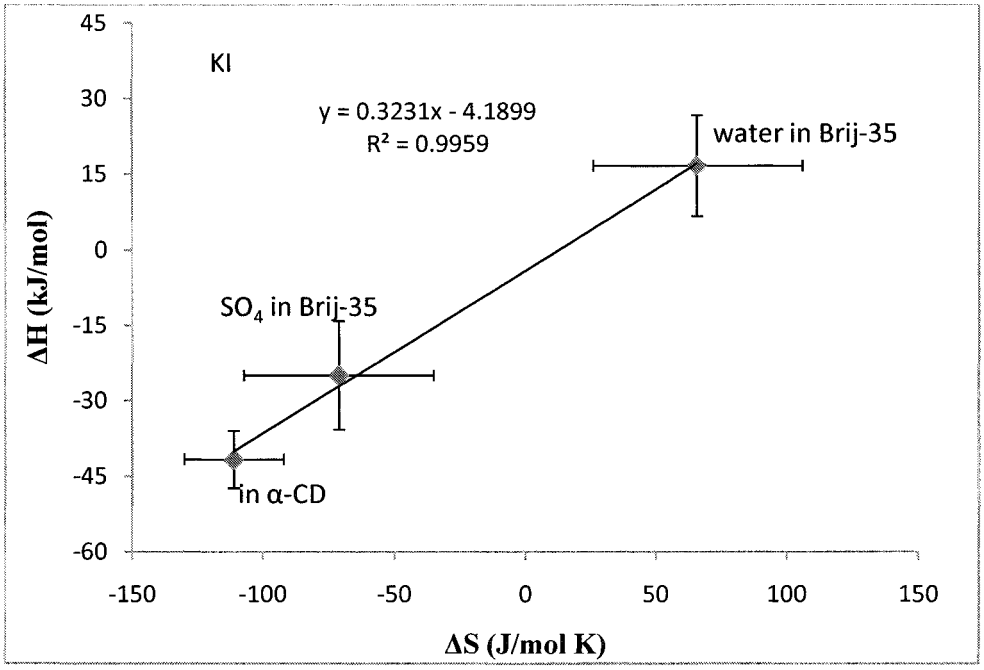

Figure 7.3 compensation plot for the binding of iodide to Brij-35 and α-CD for the reaction of iodide with MCPBA.

7.2 Recommendations for future work.

The present study shows the existence of isokinetic relationships for a series of related reaction; these related reactions being defined either by structural differences (e.g. aryl alkyl sulfides) or different reactions conditions (e.g. the peracid-iodide reaction in the presence of different salts). In most of the cases looked at in this work the presence of isokinetic or compensation effect is present which might suggest that the reaction follows the same mechanism, though no sound interpretation has been provided in this work, particularly for the transition state stabilisation correlations. There is a requirement, therefore to further investigate these relationships, perhaps looking at other reactants and other system of micelles, for example anionic and cationic ones.

In addition, the thermodynamic parameters should be obtained independently using calorimetery which should give reliable values. Exner[140] has shown that if ΔH is obtained from calorimetry measurements and ΔG from equilibrium measurement then the correct relationship can be proven from a plot of ΔH versus ΔG as they are not intercorrelated; for our study all the data came from one experimental study. For future work when investigating isokinetic relationships the thermodynamic parameters should, therefore, be derived independently from different experiment and not calculated from same data set.

In the case of the MCPBA-iodide reaction the binding of iodide was very small and could not be detected unless high concentrations of the micelle were used which was not possible for the studied surfactants as they become cloudy at high concentration, rendering the kinetics difficult; therefore a better nucleophile which bind strongly to micelle should be used or non-ionic surfactants with high solubility. In this latter respect the study did use Pluronic104 but as described the iodine formed as a result of reaction with MCPBA was very quickly consumed by a side reaction and the observed rate could not be determined. Further studies should be carried out to try and elucidate the nature of the contaminant responsible for the side reaction, with the aim of removing this problem, thus allowing the rates to be determined.

Finally, in order to further explore whether entropy-entropy compensation plots can be used as probes of molecular structure and organisation, as suggested by us for α-cyclodextrin complexes of aryl-alkyl sulfides, a similar thermodynamic binding study could be carried out using a different series of aromatic substrates.

References

1. K. Yamaguchi., K. Takada., Y. Otsuji. and k. Mizuno. in *Organic peroxide*, ed. W. Ando, John Wiley & Sons, New York., 1992, vol. 1, pp. 2-97.
2. R. Curci and J. O. Edwards, in *Organic peroxides*, ed. D. Swern, Wiley interscience New York, 1970, vol. 1, pp. 199-264.
3. J. S. Levitt, A. L. N'Guessan, K. L. Rapp and M. C. Nyman, *Water Res*, 2003, **37**, 3016-3022.
4. A. L. N'Guessan., N. Alderman., K. O'Connor., A. Z. A. Rahim. and M. C. Nyman., *Int. J. Environ. Waste Manage.* , 2006, **1**, 61-74.
5. Y. Sawaki, in *Organic peroxide,* ed. W. Ando, John Wiley, Chichester, 1992, vol. 1, pp. 425-477.
6. A. G. Davies, *Organic peroxides*, Butterworths, London, 1961.
7. C. W. Jones, *Applications of hydrogen peroxide and derivatives*, Royal Society of Chemistry, Cambridge, 1999.
8. W. D. Emmons. and A. S. Pagano, *J. Am. Chem. Soc.* , 1955, **77**, 89-92.
9. D. M. Davies and M. E. Deary, *Journal of the Chemical Society-Perkin Transactions 2*, 1991, 1549-1552.
10. W. H. T. Davidson, *J. Chem. Soc*, 1931, **9**, 4256-4261.
11. D. Swern, L. P. Witnauer, C. R. Eddy and W. E. Parker, *J. Am. Chem. Soc.* , 1955, **77**, 5537-5541.
12. P. A. Giguere. and A. W. Omles, *Can. J. Chem*, 1952, **30**, 821-830.
13. J. R. Rittenhouse, W. Lobunez, D. Swern and J. G. Miller, *J. Am. Chem. Soc.* , 1958, **80**, 4850-4852.
14. K. B. Wiberg., *J. Am. Chem. Soc*, 1955, **77**, 2519-2522.
15. N. A. Porter, in *organic peroxide* ed. W. Ando, john wiley, New York, Editon edn., 1992, p. 101.
16. C. A. Bunton., in *Peroxide reaction Mechanism*, ed. J. O. Edward, interscience, New York, 1962, p. 73.
17. F. Secco and Venturin.M, *J. Chem. Soc., Perkin Trans. 2* 1972, 2305-2308.
18. A. P. James, R. A. W. Johnstone, M. McCarron, J. P. Sankey and B. Trenbirth, *Chem. Commun.* , 1998, 429-430.
19. C. L. Hill and C. M. Prossermccartha, *Coord. Chem. Rev.*, 1995, **143**, 407-455.
20. B. Meunier, *Chem. Rev*, 1992, **92**, 1411-1456.
21. S. Yamabe and S. Yamazaki, *J. Org. Chem*, 2007, **72**, 3031-3041.

22. J. F. Goodman., P. Robson. and E. R. Wilson., *Trans. Faraday Soc* 1962, **58**, 1846-1851.
23. P. M. Paradis, Ph.D Thesis, University of Northumbria at Newcastle, 1995.
24. Y. Ogata., K. Tomizawa. and K. Furuta, in *The Chemistry of Peroxides*, ed. S. Patai,Wiley, Chichester, 1983, pp. 710-771.
25. D. L. Heywood., B. Phillips. and H. J. Stansbury, *J. Org. Chem*, 1961, **26**, 281-281.
26. D. Lefort, J. Fossey, M. Gruselle, J. Y. Nedelec and J. Sorba, *Tetrahedron*, 1985, **41**, 4237-4252.
27. D. F. Evans. and M. W. Upton, *J. Chem. Soc., Dalton Trans*, 1985, **6**, 1151-1153.
28. F. Secco, Venturin.M and S. Celsi, *J. Chem. Soc., Perkin Trans. 2* 1972, 497-501.
29. A.Ba-saif., A. K.Luthra. and A.Williams, *J. Am. Chem. Soc*, 1987, **109**, 6362-6368
30. D. Myers, *Surfaces, interfaces, and colloids : principles and applications*, 2nd ed. edn., Wiley-VCH, New York ; Chichester, 1999.
31. I. V. Berezin, K. Martinek and A. k. Yatsimirski, *Russ. Chem. Rew*, 1973, **42**, 787-802.
32. M. J. Rosen, *Surfactants and interfacial phenomena*, 3rd ed. edn., Wiley-Interscience, Hoboken, N.J., 2004.
33. K. J. Tasaki, *J. Am. Chem. Society*, 1996, **118**, 8459-8469.
34. P. Becher., *J. Colloid Sci*, 1961, **16**, 49-56.
35. G. D. J. Phillies, R. H. Hunt, K. Strang and N. Sushkin, *Langmuir*, 1995, **11**, 3408-3416.
36. M. le Maire, P. Champeil and J. V. Møller, *Biochim. Biophys. Acta, Biomembr*, 2000, **1508**, 86-111.
37. C. Tanford, Y. Nozaki and M. F. Rohde, *J. Phys. Chem*, 1977, **81**, 1555-1560.
38. K. S. Sharma, S. R. Patil, A. K. Rakshit, K. Glenn, M. Doiron, R. M. Palepu and P. A. Hassan, *J. Phys. Chem. B*, 2004, **108**, 12804-12812.
39. J. H. Fendler and E. J. Fendler, *Catalysis in micellar and macromolecular systems*, Academic Press, New York, 1975.
40. M. M and K. M, *Bull. Chem. Soc. Jpn.*, 1972, **45**, 428-431.
41. J. Zhao and B. M. Fung, *Langmuir*, 1993, **9**, 1228-1231.
42. D. Myers, *Surfactant science and technology*, 3rd ed. edn., Chichester : Wiley-Interscience, Hoboken, N.J., 2006.

43. C. Tanford, *The hydrophobic effect : formation of micelles and biological membranes*, 2nd ed. edn., Wiley, New York ; Chichester, 1980.
44. J. Clifford and B. A. Pethica, *Trans. Faraday Soc*, 1965, **61**, 182-189.
45. N. T. Southall, K. A. Dill and A. D. J. Haymet, *J. Phys. Chem. B* 2002, **106**, 521-533.
46. V. K. Paruchuri, J. Nalaskowski, D. O. Shah and J. D. Miller, *Colloids Surf., A* 2006, **272**, 157-163.
47. H. H, *Prog. Colloid Polym. Sci*, 1978, **65**, 140-157.
48. B. Simmons, V. Agarwal, G. McPherson, V. John and A. Bose, *Langmuir*, 2002, **18**, 8345-8349.
49. G. W. Zhou, G. Z. Li and W. J. Chen, *Langmuir*, 2002, **18**, 4566-4571.
50. E. Rodenas and E. Perezbenito, *J. Phys. Chem*, 1991, **95**, 4552-4556.
51. B. Lindman. and H. Wennerström., eds., *Topics in Current Chemistry*, Springer-Verlag, Berlin, 1980.
52. P. Debye and E. W. Anacker, *J. Phys. Chem*, 1951, **55**, 644-655.
53. K. J. Mysels, *J. Colloid. Sci*, 1955, **10**, 507-522.
54. M. Benrraou, B. L. Bales and R. Zana, *J. Phys. Chem. B*, 2003, **107**, 13432-13440.
55. J. B. F. N. Engberts, *Pure Appl. Chem*, 1992, **64**, 1653-1660.
56. K. J. Mysels, *Introduction to Colloid Chemistry*, Wiley, New York, 1959.
57. M. N. Islam and T. Kato, *J. Phys. Chem. B*, 2003, **107**, 965-971.
58. N. Pandit, T. Trygstad, S. Croy, M. Bohorquez and C. Koch, *J. Colloid Interface Sci*, 2000, **222**, 213-220.
59. T. M. Doscher, G. E. Myers and D. C. Atkins Jr, *J. Colloid Interface Sci*, 1951, **6**, 223-235.
60. W. N. Maclay, *J. Colloid. Sci*, 1956, **11**, 272-285.
61. H. Schott, *J. Colloid Interface Sci*, 1973, **43**, 150-155.
62. H. Schott, *J. Colloid Interface Sci*, 1995, **173**, 265-277.
63. K. Deguchi and K. Meguro, *J. Colloid Interface Sci*, 1975, **50**, 223-227.
64. F. Tokiwa and T. Matsumoto., *Bull. Chem. Soc. Jpn*, 1975, **48**, 1645-1646.
65. H. Schott and S. K. Han, *J. Pharm. Sci*, 1975, **64**, 658-664.
66. P. U. Kenkare, C. K. Hall and P. K. Kilpatrick, *J. Colloid Interface Sci*, 1996, **184**, 456-468.
67. K. S. Sharma, S. R. Patil and A. K. Rakshit, *Colloids Surf., A* 2003, **219**, 67-74.
68. J. W. McBain, *Trans. Faraday Soc*, 1913, **9**, 99-101.

69. F. M. Menger, *Acc. Chem. Res*, 1979, **12**, 111-117.
70. D. J. Mitchell and B. W. Ninham, *J. Chem. Soc., Faraday Trans. 2*, 1981, **77**, 601-629.
71. J. N. Israelachvili, D. J. Mitchell and B. W. Ninham, *J. Chem. Soc., Faraday Trans. 2*, 1976, **72**, 1525-1568.
72. K. Holmberg, B. Jonsson and B. Lindman, *Surfactants and Polymers in Aqeous Solution*, 2 edn., John Wiley, Chichester, 2003.
73. G. Stainsby and A. E. Alexander, *Trans. Faraday Soc*, 1950, **46**, 587-597.
74. H. Maeda, in *Encyclopedia of Surface and Colloid Science* eds. P. Somasundaran and A. Hubbard, Taylor and Francis, Editon edn., 2006, pp. 6221-6234.
75. M. J. Blandamer, P. M. Cullis, L. G. Soldi, J. B. F. N. Engberts, A. Kacperska, N. M. Vanos and M. C. S. Subha, *Adv. Colloid Interface Sci*, 1995, **58**, 171-209.
76. T. F. Tadros, *Applies Surfactants; Principle and Applications*, Wiley-VCH, Berlin, 2005.
77. R. V. Hanke, W. Knoche and E. Dutkiemiez, *J. Chem. Soc., Perkin Trans. 1*, 1987, **83**, 2847 - 2856.
78. M. Almgren, F. Grieser and J. K. Thomas, *J. Am. Chem. Soc*, 1979, **101**, 279-291.
79. D. J. Jobe., V. C. Reinsborough and P. J. White, *Can. J. Chem*, 1982, **60**, 279-284.
80. M. F. Emerson and A. Holtzer, *J. Phys. Chem.*, 1967, **71**, 3320-3330.
81. C. Hirose and L. Sepulveda, *J. Phys. Chem*, 1981, **85**, 3689-3694.
82. S. J. Rehfeld, *J. Phys. Chem*, 1971, **75**, 3905-3906
83. J. H. Fendler and Patterso.Lk, *J. Phys. Chem*, 1971, **75**, 3907-&.
84. R. Nagarajan, M. A. Chaiko and E. Ruckenstein, *J. Phys. Chem*, 1984, **88**, 2916-2922.
85. K. Kandori, R. J. McGreevy and R. S. Schechter, *J. Phys. Chem*, 1989, **93**, 1506-1510
86. P. Mukerjee., J. R. Cardinal. and N. R. Desai., in *Micellization, solubilization and microemulsions*, ed. K. L. Mittal., Plenum press, New York, 1977, pp. 241-261.
87. P. Mukerjee and J. R. Cardinal, *J. Phys. Chem*, 1978, **82**, 1620-1627.
88. J. A. Marqusee and K. A. Dill, *J. Chem. Phys*, 1986, **85**, 434-444.
89. C. O. Rangel-Yagui, A. Pessoa and L. C. Tavares, *J. Pharm. Pharmacol. Sci*, 2005, **8**, 147-163.
90. S. Riegelman, N. A. Allawala, M. K. Hrenoff and L. A. Strait, *J. Colloid Sci.*, 1958, **13**, 208-217.

91. M. Alauddin and R. E. Verrall, *J. Phys. Chem*, 1984, **88**, 5725-5730.
92. D. W. R. Gruen, *Prog. Colloid Polym. Sci*, 1985, **70**, 6-16.
93. C. A. Bunton and C. P. Cowell, *J. Colloid Interface Sci*, 1988, **122**, 154-162.
94. L. K. Patterson and J. H. Fendler, *J. Phys. Chem*, 1970, **74**, 4608-4609.
95. B. E. Hawrylak and D. G. Marangoni, *Can. J. Chem*, 1999, **77**, 1241-1244.
96. S. Paria and P. K. Yuet, *Ind. Eng. Chem. Res*, 2007, **46**, 108–113.
97. F. M. Menger and C. E. Portnoy, *J. Am. Chem. Soc*, 1967, **89**, 4698-4703.
98. F. Sterpone, C. Pierleoni, G. Briganti and M. Marchi, *Langmuir*, 2004, **20**, 4311-4314.
99. C. A. Bunton, E. J. Fendler and J. H. Fendler, *J. Am. Chem. Soc*, 1967, **89**, 1221-1230.
100. M. N. Khan, in *Encyclopedia of surface and colloid science, Marcel Dekker*, ed. A. Hubbard, Marcel Dekker, new york, Editon edn., 2002, pp. 3178-3191.
101. D. M. Davies, N. D. Gillitt and P. M. Paradis, *J. Chem. Soc., Perkin Trans. 2*, 1996, 659-666.
102. D. M. Davies and S. J. Foggo, *J. Chem. Soc., Perkin Trans. 2*, 1998, 247-251.
103. P. Bauduin, A. Renoncourt, D. Touraud, W. Kunz and B. W. Ninham, *Curr. Opin. Colloid Interface Sci*, 2004, **9**, 43-47.
104. E. Leontidis, *Curr. Opin. Colloid Interface Sci*, 2002, **7**, 81-91.
105. W. P. Jencks, *Catalysis in chemistry and enzymology*, McGraw-Hill, New York ; London, 1969.
106. P. Alexandridis and J. F. Holzwarth, *Langmuir*, 1997, **13**, 6074-6082.
107. W. F. McDevit and F. A. Long, *J. Am. Chem. Soc*, 1952, **74**, 1773-1777.
108. M. S. Baptista and C. D. Tran, *J. Phys. Chem*, 1995, **99**, 12952-12961.
109. S. Ta§cioglu, *Tetrahedron*, 1996, **52**, 11113-11152.
110. Y. Zhang and P. S. Cremer, *Curr. Opin. Chem. Biol*, 2006, **10**, 658-663.
111. C. A. Bunton and G. Cerichelli, *Int. J. Chem. Kinet*, 1980, **12**, 519-533.
112. V. K. Aswal and P. S. Goyal, *Phys. Rev. E: Stat. Phys., Plasmas, Fluids*, 2000, **61**, 2947-2953.
113. L. R. Romsted, R. B. Dunlap and E. H. Cordes, *J. Phys. Chem*, 1967, **71**, 4581-4583.
114. E. H. Cordes, *Reaction kinetics in micelles : proceedings*, Plenum Press, New York ; London, 1973.
115. C. A. Bunton and L. Robinson, *J. Am. Chem. Soc*, 1968, **90**, 5972-5979;(b) C. A. Bunton and L. B. Robinson, *J. Org. Chem*, 1969, **34**, 780-785.

116. L. Y. Zakharova, L. A. Kudryavtseva and A. I. Konovalov, *Mendeleev Commun*, 1998, **8**, 163-165.

117. M. D. Graciani, A. Rodriguez, M. Munoz and M. L. Moya, *React. Kinet. Catal. Lett*, 2002, **76**, 11-18.

118. S. Possidonio, F. Siviero and O. A. El Seoud, *J. Phys. Org. Chem*, 1999, **12**, 325-332.

119. O. A. El Seoud, M. F. Ruasse and S. Possidonio, *J. Phys. Org. Chem.* , 2001, **14**, 526-532.

120. N. C. Sarada and I. A. K. Reddy, *J. Indian Chem. Soc*, 1993, **70**, 35-39.

121. Kabir-ud-Din, M. Akram and Z. Khan, *Inorg. React. Mech*, 2002, **4**, 187-196.

122. C. G. Overberger and R. W. Cummins, *J. Am. Chem. Soc*, 2002, **75**, 4250-4254.

123. R. Bacaloglu, A. Blasko, C. A. Bunton and H. Foroudian, *J. Phys. Org. Chem*, 1992, **5**, 171-178.

124. D. M. Davies, M. E. Deary, K. Quill and R. A. Smith, *Chem. Eur. J*, 2005, **11**, 3552-3558.

125. G. W. Wagner, L. R. Procell, Y. C. Yang and C. A. Bunton, *Langmuir*, 2001, **17**, 4809-4811.

126. Y. C. Yang, F. J. Berg, L. L. Szafraniec, W. T. Beaudry, C. A. Bunton and A. Kumar, *J. Chem. Soc., Perkin Trans. 2* 1997, 607-613.

127. H. R. Yao and D. E. Richardson, *J. Am. Chem. Soc*, 2003, **125**, 6211-6221.

128. N. D. Gillitt, J. Domingos and C. A. Bunton, *J. Phys. Org. Chem*, 2003, **16**, 603-607.

129. C. A. Bunton, *Adv. Colloid Interface Sci*, 2006, **123-126**, 333-343.

130. A. Blasko, C. A. Bunton and S. Wright, *J. Phys. Chem*, 1993, **97**, 5435-5442.

131. G. Cerichelli, C. Grande, L. Luchetti and G. Mancini, *J. Org. Chem*, 1991, **56**, 3025-3030.

132. A. Blasko, C. A. Bunton and H. S. J. Foroudian, *J. Colloid Interface Sci*, 1995, **175**, 122-130.

133. M. Chiarini, N. D. Gillitt and C. A. Bunton, *Langmuir*, 2002, **18**, 3836-3842.

134. J. R. B. Bharathy, T. K. Ganesan, E. Rajkumar, S. Rajagopal, B. Manimaran, T. Rajendran and K. L. Lu, *Tetrahedron*, 2005, **61**, 4679-4687.

135. C. J. Drummond and F. Grieser, *J. Colloid Interface Sci*, 1989, **127**, 281-291.

136. S. Balakumar, P. Thanasekaran, E. Rajkumar, K. J. Adaikalasamy, S. Rajagopal, R. Ramaraj, T. Rajendran, B. Manimaran and K. L. Lu, *Org. Biomol. Chem*, 2006, **4**, 352-358.

137. B. Sankararaj, S. Rajagopal and K. Pitchumani, *Indian J. Chem., Sect A* 1995, **34**, 440-445.

138. A. K. Das, S. K. Mondal, D. Kar and M. Das, *Int. J. Chem. Kinet*, 2001, **33**, 173-181.

139. V. L. Lobachev, T. M. Prokop'eva and V. A. Savelova, *Theor. Exp. Chem*, 2004, **40**, 383-388.

140. O. Exner, *Chem. Commun*, 2000, 1655-1656.

141. O. Exner, *J. Phys. Org. Chem*, 1997, **10**, 797-813.

142. O. Exner, *Nature*, 1970, **227**, 366-367.

143. Z. Karpinski and R. Larsson, *J. Catal*, 1997, **168**, 532-537.

144. L. Liu and Q. X. Guo, *Chem. Rev*, 2001, **101**, 673-695.

145. A. Vailaya and C. Horvath, *J. Phys. Chem*, 1996, **100**, 2447-2455.

146. R. R. Krug, *Ind. Eng. Chem. Fundam*, 1980, **19**, 50-59.

147. T. Rispens and J. B. F. N. Engberts, *J. Org. Chem*, 2003, **68**, 8520-8528.

148. G. Cerichelli, L. Luchetti, G. Mancini, G. Savelli and C. A. Bunton, *J. Colloid Interface Sci*, 1993, **160**, 85-92.

149. V. M. F. Lai, C. Y. Lii, W. L. Hung and T. J. Lu, *Food Chem*, 2000, **68**, 319-325.

150. S. B. Sulthana, S. G. T. Bhat and A. K. Rakshit, *Langmuir*, 1997, **13**, 4562-4568.

151. J. Szejtli, *Chem. Rev*, 1998, **98**, 1743-1753.

152. W. R. Saenger, J. Jacob, K. Gessler, T. Steiner, D. Hoffmann, H. Sanbe, K. Koizumi, S. M. Smith and T. Takaha, *Chem. Rev*, 1998, **98**, 1787-1802.

153. Y. Inoue, T. Hakushi, Y. Liu, L. H. Tong, B. J. Shen and D. S. Jin, *J. Am. Chem. Soc*, 1993, **115**, 475-481.

154. E. Sabadini, T. Cosgrove and F. C. Egidio, *Carbohydr. Res*, 2006, **341**, 270-274.

155. A. Pérez-Garrido, A. M. Helguera, A. A. Guillén, M. N. D. S. Cordeiro and A. G. Escudero, *Bioorg. Med. Chem*, 2009, **17**, 896-904.

156. I. Tabushi, Y. Kiyosuke, T. Sugimoto and K. Yamamura, *J. Am. Chem. Soc*, 1978, **100**, 916-919;(b) I. Tabushi, *Acc. Chem. Res*, 1982, **15**, 66-72.

157. K. A. Connors, *Chem. Rev*, 1997, **97**, 1325-1357.

158. R. Breslow, S. Halfon and B. L. Zhang, *Tetrahedron*, 1995, **51**, 377-388.

159. R. Breslow and S. D. Dong, *Chem. Rev*, 1998, **98**, 1997-2012.

160. K. Takahashi, *Chem. Rev*, 1998, **98**, 2013-2033.

161. L. Liu and Q. X. Guo, *J. Inclusion Phenom.Macrocyclic Chem*, 2002, **42**, 1-14.

162. D. M. Davies and M. E. Deary, *J. Chem. Soc., Perkin Trans. 2* 1996, 2423-2430.

163. D. M. Davies, G. A. Garner and J. R. Savage, *J. Chem. Soc., Perkin Trans. 2* 1994, 1531-1537.
164. D. M. Davies and M. E. Deary, *J. Chem. Soc., Perkin Trans. 2* 1995, 1287-1294.
165. D. M. Davies and J. R. Savage, *J. Chem. Res., Synop* . , 1993, 94-95.
166. Q. X. Guo, S. H. Luo and Y. C. Liu, *J. Inclusion Phenom. Mol. Recognit. Chem*, 1998, **30**, 173-182.
167. M. Gerold and T. Diane, in *Encylopedia of pharmaceutical technology*, eds. J.Swarbrick. and J.C.Boylan., Informa Health Care, Editon edn., 2000, vol. 19, pp. 49-89.
168. G. Dollo, P. LeCorre, F. Chevanne and R. LeVerge, *Int. J. Pharm*, 1996, **136**, 165-174.
169. P. K. Zarzycki and H. Lamparczyk, *J. Pharm. Biomed. Anal*, 1998, **18**, 165-170.
170. P.Gornas., K.Dwiecki., M.Nogala-.Kalucka. and K.Polewski., *Acta.Agrophysica*, 2006, **7**, 73-80.
171. L. Liu, C. Yang and Q. X. Guo, *Bull. Chem. Soc. Jpn*, 2001, **74**, 2311-2314.
172. J. L. Kurz, *J. Am. Chem. Soc*, 2002, **85**, 987-991.
173. E. V. Anslyn and D. A. Dougherty, *Modern physical organic chemistry*, University Science Books, Sausalito, Calif., 2006.
174. O. S. Tee, *Adv. Phys. Org. Chem*, 1994, **29**, 1-85.
175. R. D. Mair and R. T. Hall, in *Organic peroxides*, ed. D. Swern, Wiley Interscience, New York, Editon edn., 1971, vol. 2, pp. 535-637.
176. R. J. Leatherbarrow, Erithacus Software Ltd, Horley, UK, Editon edn., 2007.
177. W. Warisnoicharoen, A. B. Lansley and M. J. Lawrence, *Aaps Pharmsci*, 2000, **2**, 20; (b) A. Berthod, S. Tomer and J. G. Dorsey, *Talanta*, 2001, **55**, 69-83; (c) Y. R. Suradkar and S. S. Bhagwat, *J. Chem. Eng. Data* 2006, **51**, 2026-2031.
178. Sigma-Aldrich Cataloge.
179. G. D'Errico, D. Ciccarelli and O. Ortona, *J. Colloid Interface Sci*, 2005, **286**, 747-754.
180. A. Patist, S. Bhagwat, K. Penfield, P. Aikens and D. Shah, *J. Surfactants Deterg*, 2000, **3**, 53-58.
181. M. N. Khan and Z. Arifin, *Langmuir*, 1996, **12**, 261-268.; M. N. Khan and Z. Arifin, *J. Colloid Interface Sci*, 1996, **180**, 9-14.
182. P. Alexandridis, V. Athanassiou, S. Fukuda and T. A. Hatton, *Langmuir*, 2002, **10**, 2604-2612.

183. S. Miyagishi, K. Okada and T. Asakawa, *J. Colloid Interface Sci*, 2001, **238**, 91-95.
184. A. Ray and G. Nemethy, *J. Am. Chem. Soc*, 1971, **93**, 6787-&.
185. K. Megure, M. Ueno and K. Esumi, in *non-ionic surfactants: physical chemistry (Surfactant science)* ed. M. J. Schick, Marcel Dekker, New York, Editon edn., 1987 p. 133.
186. L. Koshy and A. K. Rakshit, *Bull. Chem. Soc. Jpn*, 1991, **64**, 2610-2612.
187. T. Wenle. and B. Monica., *J. Chem. Soc., Perkin Trans. 2* 1998, 1957-1960;(b) E. Grunwald and C. Steel, *J. Am. Chem. Soc.* , 1995, **117**, 5687-5692
188. C. Hansch, A. Leo and R. W. Taft, *Chem. Rev*, 1991, **91**, 165-195.
189. O. S. Tee and A. A. Fedortchenko, *Can. J. Chem*, 1997, **75**, 1434-1438.
190. O. S. Tee and O. J. Yazbeck, *Can. J. Chem*, 2000, **78**, 1100-1108.
191. M. Sakurai, M. Kitagawa, H. Hoshi, Y. Inoue and R. Chujo, *Carbohydr. Res*, 1990, **198**, 181-191.
192. D. M. Davies and M. E. Deary, *J. Chem. Soc., Perkin Trans. 2* 1996, 2415-2421.
193. K. A. Connors and D. D. Pendergast, *J. Am. Chem. Soc*, 1984, **106**, 7607-7614.
194. M. V. Rekharsky and Y. Inoue, *J. Am. Chem. Soc*, 2002, **124**, 813-826.
195. J. F. Wojcik and R. P. Rohrbach, *J. Phys. Chem*, 1975, **79**, 2251-2253.
196. E. A. Lewis and L. D. Hansen, *J. Chem. Soc., Perkin Trans. 2*, 1973, 2081-2085.

Appendix A

Table A1 Data for the reaction between iodide 1.5×10^{-3} M and *ca.* 4×10^{-6} M MCPBA, in the presence of various concentration of non-ionic surfactants in 0.003 M nitric acid at 25 C^0.

[Brij58]/M	k_{obs}, s^{-1}	$[C_{12}E_{10}]$/M	k_{obs}	[brij700]/M	k_{obs}, s^{-1}
0	8.14±0.01	0	8.24± 0.01	0	8.2±0.01
3×10^{-5}	9.45±0.02	4.06×10^{-5}	8.73±0.019	4.28×10^{-5}	9.5±0.03
6.42×10^{-5}	9.36±0.01	8.1×10^{-5}	9.23±0.02	8.5×10^{-5}	9.6±0.01
1.6×10^{-4}	9.25±0.03	1.21×10^{-4}	9.27±0.02	1.28×10^{-4}	9.7±0.04
2.4×10^{-4}	9.43±0.02	3.04×10^{-4}	9.26±0.03	2.14×10^{-4}	10.1±0.01
3.21×10^{-4}	10.02±0.01	5.08×10^{-4}	9.68±0.01	4.28×10^{-4}	11.3±0.02
5.35×10^{-4}	11.51±0.01	9.1×10^{-4}	10.74±0.01	8.56×10^{-4}	13.8±0.01
1.338×10^{-3}	15.09±0.02	1.52×10^{-3}	12.24±0.01	1.71×10^{-3}	17.2±0.2
2.67×10^{-3}	18.75±0.03	2.309×10^{-3}	14.12±0.01	2.56×10^{-3}	19.7±0.02
5.35×10^{-3}	23.06±0.03	5.6×10^{-3}	17.29±0.02	3.42×10^{-3}	20.8±0.03
1.07×10^{-2}	26.84±0.03	9.2×10^{-3}	20.85±0.03	4.28×10^{-3}	21.9±0.04
1.87×10^{-2}	29.06±0.04	2.3×10^{-2}	23.93±0.05	5.35×10^{-3}	22.5±0.03
2.67×10^{-2}	29.19±0.05	4.6×10^{-2}	24.91±0.03	6.42×10^{-3}	23.5±0.0
4.01×10^{-2}	29.2±0.04	6.46×10^{-2}	25.19±0.03	8.56×10^{-3}	24.3±0.04
4.81×10^{-2}	29.27±0.04	8.3×10^{-2}	25.03±0.04	1×10^{-2}	24.9±0.04
5.88×10^{-2}	29.32±0.06	10.6×10^{-2}	24.79±0.03		

Table A2 Data for the reaction between iodide 1.5×10^{-3} M and *ca.* 4×10^{-6} M MCPBA, at various concentration of brij-35 and constant concentration of sodium sulfate in 0.003 M nitric acid at 25 C^0

[Brij-35]/M	k_{obs},[0.07]	k_{obs}, [0.13]	k_{obs},[0.2]	k_{obs}, [0.25]	k_{obs}, 0.5 M
0	8.7±0.02	8.4±0.05	8.42±0.02	8.277±0.03	8.92±0.09
2×10^{-5}	8.8±0.02	8.57±0.02	8.57±0.02	8.304±0.03	8.99±0.07
4×10^{-5}	8.9±0.02	8.93±0.07	9.107±0.06	8.514±0.03	8.90±0.08
8×10^{-5}	9.4±0.023	9.16±0.04	9.13±0.03	9.531±0.04	10.40±0.05
1.6×10^{-4}	9.49±0.01	9.086±0.01	9.1±0.02	9.779±0.03	12.40±0.07
2.4×10^{-4}	9.5±0.01	9.2±0.05	9.4±0.03	10.61±0.04	14.61±0.04
3.6×10^{-4}	9.8±0.02	9.54±0.03	9.76±0.05	11.47±0.06	15.32±0.04
4.6×10^{-4}	10.3±0.02	10.13±0.07	10.22±0.05	12.54±0.04	16.65±0.07
5.6×10^{-4}	10.8±0.02	11.74±0.08	10.72±0.05	12.68±0.04	18.18±0.08
6.6×10^{-4}	11.2±0.02	12.36±0.03	12.41±0.04	14.48±0.05	19.74±0.06
1.2×10^{-3}	13.6±0.012	15.21±0.09	16.33±0.10	18.62±0.08	26.07±0.12
2.5×10^{-3}	18.9±0.05	20.48±0.05	22.21±0.14	24.98±0.1	35.7±0.28
5×10^{-3}	25.1±0.04	25.65±0.13	28.75±0.13	31.7±0.18	43.96±0.34
1.49×10^{-2}	29.1±0.07	28.54±0.011	35.2±0.11	38.27±0.3	50.17±0.16
1.69×10^{-2}	30.8±0.08	30.76±0.07	36.14±0.13	38.1±0.2	51±0.13
2.31×10^{-2}	30.9±0.06	31.7±0.02	37.3±0.119	39.11±0.2	50.08±0.16
2.7×10^{-2}	31.2±0.09	31.63±0.03	37.1±0.16	38.96±0.3	48.6±0.19
3.3×10^{-2}	31±0.15	31.66±0.07	36.51±0.13	37.41±0.3	48.01±0.18
3.8×10^{-2}	30.3±0.10	31.4±0.09	35.32±0.013	36.49±0.23	48.21±0.11
4.5×10^{-2}	30.4±0.2	30.38±0.28	35.27±0.23	36.22±0.3	45.14±0.22
4.75×10^{-2}	29.8±0.22	29.85±0.16	34.78±0.38	34.66±0.3	44.1±0.23
5×10^{-2}	29.6±0.4	28.94±0.17	34.26±0.4	34.32±0.4	43.89±0.1

Table A2 Continue.

[Brij-35]/M	k_{obs},[0.3]	k_{obs}, [0.35]	k_{obs},[0.4]	k_{obs}, [0.003], $HN0_3$
0	8.74±0.031	8.34±0.03	8.82±0.03	8.43±0.01
2×10^{-5}	8.82±0.05	8.87±0.03	8.89±0.15	8.60±0.02
4×10^{-5}	8.86±0.04	9.10±0.04	9.18±0.08	8.80±0.03
8×10^{-5}	9.51±0.03	9.34±0.03	9.27±0.08	9.10±0.02
1.6×10^{-4}	9.79±0.02	9.60±0.04	10.6±0.05	9.40±0.02
2.4×10^{-4}	11.0±0.02	11.4±0.07	12.4±0.08	9.37±0.03
3.6×10^{-4}	11.9±0.01	12.4±0.04	14.5±0.07	9.43±0.02
4.6×10^{-4}	13.0±0.02	14.2±0.07	15.8±0.11	9.70±0.03
5.6×10^{-4}	13.9±0.07	14.8±0.07	17.1±0.21	10.1±0.02
6.6×10^{-4}	15.1±0.03	15.4±0.04	19.6±0.24	10.4±0.02
1.2×10^{-3}	19.0±0.06	21.4±0.07	24.1±0.35	12.0±0.02
2.5×10^{-3}	27.5±0.09	27.7±0.12	33.6±0.18	15.8±0.04
5×10^{-3}	34.8±0.12	34.8±0.16	39.7±0.27	18.1±0.05
9×10^{-3}	39.5±0.11	38.3±0.10	45.1±0.26	21.5±0.13
1.496×10^{-2}	39.6±0.10	41.8±0.09	46.6±0.31	23.9±0.25
1.89×10^{-2}	40.4±0.11	41.9±0.15	46.6±0.29	24.5±0.10
2.31×10^{-2}	40.2±0.15	42.3±0.15	46.1±0.20	24.8±0.32
2.7×10^{-2}	40.0±0.10	41.4±0.15	45.6±0.10	24.7±0.33
3.3×10^{-2}	37.6±0.14	40.7±0.22	44.7±0.19	24.9± 0.43
4×10^{-2}	37.3±0.23	37.4±0.43	43.3±0.24	24.3± 0.61
4.5×10^{-2}	36.3±0.49	37.2±0.71	40.87±0.3	24.3± 0.43
5×10^{-2}	35.4±0.62	36.4±0.68	39.6±0.51	24.3± 0.58

Table A3. Data for the reaction between iodide 1.5×10^{-3} M and *ca.* 4×10^{-6} M MCPBA, at various concentration of brij-35 and constant concentration of sodium perchlorate in 0.003 M nitric acid at 25 C^0

[Brij-35]	k_{obs},[0.05]/ M	k_{obs},[0.26]/ M	k_{obs},[0.4]/ M
0	8.5±0.02	8.24±0.03	7.91±0.04
1.6×10^{-4}	9.1±0.03	8.20±0.05	8.02±0.04
2.4×10^{-4}	9.0±0.04	8.12±0.07	7.95±0.01
3.6×10^{-4}	9.2±0.01	8.16±0.02	7.94±0.05
4.6×10^{-4}	9.3±0.02	8.27±0.06	7.98±0.04
5.6×10^{-4}	9.5±0.04	8.19±0.03	7.86±0.02
6.6×10^{-4}	10.0±0.01	8.14±0.03	7.64±0.07
1.2×10^{-3}	10.9±0.02	8.05±0.02	7.73±0.04
2.5×10^{-3}	11.4±0.01	7.91±0.01	7.60±0.07
5×10^{-3}	13.1±0.03	7.71±0.02	7.20±0.02
9×10^{-3}	15.4±0.02	7.50±0.05	7.03±0.03
1.496×10^{-2}	15.6±0.05	7.44±0.08	6.89±0.07
1.649×10^{-2}	15.5±0.04	7.37±0.07	6.82±0.07
2.31×10^{-2}	16.1±0.03	7.34±0.08	6.80±0.13
2.7×10^{-2}	16.1±0.04	7.26±0.10	6.76±0.03
3.3×10^{-2}	16.2±0.08	7.26±0.12	6.75±0.14
4×10^{-2}	16.3±0.12	7.23±0.09	6.79±0.09
4.5×10^{-2}	16.1±0.14	7.27±0.23	6.81±0.1
5×10^{-2}	16.2±0.10	7.27±0.19	6.85±0.16

Table A3. Continue, Data for the reaction between iodide 1.5×10^{-3} M and *ca.* 4×10^{-6} M MCPBA, at various concentration of brij-35 and constant concentration of sodium perchlorate in 0.003 M nitric acid at 25 C^0.

[Brij-35]/M	k_{obs},[0.6]/M	k_{obs}, [0.8]/M	[Brij-35]/M	k_{obs}, [0.5]/M	k_{obs}, [1]/ M
0	8.05±0.01	8.14±0.01	0	8.03±0.03	7.84±0.028
3.6×10^{-4}	7.87±0.04	7.96±0.01	2×10^{-5}	7.9±0.02	7.87±0.03
4.6×10^{-4}	7.67±0.08	7.78±0.01	4×10^{-5}	8.04±0.02	7.94±0.02
5.6×10^{-4}	7.62±0.04	7.62±0.01	8×10^{-5}	8.03±0.01	7.93±0.01
6.6×10^{-4}	7.49±0.02	7.69±0.01	1.6×10^{-4}	8.05±0.02	7.95±0.03
1.2×10^{-3}	7.48±0.05	7.5±0.02	2.4×10^{-4}	8.04±0.02	7.94±0.02
2.5×10^{-3}	7.2±0.009	7.25±0.01	3.6×10^{-4}	8.04±0.03	7.71±0.05
5×10^{-3}	7.05±0.02	6.94±0. 004	4.6×10^{-4}	8.03±0.03	7.60±0.02
9×10^{-3}	6.79±0.04	6.52±0.005	5.6×10^{-4}	8.03±0.03	7.79±0.05
1.496×10^{-2}	6.65±0.07	6.32±0.005	6.6×10^{-4}	7.99±0.01	7.86±0.2
1.89×10^{-2}	6.58±0.02	6.29±0.005	1.2×10^{-3}	7.68±0.02	7.68±0.06
2.31×10^{-2}	6.53±0.02	6.2±0.004	2.5×10^{-3}	7.59±0.02	7.30±0.02
2.7×10^{-2}	6.56±0.03	6.16±0.004	5×10^{-3}	7.18±0.01	6.80±0.03
3.3×10^{-2}	6.48±0.03	6.16±0.003	9×10^{-3}	7.01±0.02	6.72±0.02
4×10^{-2}	6.51±0.02	6.23±0.004	1.496×10^{-2}	6.76±0.02	6.59±0.03
4.5×10^{-2}	6.52±0.02	6.2±0.01	1.69×10^{-2}	6.70±0.04	6.40±0.02
5×10^{-2}	6.57±0.015	6.33±0.01	2.31×10^{-2}	6.63±0.03	6.28±0.04
			2.7×10^{-2}	6.64±0.03	6.17±0.02
			3.3×10^{-2}	6.58±0.04	6.18±0.01
			3.8×10^{-2}	6.64±0.03	6.22±0.03
			4.5×10^{-2}	6.75±0.06	6.25±0.02
			4.75×10^{-2}	6.72±0.02	6.29±0.05
			5×10^{-2}	6.72±0.04	6.21±0.03

Table A4 The kinetic data for the reaction of 1.5×10^{-3} M potassium iodide with *ca.* 4×10^{-6} M MCPBA and 0.003 M nitric acid at different temperature.

[Brij-35]	K_{obs} at 15°C	K_{obs} at 20°C	K_{obs} at 25°C	K_{obs} at 30°C	K_{obs} at 35°C
0	5.12±0.007	6.50±0.01	8.4±0.021	10.2±0.013	12.9±0.022
2×10^{-5}	5.19±0.007	6.58±0.04	8.6±0.017	10.3±0.025	13.1±0.023
4×10^{-5}	5.27±0.008	6.73±0.04	8.8±0.014	10.2±0.033	13.5±0.02
8×10^{-5}	5.49±0.012	6.75±0.07	9.1±0.023	10.3±0.025	14.1±0.03
1.6×10^{-4}	5.73±0.013	6.71±0.12	9.4±0.032	10.4±0.034	14.4±0.03
2.4×10^{-4}	5.72±0.008	6.93±0.10	9.3±0.02	10.6±0.041	14.8±0.03
3.6×10^{-4}	5.72±0.006	7.32±0.20	9.4±0.027	10.8±0.036	15.7±0.02
4.6×10^{-4}	5.97±0.006	7.59±0.28	9.7±0.016	11.4±0.035	16.5±0.01
5.6×10^{-4}	6.28±0.009	7.82±0.40	10.1±0.022	11.9±0.054	17.2±0.029
6.6×10^{-4}	6.40±0.007	8.21±0.06	10.4±0.016	12.7±0.084	18.9±0.02
1.2×10^{-3}	8.02±0.007	10.01±0.01	12.0±0.033	14.8±0.02	19.9±0.02
2.5×10^{-3}	10.6±0.010	13.16±0.01	15.8±0.024	18.7±0.047	22.1±0.03
5×10^{-3}	13.6±0.028	16.24±0.01	18.1±0.016	22.7±0.046	27.5±0.04
9×10^{-3}	15.53±0.07	19.10±0.02	21.5±0.073	27.0±0.071	32.4±0.05
1.496×10^{-2}	16.8±0.027	20.30±0.03	23.9±0.046	29.6±0.122	34.8±0.046
1.89×10^{-2}	17.1±0.016	21.00±0.02	24.5±0.18	30.8±0.062	35.9±0.048
2.31×10^{-2}	17.5±0.015	21.40±0.025	24.8±0.024	31.1±0.020	36.3±0.055
2.7×10^{-2}	17.4±0.021	21.43±0.03	24.7±0.034	31.1±0.02	36.9±0.05
3.3×10^{-2}	17.4±0.019	21.39±0.02	24.9±0.01	31.0±0.03	36.9±0.06
4×10^{-2}	17.5±0.031	21.41±0.02	24.4±0.15	30.3±0.06	36.9±0.065
4.5×10^{-2}	17.4±0.027	21.37±0.04	24.3±0.15	30.2±0.053	36.8±0.1
5×10^{-2}	17.3±0.040	21.30±0.02	24.32±0.26	30.1±0.049	36.7±0.08

Table A5 the kinetic data for the reaction of 1.5×10^{-3} M potassium iodide with *ca.* 4 x 10^{-6} M MCPBA and 0.003 M nitric acid in the presence of perchlorate 1 M at different temperature.

[Brij-35]	k_{obs}, 15°C	k_{obs}, 20°C	k_{obs}, 30°C	k_{obs}, 35°C
0	4.75±0.01	6.151±0.003	9.9±0.018	12.4±0.006
2×10^{-5}	4.83±0.02	6.2±0.014	9.86±0.020	12.4±0.023
4×10^{-5}	4.69±0.012	6.18±0.009	9.94±0.015	12.3±0.02
8×10^{-5}	4.72±0.01	6.12±0.014	9.92±0.023	12.3±0.022
1.6×10^{-4}	4.67±0.01	6.22±0.009	9.93±0.008	12.4±0.020
2.4×10^{-4}	4.78±0.02	6.24±0.002	9.87±0.009	12.4±0.022
3.6×10^{-4}	4.66±0.02	6.20±0.008	9.75±0.018	12.3±0.015
4.6×10^{-4}	4.68±0.015	6.19±0.007	9.63±0.029	12.2±0.015
5.6×10^{-4}	4.62±0.01	6.11±0.009	9.57±0.011	12.2±0.016
6.6×10^{-4}	4.48±0.013	5.94±0.008	9.56±0.012	12.1±0.015
1.2×10^{-3}	4.45±0.005	5.74±0.006	9.58±0.008	12.0±0.001
2.5×10^{-3}	4.24±0.003	5.65±0.002	9.16±0.006	11.5±0.002
5×10^{-3}	4.02±0.004	5.45±0.004	8.82±0.005	11.1±0.005
9×10^{-3}	3.82±0.003	5.19±0.003	8.38±0.007	10.5±0.009
1.496×10^{-2}	3.72±0.002	5.05±0.007	8.22±0.006	10.2±0.01
1.89×10^{-2}	3.69±0.003	4.98±0.003	8.14±0.005	10.0±0.03
2.31×10^{-2}	3.67±0.006	4.93±0.006	8.13±0.006	10.0±0.02
2.7×10^{-2}	3.65±0.007	4.96±0.005	8.07±0.007	9.9±0.027
3.3×10^{-2}	3.63±0.002	4.88±0.005	8.04±0.008	9.9±0.03
4×10^{-2}	3.7±0.01	4.91±0.004	8.03±0.018	9.9±0.04
4.5×10^{-2}	3.68±0.004	4.87±0.025	8.02±0.068	9.9±0.05
5×10^{-2}	3.67±0.002	4.90±0.012	8.04±0.140	10.0±0.05

Table A6 the kinetic data for the reaction of 1.5×10^{-3} M potassium iodide with *ca.* 4 x 10^{-6} M MCPBA and 0.003 M nitric acid in the presence of sulfate 0.35 M at different temperature.

[Brij-35]	k_{obs}, 20°C	k_{obs}, 25°C	k_{obs}, 30°C	k_{obs}, 35°C	k_{obs}, 15°C
0	6.81±0.01	8.34±0.03	10.81±0.01	13.07±0.03	5.35±0.01
1×10^{-5}	6.87±0.02	8.49±0.04	10.78±0.05	13.03±0.02	5.32±.021
2×10^{-5}	6.94±0.01	8.87±0.03	10.94±0.02	12.97±0.03	5.46±.01
4×10^{-5}	7.11±0.02	9.10±0.03	11.12±0.04	13.22±0.03	5.39±.01
8×10^{-5}	7.06±0.03	9.34±0.03	11.3±0.037	14.9±0.023	5.44±.013
1.6×10^{-4}	7.24±0.02	9.60±0.04	12.37±0.13	15.82±0.01	5.49±.009
2.4×10^{-4}	7.33±0.02	11.4±0.07	12.85±0.10	17.2±0.023	5.14±.01
3.6×10^{-4}	7.59±0.03	12.4±0.04	13.94±0.14	17.87±0.04	5.37±.017
4.6×10^{-4}	8.36±0.02	14.2±0.07	15.7±0.051	19.3±0.031	5.51±.022
5.6×10^{-4}	11.73±0.02	14.8±0.07	17.81±0.11	20.16±0.03	6.85±.005
6.6×10^{-4}	14.38±0.04	15.4±0.04	20.72±0.13	22.83±0.01	11.6±0.003
1.2×10^{-3}	17.52±0.01	21.4±0.07	24.51±0.02	28.6±0.03	14.06±0.001
2.5×10^{-3}	23.75±0.02	27.7±0.12	32.94±0.03	37.43±0.05	19.6±0.014
5×10^{-3}	29.60±0.03	34.8±0.16	42.49±0.09	47.97±0.07	23.35±0.02
9×10^{-3}	33.48±0.04	38.3±0.1	48.26±0.06	54.9±0.10	27.52±0.03
1.496×10^{-2}	34.89±0.04	41.8±0.09	51.2±0.066	58.15±0.12	28.22±0.02
1.89×10^{-2}	35.50±0.04	41.9±0.15	52.04±0.07	58.84±0.15	28.35±0.03
2.31×10^{-2}	35.51±0.05	42.3±0.14	52.13±0.05	58.96±0.23	28.25±0.04
2.7×10^{-2}	35.56±0.06	41.4±0.15	52.24±0.07	58.99±0.13	28.07±0.03
3.3×10^{-2}	35.60±0.06	40.7±0.22	51.89±0.05	58.79±0.22	27.6±0.03
4×10^{-2}	34.89±0.04	37.4±0.43	51.79±0.07	57.8±0.25	26.82±0.04
4.5×10^{-2}	34.47±0.06	37.2±0.71	50.33±0.10	57.7±0.21	26.6±0.03
5×10^{-2}	33.91±0.08	36.4±0.68	50.03±0.08	57.01±0.19	26.2±0.05

Table A7. Data for the reaction between iodide 1.5×10^{-3} M and *ca.* 4×10^{-6} M MCPBA, at various concentration of brij-35 in presence of caesium chloride in 0.003 M nitric acid at 25 C^0

[Brij-35]/M	k_{obs}, [0.2]/ M	k_{obs}, [0.5]/ M	k_{obs}, [0.8]/ M
0	9.67±0.02	10.03±0.04	11.1±0.07
2×10^{-5}	9.7±0.023	10.43±0.04	11.8±0.067
4×10^{-5}	9.9±0.03	10.85±0.03	11.73±0.1
8×10^{-5}	10.4±0.03	11.1±0.04	11.87±0.04
1.6×10^{-4}	10.4±0.02	11.01±0.06	11.84±0.05
2.4×10^{-4}	10.3±0.02	11.03±0.04	12.2±0.054
3.6×10^{-4}	10.4±0.01	11.54±0.03	13.2±0.08
4.6×10^{-4}	10.8±0.02	12.43±0.04	14.22±0.03
5.6×10^{-4}	11.1±0.01	12.7±0.03	14.89±0.05
6.6×10^{-4}	11.5±0.02	13.16±0.04	15.03±0.04
1.2×10^{-3}	13.1±0.02	16.49±0.08	17.32±0.06
2.64×10^{-3}	16.4±0.03	20.45±0.06	22.43±0.14
5.06×10^{-3}	21.7±0.03	24.55±0.05	25.98±0.1
7.04×10^{-3}	23.5±0.04	27.02±0.07	29.43±0.18
9.9×10^{-3}	24.5±0.05	28.4±0.07	31.77±0.19
1.496×10^{-2}	25.9±0.04	31.54±0.11	33.36±0.18
1.89×10^{-2}	26.4±0.06	33.64±0.16	33.46±0.12
2.31×10^{-2}	27.0±0.05	33.7±0.1	33.78±0.13
2.7×10^{-2}	27.1±0.07	33.37±0.14	33.1±0.2
3.3×10^{-2}	27.1±0.10	33.25±0.16	33.05±0.22
4×10^{-2}	26.7±0.16	32.87±0.17	32.47±0.1
4.5×10^{-2}	25.9±0.14	31.98±0.16	32.2±0.11
5×10^{-2}	25.3±0.13	31.7±0.19	31.57±0.15

Table A8. Data for the reaction between iodide 1.5×10^{-3} M and *ca.* 4×10^{-6} M MCPBA, at various concentration of brij-35 in presence of lithium chloride in 0.003 M nitric acid at 25 C^0

[Brij-35]/M	k_{obs}, [0.2]/ M	k_{obs}, [0.5]/ M	k_{obs}, [0.8]/ M
0	8.8±0.02	9.1±0.04	9.8±0.05
2×10^{-5}	8.70±0.017	9.16±0.034	9.75±0.04
4×10^{-5}	8.9±0.02	9.2±0.029	9.6±0.04
8×10^{-5}	9.5±0.035	9.914±0.03	10.3±0.05
1.6×10^{-4}	9.5±0.026	9.99±0.017	10.49±0.03
2.4×10^{-4}	9.54±0.02	10.1±0.02	10.61±0.03
3.6×10^{-4}	9.76±0.022	10.97±0.03	11.87±0.02
4.6×10^{-4}	10.27±0.01	11.47±0.03	12.61±0.04
5.6×10^{-4}	10.76±0.02	11.62±0.02	13.12±0.02
6.6×10^{-4}	11.37±0.02	12.94±0.03	13.33±0.03
1.2×10^{-3}	13.63±0.01	14.66±0.03	16.06±0.04
2.64×10^{-3}	16.64±0.03	18.57±0.04	21.3±0.07
5.0×10^{-3}	20.3±0.034	25.65±0.07	25.5±0.20
7.04×10^{-3}	21.74±0.04	26.86±0.06	28.4±0.12
$9.\times10^{-3}$	23.1±0.024	28.95±0.08	30.01±0.1
1.496×10^{-2}	24.7±0.04	29.59±0.09	31.5±0.14
1.89×10^{-2}	25.3±0.044	30.49±0.13	31.4±0.13
2.31×10^{-2}	25.5±0.06	30.37±0.08	31.5±0.10
2.7×10^{-2}	25.51±0.08	29.79±0.10	31.58±0.14
3.3×10^{-2}	25.44±0.09	29.86±0.09	31.43±0.12
4×10^{-2}	25.02±0.10	28.53±0.13	30.6±0.10
4.5×10^{-2}	24.67±0.19	27.59±0.08	29.49±0.15
5×10^{-2}	24.3±0.60	26.11±0.2	29.23±0.09

Table A9. Data for the reaction between iodide 1.5×10^{-3} M and *ca.* 4×10^{-6} M MCPBA, at various concentration of brij-35 in presence of magnesium chloride in 0.003 M nitric acid at 25 C^0

[Brij-35]/M	k_{obs}, [0.2]/ M	k_{obs}, [0.5]/ M
0	8.9 ± 0.03	10.00 ± 0.11
2×10^{-5}	9.04 ± 0.02	10.12 ± 0.078
4×10^{-5}	9.1 ± 0.03	10.40 ± 0.19
8×10^{-5}	9.91 ± 0.03	10.50 ± 0.07
1.6×10^{-4}	10.1 ± 0.04	11.00 ± 0.06
2.4×10^{-4}	10.13 ± 0.03	11.46 ± 0.04
3.6×10^{-4}	10.09 ± 0.01	11.91 ± 0.04
4.6×10^{-4}	10.18 ± 0.02	12.93 ± 0.06
5.6×10^{-4}	10.42 ± 0.02	13.5 ± 0.05
6.6×10^{-4}	11.13 ± 0.03	13.97 ± 0.04
1.2×10^{-3}	12.31 ± 0.03	16.40 ± 0.06
2.5×10^{-3}	16.1 ± 0.04	20.75 ± 0.10
5×10^{-3}	19.08 ± 0.03	23.33 ± 0.08
9×10^{-3}	22.02 ± 0.04	27.14 ± 0.14
1.496×10^{-2}	22.43 ± 0.04	28.00 ± 0.07
1.89×10^{-2}	22.7 ± 0.05	28.30 ± 0.08
2.31×10^{-2}	23.0 ± 0.04	28.19 ± 0.15
2.7×10^{-2}	23.31 ± 0.05	28.57 ± 0.13
3.3×10^{-2}	23.32 ± 0.06	28.36 ± 0.12
4×10^{-2}	22.75 ± 0.08	26.98 ± 0.16
4.5×10^{-2}	22.29 ± 0.1	26.90 ± 0.2
5×10^{-2}	22.4 ± 0.12	26.20 ± 0.14

Table A10. Data for the reaction between iodide 1.5×10^{-3} M and *ca.* 4×10^{-6} M MCPBA, at various concentration of brij-35 in presence of potassium chloride in 0.003 M nitric acid at 25 C^0

[Brij-35]/M	k_{obs}, [0.5]/ M	k_{obs},[0.8]/ M
0	8.4±0.013	9.608±0.07
2×10^{-5}	9.572±0.03	9.7±0.05
4×10^{-5}	10±0.05	9.928±0.06
8×10^{-5}	9.92±60.03	9.86±0.05
1.6×10^{-4}	10.21±0.02	10.11±0.03
2.4×10^{-4}	10.25±0.01	10.68±0.04
3.6×10^{-4}	10.8±0.02	11.96±0.03
4.6×10^{-4}	11.69±0.02	12.75±0.03
5.6×10^{-4}	12.69±0.02	13.59±0.05
7×10^{-4}	13.42±0.01	14.72±0.05
1.5×10^{-3}	16.94±0.04	17.25±0.07
2.5×10^{-3}	20.92±0.07	24.9±0.09
3.5×10^{-3}	23.13±0.1	30.61±0.11
5×10^{-3}	25.85±0.16	32.03±0.01
9×10^{-3}	31±0.1	35.63±0.01
1.32×10^{-2}	33.8±0.06	37.82±0.14
1.8×10^{-2}	34.2±0.08	38.22±0.01
2.31×10^{-2}	33.9±0.1	37.93±0.14
2.9×10^{-2}	33.62±0.14	38.4±0.13
3.5×10^{-2}	33.59±0.1	38.26±0.09
4×10^{-2}	33.5±0.2	38.18±0.13
4.5×10^{-2}	33.49±0.24	38.3±0.01
5×10^{-2}	33.32±0.32	37.96±0.2

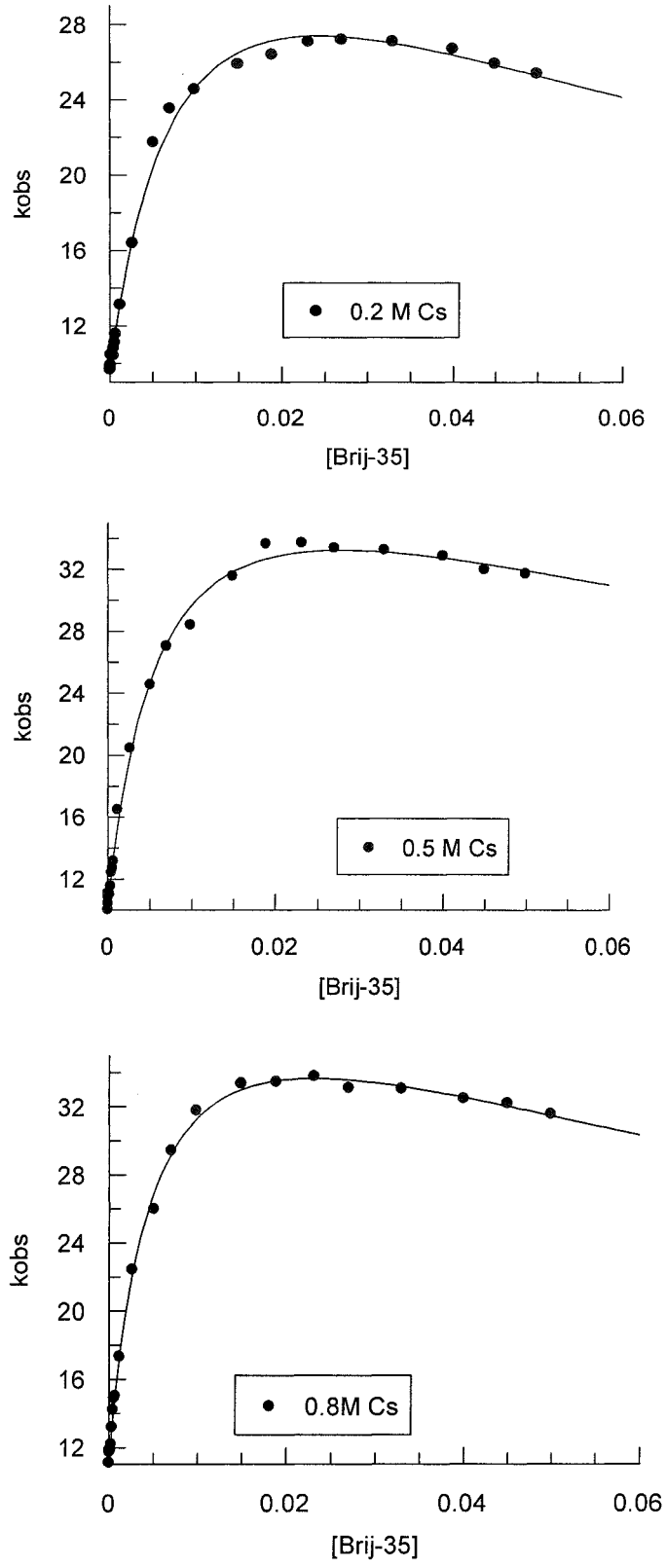

Figure A1 Plot of the observed pseudo-first order rate constant for the reaction of 3-perchloroperbenzoic acid with iodide at caesium concentrations 0.2 M upper curve, 0.5 M middle plot and 0.8 M with non-linear least square best fit line using Equation.3.6.

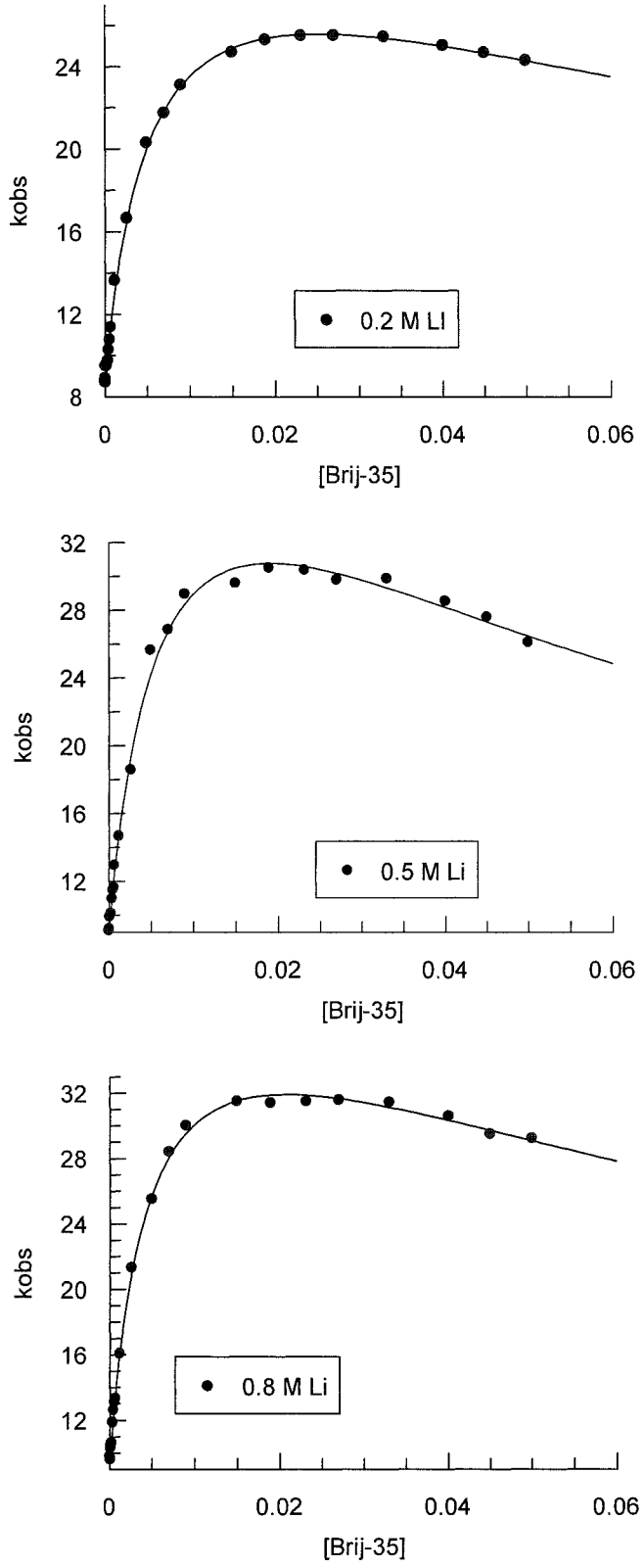

Figure A2 Plot of the observed pseudo-first order rate constant for the reaction of 3-perchloroperbenzoic acid with iodide at three lithium concentrations, with non-linear least square best fit line using Equation.3.6.

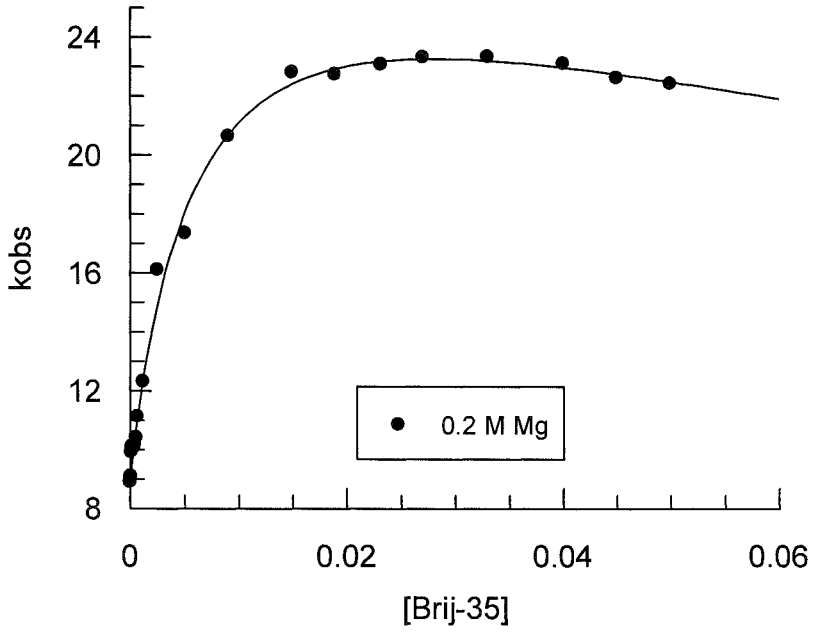

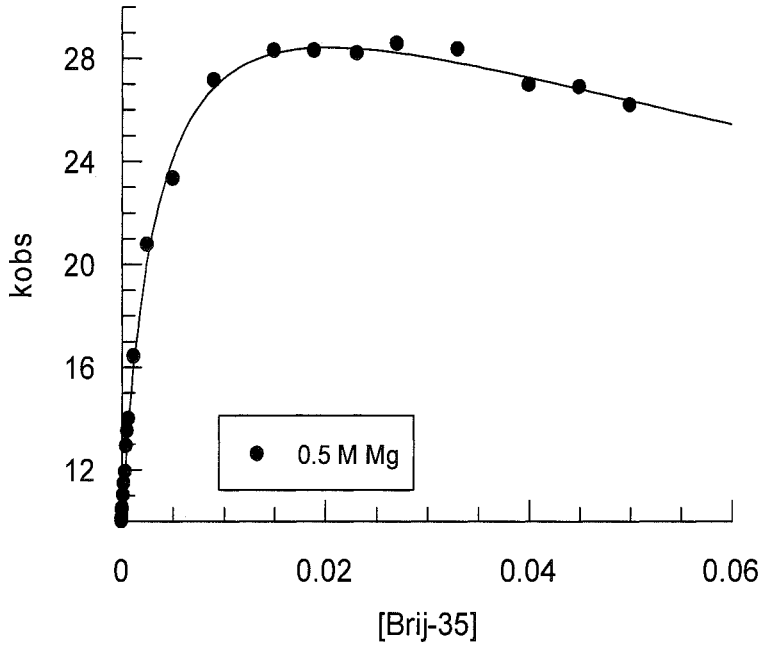

Figure A3 Plot of the observed pseudo-first order rate constant for the reaction of 3-perchloroperbenzoic acid with iodide at three magnesium concentrations 0.2 M upper curve and 0.5 M lower one with non-linear least square best fit line using Equation.3.6.

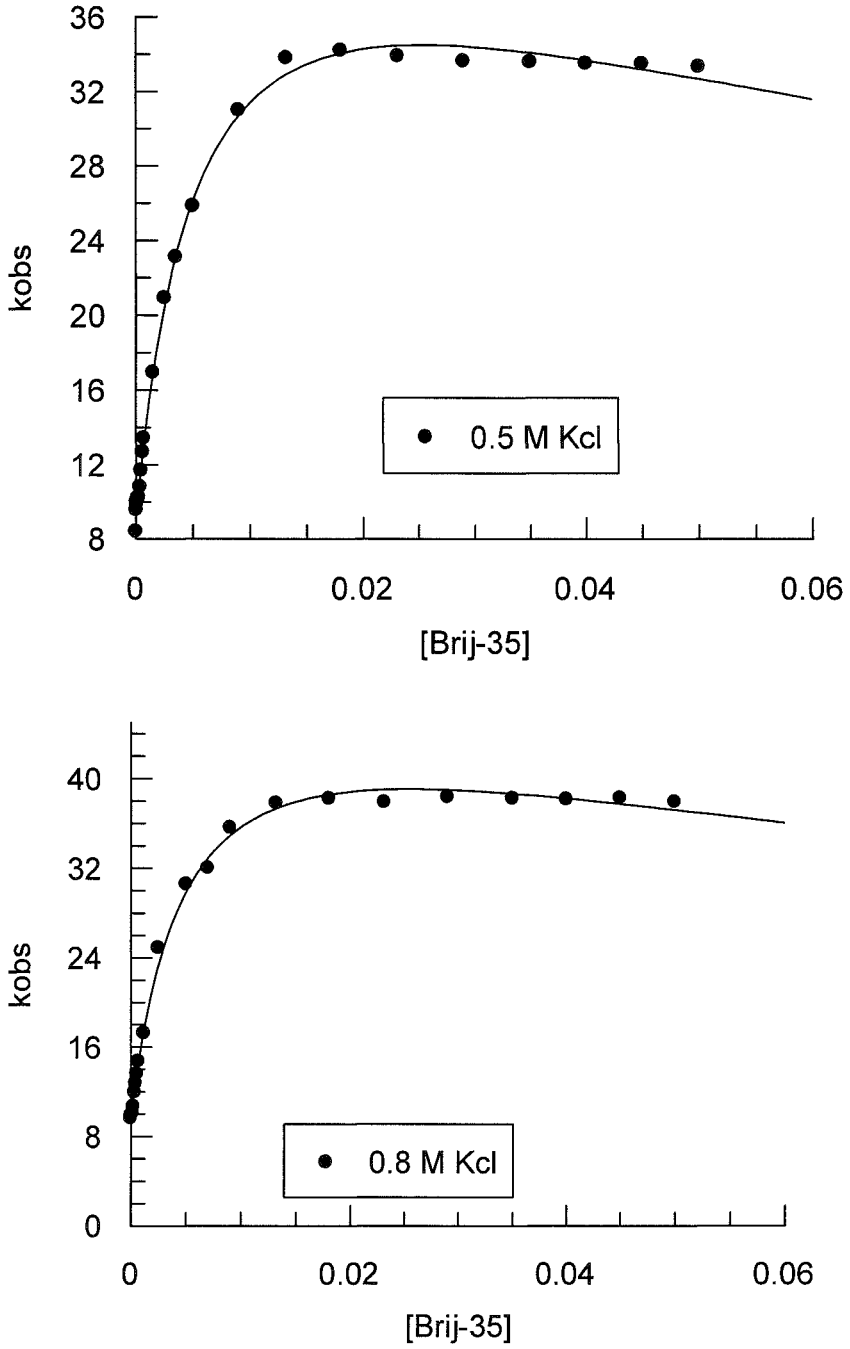

Figure A4 Plot of the observed pseudo-first order rate constant for the reaction of 3-chloroperbenzoic acid with iodide two potassium concentrations 0.5 M upper curve and 0.8 M lower one with non-linear least square best fit line using Equation.3.6.

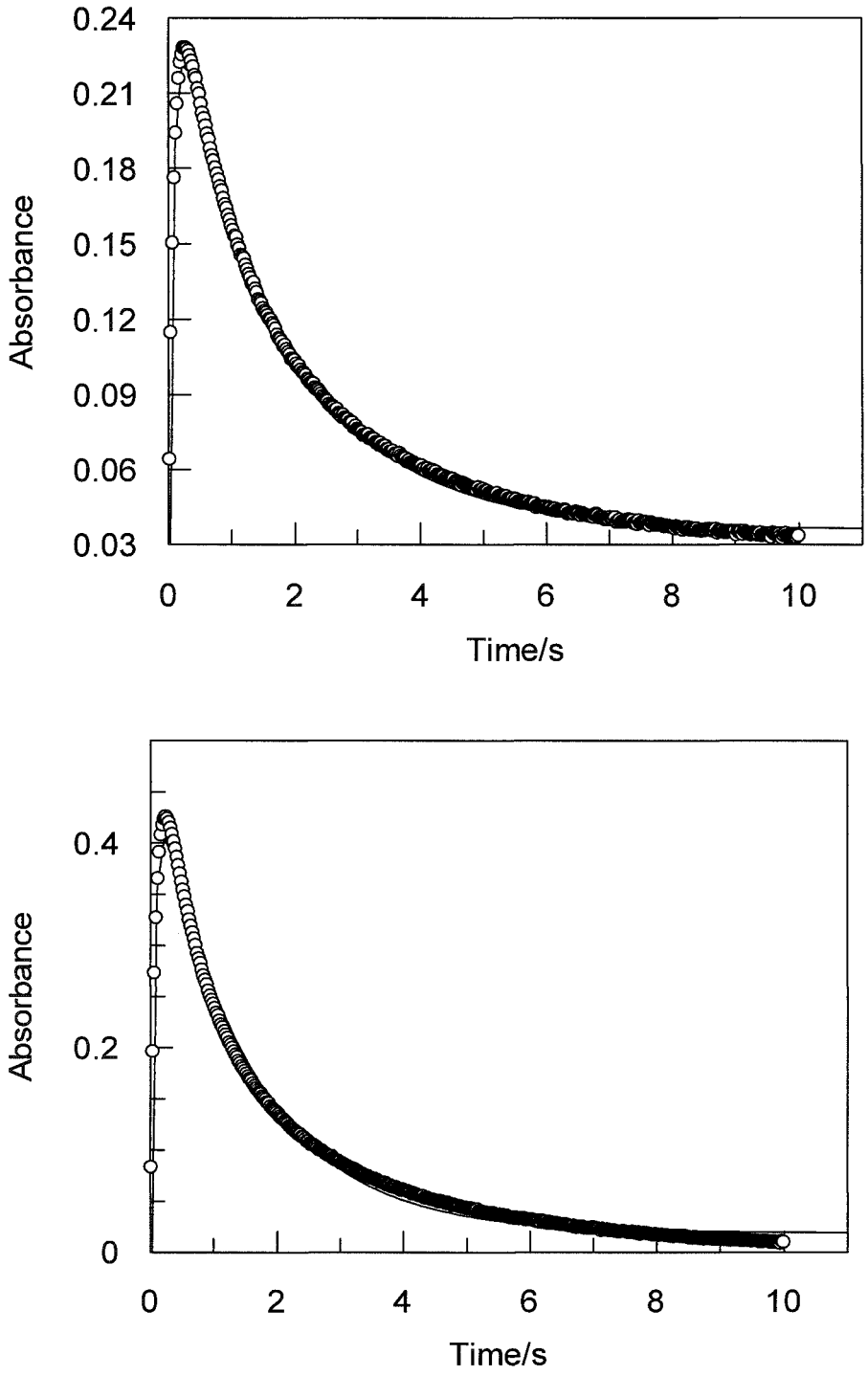

Figure A5 The absorbance versus time for the reaction of 1.1×10^{-5} M top plot and 2×10^{-5} M bottom plot of MCPBA with 0,0015 M iodide in the presence of 5×10^{-4} M P104 at 25°C .

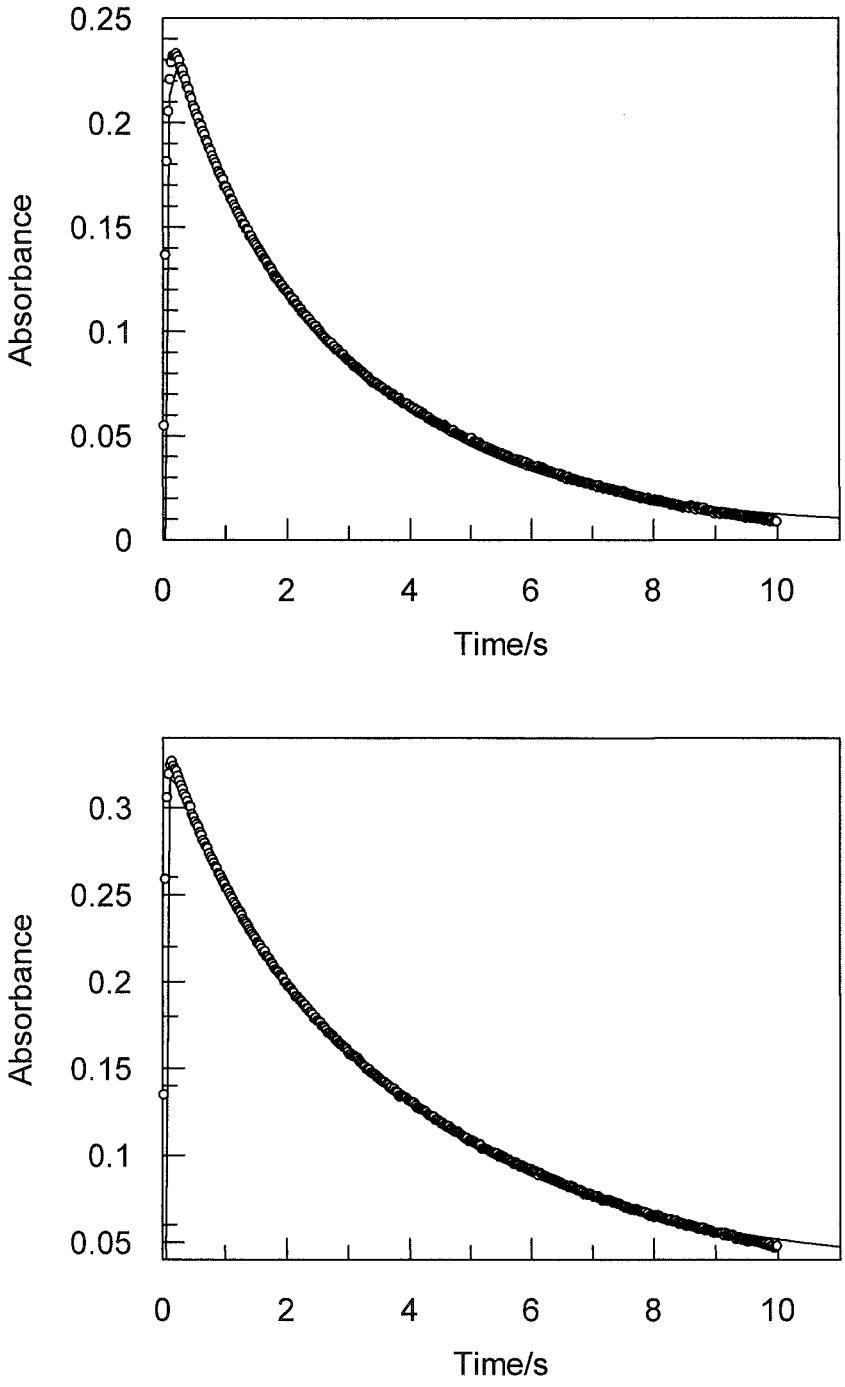

Figure A6 The absorbance versus time for the reaction of 1.5×10^{-5} M MCPBA with 0.003 M top plot and 0.006 M bottom plot of iodide in the presence of 5×10^{-4} M P104 at 25°C.

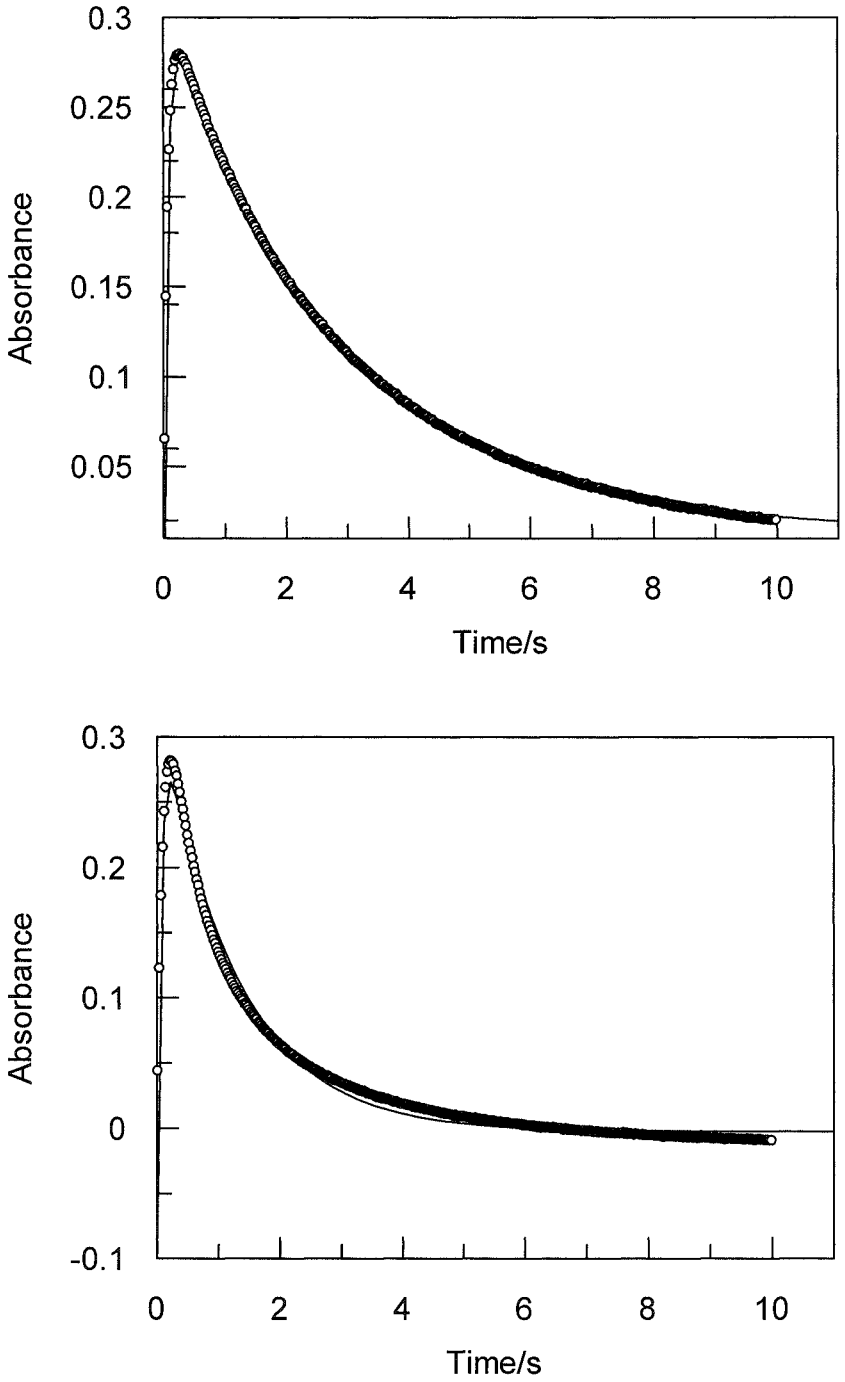

Figure A7 The absorbance versus time for the reaction of 1.5×10^{-5} M MCPBA with 0.0015 M iodide in the presence of 1×10^{-3} M top plot and 2.5×10^{-4} M bottom plot of P104 at 25°C.

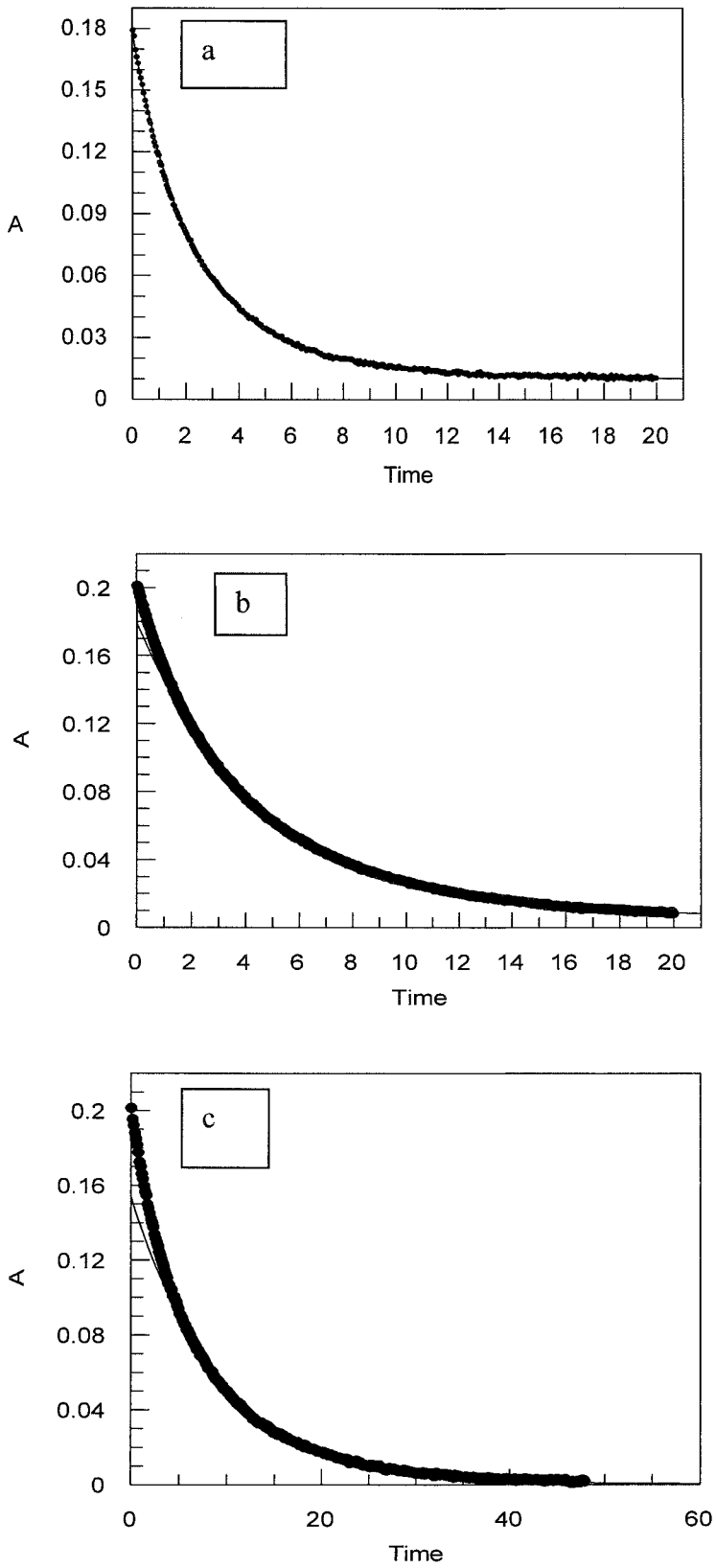

Figure A8 The absorbance versus time for the mixture of 0.0015 M KI (a), 0.003 M KI (b) and 0.006 M KI (c) and1×10^{-5} M iodine and 5×10^{-4} M of P 104 at 25°C

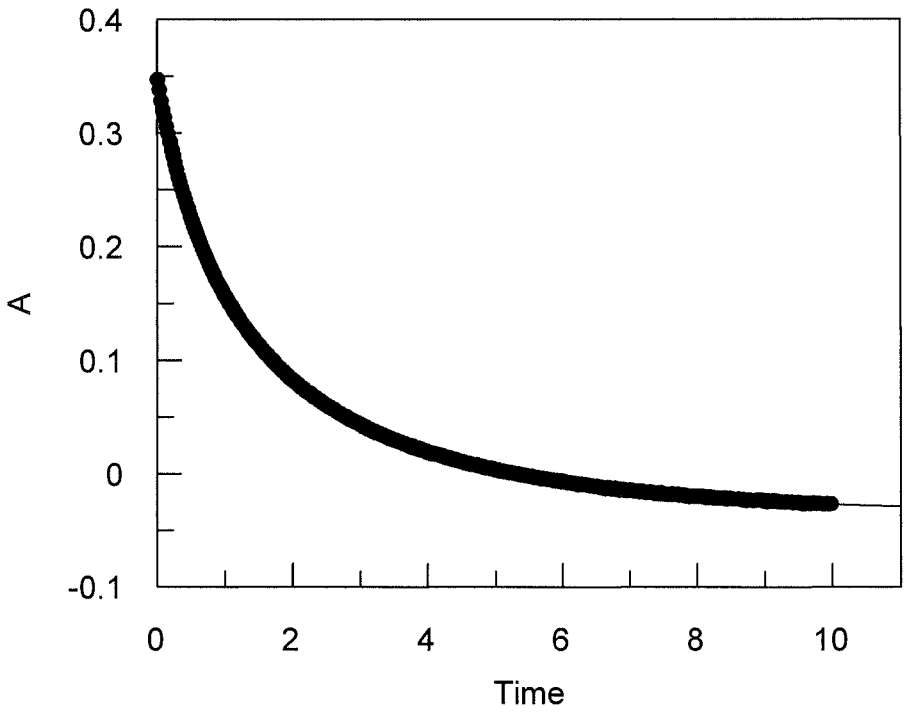

Figure A9 The absorbance versus time for the mixture of 0.0015 M and 2.5×10^{-5} M iodine and 5×10^{-4} M of P 104 at 25°C.

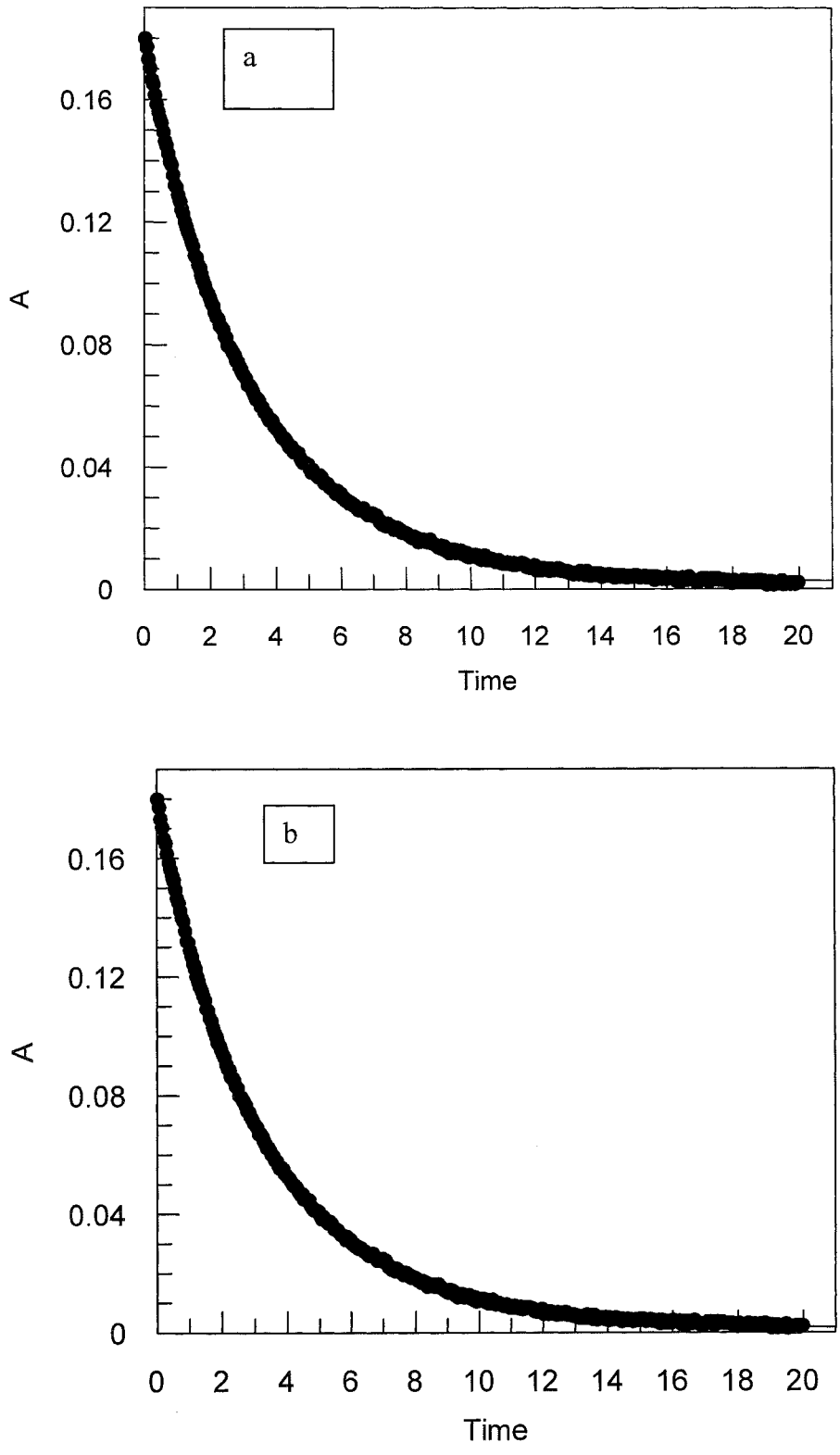

Figure A10 The absorbance versus time for the mixture of 0.0015 M and 1×10^{-5} M iodine and 2.5×10^{-4} M of P 104 (a) and 1×10^{-3} M (b) at 25°C.

The reaction of MCPBA with iodide in pluronic after dialysis is shown in Figure A11 and A12

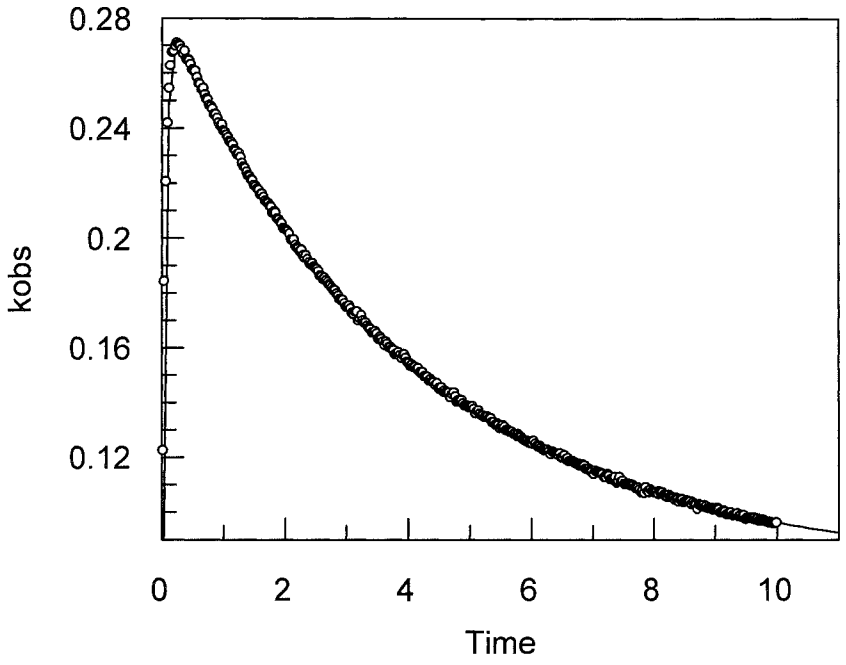

Figure A11 The absorbance versus time for the reaction of 0.0015 iodide with 5×10^{-6} MCPBA in 2.71×10^{-3} M of P104 at 25°C . After 2 dialysis

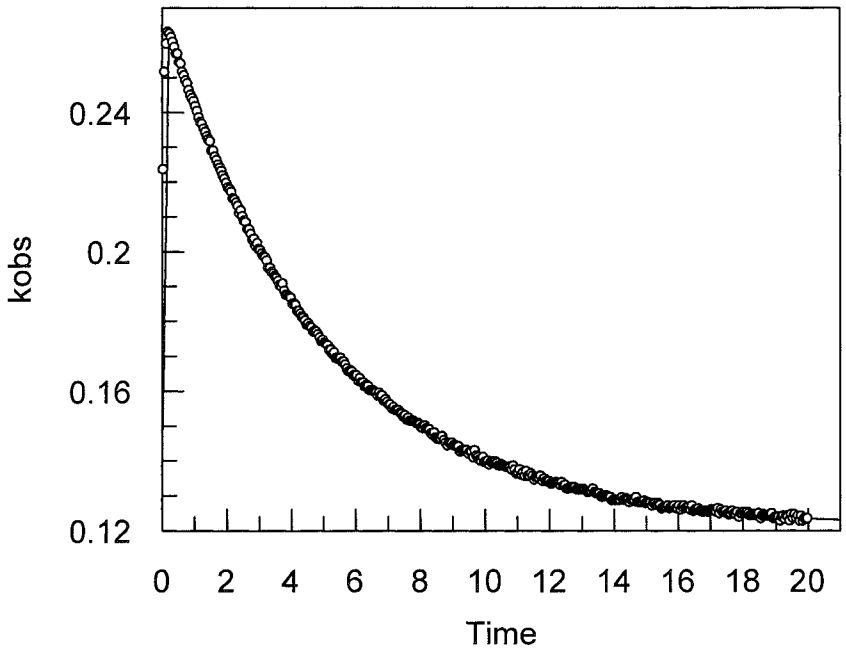

Figure A12 The absorbance versus time for the reaction of 0.0015 M iodide with 5×10^{-6} MCPBA in 5.42×10^{-3} M of P104 at 25°C. After four dialysis

Section S1. Testing the presence of isokinetic relationships using Exner plot [143].

The existence of an isokinetic relationship was inferred from the linear relationship between two series of ln *k* values, measured at two temperatures (T_1 and T_2). By plotting ln k (298K) versus ln k (308K) for the process in water, and ln k (288K) versus ln k (308K) for the process in micellar (see Figure 3.24 with correlation coefficients 0.9912 and 0.95 respectively), the value of T_{ios} was calculated from $T_{ios} = T_1T_2\,(b - 1)/(T_2b - T_1)$, where b is the slope of the Exner plot and $T_2 > T_1$. The value T_{ios} is 318 and 133 K is lower than 337 K and 255 K, calculated from the plot of $\Delta H^{\ddagger}$ versus $\Delta S^{\ddagger}$ (see Figure A13). So, as mentioned in Chapter One, the different values obtained for T_{iso} using different plots may suggest that this phenomena is either an artefact and related to an error in calculation, or the isokinetic relationships are different to isoequilibrium enthalpy-entropy compensation. However, for the peracid binding constant no linear correlation was obtained when such a plot was constructed.

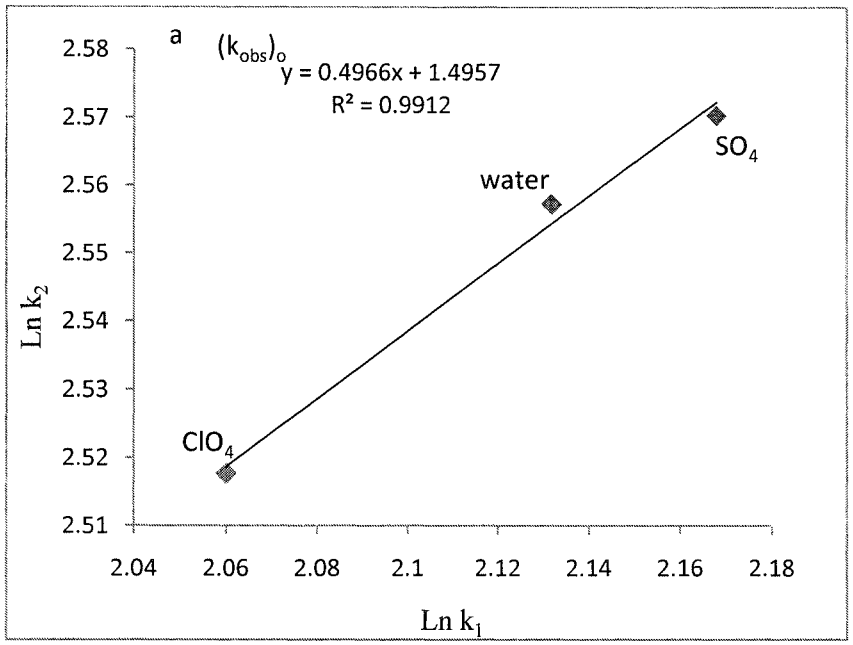

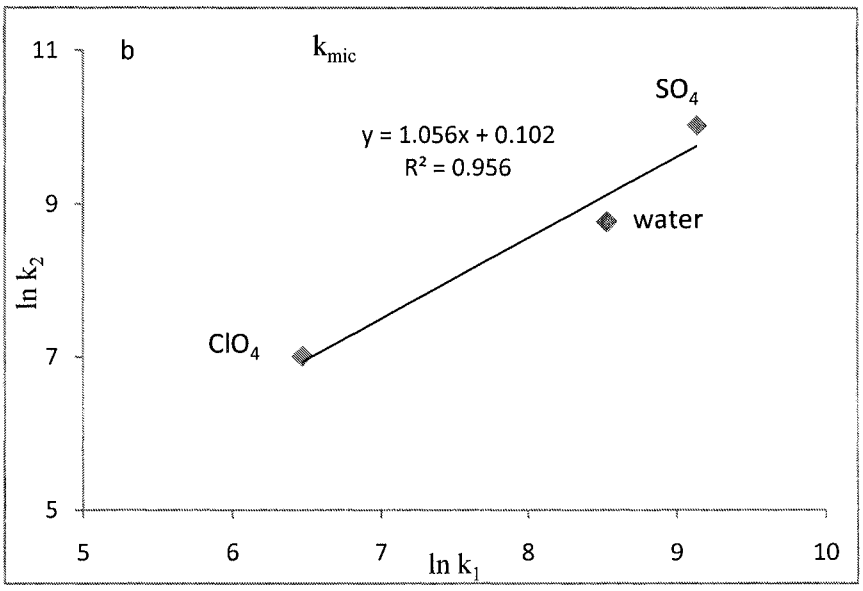

Figure A13: Logarithm of rate constant at 35°C versus that at 25°C for the reaction of iodide with MCPBA in the absence (a) and presence (b) of Brij-35. T_{iso} = 318.5 and 133 K for the process in water and the micellar system respectively.

Appendix B

Table.B1: The observed rate constant and its standard error for the reaction in the presence in 0.0113 M Brij-35 at fixed p-tolyl sulfide and various MCPBA and then various methyl *p*-tolyl sulfide and $2\times10^{-}$ 4 M of MCPBA

[4-CH_3]/ 10^6 M^{-1}	k_{obs}, s^{-1}	[MCPBA]/M	k_{obs}, s^{-1}
2	0.627±0.03	0.00003	0.0766±0.001
4	0.612±0.02	0.00009	0.270±0.002
6	0.623±0.02	0.00015	0.453±0.004
8	0.612±0.05	0.00019	0.9211±0.01
10	0.618±0.07	0.00021	0.6376±.02
13	0.616±0.05	0.00038	1.218±.01
		0.00049	1.6±0.03

Table B2: The effect of MCPBA on the reaction rate, reaction condition of 1×10^{-5} M of methyl *p*-tolyl sulfide and in 0.003 M nitric acid at 25°C.

[MCPBA]/M^{-1}	k_{obs}, s^{-1}	A_∞	A_o
0.00004	0.023±0.0001	0.0753	0.0983
0.00008	0.049±0.0003	0.112	0.161
0.00021	0.128±0.001	0.259	0.387
0.00025	0.158±0.001	0.3038	0.4618
0.00033	0.215±0.003	0.399	0.614
0.00049	0.323±0.003	0.5717	0.8947

Table.B3: Rate constant for the oxidation of $1\times10\text{-}^5$ M methyl *p*-tolyl sulfide as function of peroxymonsulfate concentrations.

[PMS]	k_{obs}, s^{-1}
0.00015	0.173±0.0004
0.00031	0.347±0.002
0.00047	0.510±0.005
0.00062	0.699±0.002
0.00077	0.842±0.006
0.00100	1.109±0.006
0.00131	1.459±0.004

Table.B4: The observed rate constant for the reaction of alkyl aryl sulfides 1×10^{-5} M with 5×10^{-4} M peroxymonsulfate and 2×10^{-4} – MCPBA at 25°C.

[Brij-35]/M	k_{obs}, 4-Br	k_{obs}, 4-CH_2OH	[Brij-35]/M	k_{obs}, 4-Br	k_{obs}, 4-CH_2OH
0	0.292 ± 0.004	0.400±0.002	0	0.0665±0.001	0.102±0.006
4.52×10^{-6}	0.294±0.003	0.402±0.002	2×10^{-6}	0.069±0.001	0.101±0.001
7×10^{-6}	0.2945±0.002	0.404±0.002	4.5×10^{-6}	0.066±0.001	0.101±0.002
1.35×10^{-5}	0.292±0.003	0.399±0.003	1.4×10^{-5}	0.071±0.001	0.099±0.008
4×10^{-5}	0.288±0.003	0.397±0.002	8.1×10^{-5}	0.098±0.001	0.103±0.004
8.10×10^{-5}	0.272±0.001	0.4±0.001	2×10^{-4}	0.198±0.003	0.113±0.001
1.98×10^{-4}	0.246±0.004	0.399±0.002	3.9×10^{-4}	0.315±0.003	0.127±0.001
3.98×10^{-4}	0.211±0.006	0.388±0.002	5.6×10^{-4}	0.471±0.004	0.162±0.001
5.65×10^{-4}	0.157±0.001	0.38±0.002	1.1×10^{-3}	0.525±0.01	0.191±0.002
8.40×10^{-4}	0.137±0.004	0.364±0.001	1.7×10^{-3}	0.556±0.01	0.239±0.002
1.13×10^{-3}	0.111±0.003	0.356±0.001	2.9×10^{-3}	0.522±0.01	0.261±0.002
2.26×10^{-3}	0.064±0.002	0.326±0.005	3.9×10^{-3}	0.484±0.01	0.286±0.009
3.95×10^{-3}	0.045±0.001	0.305±0.001	5.7×10^{-3}	0.410±0.007	0.269±0.008
5.65×10^{-3}	0.035±0.001	0.285±0.002	9×10^{-3}	0.359±0.008	0.249±0.001
9×10^{-3}	0.023±0.004	0.24±0.004	1.5×10^{-2}	0.226±0.004	0.22±0.001
1.5×10^{-2}	0.011±0.01	0.186±0.001	02×10^{-2}	0.176±0.005	0.183±0.001
2.5×10^{-2}	0.008±0.003	0.134±0.001	2.4×10^{-2}	0.149±0.003	0.168±0.001
3.3×10^{-2}	0.007±0.001	0.095±0.004	3.3×10^{-2}	0.129±0.006	0.142±0.002
4.4×10^{-2}	0.006±0.003	0.087±0.001	4.4×10^{-2}	0.109±0.002	0.115±0.001
5×10^{-2}	0.005±0.01	0.078±0.002	5×10^{-2}	0.096±0.002	0.109±0.001

Table.B5: The observed rate constant for the reaction of alkyl aryl sulfides 1×10^{-5} M with 5×10^{-4} M of peroxymonosulfate at 25°C.

[Brij-35]/M	k_{obs}, 4-Nitro	k_{obs}, 4-OCH_3
0	0.062 ± 0.0002	0.734±0.013
3.60×10^{-6}	0.063±0.0002	0.7309±0.005
1.35×10^{-5}	0.063±0.0004	0.730±0.009
4.5×10^{-5}	0.064±0.0011	0.74±0.009
8.10×10^{-5}	0.063±0.0002	0.727±0.01
1.98×10^{-4}	0.061±0.0002	0.711±0.009
3.98×10^{-4}	0.057±0.0003	0.657±0.005
5.65×10^{-4}	0.054±0.0001	0.623±0.008
1.13×10^{-3}	0.051±0.002	0.579±0.007
2.26×10^{-3}	0.041±0.0001	0.454±0.007
3.95×10^{-3}	0.030±0.0001	0.3349±0.004
5.65×10^{-3}	0.026±0.0004	0.2886±0.006
9×10^{-3}	0.018±0.0003	0.198±0.01
1.5×10^{-2}	0.023±0.0004	0.153±0.003
2.5×10^{-2}	0.008±0.0002	0.100±0.004
3.3×10^{-2}	0.0063±0.0003	0.081±0.001
4.4×10^{-2}	0.0053±0.0005	0.0684±0.003
5×10^{-2}	0.0051±0.0004	0.0516±0.002

Table.B6: The observed rate constant for the reaction of alkyl aryl sulfides 1×10^{-5} M with 2×10^{-4} M of MCPBA at 25°C.

[Brij-35]/M	k_{obs}, 4-Nitro	k_{obs}, 4-OCH_3
0	0.0109±0.0003	0.201±0.004
3.6×10^{-6}	0.0107±0.0002	0.196±0.004
1.35×10^{-5}	0.0109±0.0003	0.208±0.005
4.52×10^{-5}	0.011±0.00023	0.204±0.007
8.1×10^{-5}	0.012±0.00024	0.235±0.007
1.98×10^{-4}	0.0153±0.001	0.311±0.007
3.98×10^{-4}	0.021±0.0004	0.487±0.03
5.65×10^{-4}	0.027±0.001	0.583±0.024
1.13×10^{-3}	0.0356±0.0007	0.939±0.017
1.69×10^{-3}	0.040±0.001	1.128±0.02
2.85×10^{-3}	0.0435±0.0008	1.23±0.037
3.95×10^{-3}	0.0417±0.001	1.203±0.019
5.65×10^{-3}	0.035±0.001	1.107±0.008
9×10^{-3}	0.031±0.001	1.021±0.03
1.5×10^{-2}	0.0228±0.002	0.739±0.023
2×10^{-2}	0.0177±0.002	0.598±0.03
2.4×10^{-2}	0.0136±0.0007	0.527±0.02
3.3×10^{-2}	0.011±0.004	0.439±0.006
4.4×10^{-2}	0.0075±0.002	0.359±0.01
5×10^{-2}	0.0067±0.003	0.322±0.01

Table.B7: The observed rate constant for the reaction of alkyl aryl sulfides 1×10^{-5} M with 4×10^{-4} M of peroxymonosulfate at 25°C.

[Brij-35]/M	k_{obs}, 4-Cl	k_{obs} , 2-Cl
0	0.3249±0.002	0.0976±0.001
3.6×10^{-6}	0.329±0.001	0.098±0.0004
1.35×10^{-5}	0.3238±0.002	0.0984±0.001
4.50×10^{-5}	0.3265±0.004	0.0975±0.0004
7.68×10^{-5}	0.3234±0.002	0.095±0.0004
1.98×10^{-4}	0.2947±0.001	0.088±0.0004
3.75×10^{-4}	0.258±0.003	0.076±0.0002
5.65×10^{-4}	0.2217±0.001	0.0631±0.0001
1.13×10^{-3}	0.1628±0.007	0.0447±0.001
2.26×10^{-3}	0.101±0.005	0.0283±0.0003
3.95×10^{-3}	0.073±0.0004	0.0197±0.0002
5.65×10^{-3}	0.0555±0.002	0.0124±0.001
9×10^{-3}	0.0348±0.0005	0.009±0.0006
1.5×10^{-2}	0.0216±0.001	0.006±0.0002
2.5×10^{-2}	0.0149±.0003	0.003±0.0003
3.3×10^{-2}	0.0115±0.0007	0.0026±0.0005
4.4×10^{-2}	0.0089±0.001	0.002±0.0004
5×10^{-2}	0.0073±0.001	0.0019±0.001

Table.B8: The observed rate constant for the reaction of alkyl aryl sulfides 1×10^{-5} M with 2×10^{-4} M of MCPBA at 25°C

[Brij-35]/M	k_{obs}, 4-Cl	k_{obs} , 2-Cl
0	0.07±0.0003	0.0238±0.00023
3.6×10^{-6}	0.079±0.0003	0.0239±0.0002
1.35×10^{-5}	0.0776±0.0004	0.024±0.00022
4.5×10^{-5}	0.085±0.001	0.0254±0.0003
7.68×10^{-5}	0.099±0.0006	0.0285±0.0004
1.98×10^{-4}	0.1702±0.001	0.049±0.005
3.75×10^{-4}	0.296±0.002	0.079±0.0007
5.65×10^{-4}	0.3816±0.002	0.100±0.0005
1.13×10^{-3}	0.544±0.004	0.124±0.0072
2.80×10^{-3}	0.583±0.0036	0.127±0.0009
3.95×10^{-3}	0.536±0.0034	0.1159±0.0012
5.65×10^{-3}	0.456±0.003	0.094±0.0013
9.00×10^{-3}	0.364±0.003	0.067±0.001
1.50×10^{-2}	0.254±0.006	0.046±0.001
$2.\times10^{-2}$	0.202±0.004	0.0353±0.001
2.5×10^{-2}	0.175±0.0014	0.0286±0.0003
3.3×10^{-2}	0.1397±0.0012	0.0234±0.001
4.40×10^{-2}	0.1055±0.0014	0.0178±0.01
5×10^{-2}	0.090±0.001	0.015±0.002

Table.B9: The observed rate constant for the reaction of aryl alkyl sulphides 1×10^{-5} M with 4×10^{-4} M of peroxymonosulfate and 2×10^{-4} M of MCPBA at 25°C

[Brij-35]/M	k_{obs},3-Cl	[Brij-35]	k_{obs}, 3-Cl in MCPBA
0	0.225±0.0012	0	0.051±0.0003
3.6×10^{-6}	0.228±0.001	3.6×10^{-6}	0.0513±0.0005
1.35×10^{-5}	0.229±0.001	1.3×10^{-5}	0.0504±0.0003
3.6×10^{-5}	0.227±0.0012	6×10^{-5}	0.0528±0.0003
7.68×10^{-5}	0.226±0.001	7.68×10^{-5}	0.0619±0.001
1.98×10^{-4}	0.208±0.001	1.98×10^{-4}	0.1005±0.001
3.8×10^{-4}	0.187±0.001	3.75×10^{-4}	0.176±0.002
5.7×10^{-4}	0.145±0.001	5.65×10^{-4}	0.2368±0.005
1.13×10^{-3}	0.105±0.0003	0.00113	0.2967±0.002
0.0028	0.058±0.0002	0.0028	0.305±0.0024
0.00395	0.041±0.0011	0.00395	0.280±0.002
0.0073	0.025±0.001	0.00565	0.2415±0.002
0.009	0.0176±0.002	0.009	0.179±0.0022
0.015	0.0134±0.001	0.015	0.132±0.0013
0.02	0.0096±0.001	0.02	0.1107±0.001
0.025	0.008±0.001	0.025	0.0857±0.001
0.033	0.0063±0.001	0.033	0.069±0.001
0.044	0.0052±0.002	0.044	0.0454±0.005
0.05	0.004±0.004	0.05	0.0347±0.0016

Table.B10: The observed rate constant for the reaction of phenyl methyl sulfide1×10^{-5} M with 4×10^{-4} M of peroxymonosulfate and 2×10^{-4} M of MCPBA at 25°C

[Brij-35]/M	k_{obs}, MPS	[Brij-35]/M	k_{obs} , MCPBA
0	0.4155±0.0024	0	0.1015±0.001
1×10^{-5}	0.4047±0.0021	1×10^{-5}	0.1024±0.001
4×10^{-5}	0.4095±0.002	4×10^{-5}	0.1018±0.002
8×10^{-5}	0.4063±0.0012	8×10^{-5}	0.105±0.001
02×10^{-4}	0.383±0.0021	2×10^{-4}	0.133±0.001
3.8×10^{-4}	0.3736±0.0022	3.8×10^{-4}	0.164±0.001
5.7×10^{-4}	0.3545±0.0021	5.7×10^{-4}	0.219±0.001
1.13×10^{-3}	0.3278±0.0025	1.13×10^{-3}	0.28±0.002
2.8×10^{-3}	0.2426±0.0022	2×10^{-3}	0.342±0.002
0.00395	0.2197±0.0016	3.95×10^{-3}	0.361±0.002
0.0073	0.160±0.0013	0.00565	0.323±0.003
0.015	0.1274±0.001	0.009	0.263±0.003
0.02	0.0917±0.0014	0.015	0.204±0.0027
0.025	0.073±0.0065	0.02	0.16±0.0016
0.033	0.0479±0.0055	0.025	0.143±0.002
0.044	0.036±0.004	0.033	0.106±0.001
0.05	0.028±0.004	0.044	0.085±0.007
		0.05	0.082±0.01

Table.B11: The temperature dependence data for the reaction of methyl *p*-tolyl sulfide 1×10^{-5} M with 5×10^{-4} M peroxymonosulfate..

[Brij-35]/M	k_{obs}, 15 °C	k_{obs}, 20 °C	[Brij-35]/M	k_{obs}, 25 °C
0	0.37±0.003	0.434±0.0021	0	0.501±0.002
2×10^{-6}	0.371±0.003	0.4346±0.003	2×10^{-6}	0.504±0.0023
5×10^{-6}	0.3719±0.003	0.427±0.0029	5×10^{-6}	0.506±0.002
1.35×10^{-5}	0.3702±0.004	0.435±0.0031	1.35×10^{-5}	0.506±0.002
3.6×10^{-5}	0.370±0.002	0.432±0.0028	8×10^{-5}	0.492±0.002
8×10^{-5}	0.370±0.004	0.4236±0.0023	1.98×10^{-4}	0.488±0.002
1.98×10^{-4}	0.369±0.003	0.418±0.0027	5.6×10^{-4}	0.418±0.001
5.6×10^{-4}	0.309±0.004	0.342±0.0023	8.4×10^{-4}	0.386±0.001
8.4×10^{-4}	0.276±0.004	0.32±0.0024	1.3×10^{-3}	0.314±0.002
1.13×10^{-3}	0.245±0.003	0.284±0.0023	1.69×10^{-3}	0.273±0.002
2.26×10^{-3}	0.193±0.002	0.205±0.0031	2.260×10^{-3}	0.24±0.0018
3.95×10^{-3}	0.128±0.003	0.1479±0.0018	2.8×10^{-3}	0.217±0.003
5×10^{-3}	0.098±0.002	0.1185±0.0015	3.95×10^{-3}	0.186±0.002
9×10^{-3}	0.069±0.002	0.0753±0.001	5×10^{-3}	0.157±0.001
1.5×10^{-2}	0.0394±0.001	0.0428±0.001	9×10^{-3}	0.085±0.0012
2.5×10^{-2}	0.028±0.0004	0.033±0.0005	1.5×10^{-2}	0.062±0.0014
3.3×10^{-2}	0.021±0.0003	0.0264±0.0004	2.4×10^{-2}	0.043±0.001
4.4×10^{-2}	0.019±0.0004	0.0238±0.0002	2.8×10^{-2}	0.037±0.001
5×10^{-2}	0.0143±0.001	0.0156±0.006	3.3×10^{-2}	0.0336±0.001
			4×10^{-2}	0.028±0.0007
			5×10^{-2}	0.023±0.001

Table.B11: continue

[Brij-35]/M	k_{obs} at 30°C	k_{obs} at 35 °C
0	0.5585±0.004	0.653±0.003
2×10^{-6}	0.56±0.003	0.6469±0.004
5×10^{-6}	0.5596±0.004	0.647±0.003
1.35×10^{-5}	0.5576±0.004	0.646±0.004
3.6×10^{-5}	0.557±0.004	0.639±0.005
8×10^{-5}	0.5574±0.003	0.632±0.005
1.8×10^{-4}	0.5341±0.004	0.607±0.0046
5.6×10^{-4}	0.465±0.002	0.538±0.003
8.4×10^{-4}	0.445±0.004	0.5044±0.004
2.22×10^{-3}	0.3061±0.003	0.361±0.004
3.9×10^{-3}	0.217±0.0025	0.258±0.0037
5×10^{-3}	0.173±0.003	0.2164±0.006
9×10^{-3}	0.1235±0.002	0.149±0.003
1.5×10^{-2}	0.081±0.003	0.098±0.002
2.5×10^{-2}	0.0428±0.001	0.0558±0.001
3.3×10^{-2}	0.0374±0.002	0.0536±0.001
4.4×10^{-2}	0.0317±0.001	0.047±0.001
5×10^{-2}	0.0278±0.001	0.032±0.001

Table.B11: The temperature dependence data for the reaction of methyl methyl *p*-tolyl sulfide 1×10^{-5} M with 2×10^{-4} M MCPBA

[Brij-35]/M	k_{obs}, 20 °C	k_{obs}.30 °C	[Bri-35]/M	k_{obs}, 25 °C
0	0.1194±0.001	0.1876±0.002	0	0.1399±0.001
2×10^{-6}	0.1189±0.002	0.187±0.0026	5×10^{-6}	0.1407±0.005
3.6×10^{-6}	0.121±0.002	0.187±0.002	1.4×10^{-5}	0.142±0.003
07×10^{-6}	0.119±0.001	0.187±0.0024	3.6×10^{-5}	0.146±0.004
1.4×10^{-5}	0.122±0.002	0.189±0.002	1.8×10^{-4}	0.25±0.002
4×10^{-5}	0.117±0.001	0.198±0.002	2.3×10^{-4}	0.326±0.002
8×10^{-5}	0.136±0.0015	0.327±0.003	5.6×10^{-6}	0.47±0.005
2×10^{-4}	0.200±0.001	0.373±0.004	7.3×10^{-6}	0.683±0.004
4×10^{-4}	0.328±0.002	0.547±0.005	0.0013	0.84±0.01
5.6×10^{-4}	0.403±0.002	0.610±0.02	0.0016	0.86±0.008
7.3×10^{-4}	0.528±0.005	0.774±0.01	0.0028	0.96±0.002
1.69×10^{-3}	0.714±0.004	0.969±0.01	0.00395	0.914±0.01
2.8×10^{-3}	0.740±0.01	0.996±0.01	0.005	0.83±0.002
3.95×10^{-3}	0.727±0.01	0.987±0.01	0.0073	0.744±0.004
5.65×10^{-3}	0.671±0.01	0.913±0.008	0.009	0.714±0.004
9×10^{-3}	0.546±0.002	0.73±0.005	0.015	0.540±0.01
1.5×10^{-2}	0.400±0.01	0.557±0.004	0.02	0.44±0.0024
2×10^{-2}	0.358±0.006	0.457±0.003	0.024	0.362±0.002
2.48×10^{-2}	0.289±0.004	0.361±0.004	0.028	0.308±0.003
3.3×10^{-2}	0.241±0.003	0.286±0.005	0.33	0.257±0.01
4.46×10^{-2}	0.171±0.01	0.231±0.003	0.043	0.21±0.01
5×10^{-2}	0.146±0.003	0.197±0.004	0.05	0.189±0.003

Table 11B continue

[Brij-35]/M	k_{obs} at 35 °C	k_{obs} at 15 °C
0	0.237±0.003	0.088±0.0012
2×10^{-6}	0.233±0.0034	0.0881±0.001
3.6×10^{-6}	0.226±0.003	0.0913±0.002
7×10^{-6}	0.2275±0.003	0.091±0.001
4×10^{-5}	0.233±0.003	0.0986±0.001
8×10^{-5}	0.2679±0.01	0.1079±0.0024
2×10^{-4}	0.423±0.005	0.161±0.004
4×10^{-4}	0.584±0.01	0.351±0.01
5.6×10^{-4}	0.8013±0.02	0.268±0.01
7.3×10^{-4}	0.868±0.01	0.4318±0.01
1.69×10^{-3}	1.038±0.02	0.544±0.006
2.2×10^{-3}	1.07±0.01	0.561±0.0045
2.8×10^{-3}	1.132±0.01	0.578±0.005
3.95×10^{-3}	0.996±0.01	0.555±0.004
9×10^{-3}	0.7478±0.004	0.4005±0.003
1.5×10^{-2}	0.5936±0.005	0.355±0.006
2×10^{-2}	0.425±0.01	0.276±0.005
2.5×10^{-2}	0.385±0.002	0.2267±0.01
3.3×10^{-2}	0.327±0.007	0.1813±0.004
4.46×10^{-2}	0.267±0.004	0.121±0.003
5×10^{-2}	0.233±0.006	0.1093±0.004

Table.B12: The temperature dependence data for the reaction of (methylthio) benzyl alcohol 5×10^{-4} M with 5×10^{-4} M peroxymonosulfate..

[Brij-35]/M	k_{obs},20 °C	[Brij-35]/M	k_{obs},25 °C
0	0.3387±0.003	0	0.400±0.0014
5×10^{-6}	0.3425±0.0025	4.52×10^{-6}	0.401±0.002
1.4×10^{-5}	0.3468±0.0023	7×10^{-6}	0.403±0.002
3.6×10^{-5}	0.3427±0.002	1.35×10^{-5}	0.399±0.003
7.7×10^{-5}	0.3402±0.004	4×10^{-5}	0.397±0.002
1.98×10^{-4}	0.3415±0.003	8.1×10^{-5}	0.400±0.001
3.98×10^{-4}	0.339±0.0033	1.98×10^{-4}	0.399±0.002
5.65×10^{-4}	0.337±0.004	3.98×10^{-4}	0.388±0.002
1.13×10^{-3}	0.320±0.003	5.65×10^{-4}	0.38±0.002
2.26×10^{-3}	0.295±0.003	8.40×10^{-4}	0.364±0.001
3.95×10^{-3}	0.272±0.003	1.13×10^{-3}	0.355±0.001
5.65×10^{-3}	0.243±0.002	2.26×10^{-3}	0.326±0.002
9×10^{-3}	0.2025±0.003	3.95×10^{-3}	0.304±0.001
1.5×10^{-2}	0.1485±0.002	5.65×10^{-3}	0.285±0.001
2.5×10^{-2}	0.1129±0.001	9×10^{-3}	0.240±0.001
3.3×10^{-2}	0.084±0.002	1.5×10^{-3}	0.186±0.0013
4.4×10^{-2}	0.074±0.001	2.5×10^{-2}	0.134±0.001
5×10^{-2}	0.058±0.001	3.3×10^{-2}	0.094±0.004
		4.4×10^{-2}	0.089±0.001
		5×10^{-2}	0.0785±0.001

Table.B12 continue

[Brij-35]/M	k_{obs},35 °C	k_{obs},15 °C	k_{obs},30 °C
0	0.5418±0.003	0.2719±0.001	0.4627±0.003
5×10^{-6}	0.546±0.002	0.2778±0.002	0.4685±0.002
1.4×10^{-5}	0.549±0.002	0.2768±0.002	0.469±0.0023
3.6×10^{-5}	0.544±0.0018	0.281±0.0015	0.4687±0.002
7.7×10^{-5}	0.5476±0.003	0.285±0.002	0.4703±0.005
1.98×10^{-4}	0.548±0.003	0.278±0.001	0.4617±0.001
3.98×10^{-4}	0.546±0.002	0.277±0.001	0.460±0.003
5.65×10^{-4}	0.538±0.003	0.2769±0.001	0.459±0.002
1.13×10^{-3}	0.5156±0.002	0.262±0.001	0.440±0.001
2.26×10^{-3}	0.478±0.003	0.242±0.002	0.409±0.003
3.95×10^{-3}	0.438±0.002	0.223±0.001	0.3746±0.002
5.65×10^{-3}	0.401±0.0015	0.1995±0.001	0.3428±0.004
9×10^{-3}	0.366±0.002	0.166±0.001	0.313±0.001
1.5×10^{-2}	0.302±0-.003	0.1218±0.001	0.242±0.0017
2.5×10^{-2}	0.214±0.002	0.0845±0.0014	0.164±0.002
3.3×10^{-2}	0.172±0.003	0.068±0.001	0.137±0.003
4.4×10^{-2}	0.141±0.001	0.0528±0.004	0.1174±0.002
5×10^{-2}	0.1165±0.001	0.045±0.001	0.0937±0.003

Table.B12: The temperature dependence data for the reaction of 4-(methylthio) benzyl alcohol with 2×10^{-4} M of MCPBA

[Brij-35]/M	k_{obs} at 15 °C	[Brij-35]/M	k_{obs} at 20 °C	[Brij-35]/M	k_{obs} at 25 °C
0	0.0638±0.006	0	0.082±0.003	0	0.102±0.006
3.6×10^{-6}	0.0636±0.005	2×10^{-6}	0.082±0.001	2×10^{-6}	0.101±0.005
1.35×10^{-5}	0.068±0.005	4.5×10^{-6}	0.083±0.002	4.5×10^{-6}	0.1013±0.005
6×10^{-5}	0.0654±0.004	1.35×10^{-5}	0.082±0.002	1.35×10^{-5}	0.099±0.005
9×10^{-5}	0.065±0.003	8×10^{-5}	0.083±0.003	9×10^{-5}	0.103±0.004
2×10^{-4}	0.073±0.005	1.7×10^{-4}	0.096±0.002	2×10^{-4}	0.113±0.006
3.8×10^{-4}	0.087±0.007	2.8×10^{-4}	0.104±0.003	3.8×10^{-4}	0.1277±0.001
5.7×10^{-4}	0.1079±0.007	3.6×10^{-4}	0.111±0.003	5.7×10^{-4}	0.1628±0.001
1.13×10^{-3}	0.1315±0.002	5.7×10^{-4}	0.152±0.003	1.13×10^{-3}	0.191±0.002
1.98×10^{-3}	0.1826±0.001	1.13×10^{-3}	0.183±0.002	1.69×10^{-3}	0.239±0.001
2.82×10^{-3}	0.198±0.001	2.85×10^{-3}	0.218±0.003	2.85×10^{-3}	0.260±0.002
3.955×10^{-3}	0.206±0.001	3.95×10^{-3}	0.246±0.001	3.95×10^{-3}	0.286±0.009
6.78×10^{-3}	0.198±0.003	5.65×10^{-3}	0.238±0.002	5.65×10^{-3}	0.269±0.008
1×10^{-2}	0.1827±0.001	9×10^{-3}	0.222±0.001	9×10^{-3}	0.249±0.009
1.9×10^{-2}	0.1415±0.002	1.5×10^{-2}	0.200±0.001	1.5×10^{-2}	0.221±0.001
2.5×10^{-2}	0.1209±0.001	2.4×10^{-2}	0.157±0.003	2×10^{-2}	0.182±0.001
3.3×10^{-2}	0.1017±0.009	3.3×10^{-2}	0.127±0.002	2.5×10^{-2}	0.1677±0.009
4.4×10^{-2}	0.087±0.001	4.4×10^{-2}	0.099±0.001	3.3×10^{-2}	0.1418±0.002
5×10^{-2}	0.079±0.007	5×10^{-2}	0.087±0.002	4.4×10^{-2}	0.1154±0.009
				5×10^{-2}	0.1088±0.007

Table.B12 continue

[Brij-35]/M	k_{obs} at35 °C	[Brij-35]/M	k_{obs} at 30 °C
0	0.155±0.001	0	0.1267±0.003
4.36×10^{-5}	0.1579±0.0012	2×10^{-6}	0.1205±0.002
1.35×10^{-5}	0.154±0.001	4.5×10^{-6}	0.120±0.002
5.8×10^{-5}	0.158±0.001	1.35×10^{-5}	0.1179±0.0024
9×10^{-5}	0.1618±0.001	8×10^{-5}	0.1217±0.002
2×10^{-4}	0.1889±0.001	1.7×10^{-4}	0.127±0.002
3.8×10^{-4}	0.204±0.0013	2.8×10^{-4}	0.1495±0.003
5.7×10^{-4}	0.239±0.002	3.6×10^{-4}	0.158±0.004
1.13×10^{-3}	0.295±0.006	5.7×10^{-4}	0.197±00.003
1.98×10^{-3}	0.3618±0.004	1.3×10^{-3}	0.230±00.002
2.82×10^{-3}	0.379±0.005	2.85×10^{-3}	0.295±0.003
3.95×10^{-3}	0.3847±0.001	3.95×10^{-3}	0.3277±0.003
6.78×10^{-3}	0.361±0.002	5.65×10^{-3}	0.318±0.003
1×10^{-2}	0.338±0.002	9×10^{-3}	0.301±0.002
1.9×10^{-2}	0.267±0.002	1.5×10^{-2}	0.256±0.002
2.5×10^{-2}	0.223±0.002	2.4×10^{-2}	0.196±0.001
3.3×10^{-2}	0.193±0.001	3.3×10^{-2}	0.1577±0.002
4.4×10^{-2}	0.1589±0.001	4.4×10^{-2}	0.1275±0.001
5×10^{-2}	0.1462±0.008	5×10^{-2}	0.1156 ±0.0025

Table.B13: The temperature dependence data for the reaction of 4-Bromothioanisole 1×10^{-5} M with 5×10^{-4} M peroxymonosulfate..

[Brij-35]/M	k_{obs} at 15 °C	[Brij-35]/M	k_{obs} at 20 °C	k_{obs} at 25 °C
0	0.2175±0.002	0	0.2509±0.004	0.2915±0.004
2×10^{-6}	0.220±0.001	4.5×10^{-6}	0.2537±0.004	0.294±0.002
4.8×10^{-6}	0.216±0.001	6.8×10^{-6}	0.2568±0.003	0.2945±0.002
1.35×10^{-5}	0.217±0.001	1.35×10^{-5}	0.252±0.002	0.2924±0.002
4×10^{-5}	0.2155±0.001	4×10^{-5}	0.249±0.003	0.2878±0.001
8×10^{-5}	0.2145±0.001	8.1×10^{-5}	0.2457±0.003	0.2718±0.001
1.98×10^{-4}	0.198±0.001	1.98×10^{-4}	0.2184±0.005	0.2463±0.001
3.98×10^{-4}	0.161±0.002	3.98×10^{-4}	0.1705±0.003	0.211±0.006
5.7×10^{-4}	0.128±0.001	5.7×10^{-4}	0.1426±0.003	0.157±0.005
8.4×10^{-4}	0.1026±0.007	8.4×10^{-4}	0.1188±0.003	0.1374±0.004
0.00113	0.087±0.008	0.00113	0.0989±0.002	0.1116±0.003
0.00226	0.048±0.006	0.00226	0.0619±0.002	0.065±0.005
0.00395	0.0297±0.003	0.00395	0.0369±0.001	0.0459±0.005
0.00565	0.026±0.002	0.00565	0.0307±0.008	0.0358±0.006
0.009	0.015±0.002	0.009	0.0188±0.005	0.0233±0.004
0.015	0.0086±0.003	0.015	0.01±0.004	0.0117±0.004
0.025	0.007±0.001	0.025	0.008±0.002	0.0089±0.003
0.033	0.0065±0.002	0.033	0.007±0.002	0.0079±0.001
0.044	0.0053±0.002	0.044	0.0056±0.005	0.0065±0.001
0.05	0.0039±0.001	0.05	0.005±0.005	0.0053±0.002

Table.B13 continue

[Brij-35]/M	k_{obs} at 30 °C	[Brij-35]/M	k_{obs} at 35 °C
0	0.354±0.002	0	0.412±0.002
4×10^{-6}	0.3548±0.002	2.3×10^{-6}	0.410±0.0024
6.8×10^{-6}	0.3526±0.002	6.8×10^{-6}	0.4132±0.003
1.35×10^{-5}	0.3527±0.001	1.35×10^{-5}	0.413±0.002
4×10^{-5}	0.3486±0.003	4×10^{-5}	0.4065±0.003
7.7×10^{-5}	0.3419±0.004	7.7×10^{-5}	0.4008±0.002
1.980×10^{-4}	0.3084±0.002	1.98×10^{-4}	0.3715±0.003
3.980×10^{-4}	0.2564±0.004	3.980×10^{-4}	0.305±0.002
5.700×10^{-4}	0.2125±0.002	5.7×10^{-4}	0.241±0.002
0.00113	0.159±0.001	0.00113	0.192±0.002
0.00226	0.0896±0.001	0.00226	0.107±0.002
0.00395	0.0639±0.001	0.00395	0.076±0.003
0.00565	0.0446±0.005	0.0056	0.0531±0.001
0.009	0.0278±0.003	0.009	0.0331±0.001
0.015	0.0197±0.004	0.015	0.0234±0.003
0.025	0.0116±0.002	0.025	0.0137±0.003
0.033	0.0098±0.002	0.033	0.0118±0.001
0.044	0.0073±0.002	0.044	0.0085±0.001
0.05	0.0061±0.0016	0.05	0.0074±0.004

Table.B13: The temperature dependence data for the reaction of 4-Bromothioanisole 1×10^{-5} M with 5×10^{-4} M MCPBA.

[Brij-35]/M	k_{obs} at 15 °C	k_{obs} at 20 °C	k_{obs} at 30 °C
0	0.0413±0.001	0.0518±0.0004	0.085±0.001
4.25×10^{-6}	0.0414±0.0005	0.051±0.0006	0.084±0.0006
9×10^{-6}	0.0413±0.001	0.051±0.0006	0.085±0.002
3.65×10^{-5}	0.0415±0.001	0.060±0.001	0.096±0.001
7.68×10^{-5}	0.0594±0.002	0.078±0.001	0.119±0.001
1.25×10^{-4}	0.068±0.002	0.133±0.001	0.166±0.003
1.98×10^{-4}	0.104±0.001	0.170±0.002	0.230±0.002
3.75×10^{-4}	0.184±0.003	0.280±0.003	0.371±0.004
5.7×10^{-4}	0.2624±0.002	0.366±0.004	0.532±0.003
0.00113	0.2924±0.006	0.420±0.005	0.630±0.005
0.0028	0.273±0.004	0.414±0.007	0.618±0.007
0.00395	0.235±0.003	0.378±0.005	0.565±0.007
0.0073	0.1815±0.001	0.332±0.006	0.489±0.006
0.009	0.1496±0.001	0.279±0.005	0.415±0.005
0.0146	0.1089±0.001	0.203±0.003	0.297±0.004
0.02	0.088±0.006	0.157±0.002	0.233±0.002
0.033	0.05±0.005	0.103±0.004	0.160±0.002
0.044	0.036±0.002	0.072±0.003	0.125±0.004
0.05	0.03±0.002	0.061±0.003	0.101±0.005

Table.B13 continue.

[Brij-35]/M	k_{obs} at 25 °C	[Brij-35]/M	k_{obs} at 35 °C
0	0.066±0.0006	0	0.107±0.0007
2×10^{-6}	0.068±0.0006	4.25×10^{-6}	0.110±0.0007
4.52×10^{-6}	0.065±0.0005	9×10^{-6}	0.105±0.004
1.35×10^{-5}	0.070±0.0006	3.65×10^{-5}	0.117±0.001
8.1×10^{-5}	0.098±0.001	7.68×10^{-5}	0.139±0.001
1.98×10^{-4}	0.198±0.003	0.000125	0.197±0.002
3.98×10^{-4}	0.315±0.004	0.000198	0.273±0.001
5.65×10^{-4}	0.471±0.005	0.000375	0.427±0.003
0.00113	0.525±0.006	0.00057	0.613±0.004
0.00169	0.555±0.006	0.00113	0.736±0.006
0.00285	0.521±0.009	0.0028	0.681±0.008
0.00395	0.483±0.008	0.00395	0.647±0.006
0.00565	0.410±0.007	0.0073	0.549±0.007
0.009	0.358±0.008	0.009	0.472±0.005
0.015	0.226±0.004	0.0146	0.368±0.006
0.02	0.175±0.003	0.02	0.290±0.003
0.024	0.148±0.003	0.033	0.193±0.003
0.033	0.129±0.002	0.044	0.140±0.002
0.044	0.109±0.002	0.05	0.135±0.003
0.05	0.096±0.002		

Appendix C

Table.C1: The Observed first order rate for the oxidation of 4-nitrothioanisole by MCPBA in 0.003 M nitric acid at different temperature.

[α-CD] / M	k_{obs} ,15	k_{obs} ,20	k_{obs} ,25
0	0.0065±0.0002	0.0085±0.0004	0.0109±0.005
0.00008	0.0105±0.0003	0.0137±0.0004	0.016±0.001
0.0004	0.0209±0.001	0.0272±0.001	0.0273±0.001
0.0006	0.0275±0.001	0.0357±0.0004	0.0346±0.01
0.0008	0.0304±0.0007	0.0396±.0004	0.0387±0.001
0.0014	0.0357±0.001	0.0432±0.0001	0.0475±0.0001
0.004	0.0287±.001	0.0374±0.001	0.0508±0.001
0.006	0.0189±0.0006	0.0265±0.0004	0.0396±0.001
0.008	0.0137±.0004	0.0218±0.001	0.032±0.0006
0.01	0.0101±0.0003	0.0164±0.0002	0.0267±0.001
0.015	0.0062±0.0004	0.0096±0.001	0.0159±0.004
0.02	0.0035±0.0002	0.0059±0.0004	0.0099±.0002
0.025	0.0021±0.0003	0.0032±0.0004	0.0069±0.0002
0.03	0.0016±0.0002	0.0024±0.0002	0.0052±0.0003

Table.C1: continue

[α-CD] / M	k_{obs},30	k_{obs},35
0	0.0165±0.0004	0.0224±0.001
8×10^{-5}	0.0203±0.0003	0.0246±0.0021
4×10^{-4}	0.0312±0.0002	0.0377±0.001
6×10^{-4}	0.0382±0.0001	0.046±0.001
8×10^{-4}	0.0414±0.0005	0.0501±0.001
0.0014	0.0551±0.0005	0.0633±0.0002
0.004	0.0652±0.0004	0.080±0.00023
0.006	0.0581±0.001	0.0715±0.0003
0.008	0.0476±0.001	0.063±0.002
0.01	0.0412±0.0003	0.0548±0.001
0.015	0.0301±0.0002	0.040±0.001
0.02	0.0201±0.001	0.0268±0.0006
0.025	0.0145±0.0002	0.0192±0.001
0.03	0.0106±0.0004	0.0142±0.001

Table.C2: The Observed first order rate for the oxidation of 4-nitrothioanisole by peroxymonosulfate in 0.003 M nitric acid at different temperature

[α-CD] / M	k_{obs} ,15	k_{obs} ,20	[α-CD] / M	k_{obs} ,25
0	0.040 ± 0.0001	0.050 ± 0.0004	0	0.062 ± 0.002
8×10^{-5}	0.040 ± 0.0014	0.051 ± 0.001	8×10^{-5}	0.060 ± 0.003
4×10^{-4}	0.040 ± 0.0001	0.0507 ± 0.001	4×10^{-4}	0.0598±0.003
6×10^{-4}	0.039 ± 0.0001	0.0503 ± 0.004	6×10^{-4}	0.0583 ± 0.002
8×10^{-4}	0.037 ± 0.0001	0.0492 ± 0.004	8×10^{-4}	0.058 ± 0.002
0.0014	0.033 ± 0.001	0.043 ± 0.004	0.0014	0.0537 ± 0.001
0.002	0.028 ± 0.001	0.0375 ± 0.005	0.002	0.0488 ± 0.002
0.004	0.018 ± 0.001	0.0243 ± 0.006	0.004	0.0371 ± 0.001
0.006	0.011 ± 0.0003	0.0151 ± 0.001	0.006	0.0273 ± 0.007
0.008	0.008 ± 0.0006	0.0108 ± 0.001	0.008	0.0207 ± 0.005
0.015	0.003 ± 0.001	0.0051 ± 0.001	0.01	0.016 ± 0.004
0.025	0.0019 ± 0.001	0.0025 ± 0.004	0.015	0.011 ± 0.003
0.03	0.0015 ± 0.001	0.0019 ± 0.003	0.02	0.0073 ± 0.005
			0.03	0.0043 ± 0.003

Table.C2: continue

[α-CD] / M	k_{obs},30	k_{obs},35
0	0.0785 ± 0.0003	0.094 ± 0.0005
8×10^{-5}	0.078± 0.00027	0.094 ± 0.0003
4×10^{-4}	0.075 ± 0.0002	0.090 ± 0.0002
6×10^{-4}	0.075 ± 0.0004	0.090 ± 0.0002
8×10^{-4}	0.073 ± 0.0004	0.088 ± 0.0003
0.0014	0.068 ± 0.0003	0.084 ± 0.0002
0.002	0.065 ± 0.0003	0.08 0± 0.0002
0.004	0.053 ± 0.0004	0.065 ± 0.0001
0.006	0.042 ± 0.0004	0.053 ± 0.0001
0.008	0.035 ± 0.0002	0.044 ± 0.0001
0.01	0.029 ± 0.0005	0.037 ± 0.0008
0.015	0.020 ± 0.0005	0.026 ± 0.0006
0.02	0.014 ± 0.0003	0.018 ± 0.0004
0.025	0.010 ± 0.0003	0.014 ± 0.0004
0.03	0.0089± 0002	0.011 ± 0.0005

Table.C3: The Observed first order rate for the oxidation of 4-methoxythioanisole by 2×10^{-4} M MCPBA in 0.003 M nitric acid at different temperature

[α-CD] / M	k_{obs},20	k_{obs},25	k_{obs},15	k_{obs},30	k_{obs},35
0	0.169±0.003	0.20±0.005	0.128±0.003	0.274±0.005	0.356±0.01
8×10^{-5}	0.228±0.004	0.26±0.004	0.193±0.002	0.326±0.008	0.382±0.006
4×10^{-4}	0.39±0.007	0.47±0.007	0.309±0.004	0.482±0.01	0.539±0.01
6×10^{-4}	0.491±0.006	0.56±0.01	0.425±0.005	0.578±0.01	0.635±0.01
8×10^{-4}	0.575±0.008	0.63±0.01	0.519±0.007	0.666±0.013	0.711±0.01
0.0014	0.681±0.01	0.77±0.013	0.594±0.006	0.794±0.02	0.866±0.02
0.002	0.714±0.01	0.80±0.02	0.627±0.01	0.861±0.02	0.98±0.018
0.004	0.749±0.014	0.90±0.02	0.596±0.01	1.04±0.02	1.209±0.03
0.006	0.61±0.02	0.80±0.012	0.425±0.008	0.965±0.03	1.13±0.029
0.008	0.470±0.013	0.65±0.015	0.288±0.009	0.86±0.029	1.05±0.028
0.01	0.354±0.02	0.51±0.005	0.193±0.005	0.734±0.035	0.991±0.03
0.015	0.213±0.003	0.32±0.006	0.102±0.004	0.466±0.002	0.708±0.02
0.02	0.134±0.002	0.19±0.004	0.07±0.003	0.328±0.003	0.533±0.01
0.025	0.096±0.004	0.15±0.003	0.043±0.002	0.236±0.005	0.407±0.01
0.03	0.067±0.003	0.10±0.028	0.033±0.002	0.175±0.006	0.271±0.006
0.0375	0.031±0.005	0.05±0.002	0.011±0.003	0.119±0.004	0.178±0.006
0.0475	0.026±0.004	0.04±0.001	0.010±0.008	0.089±0.01	0.165±0.001

Table.C4: The Observed first order rate for the oxidation of 4-methoxythioanisole by 4.8×10^{-4} M peroxymonosulfate in 0.003 M nitric acid at different temperature.

[α-CD] / M	k_{obs},15	k_{obs},20	k_{obs},25	k_{obs},30	k_{obs},35
0	0.56±0.02	0.629±0.009	0.702±0.01	0.768±0.006	0.845±0.014
8×10^{-5}	0.54±0.01	0.615±0.016	0.691±0.006	0.765±0.014	0.839±0.006
4×10^{-4}	0.51±0.018	0.610±0.02	0.687±0.004	0.761±0.01	0.84±0.008
6×10^{-4}	0.49±0.009	0.583±0.015	0.669±0.01	0.751±0.01	0.837±0.02
8×10^{-4}	0.48±0.013	0.576±0.01	0.667±0.01	0.751±0.01	0.835±0.03
0.0014	0.41±0.008	0.519±.02	0.627±0.009	0.703±0.011	0.78±0.01
0.002	0.36±0.006	0.453±.019	0.544±0.009	0.634±0.009	0.72±0.02
0.004	0.21±0.005	0.322±..02	0.429±0.007	0.549±0.013	0.67±0.007
0.006	0.15±0.005	0.237±.014	0.320±0.006	0.425±0.008	0.53±0.01
0.008	0.12±0.004	0.186±.008	0.247±0.005	0.355±0.007	0.463±0.01
0.01	0.07±0.002	0.136±0.009	0.200±0.006	0.298±0.003	0.396±0.009
0.015	0.04±0.002	0.087±0.008	0.126±0.003	0.216±0.003	0.307±0.007
0.02	0.03±0.007	0.060±0.006	0.092±0.00	0.163±0.002	0.234±0.007
0.025	0.019±0.005	0.040±0.006	0.060±0.002	0.105±0.005	0.15±0.004
0.03	0.015±0.007	0.033±0.005	0.051±0.002	0.089±0.006	0.126±0.006
0.0375	0.013±0.004	0.027±0.004	0.042±0.006	0.074±0.002	0.106±0.005
0.045	0.007±0.003	0.016±0.005	0.025±0.01	0.050±0.001	0.075±0.004

Table.C5: The Observed first order rate for the oxidation of 4-(methylthio) benzyl alcohol by 2×10^{-4} M MCPBA in 0.003 M nitric acid at different temperature

[α-CD] / M	k_{obs},15	k_{obs},20	k_{obs},25	k_{obs},30	k_{obs},35
0	0.063±0.001	0.082±0.005	0.101±0.001	0.126±0.002	0.155±0.003
8×10^{-5}	0.117±0.004	0.13±0.002	0.150±0.001	0.190±0.001	0.230±0.001
4×10^{-4}	0.23±0.002	0.248±0.001	0.285±0.002	0.317±0.002	0.349±0.002
6×10^{-4}	0.287±0.002	0.321±0.002	0.362±0.002	0.398±0.003	0.436±0.003
8×10^{-4}	0.34±0.002	0.380±0.003	0.423±0.002	0.459±0.003	0.495±0.002
0.0014	0.453±0.004	0.493±0.004	0.552±0.003	0.599±0.004	0.646±0.004
0.002	0.486±0.004	0.555±0.003	0.642±0.004	0.700±0.003	0.759±0.005
0.004	0.525±0.005	0.669±0.004	0.762±0.005	0.864±0.006	0.966±0.007
0.006	0.484±0.004	0.614±0.007	0.772±0.005	0.904±0.007	1.036±0.009
0.008	0.432±0.004	0.560±0.006	0.723±0.005	0.870±0.007	1.018±0.008
0.01	0.377±0.004	0.508±0.004	0.682±0.004	0.836±0.005	0.990±0.008
0.015	0.276±0.002	0.390±0.003	0.553±0.003	0.730±0.006	0.908±0.007
0.02	0.199±0.002	0.302±0.003	0.427±0.004	0.599±0.005	0.771±0.006
0.025	0.151±0.001	0.238±0.003	0.341±0.002	0.497±0.004	0.653±0.005
0.03	0.116±0.001	0.189±0.002	0.289±0.002	0.428±0.003	0.568±0.004
0.035	0.094±0.001	0.140±0.002	0.240±0.002	0.369±0.003	0.499±0.003
0.045	0.063±0.002	0.099±0.008	0.174±0.001	0.285±0.004	0.396±0.003

Table.C6: The Observed first order rate for the oxidation of 4-(methylthio) benzyl alcohol by 4.8×10^{-4} M peroxymonosulfate in 0.003 M nitric acid at different temperature

[α-CD] / M	k_{obs},15	k_{obs},20	k,25	k_{obs},30	k_{obs},35
0	0.271±0.001	0.34±0.002	0.40±0.002	0.46±0.003	0.54±0.002
8×10^{-5}	0.275±0.002	0.339±0.0016	0.403±0.002	0.461±0.002	0.540±0.003
4×10^{-4}	0.274±0.002	0.336±0.0015	0.398±0.002	0.458±0.003	0.539±0.004
6×10^{-4}	0.270±0.002	0.334±0.002	0.397±0.002	0.454±0.002	0.53±0.003
8×10^{-4}	0.269±0.002	0.329±0.003	0.390±0.002	0.450±0.002	0.531±0.004
0.0014	0.259±0.002	0.320±0.002	0.381±0.002	0.443±0.004	0.523±0.003
0.002	0.252±0.002	0.312±0.004	0.372±0.002	0.427±0.003	0.501±0.002
0.004	0.213±0.002	0.266±0.002	0.319±0.002	0.378±0.002	0.454±0.002
0.006	0.174±0.001	0.227±0.003	0.281±0.002	0.340±0.004	0.414±0.002
0.008	0.148±0.009	0.198±0.003	0.249±0.001	0.304±0.003	0.374±0.002
0.01	0.129±0.008	0.176±0.001	0.223±0.002	0.282±0.003	0.355±0.001
0.015	0.090±0.008	0.131±0.002	0.173±0.001	0.224±0.002	0.286±0.002
0.02	0.0631±0.005	0.099±0.001	0.135±0.008	0.182±0.005	0.237±0.001
0.025	0.048±0.003	0.077±0.006	0.107±0.007	0.152±0.004	0.203±0.002
0.03	0.036±0.002	0.062±0.001	0.088±0.006	0.130±0.003	0.179±0.001
0.035	0.027±0.002	0.049±0.004	0.071±0.001	0.106±0.003	0.146±0.001
0.045	0.019±0.003	0.036±0.003	0.053±0.002	0.080±0.005	0.111±0.006

Table.C7: The Observed first order rate for the oxidation of methyl *p*-tolyl sulfide by 2×10^{-4} M MCPBA in 0.003 M nitric acid at different temperature

[α-CD] / M	k_{obs},15	k_{obs},20	k_{obs},30
0	0.089±0.002	0.117±0.004	0.187±0.003
8×10^{-5}	0.165±0.0045	0.195±0.004	0.258±0.002
4×10^{-4}	0.345±0.005	0.37±0.006	0.434±0.006
6×10^{-4}	0.443±0.0053	0.470±0.005	0.539±0.006
8×10^{-4}	0.494±0.68	0.551±0.006	0.619±0.007
0.0014	0.619±0.006	0.635±0.007	0.818±0.009
0.002	0.591±0.004	0.680±0.007	0.892±0.01
0.004	0.399±0.002	0.593±0.006	0.923±0.008
0.006	0.246±0.002	0.407±0.007	0.748±0.007
0.008	0.158±0.001	0.289±0.004	0.576±0.005
0.01	0.108±0.005	0.201±0.003	0.471±0.005
0.015	0.061±0.007	0.117±0.004	0.275±0.003
0.02	0.033±0.003	0.060±0.005	0.177±0.002
0.025	0.026±0.008	0.039±0.005	0.132±0.004
0.03	0.019±0.005	0.030±0.003	0.088±0.002
0.035	0.015±0.004	0.029±0.006	0.062±0.009
0.045	0.013±0.001	0.020±0.004	0.040±0.005

[α-CD] / M	k_{obs},25	[α-CD] / M	k_{obs},35
0	0.141±0.001	0	0.24±0.002
8×10^{-5}	0.198±.003	8×10^{-5}	0.27±0.004
4×10^{-4}	0.396±0.005	4×10^{-4}	0.478±0.005
6×10^{-4}	0.483±0.01	6×10^{-4}	0.567±0.004
8×10^{-4}	0.575±0.006	8×10^{-4}	0.655±0.003
0.002	0.799±0.01	0.002	0.977±0.008
0.004	0.718±0.01	0.004	1.032±0.006
0.006	0.547±0.006	0.006	0.956±0.004
0.008	0.383±0.004	0.008	0.785±0.003
0.01	0.303±0.003	0.01	0.642±0.002
0.015	0.161±0.002	0.015	0.438±0.004
0.02	0.102±0.001	0.02	0.303±0.004
0.025	0.075±0.002	0.025	0.201±0.003
0.03	0.055±0.0006	0.03	0.138±0.004
0.035	0.041±0.0008	0.035	0.111±0.007
0.045	0.023±0.0006	0.045	0.063±0.002

Table.C8: Observed first order rate for the oxidation of methyl *p*-tolyl sulfide by 4.8×10^{-4} M peroxymonosulfate in 0.003 M nitric acid at different temperature.

[α-CD] / M	k_{obs} ,15	k_{obs},20	k_{obs},25	k_{obs} ,30	k_{obs} ,35
0	0.37±0.005	0.434±0.004	0.501±0.0052	0.559±0.004	0.653±0.01
8×10^{-5}	0.377±0.005	0.442±0.006	0.503±0.0054	0.567±0.006	0.6593±0.01
4×10^{-4}	0.371±0.004	0.438±0.005	0.505±0.004	0.554±0.006	0.661±0.008
6×10^{-4}	0.362±0.0048	0.422±0.005	0.498±0.005	0.540±0.004	0.655±0.008
8×10^{-4}	0.323±0.004	0.406±0.005	0.470±0.006	0.512±0.006	0.648±0.008
0.0014	0.282±0.003	0.342±0.004	0.447±0.004	0.489±0.005	0.616±0.007
0.002	0.227±0.003	0.294±0.002	0.408±0.0035	0.452±0.004	0.569±0.006
0.004	0.123±0.001	0.194±0.004	0.274±0.002	0.342±0.003	0.445±0.006
0.006	0.074±0.007	0.129±0.007	0.191±0.002	0.245±0.002	0.333±0.005
0.008	0.050±0.006	0.088±0.003	0.132±0.001	0.182±0.002	0.258±0.0053
0.01	0.040±0.004	0.067±0.002	0.092±0.001	0.147±0.01	0.209±0.003
0.015	0.018±0.002	0.037±0.005	0.063±0.0008	0.086±0.006	0.129±0.002
0.02	0.010±0.005	0.022±0.007	0.037±0.004	0.055±0.004	0.086±0.001
0.025	0.007±0.008	0.017±0.007	0.027±0.003	0.038±0.005	0.061±0.002
0.03	0.005±0.005	0.012±0.004	0.020±0.003	0.031±0.005	0.047±0.008
0.035	0.004±0.005	0.008±0.004	0.014±0.004	0.022±0.003	0.036±0.003
0.045	0.0029±0.004	0.005±0.003	0.010±0.006	0.016±0.0042	0.025±0.0027

Table.C9: The Observed first order rate for the oxidation of 4-bromothioanisole by 2×10^{-4} M MCPBA in 0.003 M nitric acid at different temperature

[α-CD]/M	$k_{obs},15^0$	$k_{obs},20$	$k_{obs},25$	$k_{obs},30$	$k_{obs},35$
0	0.0413±0.003	0.0529±0.002	0.066±0.004	0.085±0.002	0.107±0.006
$8.\times10^{-5}$	0.0588±0.005	0.0789±0.004	0.092±0.005	0.110±.002	0.129±0.008
4×10^{-4}	0.1148±0.008	0.1295±0.007	0.148±0.01	0.173±0.001	0.198±0.001
6×10^{-4}	0.125±0.008	0.1468±0.006	0.184±0.001	0.194±0.003	0.220±0.001
8×10^{-4}	0.130±0.007	0.1557±0.007	0.196±0.001	0.216±0.001	0.255±0.002
0.0014	0.1057±0.008	0.146±0.006	0.196±0.001	0.230±0.009	0.272±0.002
0.002	0.0822±0.003	0.1219±0.003	0.166±0.002	0.216±0.005	0.27±.001
0.004	0.0338±0.001	0.062±.002	0.091±0.006	0.148±0.003	0.202±0.001
0.006	0.0168±0.008	0.0351±0.002	0.054±0.005	0.099±0.002	0.144±0.007
0.008	0.011±0.007	0.0234±0.01	0.036±0.003	0.067±0.001	0.098±0.006
0.01	0.0074±0.003	0.015±.004	0.023±0.002	0.047±0.001	0.070±0.003
0.015	0.0046±0.006	0.0093±0.007	0.014±0.002	0.029±.001	0.043±0.003
0.02	0.0027±0.002	0.0078±0.003	0.009±0.007	0.018±0.002	0.027±0.001
0.025	0.002±0.003	0.0046±0.004	0.007±0.004	0.013±0.004	0.017±0.002
0.03	0.001±0.0058		0.0045±0.001		
0.035		0.0027±0.002		0.0093±0.002	0.012±0.006

Table.C10: the Observed first order rate for the oxidation of 4-bromothioanisole by 4.8×10^{-4} M peroxymonosulfate in 0.003 M nitric acid at different temperature.

[α-CD]/M	k_{obs} ,15	k_{obs} ,20	k_{obs} ,25	k_{obs} ,30	k_{obs} ,35
0	0.217±0.002	0.250±0.004	0.291±0.003	0.354±0.002	0.412±0.003
8×10^{-5}	0.216±0.001	0.249±0.002	0.282±0.002	0.341±0.006	0.397±0.002
4×10^{-4}	0.191±0.002	0.219±0.001	0.274±0.002	0.342±0.01	0.381±0.003
6×10^{-4}	0.167±0.001	0.197±0.002	0.239±0.002	0.314±0.009	0.366±0.002
8×10^{-4}	0.151±0.09	0.188±0.005	0.224±0.001	0.292±.006	0.314±0.002
0.0014	0.111±0.006	0.149±0.005	0.182±0.001	0.233±0.001	0.280±0.003
0.002	0.079±0.005	0.110±0.004	0.150±0.01	0.198±0.003	0.184±0.002
0.004	0.040±0.002	0.063±0.003	0.082±0.005	0.121±0.003	0.141±0.001
0.006	0.027±0.002	0.043±0.005	0.055±0.004	0.089±0.005	0.101±0.008
0.008			0.039±0.003	0.064±0.002	0.084±0.007
0.01	0.016±0.001	0.025±0.003	0.032±0.003	0.053±0.004	0.061±0.004
0.015			0.022±0.002	0.038±0.003	0.044±0.006
0.02	0.007±0.005	0.0128±0.004	0.016±0.001		
0.025			0.012±0.008		
0.03	0.005±0.003	0.008±0.002	0.010±0.007	0.017±0.01	0.028±0.002
0.035				0.014±0.004	0.024±0.002
0.04	0.003±0.003	0.005±0.002		0.014±0.005	0.021±0.002

Equation.C1: Computer programme used for fitting kinetic data utilizing bisection method

If solvent=1 Then
Return ($k_a + k_{a1}$*cdt + k_{a2}*cdt^2)/((1+(K_P+K_I)*cdt + K_P*K_I*cdt^2))

Endif

If solvent=2 Then
cdu := cdt
cdl := 0
:bisect
diff := cdu - cdl
If abs(diff) < 1e-13 Then
Goto done
Endif
cdf := (cdu+cdl)/2
cdclo :=Kclo*cdf*clo
cdi :=KI*cdf*I
func := cdf + cdclo + cdi
If func > cdt Then
cdu := cdf
Else
cdl := cdf
Endif
Goto bisect
:done
cdf := (cdl + cdu)/2

Return ($k_b + k_{b1}$*cdf + k_{b2}*cdf^2)/((1+(K_P+K_I)*cdf + K_P*K_I*cdf^2))

Endif
If solvent=3 Then
cdf=cdt/(Kso4*so4+1)
Return ($k_c + k_{c1}$*cdf + k_{c2}*cdf^2)/((1+(K_P+K_I)*cdf + K_P*K_I*cdf^2))

Endif
If solvent=4 Then
cdu := cdt
cdl := 0
:bisect1
diff := cdu - cdl
If abs(diff) < 1e-13 Then
Goto done1
Endif
cdf := (cdu+cdl)/2
cdclo :=Kclo*cdf*clo1
cdi :=K_I*cdf*I
func := cdf + cdclo + cdi
If func > cdt Then
cdu := cdf
Else

```
cdl := cdf
Endif
Goto bisect1
:done1
cdf := (cdl + cdu)/2

Return (k_d + k_dl*cdf + kd2*cdf^2 )/((1+(K_P+K_I)*cdf + K_P*K_I*cdf^2))

Endif
```

Solvent 1, 2, 3 and 4 represent the reaction in nitric acid, 1M $NaClO_4$, 0.35 M Na_2SO_4 and 0.2 M $NaClO_4$

Cdf is the free cyclodextrin, cdt is total cyclodextrin concentrations.

A Kinetic and Thermodynamic Study of the Reduction of Peroxyacids by Iodide and Aryl Alkyl Sulfides in the Presence of Non-ionic Surfactants and α-Cyclodextrin.

SALEM MANSOUR MOUSA

PhD

2009

A Kinetic and Thermodynamic Study of the Reduction of Peroxyacids by Iodide and Aryl Alkyl Sulfides in the Presence of Non-ionic Surfactants and α-Cyclodextrin.

A thesis submitted in partial fulfilment

of the requirements of the

University of Northumbria at Newcastle

For the degree of

Doctor of Philosophy

Research undertaken in the School of applied Science

at Northumbria University

2009

ACKNOWLEDGMENT

All powers belong to almighty God, the creator of whole universe, who provide me the knowledge and strength to complete this work.

I wish to express my sincere gratitude to my supervisors Dr. Michael Deary and Dr. Martin Davies for their guidance and cooperation throughout this work, and also speciall thanks to Dr Michael Deary for reading the manuscript of this thesis and making many suggestions which helped materially to clear and improve this thesis.

Also I wish to express my thanks to Mr Gary Askwith, for his assistance during this research work.

Also I am indebted to my sponsor, Libyan Government, for paying the fees and living expense during my study.

Finally I would like to acknowledge my parents and wife for their help and encouragement at each and every step.

Declaration

I declare that the work contained in this thesis has not been submitted for any other award and that it is all my own work.

Name: SALEM MANSOUR MOUSA

Signature:

Date: 07/05/2009

Table of content

Abstract

The objectives of this study were two-fold: firstly to add to existing knowledge about the reaction of peracid with both iodide and sulfides in the presence of micelles (anionic and non-ionic) and α-cyclodextrin. The reaction between iodide and peracid had previously been studied only at 25°C in non-ionic, anionic micellar and alpha cyclodextrin; while the reaction of sulfides and peracid had only been investigated in the presence of α-cyclodextrin at one temperature. This study has investigated the previously undetermined effect of temperature on these reactions and how changes in temperature can affect the process of reactants binding to the micelle or cyclodextrin catalyst. The second objective was to obtain quantitative information about reactivity in ordered aqueous media such as micellar systems and cyclodextrins, and find out how these media can affect and control these reactions. This might have implications for fields such as cell biology, specifically for process occurring in living cells since both cyclodextrins and micelles might be considered simple models for protein and membranes in terms of their hydrophobicity. In addition, little information is known about bimolecular reactions involving two neutral reactants in non-ionic micelles where only the hydrophobic interaction is likely to influence the reaction due to the absence of charge-charge interaction.

A kinetic and thermodynamic investigation of the reactions between peracids and different reductants i.e. iodide and series of aryl alkyl sulfides in presence non-ionic micelle and α- cyclodextrin is reported in this work. The kinetics were conducted by monitoring spectrophotometrically the increase or decrease in the absorbance due to formation of triioidide or disappearance of sulfides respectively, and absorbance versus time plots were fitted to nonlinear equation in order to obtain the observed pseudo first order rate constants.

For reactions carried out in micellar systems the kinetic data were treated using the multiple micellar pseudophase model developed by Davies which considers the partition of reactants between water in the bulk aqueous phase and that in the micellar pseudophases. Important parameters in this model include the binding constant of reactants to Brij (non-ionic micelle) and k_{mic} (reaction rate in micelle). For reactions in α-cyclodextrin, data was fitted to rate equations containing first and second order dependencies on cyclodextrin using non linear regression techniques.

The work was carried out in the presence of 0.003 M nitric acid as reaction medium. The effect of inorganic electrolytes (sodium nitrate, sulfate, actetate, perchlorate and chloride)

on the rate of oxidation of iodide in the absence and presence of non-ionic surfactant brij-35 was also studied. The critical micelle concentration (CMC) of the surfactants was determined using kinetic techniques and was found to be inversely proportional to the salt concentration and also to the temperature. The CMC was also found to decrease as the length of the hydrophobic part of the Brij surfactants was increased, possibly due to the decrease of interfacial energy on micellization, which generally increases in with increasing hydrophobic chain length.

It was shown from analysis of the kinetic data that all non-ionic micelles in the (absence of salts) and α-CD studied in this work enhanced the rate of the iodide oxidation by MCPBA and that the rate showed saturation type kinetics. Sulfate ions were shown to accelerate the reaction further, whereas perchlorate caused an inhibition of the iodide oxidation (compared to the reaction only in nitric acid) in presence of Brij-35, but an increase in the presence of α-cyclodextrin. For the oxidation of sulfides by MCPBA in micelles and α-CD the observed rate increases to a maximum with increasing micelle or α-CD concentration and then subsequently declines. In the case of sulfide oxidation by the anionic peracid, peroxymonosulfate (PMS), there was only inhibition in the rate, due to separation of reactants.

The effect of temperature on both rate and equilibrium processes for these systems was determined over the range 15 to 35°C. The results showed a linear decrease in the binding of metachloroperbenzoic (MCPBA) acid and aryl alkyl sulfides to both micelle and α-CD with increasing the temperature.

The thermodynamic and activation parameters for the reactions were determined by using Van't Hoff and Eyring plots. Comparison of the micellar association constants of MCPBA and the apparent micellar association constant of the transition state for the reaction with iodide, suggested that orientational restriction imposed on the peracid by Brij-35 are similar to that in the transition state. For the same reactions carried out in α-cyclodextrin at different temperatures it was determined that the binding constant enthalpy and entropy of substrates, (peracid and iodide) are more negative than that obtained in the presence of brij-35 which indicates that stronger interactions are involved and more restriction imposed on the reactant in presence of α-CD compared to brij-35.

A similar approach was employed for the reaction of series of aryl alkyl sulfides with peracids (PMS and MCPBA) in presence of Brij-35 and α-CD. The aryl alkyl sulfides can form both 1:1 and 2:1 host: guest complexes in cyclodextrin; the 2:1 inclusion

complexes for some sulfides were larger than the 1:1 complexes, indicating cooperative binding, with the driving force for this possibly being a substrate induced dipole-dipole interaction between the two cyclodextrin molecules. Linear free energy studies indicate that the catalytic species is the bound peracid reacting with the unbound sulfides; sulfide binding results in steric inhibition of the reaction. The reaction of the non-binding PMS with sulfides results only in inhibition as cyclodextrin concentration is increased.

The enthalpy and entropy for sulfide oxidation by peracids was calculated by means of a Van't Hoff plot. The reaction in α-CD associated with more negative entropy and enthalpy for the inclusion 2:1 while for 1:1 some substrates associated with positive entropy and small negative enthalpy while other show the usual behaviour observed for complex formation (negative values for both enthalpy and entropy).

In all studied reactions (related reactions) there were good relationships between enthalpy and entropy (isokinetic relationships or enthalpy-entropy compensation). Whilst in some cases it is difficult to explain why enthalpy-entropy compensation might be observed, we have suggested that in the case of binding of sulfides to cyclodextrin these plots can act as probes into the orientation of the substrate within the cyclodextrin cavity.

The nature of the catalytic mechanism for the reactions of peracids with sulfides and iodide in the presence of micelles and α-cyclodextrin was examined by comparing the transition state stabilisation parameters, K_{TS1}, for the same reaction in the two catalytic systems. It was found that for three out of five sulfides the degree of transition state stabilisation was almost identical in both Brij-35 and α-cyclodextrin, perhaps suggesting the same catalytic mechanism in each system; this could be via either decreased stabilisation of the peracid ground state in the absence of a protic solvent and / or the prevention of significant charge development in the transition state as a result of an intramolecular proton transfer step involving the peracid that is facilitated by the absence of water. Other possibilities exist, such as general acid catalysis, though these would be more dependent on the nature of the catalytic system. There was a less clear relationship for iodide.

Abstract

The objectives of this study were two-fold: firstly to add to existing knowledge about the reaction of peracid with both iodide and sulfides in the presence of micelles (anionic and non-ionic) and α-cyclodextrin. The reaction between iodide and peracid had previously been studied only at 25°C in non-ionic, anionic micellar and alpha cyclodextrin; while the reaction of sulfides and peracid had only been investigated in the presence of α-cyclodextrin at one temperature. This study has investigated the previously undetermined effect of temperature on these reactions and how changes in temperature can affect the process of reactants binding to the micelle or cyclodextrin catalyst. The second objective was to obtain quantitative information about reactivity in ordered aqueous media such as micellar systems and cyclodextrins, and find out how these media can affect and control these reactions. This might have implications for fields such as cell biology, specifically for process occurring in living cells since both cyclodextrins and micelles might be considered simple models for protein and membranes in terms of their hydrophobicity. In addition, little information is known about bimolecular reactions involving two neutral reactants in non-ionic micelles where only the hydrophobic interaction is likely to influence the reaction due to the absence of charge-charge interaction.

A kinetic and thermodynamic investigation of the reactions between peracids and different reductants i.e. iodide and series of aryl alkyl sulfides in presence non-ionic micelle and α- cyclodextrin is reported in this work. The kinetics were conducted by monitoring spectrophotometrically the increase or decrease in the absorbance due to formation of triioidide or disappearance of sulfides respectively, and absorbance versus time plots were fitted to nonlinear equation in order to obtain the observed pseudo first order rate constants.

For reactions carried out in micellar systems the kinetic data were treated using the multiple micellar pseudophase model developed by Davies which considers the partition of reactants between water in the bulk aqueous phase and that in the micellar pseudophases. Important parameters in this model include the binding constant of reactants to Brij (non-ionic micelle) and k_{mic} (reaction rate in micelle). For reactions in α-cyclodextrin, data was fitted to rate equations containing first and second order dependencies on cyclodextrin using non linear regression techniques.

The work was carried out in the presence of 0.003 M nitric acid as reaction medium. The effect of inorganic electrolytes (sodium nitrate, sulfate, actetate, perchlorate and chloride)

on the rate of oxidation of iodide in the absence and presence of non-ionic surfactant brij-35 was also studied. The critical micelle concentration (CMC) of the surfactants was determined using kinetic techniques and was found to be inversely proportional to the salt concentration and also to the temperature. The CMC was also found to decrease as the length of the hydrophobic part of the Brij surfactants was increased, possibly due to the decrease of interfacial energy on micellization, which generally increases in with increasing hydrophobic chain length.

It was shown from analysis of the kinetic data that all non-ionic micelles in the (absence of salts) and α-CD studied in this work enhanced the rate of the iodide oxidation by MCPBA and that the rate showed saturation type kinetics. Sulfate ions were shown to accelerate the reaction further, whereas perchlorate caused an inhibition of the iodide oxidation (compared to the reaction only in nitric acid) in presence of Brij-35, but an increase in the presence of α-cyclodextrin. For the oxidation of sulfides by MCPBA in micelles and α-CD the observed rate increases to a maximum with increasing micelle or α-CD concentration and then subsequently declines. In the case of sulfide oxidation by the anionic peracid, peroxymonosulfate (PMS), there was only inhibition in the rate, due to separation of reactants.

The effect of temperature on both rate and equilibrium processes for these systems was determined over the range 15 to 35°C. The results showed a linear decrease in the binding of metachloroperbenzoic (MCPBA) acid and aryl alkyl sulfides to both micelle and α-CD with increasing the temperature.

The thermodynamic and activation parameters for the reactions were determined by using Van't Hoff and Eyring plots. Comparison of the micellar association constants of MCPBA and the apparent micellar association constant of the transition state for the reaction with iodide, suggested that orientational restriction imposed on the peracid by Brij-35 are similar to that in the transition state. For the same reactions carried out in α-cyclodextrin at different temperatures it was determined that the binding constant enthalpy and entropy of substrates, (peracid and iodide) are more negative than that obtained in the presence of brij-35 which indicates that stronger interactions are involved and more restriction imposed on the reactant in presence of α-CD compared to brij-35.

A similar approach was employed for the reaction of series of aryl alkyl sulfides with peracids (PMS and MCPBA) in presence of Brij-35 and α-CD. The aryl alkyl sulfides can form both 1:1 and 2:1 host: guest complexes in cyclodextrin; the 2:1 inclusion

complexes for some sulfides were larger than the 1:1 complexes, indicating cooperative binding, with the driving force for this possibly being a substrate induced dipole-dipole interaction between the two cyclodextrin molecules. Linear free energy studies indicate that the catalytic species is the bound peracid reacting with the unbound sulfides; sulfide binding results in steric inhibition of the reaction. The reaction of the non-binding PMS with sulfides results only in inhibition as cyclodextrin concentration is increased.

The enthalpy and entropy for sulfide oxidation by peracids was calculated by means of a Van't Hoff plot. The reaction in α-CD associated with more negative entropy and enthalpy for the inclusion 2:1 while for 1:1 some substrates associated with positive entropy and small negative enthalpy while other show the usual behaviour observed for complex formation (negative values for both enthalpy and entropy).

In all studied reactions (related reactions) there were good relationships between enthalpy and entropy (isokinetic relationships or enthalpy-entropy compensation). Whilst in some cases it is difficult to explain why enthalpy-entropy compensation might be observed, we have suggested that in the case of binding of sulfides to cyclodextrin these plots can act as probes into the orientation of the substrate within the cyclodextrin cavity.

The nature of the catalytic mechanism for the reactions of peracids with sulfides and iodide in the presence of micelles and α-cyclodextrin was examined by comparing the transition state stabilisation parameters, K_{TS1}, for the same reaction in the two catalytic systems. It was found that for three out of five sulfides the degree of transition state stabilisation was almost identical in both Brij-35 and α-cyclodextrin, perhaps suggesting the same catalytic mechanism in each system; this could be via either decreased stabilisation of the peracid ground state in the absence of a protic solvent and / or the prevention of significant charge development in the transition state as a result of an intramolecular proton transfer step involving the peracid that is facilitated by the absence of water. Other possibilities exist, such as general acid catalysis, though these would be more dependent on the nature of the catalytic system. There was a less clear relationship for iodide.

Abstract

The objectives of this study were two-fold: firstly to add to existing knowledge about the reaction of peracid with both iodide and sulfides in the presence of micelles (anionic and non-ionic) and α-cyclodextrin. The reaction between iodide and peracid had previously been studied only at 25°C in non-ionic, anionic micellar and alpha cyclodextrin; while the reaction of sulfides and peracid had only been investigated in the presence of α-cyclodextrin at one temperature. This study has investigated the previously undetermined effect of temperature on these reactions and how changes in temperature can affect the process of reactants binding to the micelle or cyclodextrin catalyst. The second objective was to obtain quantitative information about reactivity in ordered aqueous media such as micellar systems and cyclodextrins, and find out how these media can affect and control these reactions. This might have implications for fields such as cell biology, specifically for process occurring in living cells since both cyclodextrins and micelles might be considered simple models for protein and membranes in terms of their hydrophobicity. In addition, little information is known about bimolecular reactions involving two neutral reactants in non-ionic micelles where only the hydrophobic interaction is likely to influence the reaction due to the absence of charge-charge interaction.

A kinetic and thermodynamic investigation of the reactions between peracids and different reductants i.e. iodide and series of aryl alkyl sulfides in presence non-ionic micelle and α- cyclodextrin is reported in this work. The kinetics were conducted by monitoring spectrophotometrically the increase or decrease in the absorbance due to formation of triioidide or disappearance of sulfides respectively, and absorbance versus time plots were fitted to nonlinear equation in order to obtain the observed pseudo first order rate constants.

For reactions carried out in micellar systems the kinetic data were treated using the multiple micellar pseudophase model developed by Davies which considers the partition of reactants between water in the bulk aqueous phase and that in the micellar pseudophases. Important parameters in this model include the binding constant of reactants to Brij (non-ionic micelle) and k_{mic} (reaction rate in micelle). For reactions in α-cyclodextrin, data was fitted to rate equations containing first and second order dependencies on cyclodextrin using non linear regression techniques.

The work was carried out in the presence of 0.003 M nitric acid as reaction medium. The effect of inorganic electrolytes (sodium nitrate, sulfate, actetate, perchlorate and chloride)

on the rate of oxidation of iodide in the absence and presence of non-ionic surfactant brij-35 was also studied. The critical micelle concentration (CMC) of the surfactants was determined using kinetic techniques and was found to be inversely proportional to the salt concentration and also to the temperature. The CMC was also found to decrease as the length of the hydrophobic part of the Brij surfactants was increased, possibly due to the decrease of interfacial energy on micellization, which generally increases in with increasing hydrophobic chain length.

It was shown from analysis of the kinetic data that all non-ionic micelles in the (absence of salts) and α-CD studied in this work enhanced the rate of the iodide oxidation by MCPBA and that the rate showed saturation type kinetics. Sulfate ions were shown to accelerate the reaction further, whereas perchlorate caused an inhibition of the iodide oxidation (compared to the reaction only in nitric acid) in presence of Brij-35, but an increase in the presence of α-cyclodextrin. For the oxidation of sulfides by MCPBA in micelles and α-CD the observed rate increases to a maximum with increasing micelle or α-CD concentration and then subsequently declines. In the case of sulfide oxidation by the anionic peracid, peroxymonosulfate (PMS), there was only inhibition in the rate, due to separation of reactants.

The effect of temperature on both rate and equilibrium processes for these systems was determined over the range 15 to 35°C. The results showed a linear decrease in the binding of metachloroperbenzoic (MCPBA) acid and aryl alkyl sulfides to both micelle and α-CD with increasing the temperature.

The thermodynamic and activation parameters for the reactions were determined by using Van't Hoff and Eyring plots. Comparison of the micellar association constants of MCPBA and the apparent micellar association constant of the transition state for the reaction with iodide, suggested that orientational restriction imposed on the peracid by Brij-35 are similar to that in the transition state. For the same reactions carried out in α-cyclodextrin at different temperatures it was determined that the binding constant enthalpy and entropy of substrates, (peracid and iodide) are more negative than that obtained in the presence of brij-35 which indicates that stronger interactions are involved and more restriction imposed on the reactant in presence of α-CD compared to brij-35.

A similar approach was employed for the reaction of series of aryl alkyl sulfides with peracids (PMS and MCPBA) in presence of Brij-35 and α-CD. The aryl alkyl sulfides can form both 1:1 and 2:1 host: guest complexes in cyclodextrin; the 2:1 inclusion

complexes for some sulfides were larger than the 1:1 complexes, indicating cooperative binding, with the driving force for this possibly being a substrate induced dipole-dipole interaction between the two cyclodextrin molecules. Linear free energy studies indicate that the catalytic species is the bound peracid reacting with the unbound sulfides; sulfide binding results in steric inhibition of the reaction. The reaction of the non-binding PMS with sulfides results only in inhibition as cyclodextrin concentration is increased.

The enthalpy and entropy for sulfide oxidation by peracids was calculated by means of a Van't Hoff plot. The reaction in α-CD associated with more negative entropy and enthalpy for the inclusion 2:1 while for 1:1 some substrates associated with positive entropy and small negative enthalpy while other show the usual behaviour observed for complex formation (negative values for both enthalpy and entropy).

In all studied reactions (related reactions) there were good relationships between enthalpy and entropy (isokinetic relationships or enthalpy-entropy compensation). Whilst in some cases it is difficult to explain why enthalpy-entropy compensation might be observed, we have suggested that in the case of binding of sulfides to cyclodextrin these plots can act as probes into the orientation of the substrate within the cyclodextrin cavity.

The nature of the catalytic mechanism for the reactions of peracids with sulfides and iodide in the presence of micelles and α-cyclodextrin was examined by comparing the transition state stabilisation parameters, K_{TS1}, for the same reaction in the two catalytic systems. It was found that for three out of five sulfides the degree of transition state stabilisation was almost identical in both Brij-35 and α-cyclodextrin, perhaps suggesting the same catalytic mechanism in each system; this could be via either decreased stabilisation of the peracid ground state in the absence of a protic solvent and / or the prevention of significant charge development in the transition state as a result of an intramolecular proton transfer step involving the peracid that is facilitated by the absence of water. Other possibilities exist, such as general acid catalysis, though these would be more dependent on the nature of the catalytic system. There was a less clear relationship for iodide.

Abstract

The objectives of this study were two-fold: firstly to add to existing knowledge about the reaction of peracid with both iodide and sulfides in the presence of micelles (anionic and non-ionic) and α-cyclodextrin. The reaction between iodide and peracid had previously been studied only at 25°C in non-ionic, anionic micellar and alpha cyclodextrin; while the reaction of sulfides and peracid had only been investigated in the presence of α-cyclodextrin at one temperature. This study has investigated the previously undetermined effect of temperature on these reactions and how changes in temperature can affect the process of reactants binding to the micelle or cyclodextrin catalyst. The second objective was to obtain quantitative information about reactivity in ordered aqueous media such as micellar systems and cyclodextrins, and find out how these media can affect and control these reactions. This might have implications for fields such as cell biology, specifically for process occurring in living cells since both cyclodextrins and micelles might be considered simple models for protein and membranes in terms of their hydrophobicity. In addition, little information is known about bimolecular reactions involving two neutral reactants in non-ionic micelles where only the hydrophobic interaction is likely to influence the reaction due to the absence of charge-charge interaction.

A kinetic and thermodynamic investigation of the reactions between peracids and different reductants i.e. iodide and series of aryl alkyl sulfides in presence non-ionic micelle and α- cyclodextrin is reported in this work. The kinetics were conducted by monitoring spectrophotometrically the increase or decrease in the absorbance due to formation of triioidide or disappearance of sulfides respectively, and absorbance versus time plots were fitted to nonlinear equation in order to obtain the observed pseudo first order rate constants.

For reactions carried out in micellar systems the kinetic data were treated using the multiple micellar pseudophase model developed by Davies which considers the partition of reactants between water in the bulk aqueous phase and that in the micellar pseudophases. Important parameters in this model include the binding constant of reactants to Brij (non-ionic micelle) and k_{mic} (reaction rate in micelle). For reactions in α-cyclodextrin, data was fitted to rate equations containing first and second order dependencies on cyclodextrin using non linear regression techniques.

The work was carried out in the presence of 0.003 M nitric acid as reaction medium. The effect of inorganic electrolytes (sodium nitrate, sulfate, actetate, perchlorate and chloride)

on the rate of oxidation of iodide in the absence and presence of non-ionic surfactant brij-35 was also studied. The critical micelle concentration (CMC) of the surfactants was determined using kinetic techniques and was found to be inversely proportional to the salt concentration and also to the temperature. The CMC was also found to decrease as the length of the hydrophobic part of the Brij surfactants was increased, possibly due to the decrease of interfacial energy on micellization, which generally increases in with increasing hydrophobic chain length.

It was shown from analysis of the kinetic data that all non-ionic micelles in the (absence of salts) and α-CD studied in this work enhanced the rate of the iodide oxidation by MCPBA and that the rate showed saturation type kinetics. Sulfate ions were shown to accelerate the reaction further, whereas perchlorate caused an inhibition of the iodide oxidation (compared to the reaction only in nitric acid) in presence of Brij-35, but an increase in the presence of α-cyclodextrin. For the oxidation of sulfides by MCPBA in micelles and α-CD the observed rate increases to a maximum with increasing micelle or α-CD concentration and then subsequently declines. In the case of sulfide oxidation by the anionic peracid, peroxymonosulfate (PMS), there was only inhibition in the rate, due to separation of reactants.

The effect of temperature on both rate and equilibrium processes for these systems was determined over the range 15 to 35°C. The results showed a linear decrease in the binding of metachloroperbenzoic (MCPBA) acid and aryl alkyl sulfides to both micelle and α-CD with increasing the temperature.

The thermodynamic and activation parameters for the reactions were determined by using Van't Hoff and Eyring plots. Comparison of the micellar association constants of MCPBA and the apparent micellar association constant of the transition state for the reaction with iodide, suggested that orientational restriction imposed on the peracid by Brij-35 are similar to that in the transition state. For the same reactions carried out in α-cyclodextrin at different temperatures it was determined that the binding constant enthalpy and entropy of substrates, (peracid and iodide) are more negative than that obtained in the presence of brij-35 which indicates that stronger interactions are involved and more restriction imposed on the reactant in presence of α-CD compared to brij-35.

A similar approach was employed for the reaction of series of aryl alkyl sulfides with peracids (PMS and MCPBA) in presence of Brij-35 and α-CD. The aryl alkyl sulfides can form both 1:1 and 2:1 host: guest complexes in cyclodextrin; the 2:1 inclusion

complexes for some sulfides were larger than the 1:1 complexes, indicating cooperative binding, with the driving force for this possibly being a substrate induced dipole-dipole interaction between the two cyclodextrin molecules. Linear free energy studies indicate that the catalytic species is the bound peracid reacting with the unbound sulfides; sulfide binding results in steric inhibition of the reaction. The reaction of the non-binding PMS with sulfides results only in inhibition as cyclodextrin concentration is increased.

The enthalpy and entropy for sulfide oxidation by peracids was calculated by means of a Van't Hoff plot. The reaction in α-CD associated with more negative entropy and enthalpy for the inclusion 2:1 while for 1:1 some substrates associated with positive entropy and small negative enthalpy while other show the usual behaviour observed for complex formation (negative values for both enthalpy and entropy).

In all studied reactions (related reactions) there were good relationships between enthalpy and entropy (isokinetic relationships or enthalpy-entropy compensation). Whilst in some cases it is difficult to explain why enthalpy-entropy compensation might be observed, we have suggested that in the case of binding of sulfides to cyclodextrin these plots can act as probes into the orientation of the substrate within the cyclodextrin cavity.

The nature of the catalytic mechanism for the reactions of peracids with sulfides and iodide in the presence of micelles and α-cyclodextrin was examined by comparing the transition state stabilisation parameters, K_{TS1}, for the same reaction in the two catalytic systems. It was found that for three out of five sulfides the degree of transition state stabilisation was almost identical in both Brij-35 and α-cyclodextrin, perhaps suggesting the same catalytic mechanism in each system; this could be via either decreased stabilisation of the peracid ground state in the absence of a protic solvent and / or the prevention of significant charge development in the transition state as a result of an intramolecular proton transfer step involving the peracid that is facilitated by the absence of water. Other possibilities exist, such as general acid catalysis, though these would be more dependent on the nature of the catalytic system. There was a less clear relationship for iodide.